AN *IN VITRO* INVESTIGATION INTO THE MECHANISM OF THE CLINICALLY RELEVANT DRUG-DRUG INTERACTION BETWEEN OMEPRAZOLE OR ESOMEPRAZOLE AND CLOPIDOGREL

BY

BRIAN WAYNE OGILVIE

Submitted to the graduate degree program in Pharmacology, Toxicology & Therapeutics and the Graduate Faculty of the University of Kansas in partial fulfillment of the requirements for the degree of Doctor of Philosophy.

_____

Committee Chair: Gregory Reed, Ph.D.

_____

Andrew Parkinson, Ph.D.

_____

Bruno Hagenbuch, Ph.D.

_____

Scott Weir, PharmD, Ph.D.

_____

Robert Hanzlik, Ph.D.

Date Defended: April 23rd, 2015

The Dissertation Committee for BRIAN WAYNE OGILVIE
certifies that this is the approved version of the following dissertation:

AN *IN VITRO* INVESTIGATION INTO THE MECHANISM OF THE CLINICALLY RELEVANT DRUG-DRUG INTERACTION BETWEEN OMEPRAZOLE OR ESOMEPRAZOLE AND CLOPIDOGREL

_____

Committee Chair: Greg Reed, Ph.D.

Date Approved: April 23rd, 2015

ABSTRACT

Clopidogrel is a thienopyridine antiplatelet prodrug that was approved by the US FDA in 1997 and quickly supplanted ticlopidine as the primary drug therapy for reducing atherothrombotic events. It is converted to its pharmacologically active metabolite H4, which irreversibly inactivates the $P2Y_{12}$ receptor on platelets, through two sequential reactions that are catalyzed mainly by CYP2C19. Common clinical practice involved the coadministration of a proton pump inhibitor (PPI, including omeprazole, esomeprazole, lansoprazole, pantoprazole, and rabeprazole) with clopidogrel to decrease the risk of upper gastrointestinal bleeding. This practice was formalized for high risk patients by the American Heart Association (and others) in 2008. By 2009, numerous publications described an unexpected decrease in clopidogrel efficacy when coadministered with PPIs, prompting both the US Food & Drug Administration (FDA) and European Medicines Agency (EMA) to issue recommendations discouraging the concomitant use of PPIs and clopidogrel. Proton pump inhibitors are also metabolized by CYP2C19. It seemed reasonable to conclude that, despite their relatively short plasma half-lives, PPIs might competitively inhibit CYP2C19, thereby reducing the efficacy of clopidogrel. In 2010, as numerous publications emerged, both regulatory agencies restricted subsequent warnings to only omeprazole and esomeprazole. The interaction between clopidogrel and PPIs, and the potential mechanisms responsible for it, continues to be a subject of much debate in 2015.

This dissertation describes research that contributes to the progress made in understanding the basis for the interaction between clopidogrel and PPIs since the time of the initial regulatory statements, and in particular, why only omeprazole and esomeprazole are implicated in this drug interaction.

The initial studies in this dissertation identified omeprazole (a racemic mixture of *R*- and *S*-enantiomers) and esomeprazole (the *S*-enantiomer) as not only competitive inhibitors, but

more importantly, metabolism-dependent inhibitors (MDIs) of CYP2C19 in human liver microsomes (HLM), human hepatocytes and recombinant CYP2C19. In contrast, lansoprazole and pantoprazole did not cause metabolism-dependent inhibition (MDI) of CYP2C19. In addition to its clinical relevance, these observations are important because they underscore the importance of using a low concentration of enzyme and a short incubation time with the CYP marker substrate in order to detect MDI of CYP enzymes in vitro. In many previous studies of CYP2C19 inhibition by omeprazole or esomeprazole, the concentration of HLM was too high and/or the substrate incubation time was too long to detect MDI. The kinetic parameters for CYP2C19 inactivation by omeprazole, namely k_{inact} and K_I, were determined and used in a physiologically based pharmacokinetic (PBPK) model to predict the degree of CYP2C19 inactivation under clinical conditions. Omeprazole and esomeprazole were subsequently shown to be irreversible MDIs of CYP2C19, which explained why the decrease in clopidogrel efficacy could not be prevented in clinical studies by simply separating the doses of clopidogrel from omeprazole or esomeprazole.

Subsequent studies demonstrated that, like the parent drug, two of the three major metabolites of omeprazole are also irreversible MDIs of CYP2C19. The kinetic parameters for CYP2C19 inactivation by these metabolites were determined and, along with those for omeprazole and esomeprazole, used in a mechanistic static model to predict the reduction of H4 formation from clopidogrel under clinical conditions. The model slightly overpredicted (by a factor of 2) the ability of omeprazole to block the conversion of clopidogrel to H4, its pharmacologically active metabolites, but otherwise established that inactivation of CYP2C19 is the likely mechanism for the clinical interaction between omeprazole/esomeprazole and clopidogrel.

Esomeprazole and its two inhibitory metabolites, namely omeprazole sulfone and 5-*O*-desmethylomeprazole, were subsequently determined to meet several criteria for

mechanism-based inhibition (a special case of irreversible MDI). In addition, studies were initiated to test the hypothesis that the mechanism of CYP2C19 inactivation by esomeprazole and its metabolites involves the formation of a benzylic radical (on the 5′-methyl group) that binds covalently to the heme moiety. This hypothesis was based on the observation that the 5′-methyl group is present on the pyridine ring of those compounds that irreversibly inactivate CYP2C19, namely omeprazole, esomeprazole, omeprazole sulfone and 5-*O*-desmethylomeprazole, but absent from those compounds that did not inactivate CYP2C19, namely lansoprazole, pantoprazole and 5′-hydroxyomeprazole. Based on this hypothesis, the investigational PPI, tenatoprazole, which contains a 5′-methyl group, was correctly predicted to cause MDI of CYP2C19 whereas ilaprazole and rabeprazole, which lack a 5′-methyl group, did not cause MDI of CYP2C19. These results suggest that the investigational PPI, tenatoprazole, but not the clinically used PPIs ilaprazole or rabeprazole, may compromise the therapeutic effectiveness of clopidogrel.

Finally, studies were performed in an attempt to provide direct evidence for the proposed mechanism of inactivation of CYP2C19 by esomeprazole, namely the formation of a heme adduct. The potential for the formation of a heme adduct in incubations of esomeprazole in HLM was evaluated by UHPLC analysis with UV/VIS detection and high resolution mass spectrometry (HRMS) with post-acquisition mass-defect filtering to identify heme and heme-containing adducts. Incubation of esomeprazole with NADPH-fortified HLM resulted in a substantial decrease in the amount of heme detectable by UHPLC with either UV absorbance or HRMS and *appeared* to show the formation of a heme adduct based on mass-defect filtering and isotopic distribution. However, the putative heme adduct was subsequently identified as a dimer of esomeprazole sulfone (a metabolite of esomeprazole formed by CYP3A4/5). Although an adduct between heme and a metabolite of esomeprazole was not ultimately identified, the potential for an unusual analytical artifact was revealed; namely, that sulfur-containing drugs

can be converted to metabolites that closely resemble a heme adduct based on mass-defect filtering and isotopic distribution.

In summary, this dissertation supports the hypothesis that irreversible inactivation of CYP2C19 is the mechanism by which omeprazole and esomeprazole reduce the efficacy of clopidogrel. This property is not shared by lansoprazole, pantoprazole, rabeprazole or ilaprazole. These findings support regulatory agencies' recommendations that, in order to reduce the risk of gastrointestinal bleeding, clopidogrel should not be coadministered with omeprazole or esomeprazole but should be coadministered with other PPIs that do not inactivate CYP2C19.

Dedicated to my daughter:

Olivia Ashley Ogilvie

ACKNOWLEDGEMENTS

First and foremost a very special thanks to my wife, Monika, for your love and encouragement along the way, not to mention bringing dinner with Olivia to my office on many Saturday or Sunday evenings. I also can't thank you enough for no longer asking "are you going into the lab this weekend?" after about the first two years. Seriously, though, I truly can't thank you enough for everything you do, and I certainly know I couldn't have done this without you.

My deepest gratitude goes to my mentor and friend, Dr. Andrew Parkinson, whose mentorship commenced an entire decade before I began graduate school. I will be eternally grateful for everything you have done for me, which is more than I could have ever imagined, including giving me the opportunity to pursue a Ph.D. while still maintaining my career. I can't thank you enough for your patience, sense of humor, generosity, your infectious - almost giddy, enthusiasm for all things related to science, and for always setting the bar high, scientifically, grammatically and personally. I am truly grateful for the extensive time and effort you spent discussing and reviewing experimental designs with me, interpretation of data and reviewing my writing. You have been truly selfless in too many ways to count and supported me through some very difficult times, especially in the last three years. From my first days at XenoTech, you made Monika and me feel like part of your family.

Special thanks go to Kay Parkinson for allowing me to have so much of Andrew's time over the years; for all the dinners, conversation and your incredible generosity. And while I'm on the Parkinsons, I would like to express my sincere thanks to Oliver, Simon and Hannah for great conversations and support over the years. It is hard to believe I've known you all since Hannah played the harp and Oliver still wanted to be an astronaut.

I express my sincere thanks to each of the members of my dissertation committee (past and present), especially to Dr. Greg Reed for agreeing to take over as my committee chair, Dr. Bruno Hagenbuch, Dr. Robert Hanzlik, Dr. Scott Weir and Dr. Curtis Klaassen for your guidance and patience, and the significant time and effort you committed to my research.

I would also like to take this opportunity to express a very sincere thanks to the many professors at KUMC who devoted significant time and effort to lectures starting with the IGBPS courses. A special thanks should also go to Dr. Tom Pazdernik for the Saturday morning review sessions during the toxicology and pharmacology courses, which helped me in my academic, professional and even personal life more than you know.

The day-to-day support of my friends at KUMC and colleagues at XenoTech, past and present, was priceless. There are too many people to name, but you have all made a lasting impact on me, and special thanks go to a number of you below.

A very special thanks goes to Dr. Joanna Barbara for your time, effort and patience with me, as you endlessly re-explained mass spectrometry concepts and terminology to me, helped me to understand what the data were telling us and why, and especially for your hours in the lab and at the computer to acquire the high resolution MS data. Chapter 7 would not have been possible without you.

Likewise, special thanks go to Dr. Sylvie Kandel for your assistance with the mass spectrometry data presented in Chapter 7. Thanks especially for bearing with me in my seemingly endless requests for more sets of chromatograms or spectra that were acquired quite some time ago.

I also take this opportunity to express a very special thanks to Dr. David Buckley. Your support and patience with me has been invaluable.

Another special thanks goes to Phyllis Yerino for your help and support over the years. I don't know where to start, so I will leave it at that.

I would also like to thank the Hepatocellular Products and Services Department of XenoTech for providing the historical data on CYP2C19 activity to observe the effect of 3-day omeprazole treatment on many fresh cultures of hepatocytes.

Faraz Kazmi also deserves special mention for his help with, among other things, the UV/VIS spectrophotometer. When I tried to use it on my own, I obtained data that looked like an EKG trace.

I express gratitude to my former collaborators at XenoTech not already named, including Brandy Paris, Ken Goodell and Dr. Paul Toren.

I would also like to thank my collaborator, Dr. Amin Rostami-Hodjegan from the Centre for Applied Pharmacokinetic Research, Manchester Pharmacy School, University of Manchester, Manchester, UK and Simcyp, Ltd. for his invaluable assistance with the PBPK modelling presented in Chapter 4.

Many thanks also go to the administrative staff within the department (past and present), especially including Rosa Meagher and Cody Tully, who helped guide me through my rather non-traditional studentship.

I am of course indebted to my parents, Jerry and Patricia for opening so many doors for me at an early age. I would not be a scientist without you. I'm also grateful to the rest of my family including my step-mother Annie, step-father Sam, mother-in-law Betty, father-in-law Ken, my brother Blake, step-sisters Kate and Emily and all the rest of you for your support and especially for listening to me go on and on about science and medicine even when you probably have no idea what I'm talking about. This list would not be complete without gratitude for the love and support of my late grandparents, Gladys Ogilvie, and Ethenelle and James Robert McNinch. A special mention should go to the pharmacists in my family, Emily and Sam who do their best to answer my questions. Finally a very special thanks to the first pharmacist I knew, my grandfather, Wayne, who let my brother and I explore his pharmacy from a very young age, and sparked my imagination and interest in medicine and science. My grandfather gave me his expired USP Dispensing Information books in high school, and my father gave me his old pathology and other textbooks from dental school (which for better or worse, I read with great interest in the days before the internet). A career in drug metabolism and toxicology seems almost inevitable in retrospect, even though I thought I wanted to be a physician.

I would also like to express thanks for the financial support for this research from XenoTech and Sekisui Medical, Co., Ltd., as well as through the National Institutes of Health Training Program in Environmental Toxicology T32ES007079 (2009).

Finally, to end where I started (i.e., the dedication to my daughter Olivia): I hope you pull this off the shelf some day and see your name and know how much you mean to me. You have taught me more about hypothesis testing than any scientific research I could ever conduct.

Table of Contents

LIST OF ABBREVIATIONS

Abbreviation	Full name
1-ABT	1-Aminobenzotriazole
ACCF	American College of Cardiology Foundation
ACG	American College of Gastroenterology
AHA	American Heart Association
ADP	Adenosine diphosphate
ADR	Adverse drug reaction
AUC	Area under the plasma drug concentration-time curve
AUC_i	AUC under inhibited conditions
AUCR	AUC ratio (i.e., change in exposure: AUC_i/AUC)
C_{max}	The maximum plasma concentration of the drug
CYP	Cytochrome P450
Da	Dalton (i.e., unified atomic mass unit or u)
DAPT	Dual antiplatelet therapy
DDI	Drug-drug interaction
DMSO	Dimethyl sulfoxide
EMs	Extensive metabolizers
EMA	European Medicines Agency
FDA	U.S. Food and Drug Administration
GPIIb/IIIa	Glycoprotein IIb/IIIa
GSH	Glutathione
H4	Clopidogrel active metabolite (a.k.a. 4b-*cis* thiol isomer)
HCE1	Human carboxylesterase 1
HLM	Human liver microsomes
HRMS	High resolution mass spectrometry
IMs	Intermediate metabolizers
k_{deg}	The rate constant for enzyme degradation
Ki	The reversible dissociation constant for an enzyme-inhibitor complex
K_I	Inhibitor concentration that supports half the maximal rate of inactivation
k_{inact}	Maximal rate of enzyme inactivation

K_m	Michaelis-Menten constant (i.e., the substrate concentration that supports the half-maximal rate of reaction)
k_{obs}	The initial rate of enzyme inactivation
LC-MS/MS	Liquid chromatography tandem mass spectrometry
MACE	Major adverse cardiac events
MBI	Mechanism-based inhibition
mDa	MilliDaltons
MDF	Mass-defect filtering
MDI	Metabolism-dependent inhibition
MDM	Mechanistic dynamic model
MI	Myocardial infarction
MIC	Metabolite inhibitory complex
MS/MS	Tandem mass spectrometry
MS^E	Elevated energy mass-spectrometry
MSM	Mechanistic static model
MTDI	University of Washington Metabolism and Transport Drug Interaction Database™: http://www.druginteractioninfo.org
m/*z*	Mass-to-charge ratio
NADPH	Nicotinamide adenine dinucleotide phosphate, reduced
5-ODM omeprazole	5-*O*-Desmethylomeprazole
$P2Y_{12}$	Platelet membrane G-protein-coupled purinergic receptor
P450	Cytochrome P450
PBPK	Physiologically based pharmacokinetic model
PCI	Percutaneous coronary intervention
PD	Pharmacodynamic
P-gp	P-glycoprotein
PMs	Poor metabolizers
PK	Pharmacokinetic
PON1	Paraoxonase 1
rh	Recombinant human
$t_{1/2}$	Elimination half-life
TDI	Time-dependent inhibition
TIC	Total ion chromatogram
UHPLC	Ultra-high performance liquid chromatography

UMs	Ultra-rapid metabolizers
UV	Ultraviolet (wavelengths from 200 – 400 nm [i.e., far ultraviolet to ultraviolet A])
V_{max}	The maximal rate of an enzymatic reaction
λ	Wavelength (nm)

LIST OF TABLES

LIST OF FIGURES

LIST OF EQUATIONS

Portions of this dissertation are reproduced from the following publications, with permission from the publishers as applicable:

1. **Ogilvie BW**, Yerino P, Kazmi F, Buckley DB, Rostami-Hodjegan A, Paris BL, Toren P and Parkinson A. (2011) The proton pump inhibitor, omeprazole, but not lansoprazole or pantoprazole, is a metabolism-dependent inhibitor of CYP2C19: implications for coadministration with clopidogrel. *Drug Metab Dispos* **39**:2020-2033.

2. **Ogilvie BW**, Toren P, Kazmi F, and Parkinson A. (2011) Esomeprazole and omeprazole sulfone are in vitro metabolism-dependent inactivators of CYP2C19: Determination of K_I and k_{inact} values. *Drug Metab Rev* **43**(S2): abstract 145.

3. **Ogilvie BW** and Parkinson A. (2012) Mechanistic studies on the inactivation of CYP2C19 by esomeprazole, 5-*O*-desmethyl omeprazole, and omeprazole sulfone. *Drug Metab Rev* **44**(S1): abstract 40.

4. **Ogilvie BW**, Barbara JE, and Parkinson A. (2013) Esomeprazole modifies heme in human liver microsomes: Preliminary high resolution mass spectrometric evidence for the mechanism of inactivation of cytochrome P450. *Drug Metab Rev* 45(S1): abstract 127.

Chapter 1. BACKGROUND AND INTRODUCTION

1.1. The cytochromes P450 in drug metabolism

The human cytochromes P450 (CYPs) are a superfamily of 55 functional heme-thiolate-containing proteins that catalyze the biotransformation of a large number of endobiotic and xenobiotic compounds, the latter of which includes drugs, pesticides, and other commonly encountered small molecules (1). Nearly 80% of all oxidative metabolism of currently used drugs is catalyzed by one or more of the major "drug-metabolizing CYPs" (i.e., CYP1A2, 2A6, 2B6, 2C8, 2C9, 2C19, 2D6, 2E1, 2J2, 3A4, and 3A5), with CYP2D6 or CYP3A4/5 involved in the metabolism of the majority of orally administered drugs (1-3). CYPs are expressed prominently in human liver endoplasmic reticulum (microsomes), which is the major site involved in drug elimination, but they are also expressed to a significant extent in many other tissues, with the next most important site for drug metabolism being the intestinal mucosa (1,4). Because CYPs represent the rate-limiting step in the metabolism of many drugs, they play a key role in determining the potency and duration of action of these same drugs. Therefore, a decrease in the activity of these enzymes can lead directly to type A toxicity (defined below), especially upon repeated dosing, thus allowing accumulation of a "victim drug" (defined below).

Relevance of drug-drug interactions to toxicology

To appreciate the relevance of adverse drug reactions to the study of toxicology, certain definitions must first be considered. Much of the current literature attempts to use various terms to describe the same thing, and to some extent the choice of term depends on the intended audience or other context of the particular communication. For instance, the FDA frequently uses the term "side effects", but generally only in information intended to be disseminated to the public at large, because the term "side effect" is often used informally to refer to *any* adverse drug reaction (ADR) (5). In contrast, FDA-approved drug labels (a.k.a. prescribing information) do not use the term "side effects" and instead use the term "adverse reactions". Alternatively,

some authors use the phrase “adverse drug event” when describing any harmful or unpleasant event that occurs while a patient is taking a drug, so it has been suggested that this term is confusing and should not be used (6). For instance, adverse events encountered during the course of drug therapy can include any untoward or unplanned occurrence (e.g., unplanned pregnancy while a patient is on an oral contraceptive, an accident, or deterioration in a concurrent illness), and may or may not be due to the drug therapy itself (6). The term “adverse drug reactions” (ADRs) will therefore be used in this dissertation as defined by Aronson: “an appreciably harmful or unpleasant reaction, resulting from an intervention related to the use of a medicinal product" (6). ADRs can occur in monotherapy, the majority of which are predictable from their known pharmacologic mechanism of action (7), but they can also occur when combinations of two or more drugs are coadministered (i.e., ADRs resulting from drug-drug interactions). Drug-drug interactions can be pharmacodynamic in nature. For example, drugs that have antiplatelet activity and drugs that impede vitamin K absorption potentiate the anticoagulant effect of warfarin without necessarily impacting its pharmacokinetic disposition, and can lead to serious ADRs.

The relevance of increased toxicity resulting from pharmacokinetic drug-drug interactions to public safety has been indirectly addressed in a number of studies. To estimate the impact of drug-drug interactions on public safety, the overall number of ADRs of any kind must first be considered. The frequently-cited study by Lazarou and colleagues on the incidence of ADRs in hospitalized patients over the 30-year period from 1966-1996 suggests that over 2.2 million serious ADRs occurred annually during this time, with 106,000 deaths occur per year in the U.S. alone due solely to ADRs (8). If still true, it would mean that ADRs are the fourth leading cause of death in the U.S. ahead of diabetes, pneumonia, and automobile accidents. It has also been estimated that over 350,000 ADRs occur in U.S. nursing homes each year, six percent of which were life-threatening, and 51% of which were judged to be

preventable (9). Importantly, these estimates do not include the number of ADRs in ambulatory settings. While there may be many reasons for these ADRs, it is reasonable to hypothesize that many are caused by an increased or decreased exposure to victim drugs by perpetrator drugs (i.e., other drugs, genetic polymorphisms or other factors that alter the disposition of the victim drug). Certain statistics underlie this hypothesis. For instance, 69% of all patient visits to primary care physicians result in a prescription, with 21% of those visits resulting in four or more drugs being prescribed (10). In total, there were 3.9 billion retail prescriptions filled in 2013, or approximately 12 prescriptions for every person in the U.S (11). Most importantly, the rate of ADRs increases exponentially after a patient is prescribed four or more drugs (12). While many of these ADRs result from pharmacodynamic interactions, there are also many cases that suggest a pharmacokinetic origin. For instance, it has been found that a known pharmacokinetic drug interaction was the suspected cause of the ADR in 26% of cases in one study (13). Leape and colleagues also estimated that known drug-drug interactions represent 3-5% of all in-hospital medication errors. Even if many of these interactions are pharmacodynamic in nature, the fact that most pharmacodynamic interactions are easily predictable from their pharmacological action underscores the importance of pharmacokinetic drug-drug interactions which can be difficult for a clinician to predict from the more obvious characteristics of the interacting drugs.

Types of drug-induced toxicities

The types of toxicity caused by drugs and/or their metabolites have been historically classified according to various systems. More recent systems propose four major types (A, B, C, and D, define below) (5,6,14,15). Some ADRs can be difficult to classify or overlap with other categories, so two additional categories, types E and F have also been proposed (5). In type A toxicity, there is a pharmacological basis for the effect, one based on the

pharmacological target of the active drug (type A1) and the other based on off-target pharmacology (type A2), but in either case, the toxic effects are “selective”, and for the most part, dose-related and predictable on the basis of their pharmacological mechanism of action. This type of toxicity can be thought of as an extension of pharmacological effect, and can occur when the drug, or its pharmacologically active metabolites, reach supratherapeutic concentrations at the target as in overdose situations, or even with typical dosing in so-called poor metabolizers of the drug (16,17). Examples of type A1 toxicity can include the extrapyramidal effects of dopamine receptor agonists, gastrointestinal bleeding due to inhibition of cyclooxygenase-1 (COX1) by nonsteroidal anti-inflammatory drugs, or hypotension upon administration of propofol. Type A2 toxicity occurs when the drug or its metabolites bind to and alter the activity of an enzyme or receptor that is not the designated pharmacological target. A very well-known example of this type of toxicity is the binding of terfenadine (a non-sedating H_1 receptor antagonist) to the rapidly-acting delayed rectifier (I_{Kr}) potassium channels in the heart which can lead to QT interval prolongation and fatal torsade de pointes (18). Most side effects are examples of minor Type A toxicity, and many inhibitory pharmacokinetic drug-drug interactions cause Type A toxicity.

Types B, C, and D toxicities are typically thought of as nonselective. Type B toxicity refers generally to toxicities that do not necessarily display typical dose-response relationships, are observed in very few patients, and are therefore frequently termed “idiosyncratic” or occasionally “bizarre”, and are generally not described as dose-dependent. Strictly speaking, however, “idiosyncratic” toxicity refers to toxicity that occurs due to a *known* genetic predisposition, for instance, the prolonged muscle relaxation and apnea that occurs with a standard dose of succinylcholine in individuals that possess a genetic polymorphism for butyrylcholinesterase that confers a low activity or complete lack of this enzyme (19). Type B toxicity is, however, frequently referred to as “idiosyncratic” in the contemporary literature, in

spite of the fact that an underlying genetic predisposition may not be known. Type C toxicity refers to cases in which the drug or its metabolites reacts chemically with tissue macromolecules, and is both dose and time-related (20). Type C toxicity is not frequently associated with drugs with notable exceptions including alkylating agents used in cancer chemotherapy, which are designed to react directly with macromolecules in tumor cells. Additionally, in some cases, drugs can be bioactivated to chemically reactive species that covalently bind to proteins, which is the case with the CYP2C9 inhibitor, tienilic acid, which was withdrawn from the market due to formation of an electrophilic thiophene sulfoxide within the CYP2C9 active site and subsequent formation of anti-liver and kidney microsome antibodies (anti-LKM_2) (16). Type D toxicity has underlying mechanisms that are similar to types B and C, although the response is time- but not typically dose-related. The effect can be quite delayed (e.g., months to years), and therefore includes the toxicity caused by carcinogens and teratogens. Type E toxicity refers to so-called “end of treatment effects” (e.g., discontinuation symptoms after prolonged use of selective serotonin reuptake inhibitors, rebound hypertension after cessation of clonidine, opioid withdrawal syndrome, etc.) and the effects are generally ameliorated by reintroduction of the drug. Type F toxicity refers to adverse events that result from “failure of therapy”, which can have different causes as described below (5,20,21).

Type F toxicity, or failure of therapy bears special mention here because this type of adverse drug reaction is frequently the result of genetic polymorphisms when a prodrug must first be converted to an active metabolite. For instance, codeine must be *O*-demethylated to form morphine (predominantly by CYP2D6) in order to exert its pharmacological effect (i.e., analgesia). Genetic polymorphisms of CYP2D6 have been well described with some individuals completely lacking an active form of CYP2D6. The frequency of the CYP2D6 poor-metabolizer (PM) phenotype varies from one ethnic group to another, but it is generally held that 5-7% of Caucasians, 2–4% of black Africans and African Americans, and 1–2% of Asians (Chinese and

Japanese) populations are CYP2D6 PMs, with higher rates in South Asians (1,20). Thus, in PM patients, codeine is a much less effective analgesic than in patients with higher CYP2D6 activity (i.e., intermediate, extensive and ultrarapid metabolizers [IMs, EMs and UMs, respectively]). CYP2D6 also converts tamoxifen to endoxifen, which is 30- to 100-fold more potent than tamoxifen in suppressing estrogen-dependent cell proliferation, and thus prevents breast cancer. Therefore, postmenopausal women who previously had estrogen receptor–positive breast cancer and are also CYP2D6 PMs treated with tamoxifen for > 5 years are at an increased risk for breast cancer recurrence (1,22). The polymorphic enzyme CYP2C19 has also been strongly implicated for its role in the multi-step conversion of the antiplatelet drug clopidogrel to its pharmacologically active metabolite, a reactive thiol often referred to as H4 (1,23). The evidence for the involvement of CYP2C19 in the conversion of clopidogrel to H4 will be discussed in greater detail in later sections.

Failure of therapy is also frequently the result of drug-drug interactions. This is most commonly discussed in the setting of a pharmacokinetic interaction when the perpetrator drug induces an enzyme involved in the clearance of the victim drug (e.g., oral contraceptive failure upon coadministration of rifampin) (1). Pharmacodynamic interactions can also lead to failure of therapy, such as when amphetamines are coadministered with antihypertensives, thus decreasing the antihypertensive effect because these drugs increase blood pressure (24). Finally, just as genetic polymorphisms are implicated in failure of therapy of prodrugs as discussed above, inhibition of the enzymes involved in the conversion such prodrugs through coadministration of a perpetrator drug can also lead to failure of therapy. It is specifically for this reason that the 2013 FDA prescribing information for clopidogrel states that “concomitant use of certain drugs that inhibit the activity of [CYP2C19] results in reduced plasma concentrations of the active metabolite of clopidogrel and a reduction in platelet inhibition” (25). Likewise, the 2013 FDA prescribing information for codeine states that “drugs that are strong inhibitors of

codeine *O*-demethylation (cytochrome P-450 2D6) may decrease the plasma concentrations of codeine's active metabolites, morphine and morphine-6-glucuronide" (26).

The broad focus of this dissertation is on the pharmacokinetic interaction between omeprazole or esomeprazole (perpetrators) and victim drugs that are CYP2C19 substrates. Although this interaction has implications for any drug that is metabolized in large part by CYP2C19 such as moclobemide, diazepam, *R*-mephobarbital, proton-pump inhibitors (PPIs) (due to reaching supratherapeutic concentrations, i.e., Types A1 and A2 toxicities), the interaction with the CYP2C19 substrate and prodrug, clopidogrel, is of special importance as an example of failure of therapy caused by a drug-drug interaction (27). Therefore, the main *toxicological* focus of this dissertation will be on Type F toxicity.

1.2. Drugs as victims and perpetrators of pharmacokinetic drug-drug interactions

From a drug-drug interaction perspective, drugs can be evaluated for their victim and perpetrator potential. Victims are those drugs whose clearance is predominantly determined by a single route of elimination, such as metabolism by a single cytochrome P450 (CYP) enzyme. Such drugs have a high victim potential because inhibition or complete loss of that elimination pathway, either due to a genetic deficiency in the relevant CYP enzyme or due to its inhibition by another, concomitantly administered drug, will result in a large decrease in clearance and a correspondingly large increase in exposure to the victim drug (e.g., area under the plasma concentration-time curve or AUC). Perpetrators are those drugs (or other environmental factors) that inhibit or induce the enzyme that is otherwise responsible for clearing a victim drug. Genetic polymorphisms that result in the partial or complete loss of enzyme activity (i.e., the intermediate and poor metabolizer genotypes) can also be viewed as perpetrators because they

have the same effect as an enzyme inhibitor: they cause a decrease in the clearance of – and an increase in exposure to – victim drugs. Likewise, genetic polymorphisms that result in the over-expression of enzyme activity (i.e., the UM genotype) can be viewed as perpetrators because they have the same effect as an enzyme inducer: they cause an increase in the clearance of – and a decrease in exposure to – victim drugs. Several drugs whose elimination is largely determined by their CYP2C9- CYP2C19- or CYP2D6-mediated metabolism (three genetically polymorphic enzymes), are victim drugs because their clearance is diminished in PMs, i.e., individuals who are genetically deficient in one of these enzymes. Drugs for which disposition is largely dependent on uptake or efflux by a transporter or on metabolism by a drug-metabolizing enzyme other than cytochrome P450 can also be considered from the victim/perpetrator perspective. From a drug interaction perspective, victim drugs are also known as objects, whereas perpetrators are also occasionally referred to as precipitants (16).

Cerivastatin, terfenadine, cisapride, dofetilide and astemizole, are all victim drugs, to such an extent that they have all been withdrawn from the market or, in the case of cisapride and dofetilide, made available with severe restrictions (28). These drugs are victim drugs because they are metabolized to a large extent by CYP3A4, the most abundant drug-metabolizing CYP in the small intestine and the liver. Inhibition of CYP3A4 by various antimycotic drugs such as ketoconazole, and antibiotic drugs such as erythromycin, decreases the clearance of terfenadine, cisapride, dofetilide and astemizole and increase their plasma concentrations to levels that, in some individuals, can cause fatal ventricular arrhythmias (i.e., QT prolongation and torsade de pointes) (16,28).

The primary purpose of evaluating drugs as inhibitors of CYP enzymes *in vitro* is to determine their perpetrator or precipitant potential before advancing a candidate drug to a late stage of development. However, identifying a drug as an *in vitro* inhibitor of a given CYP

enzyme does not imply that the drug will necessarily cause clinically relevant drug interactions. The clinical relevance of the inhibition must be considered in the following context:

(1) The pharmacokinetics of the perpetrator (inhibitory) drug.
(2) The potential of administering the perpetrator with a victim drug.
(3) The extent to which the clearance of the victim drug is dependent on the inhibited CYP enzyme (i.e., $f_{m(CYP)}$).
(4) The potential for saturating or inactivating the enzyme that metabolizes the victim drug.
(5) The clinical consequences of altering the pharmacokinetics of the victim drug (which may or may not be a cause for concern depending on the drug's therapeutic index).
(6) The therapeutic indication of the perpetrator and victim drug. Drugs used to treat life-threatening diseases (e.g., cancer, HIV) are permitted more regulatory leeway than life-style enhancing drugs (such as drugs to treat baldness) or drugs that are not first-in-class (as in the case of mibefradil, the withdrawal of which was facilitated by its being one of many calcium channel blockers on the market) (16).

The *in vitro* studies detailed in this dissertation describe a set of tools for predicting the potential for inhibitory drug interactions. Needless to say, a well-designed *in vitro* study can in most cases be a powerful predictor of clinical outcome. Unfortunately, it is easy to design an *in vitro* experiment that is analytically sound but is so seriously flawed that it provides meaningless data. For example, if amodiaquine (a high-turnover marker substrate for CYP2C8) is incubated under the same conditions (i.e., up to 1 mg/mL microsomal protein and 30 min incubation time) that are sometimes used for *S*-mephenytoin (a low turnover marker substrate for CYP2C19), then most of the amodiaquine would be converted to *N*-desethylamodiaquine. Under such conditions, a drug candidate that partially inhibits CYP2C8 may go undetected because only marked inhibition of CYP2C8 will prevent complete metabolism of amodiaquine and decrease the amount of *N*-desethylamodiaquine formed.

1.3. Site of pharmacology versus site of toxicity

In most cases when type A toxicity results from pharmacokinetic drug-drug interactions, it is simply because the victim drug accumulates in the systemic circulation upon repeated dosing, and the concentration of the drug is essentially the same at the site of pharmacology and the site of toxicity. In some cases the drug is actively excluded from what would otherwise be the site of toxicity. Such is the case with loperamide which slows gastric motility by interaction with opioid receptors in the gastrointestinal tract, but is actively excluded from the central nervous system in large part by the action of P-glycoprotein (MDR1), thus greatly minimizing the typical central toxicity observed with most opioid agonist analgesics (e.g., respiratory depression, lethargy) (29). In other cases, the site of pharmacology for a drug is limited to a single organ, and low systemic bioavailability is desirable if the drug can be selectively delivered. Such is the case with some of the statins, which generally have low systemic bioavailability (i.e., <5 to 20%, with only three, namely fluvastatin, cerivastatin and pitavastatin having more than 30%) (30), and are avidly taken up into hepatocytes, where they exert their desired pharmacological effect (i.e., inhibition of hepatic cholesterol synthesis).

1.4. Overview of the in vitro evaluation of CYP inhibition

Two major types of CYP inhibition are possible: direct inhibition and time-dependent inhibition (sometimes termed “reversible” and “irreversible”). Direct inhibition occurs when a drug inhibits a CYP enzyme without a significant lag (i.e., as soon as it binds to the CYP enzyme) and without requiring biotransformation. Examples of direct inhibition include inhibition of CYP2D6 and CYP3A4 by quinidine and ketoconazole, respectively. Direct inhibition can occur with typical (Michaelis-Menten) or atypical kinetics, including partial inhibition, or two-site binding with heterotrophic cooperation. Time-dependent inhibition occurs when the inhibitory

potency of the drug candidate increases with incubation time, which may simply reflect a slow on-rate or more commonly, biotransformation of the drug to a more potent inhibitor of the enzyme. Time-dependent inhibition includes the quasi-irreversible or irreversible metabolism-dependent inhibition caused by drugs such as troleandomycin, mibefradil, diltiazem, tienilic acid, halothane, and furafylline (1,16).

Guidelines for detecting these types of CYP inhibition *in vitro* have been described in some detail by regulatory agencies such as the FDA and EMA, and in publications (31,32). The hallmark of methods that meet or exceed the recommendations in these sources is the use of clinically used CYP-selective marker substrates in an appropriate *in vitro* test system (typically pooled human liver microsomes; for examples, see (33-35) and Chapters 3-6 in this dissertation. Because the FDA and EMA prefer that these substrates are clinically used drugs whenever possible, none of these are amenable to rapid analytical methods that make use of optical plate readers. Because of this, most definitive CYP inhibition studies must employ some type of separation technique such as HPLC, GC, capillary electrophoresis, etc. These methods can be coupled with flow-through (or occasionally stop-flow) detection such as UV, fluorescence, radiometric, mass spectrometry, etc. With the exception of LC-MS/MS methods, most of these methods require relatively long analytical run-times, which may limit throughput regardless of any automation applied to the incubation step.

In the absence of analytical equipment that can detect extremely low (sub-nanomolar) concentrations of all typical CYP marker metabolites (e.g. << 0.3 ng/mL), certain compromises in the design of CYP inhibition studies are required. The optimal design of an *in vitro* CYP inhibition study should therefore be based on a balance of microsomal protein concentrations, incubation times, marker substrates, positive control inhibitors, buffer components, automated liquid-handling systems, and analytical techniques all chosen specifically to minimize the limitations of each component. For instance, protein concentrations can have a dramatic effect

on the results due to partitioning of the test compound into microsomal membranes (often referred to simply as “nonspecific binding”), such that lower protein concentrations generally provide results that are less likely to provide a false-negative result (i.e., a result of little or no inhibition in vitro, but clinically significant inhibition) (16,35,36). Additionally, the substrate incubation time can also have a dramatic effect on the interpretation of metabolism-dependent inhibition, such that a shorter substrate incubation time provides a more accurate result (16,35). The methods described in this dissertation generally make use of very low protein concentrations (≤0.1 mg/mL) and uniform substrate incubation times (5 min). Analytical methodology is central to achieving these conditions, and the methods have lower limits of quantitation as low as 0.3 ng/mL, as described previously (16,33-35,37,38).

The starting point for these studies is a single experiment to determine three IC_{50} values from the same seven concentrations of drug: one for direct inhibition (zero-min pre-incubation with NADPH), one for time-dependent inhibition (30-min pre-incubation without NADPH), and one for NADPH- (and therefore metabolism-dependent) inhibition. If these IC_{50} determinations are designed with the substrate concentration approximately equal to *Km* for the marker reaction, the *K*i value will be equal to one-half the IC_{50} value if the inhibition is competitive and equal to the *K*i value if inhibition is noncompetitive (16,39). This simple relationship provides more reason to begin an evaluation of CYP inhibition with IC_{50} rather than *K*i determinations because a conservative estimate of the *K*i value can be used to estimate the potential clinical significance of such in vitro inhibition (31). In follow up studies (e.g., determinations of *K*i for direct inhibition, or K_I and k_{inact} for metabolism-dependent inhibition), most of the basic principles outlined above apply as well. These studies can provide a quantitative measure of both direct and metabolism-dependent inhibition (i.e., inhibition by one or more CYP-dependent metabolites). A potential limitation of this approach in human liver microsomes is the fact that potentially important non-CYP-dependent metabolites will not be formed if an added co-factor is

required (e.g. UDP-glucuronic acid). For instance, glucuronidation converts gemfibrozil to a potent inactivator of CYP2C8 in vitro and causes clinically significant inhibition of CYP2C8 at even small multiple doses (i.e., 30 mg b.i.d. for 5 days, or 1/20 the normal dose) (33,40-43).

1.5. Clopidogrel as a victim drug

Clopidogrel is an antiplatelet thienopyridine prodrug indicated for prevention of cardiovascular death, myocardial infarction (MI), stroke or other major adverse cardiac events (MACE) in the setting of recent acute coronary syndrome, MI, stroke, or established peripheral arterial disease as well as prevention of stent thrombosis in patients undergoing percutaneous coronary intervention (PCI) (25). Most of the absorbed clopidogrel (85-92% of circulating metabolites) is hydrolyzed by human carboxylesterase 1 (HCE1; gene symbol CES1) and other esterases to an inactive acid metabolite (1,44). The remaining clopidogrel must undergo a multistep activation by multiple CYP enzymes, notably including CYP2C19, via the intermediacy of 2-oxo-clopidogrel, as shown in Figure 1.1 to the active 4b-*cis*-thiol metabolite, frequently called H4 (45-49). The second CYP-mediated step converts 2-oxo-clopidogrel to a highly reactive *S*-oxide which readily reacts with water to produce sulfenic acid intermediates that are subsequently reduced to thiols (50) (for simplicity, the proposed intermediate steps are not shown in Figure 1.1). The thiol "metabolite" of clopidogrel frequently referred to in literature actually exists as a mixture of four diastereomers, H1-H4, as well as a fifth "endo" thiol formed by PON1, but only H4 is responsible for clopidogrel's antiplatelet activity (50-52). H4 exerts its pharmacological effect by irreversibly inactivating the platelet membrane G-protein coupled purinergic receptor known as $P2Y_{12}$, which thereby decreases platelet activation by diminishing the ADP-dependent activation of the GpIIb-IIIa complex, the major receptor for fibrinogen on platelets (52).

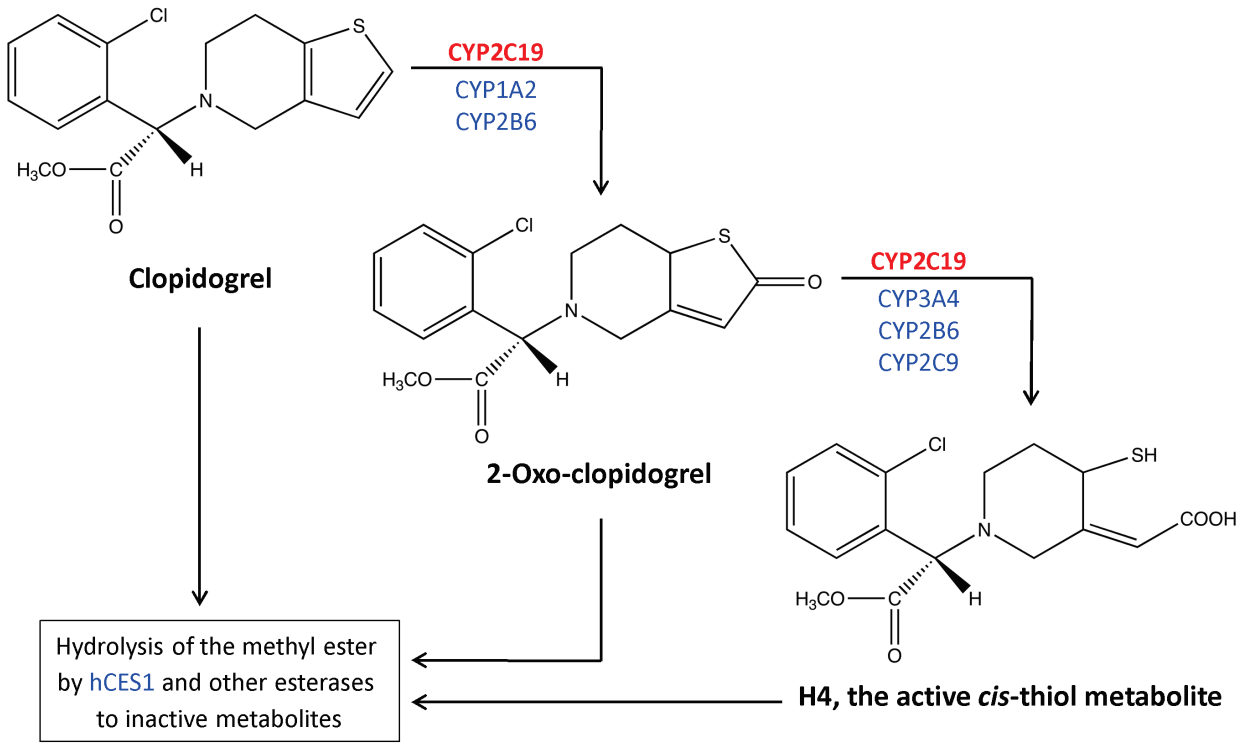

Figure 1.1. Activation of clopidogrel by CYP enzymes

The major CYP-dependent pathway is in red and other reactions are in blue. Note that the second CYP-mediated step has been proposed to involve the intermediacy of an *S*-oxide which readily reacts with water to produce sulfenic acid intermediates that are subsequently reduced to thiols, including H4 (50). For simplicity, the proposed intermediate steps are not shown.

The possibility of an interaction between proton pump inhibitors and clopidogrel is central to this dissertation because PPIs are coadministered with this anti-platelet drug in up to two-thirds of patients after discharge from the hospital for acute coronary syndromes (53). PPIs are a well-characterized class of drugs, first introduced with the 1989 approval of omeprazole, that irreversibly inactivate the gastric parietal cell H^+/K^+ ATPase (gene symbol ATP4A). All currently marketed PPIs are 2-pyridylmethylsulfinylbenzimidazole derivatives, with one imidazopyridine (i.e., tenatoprazole) in development (for a general structural scheme of PPIs, see Table 1.1). The gastric proton pumps couple ATP hydrolysis with the exchange of extracellular K^+ ions for cytoplasmic protons in the gastric parietal cell canaliculi in the final step of hydrochloric acid production. PPIs are neutral lipophilic prodrugs that become protonated to form a sulfenic acid in the acidic parietal cell canaliculi. The reactive sulfenic acid then hydrolyzes to the active cyclic sulfenamide form of the drug which covalently binds to cysteine residues of the gastric parietal cell H^+/K^+ ATPase as illustrated in Figure 1.2.

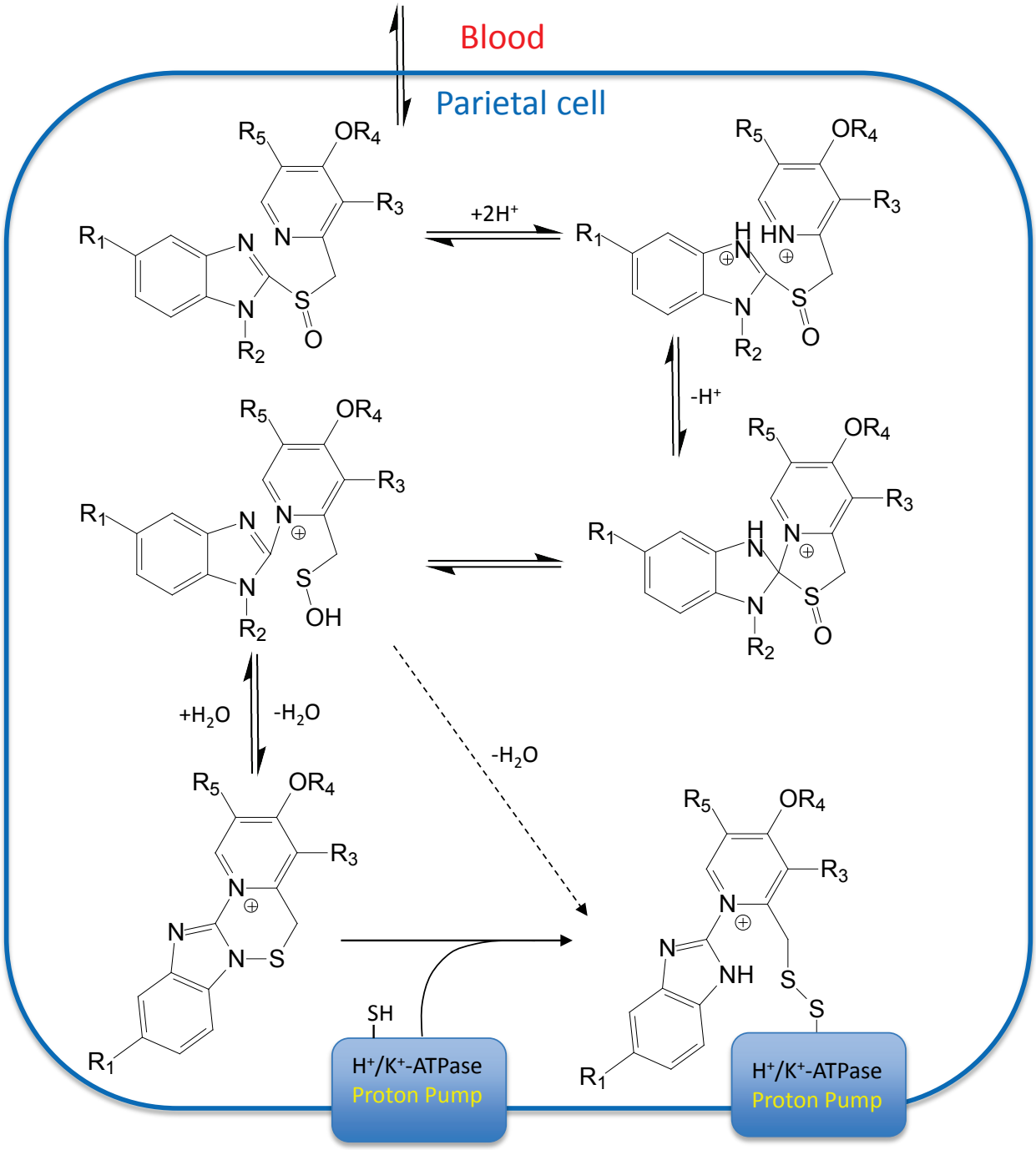

Figure 1.2. Acid catalyzed activation of proton pump inhibitors

The activation of PPIs in the acidic environment of the gastric parietal cell canaliculi is shown. *R*-groups are as defined in Table 1.1.

Because this inactivation is irreversible, PPIs provide up to 48 h of acid suppression in spite of their short pharmacokinetic half-lives (typically <2 h; see Table 1.2) (54). The major motivation for coadministration of PPIs and clopidogrel is to decrease the incidence of bleeding gastric ulcers because up to 12% of patients experience a bleeding ulcer within one year of starting clopidogrel, and PPI coadministration can decrease this risk of severe gastrointestinal bleeding (55). Although clopidogrel does not cause gastrointestinal ulcers or erosions on its own, it is obvious that its mechanism of action can promote bleeding at lesions that are caused by the typically-coadministered aspirin (i.e., dual antiplatelet therapy – DAPT) or other drugs that can injure the gastric mucosa (e.g., NSAIDs). H2 receptor antagonists (e.g., famotidine) have been found to confer only a modest benefit in preventing GI bleeding in clopidogrel-treated patients, whereas PPIs can reduce GI bleeding in this clinical setting by up to 50% (47). Because of these findings, the expert consensus report from the American College of Cardiology Foundation (ACCF), the American College of Gastroenterology (ACG), and the American Heart Association (AHA) recommend the coadministration of a PPI with thienopyridines in patients at high risk of gastrointestinal bleeding (47,56).

Table 1.1 General structural scheme of proton pump inhibitors

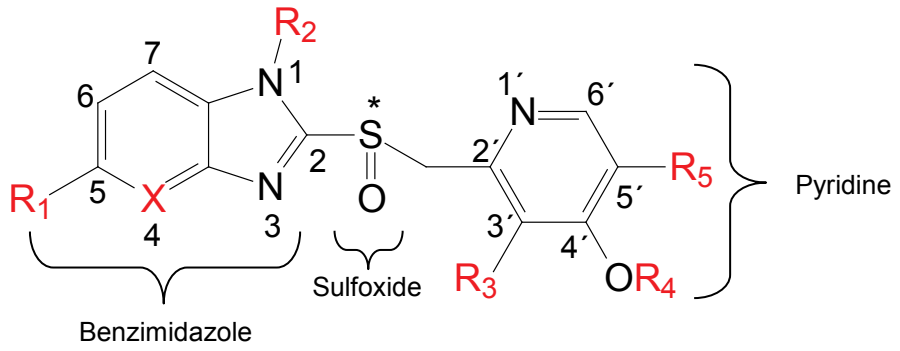

Compound	Substituents						Stereochemistry
	X	R_1	R_2	R_3	R_4	R_5	
Omeprazole	CH	OCH_3	H	CH_3	CH_3	CH_3	Racemate
Esomeprazole	CH	OCH_3	H	CH_3	CH_3	CH_3	*S*-Enantiomer of omeprazole
Lansoprazole	CH	H	H	CH_3	CH_2CF_3	H	Racemate
Dexlansoprazole	CH	H	H	CH_3	CH_2CF_3	H	*R*-Enantiomer of lansoprazole
Pantoprazole	CH	$OCHF_2$	H	OCH_3	CH_3	H	Racemate
Rabeprazole	CH	H	H	CH_3	$(CH_2)_3OCH_3$	H	Racemate
Ilaprazole [a]	CH	Pyrrole	H	CH_3	CH_3	H	Racemate
Tenatoprazole [b]	N	OCH_3	H	CH_3	CH_3	CH_3	Racemate
AGN201904 [c]	CH	OCH_3	§§	CH_3	CH_3	CH_3	Prodrug of racemic omeprazole

* Chiral center

Sources: (57-63)

[a] Ilaprazole is not currently FDA-approved.

[b] Tenatoprazole, unlike the other PPIs is not a benzimidazole derivative, and consists of an imidazopyridine ring connected to a pyridine ring by a sulfinylmethyl chain. It is not currently FDA-approved.

[c] AGN201904 is not currently FDA-approved.

§§ For AGN201904, R_2 is sulfonylphenoxyacetate ($-SO_2-Ø-OCH_2COOH$). Hydrolysis of this substituent releases omeprazole.

Table 1.2 Pharmacokinetics of selected PPIs

PPI	Molecular weight (g/mol)	Dose (mg)	AUC (μg·h/mL)	C_{max} (μg/mL)	C_{max} (μM)	T_{max} (h)	$t_{1/2}$ (h)	BA (%)
Omeprazole	345.4	20	0.2-2.0	0.08-8.0	0.23-23	1-3	0.6-1.5	40–65
Esomeprazole	345.4	40	7.3-13	3.5-5.1	10-15	1.6	1.1-1.6	>80
Lansoprazole	369.4	30	1.7-5.2	0.6-1.2	1.6-3.2	1.7	0.9-1.6	>80
Pantoprazole	383.4	40	2-16	1.1-3.3	2.9-8.6	2.5-4	0.9-1.9	77
Rabeprazole	359.4	20	0.8-2.2	0.41-0.98	1.1-2.7	3.1	1-1.1	52
Ilaprazole [a]	366.4	40	7.6	0.11	3.0	3.5	5.0	ND
Tenatoprazole [b]	346.4	40	75-100	5.3-7.0	15-20	2-4	5.6-9.3	ND

Sources: (59,61-63)

BA: Oral bioavailability

[a] Ilaprazole is not currently FDA-approved.

[b] Tenatoprazole is not currently FDA-approved.

ND: Not determined

Note: Dexlansoprazole is not included in this table because the clinically used form of this drug consists of a mixture of two types of enteric-coated granules with different pH-dependent dissolution profiles, such that its pharmacokinetics are not comparable with other PPI formulations.

Published clinical evidence for the importance of CYP2C19 in the activation of clopidogrel

As illustrated in Figure 1.1, CYP2C19 plays a prominent role in the conversion of clopidogrel to 2-oxo-clopidogrel and on to the active metabolite, H4. The role of CYP2C19 in one or both of these steps has been a matter of considerable debate in the scientific literature since the first paper on the topic was published nine years after the FDA approved clopidogrel (64). A search in PubMed for CYP2C19 and clopidogrel shows that over 600 papers cover these topics together to some extent. The interest in the activation of clopidogrel by this enzyme in particular stems largely from the fact that CYP2C19 is polymorphically expressed with 34 alleles named through 2013 (65). CYP2C19*1 homozygotes are considered the "wild-type", or extensive metabolizers (EMs). The CYP2C19*2 and *3 alleles generate a CYP2C19 enzyme with no activity and individuals who are homozygous or compound heterozygous for them account for the vast majority of CYP2C19 poor-metabolizers (PMs). The *4, *5, *6, *7 and *8 alleles also confer no, or decreased activity, but their frequency is low compared with *2 and *3 (65). The *17 allele confers increased CYP2C19 activity and is reportedly present in 10–27% of Europeans or Africans, with very low frequencies in Asians (i.e., <1%), and is considered by most authors to confer an ultra-rapid metabolizer phenotype (UMs) (65). Heterozygotes carrying a normal or increased activity allele and a loss-of-function allele are generally considered intermediate metabolizers (IMs), or occasionally "reduced metabolizers" (66). The frequency of the CYP2C19 PM phenotype varies markedly by ethnic group and is found in 13-23% of Japanese, Chinese, Korean, Vietnamese and Indian populations, 3–5% in black African and African Americans, 1-7% in Caucasians (dependent on location), ~26% of Australian aboriginals, ~14% in South Pacific Islanders, and with a very high incidence (79%) on the island of Vanuatu (1).

Between 2007 and 2014 at least 30 clinical studies have examined the effects of the most common CYP2C19 loss-of-function alleles on the pharmacodynamics and/or pharmacokinetics of clopidogrel (27,67). Several of these studies suggest that the presence of a CYP2C19 loss-of-function allele decreases the antiplatelet effect of clopidogrel, but there is considerable variability in the results, especially when pharmacodynamic endpoints alone are assessed (the vast majority of studies). However, the reported association between decreased efficacy of clopidogrel and either CYP2C19 loss-of-function alleles or its inhibition by PPIs (discussed in greater detail below) prompted the FDA to take the unusual step of requiring the manufacturers of Plavix® (Sanofi-Aventis and Bristol-Myers Squibb) to conduct post-marketing studies to investigate the role of CYP enzymes in the bioactivation of clopidogrel (which had not been performed prior to its original approval in 1997), as well as to assess the impact of CYP2C19 loss-of-function alleles and interactions with PPIs (51). The resulting clinical study sponsored by Sanofi-Aventis and Bristol-Myers Squibb in 40 healthy subjects (n=10 each from genetically determined CYP2C19 UMs, EMs, IMs and PMs) demonstrated that the mean exposure to H4 was 58–71% lower in PMs than in EMs (68). The sponsor also conducted a pooled analysis of $P2Y_{12}$ receptor, CYP1A2, CYP2B6, CYP2C9, CYP2C19, CYP3A5, CYP2D6, and P-gp polymorphisms in 396 healthy subjects and found that only CYP2C19 status had a significant impact on the antiplatelet effect of clopidogrel (68).

The clinical study required by the FDA and sponsored by Sanofi-Aventis and Bristol-Myers Squibb (68) would seem to have settled the question of the importance of CYP2C19 vs. CYP3A4 or other enzymes in the activation of clopidogrel. In a previous study, coadministration of the strong CYP3A4 inhibitor, ketoconazole, with clopidogrel decreased exposure to H4 by only 22% (69). In spite of these studies, there are several authors who maintain that CYP3A4, not CYP2C19, is the major CYP involved in the bioactivation of clopidogrel, and some further speculate that the “link of CYP2C19 genotype to platelet activity may be because an

endogenous substrate of CYP2C19, perhaps a polyunsaturated acid that yields a product that inhibits platelet aggregation" (70). The latter hypothesis could only explain the link between CYP2C19 polymorphisms and pharmacodynamic endpoints such as platelet aggregation, or time to first MACE, not the link to decreased exposure to H4. A later paper by one of these authors further states that clopidogrel "is primarily a CYP3A substrate. The TV commercials that tell one not to take clopidogrel with Nexium [esomeprazole] are not supported by the data" (71). It is notable that neither of the papers above cite the 2011 Simon paper sponsored by Sanofi-Aventis and Bristol-Myers Squibb (68). I very much disagree that the advice from the FDA to avoid clopidogrel coadministration with esomeprazole is "not supported by the data", especially given that there are alternative PPIs that do *not* cause clinically significant interactions with CYP2C19 substrates (covered in more detail below). I concede that as several authors have pointed out, many factors (e.g., diet, co-medications, compliance, exercise, genetic susceptibility to cardiovascular disease) undoubtedly come into play when considering the pharmacodynamic response or especially long-term outcomes with clopidogrel treatment across even a relatively large patient population. However, I propose that if it is accepted that clopidogrel exerts its pharmacological effect through formation of H4 and that CYP2C19 plays even some role in two separate steps involved in its formation, then it logically follows that a significant decrease in CYP2C19 activity and therefore H4 formation *in a particular patient* (whether that patient is a CYP2C19 PM due to genetic polymorphisms {up to a 71% decrease in H4 AUC (68)} or inactivation of the enzyme by omeprazole {up to a 48% decrease in H4 AUC (72)}) will decrease the benefit of clopidogrel in that *individual*. This sentiment is echoed by a quote from Leeder in the context of preemptive pharmacogenetic testing:

> For example, the proximal phenotype for CYP2C19 technically is the disappearance of the substrate (clopidogrel) and formation of the active platelet inhibiting metabolite; this genotype–phenotype association is several steps removed from the cardiovascular events to be reduced by preemptive genotyping. Is it necessary to demonstrate a robust association between CYP2C19 genotype and a reduction in intervention-related cardiovascular events

at a population level to establish sufficient clinical utility for widespread acceptance? (73)

In addition, although investigation of CYP3A4 inhibition by omeprazole or esomeprazole was not a specific aim of this dissertation, there are some data to suggest that omeprazole, esomeprazole or some of its metabolites may also act as clinically relevant inhibitors of CYP3A4, causing 25, 30 and 90% increases in exposure to the CYP3A4 substrates nifedipine, cisapride and carbamazepine (74-78). Both CYP2C19 and CYP3A4 were found to be involved in the *second* CYP-dependent step in the activation of clopidogrel with a Simcyp-predicted 21.1% and 33.5% contribution to the total CYP-dependent pathway, respectively (Figure 1.1) (44). Therefore, the *combined* impact of inhibition of two enzymes involved in H4 formation by omeprazole or esomeprazole *and* its metabolites, would be expected to have a super-proportional impact on the decrease in H4 exposure, similarly to the observed impact of grapefruit juice (which affects both CYP2C19 and CYP3A4 in the small intestine and causes an unexpectedly large 80% decrease in H4 exposure, discussed below), but in contrast to inhibition of CYP3A4 alone by ketoconazole (i.e., only a 22% decrease in H4 exposure) (17,44,69,79). These findings bolster the argument that coadministration of omeprazole or esomeprazole with clopidogrel would be expected to decrease H4 exposure by inhibition of CYP2C19 in the conversion of clopidogrel to 2-oxo-clopidogrel, and inhibition of both CYP2C19 and CYP3A4 by their metabolites in the conversion of 2-oxo-clopidogrel to H4.

Still other authors implicated polymorphisms in paraoxonase 1 (PON1) as the major factor accounting for the variable clinical response to clopidogrel (80). This finding was essentially discredited by other authors (52,81,82), largely due to the apparent inability of the analytical method used by Bouman and colleagues to separate the endo metabolite from H1-H4 (see further detail below). It is possible that the PON1 polymorphisms described by Bouman et. al., can affect levels of the “inactive” metabolites which may have as yet poorly understood actions on platelet aggregation.

Adding to the apparent confusion regarding the role of CYP2C19 in the activation of clopidogrel is the fact that nine systematic reviews or meta-analyses were published from 2010 to 2015 that reported differing conclusions on the association of CYP2C19 loss-of-function alleles and the risk of adverse cardiovascular events in patients treated with clopidogrel (reviewed by Sorich and colleagues (67)). Each review evaluated between 7 and 26 primary studies (out of >30 primary clinical studies) representing between 8,043 to 26,251 patients. These reviews reported that carriage of reduced function CYP2C19 alleles conferred a relative risk for adverse cardiovascular events of 1.11 to 1.96 (67), with the lower value not reaching statistical significance. Sorich and colleagues discussed the possible reasons for the differences in conclusions, including differences in event definitions, genotype grouping, and meta-analytic methods (67). To this list, I would add that *none* of the reviewed studies attempted to correlate exposure to H4 with CYP2C19 phenotype, which would have been informative, at least for the studies that correctly grouped CYP2C19 phenotypes. The main reason for the lack of H4 quantification was presumably the fact that an analytical method to quantify only H4, separately from the other inactive thiols, requires chiral chromatography along with a thorough understanding of the tandem mass spectral transitions of H1-H4 vs. the endo metabolite. An analytical method that fully accounted for these aspects was not developed and fully validated until 2011, sponsored by Sanofi-Aventis and Bristol-Myers Squibb (83) in support of the clinical pharmacogenomic and PPI drug-drug interaction trials (68,84). Studies that claim to have quantified H4 (e.g., (80)) without the use of a properly validated analytical method may have actually quantified either a mixture of diastereomers, or possibly only the inactive “endo” thiol isomer, which was later shown to be formed by PON1 (52,85). Quantification of the endo thiol metabolite would lead to erroneous conclusions regarding the effects of polymorphisms in PON1 vs. CYP2C19. Even if a validated chromatographic method succeeds in separating the diastereomers, one must also be familiar with the individual mass transitions in the MS/MS method because the 356→212 *m*/*z* transition is diagnostic of the “endo” thiol while the active *cis*

thiol (i.e., H4) eliminates H_2S. The 356→322 *m*/*z* transition detects two *trans* and two *cis* thiol isomers (H1-H4) that also must be separated chromatographically (Dansette, personal communication and (52,85). Indeed, in response to Dansette (86), Bouman and colleagues later acknowledged "we did not discriminate between the different putative thiol stereoisomers in our LC-MS-MS assay; instead we supposed a constant ratio of the formation of active and inactive thiol metabolites" (87).

Nine clinical studies published from 2011 to 2014 have examined the pharmacokinetics of the clopidogrel active metabolite with regard to CYP2C19 (or other clopidogrel poor responder-associated genes) with validated analytical methods that appear to adequately separate H4 from the other inactive thiols (68,82,85,88-93). Of these studies, only the study sponsored by Sanofi-Aventis and Bristol-Myers Squibb (68) was conducted as a randomized, double-blind placebo controlled study. The results of this study are described in the prescribing information for clopidogrel (25), which states in a black box to "consider alternative treatment or treatment strategies in patients identified as CYP2C19 poor metabolizers". In spite of possible limitations of the other eight studies, *all* concluded that CYP2C19 poor-metabolizers (e.g., *2/*2, *3/*3 homozygotes, or *2/*3 compound heterozygotes, etc.) had significantly less exposure to H4 than did extensive metabolizers. Five of these studies also examined one or more intermediate metabolizer genotypes, and three (88,91,93) showed that CYP2C19 intermediate metabolizers also had significantly less H4 exposure than did extensive metabolizers. Importantly, of the studies listed above that examined individuals with decreased function variants of other clopidogrel poor responder-associated genes including PON1, ABCB1 (i.e., P-gp), and CYP2B6, none reported a significantly decreased H4 exposure relative to their "wild-type" counterparts (82,85,91). Finally, additional analyses of the Simon et al. and Angiolillo et al. clinical studies (i.e., (68,84), sponsored by Sanofi-Aventis and BMS in collaboration with Simcyp to model the two sequential steps in clopidogrel activation, provided estimates of the

overall $f_{m(CYP2C19)}$ for H4 formation of 0.64 (range 0.58 to 0.72, depending on population and simulation parameters) (94). Although the foregoing publications do not conclude that CYP2C19 polymorphisms account for 100% of the variability in clinical response to clopidogrel, and furthermore cannot exclude the importance of other, as yet unknown, genetic polymorphisms or other factors in the variable response to clopidogrel, they do underscore the importance of CYP2C19 in the bioactivation of, and therefore clinical response to clopidogrel.

Clinical studies implicating CYP2C19 inhibition as a cause for decreased clopidogrel efficacy

All currently FDA-approved PPIs (i.e., omeprazole, esomeprazole, lansoprazole, dexlansoprazole, pantoprazole and rabeprazole) are metabolized in part by CYP2C19 (e.g., lansoprazole $f_{mCYP2C19}$ = 0.82 and 0.87 for omeprazole (17)), and might be expected to inhibit this enzyme to some extent (27). A search strategy in PubMed for any PPI and clopidogrel reveals that over 550 papers that cover these terms together have been published between 2002 and 2014. A search strategy limited to only omeprazole or esomeprazole and clopidogrel shows that nearly 200 of these papers cover these two PPIs with clopidogrel to some extent.

In contrast to the >30 clinical studies examining the effect of loss-of-function alleles of CYP2C19 or other genes, 19 clinical drug-drug interactions studies conducted with clopidogrel as the victim drug have been published between 2004 and 2014, including two in new drug application (NDA) review documents for prasugrel and apixaban from 2009 and 2012, respectively; (27)). The majority of these studies examined the effects of one or more drugs (including aspirin, apixaban, atorvastatin, dabigatran, fluoxetine, ketoconazole, morphine, ranitidine, or rosuvastatin) or “life-style” environmental factors (including grapefruit juice intake, cigarette smoking or St. John’s wort intake) (69,79,82,95-103). No interaction was reported for

aspirin, dabigatran or ranitidine, but at least a 20% induction or 20% inhibitory effect on either the pharmacokinetics of clopidogrel or its active metabolite, or on the pharmacodynamics of clopidogrel, was reported in at least one study for morphine, grapefruit juice, fluoxetine, rosuvastatin, St. John's wort, atorvastatin, apixaban, ketoconazole and cigarette smoking. A variety of mechanisms including delayed gastric emptying (i.e., morphine), transporter interactions (e.g., P-gp), induction or inhibition of minor enzymes involved in formation of H4 such as CYP1A2 and 3A4 were implicated in these interactions, but with the exception of grapefruit juice (~80% decrease in active metabolite formation attributed to inhibition of *both* intestinal CYP2C19 and 3A4 (79)), most of the effects were relatively small (<30% change in active metabolite formation). Some of these studies provided contradictory results depending on the study design or end-points (e.g., atorvastatin and ketoconazole).

Seven clinical DDI studies examined the effects of one or more PPIs on clopidogrel (i.e., omeprazole, esomeprazole, lansoprazole, dexlansoprazole, pantoprazole or rabeprazole – six with omeprazole and/or esomeprazole), six of which report the pharmacokinetics of the active metabolite of clopidogrel as well as the effects on clopidogrel pharmacodynamics (i.e., (72,104-108) whereas the remaining study examined only the effects of PPIs on the pharmacodynamics of clopidogrel (66). Of the studies reporting plasma concentrations of the active metabolite of clopidogrel, all concluded that coadministration of omeprazole and/or esomeprazole with clopidogrel caused a significantly decreased exposure to H4 (up to 50 % decrease in AUC or 45% decrease in C_{max}). Of particular importance is that the study by Angiolillo found that separation of omeprazole and clopidogrel dosing by 12 hours did not mitigate the effects of omeprazole, which is consistent with irreversible inhibition of CYP2C19 given the short half-lives of omeprazole and its metabolites (<2 h) (84). All but one study (104), demonstrated a significantly decreased pharmacodynamic effect of clopidogrel (e.g., ex vivo ADP-induced maximum platelet aggregation) upon coadministration of omeprazole and/or esomeprazole.

With one exception, studies that examined lansoprazole, dexlansoprazole or pantoprazole concluded that there was no significant effect on the pharmacokinetics of H4 or on the pharmacodynamics of clopidogrel (84,106,107). Only Andersson and colleagues found that high-dose lansoprazole (60 mg q.d.) significantly decreased H4 formation by 30% (108). Finally, of the two clinical studies that examined the effects of rabeprazole on clopidogrel, the one that reported pharmacokinetic and pharmacodynamic data concluded there was no interaction (104), whereas Furuta and colleagues concluded that rabeprazole caused a significant decrease in clopidogrel pharmacodynamic action, but only in CYP2C19 "reduced metabolizers" (i.e., carriers of one or more reduced function CYP2C19 alleles, so IMs or PMs) (66).

From the foregoing, it can also be concluded that the interaction between omeprazole or esomeprazole and clopidogrel is not caused by decreased absorption due to decreased gastric acid because there should be a class-effect if true, and ranitidine would also be expected to cause an interaction with clopidogrel, which it does not (103). In addition, the FDA and EMA have issued various warnings against coadministration of omeprazole or esomeprazole at various times, with the FDA in 2010 noting specifically:

> With regard to the proton pump inhibitor (PPI) drug class, this recommendation applies only to omeprazole and not to all PPIs. Not all PPIs have the same inhibitory effect on the enzyme (CYP 2C19) that is crucial for conversion of Plavix into its active form. Pantoprazole (Protonix) may be an alternative PPI for consideration. It is a weak inhibitor of CYP2C19 and has less effect on the pharmacological activity of Plavix than omeprazole. (109)

In addition, the FDA- approved prescribing information for clopidogrel updated in December, 2013 states:

> Avoid concomitant use of Plavix with omeprazole or esomeprazole. In clinical studies, omeprazole was shown to reduce the antiplatelet activity of Plavix when given concomitantly or 12 hours apart. A higher dose regimen of clopidogrel concomitantly administered with omeprazole increases antiplatelet

> response; an appropriate dose regimen has not been established. A similar reduction in antiplatelet activity was observed with esomeprazole when given concomitantly with Plavix. Consider using another acid-reducing agent with minimal or no CYP2C19 inhibitory effect on the formation of clopidogrel active metabolite. Dexlansoprazole, lansoprazole and pantoprazole had less effect on the antiplatelet activity of Plavix than did omeprazole or esomeprazole. (25)

The latter point made by the FDA, namely that dexlansoprazole, lansoprazole and pantoprazole had less of an impact on clopidogrel than did omeprazole or esomeprazole, is particularly interesting in light of the in vitro data regarding inhibition of CYP2C19 by PPIs, which will be covered in the next section. In spite of the warnings and label changes by the FDA, data collected from a retail database of >200,000 patients receiving both clopidogrel and a PPI between January 1 and March 31, 2012, showed that approximately 60% were taking an omeprazole- or esomeprazole-containing product (110).

1.6. In vitro and clinical studies demonstrating CYP2C19 inhibition by PPIs

A total of 103 studies examining one or more PPIs as in vitro inhibitors of drug-metabolizing enzymes were published between 1986 and 2014 (27). Of these, 93 studies examined omeprazole or esomeprazole as in vitro inhibitors of drug-metabolizing enzymes. Through 2014, approximately 60 IC_{50} or *K*i values for the direct inhibition of CYP2C19 by a PPI were published. Only lansoprazole and omeprazole (and their *S*-enantiomers) directly inhibited CYP2C19 with IC_{50} or *K*i values <1 μM, whereas the lowest reported IC_{50} or *K*i values for rabeprazole and pantoprazole were 9.2 and 17 μM, respectively (27). Both lansoprazole and omeprazole have similar half-lives, plasma protein binding and C_{max} values and would be predicted to cause clinically relevant direct inhibition of CYP2C19 (see Table 1.2 for a summary of PPI pharmacokinetics) (111). However, neither lansoprazole nor PPIs other than omeprazole and esomeprazole have been reported to cause clinically relevant interactions with any

CYP2C19 substrate (27). In contrast, omeprazole does cause clinically significant inhibitory interactions with the CYP2C19 substrates, including moclobemide, escitalopram, proguanil, etravirine and voriconazole (27). This apparent discrepancy would be explained if omeprazole and/or esomeprazole, but not lansoprazole or the other PPIs, were a metabolism-dependent inhibitor of CYP2C19.

Clinical evidence for metabolism-dependent inhibition of CYP2C19 by omeprazole is in fact present in literature (with the benefit of hindsight). For instance, in CYP2C19 extensive metabolizers (but not in poor metabolizers), the AUC of moclobemide ($f_{mCYP2C19} \approx 0.72$ calculated from a comparison of AUC values in PMs and EMs (17)) increased by ~31% after a single 40-mg dose of omeprazole, but increased by 121% after 8 days of dosing with 40 mg omeprazole (112). Such an apparent increase in the exposure of a victim drug with repeated dosing of the perpetrator drug can be indicative of metabolism-dependent inhibition. In addition, in vivo evidence for metabolism-dependent inhibition of CYP2C19 comes from the pharmacokinetic data for omeprazole itself (and its individual enantiomers), as summarized by Andersson and Weidolf (113). In the studies presented, 15 mg of either omeprazole (i.e., the racemate), esomeprazole or *R*-omeprazole, were administered orally for seven days. Exposure to esomeprazole (AUC) increased by 113% over 7 days, whereas exposure to omeprazole increased by only 52%, and exposure to *R*-omeprazole actually decreased by 9%. Such time-dependent changes in pharmacokinetics were initially attributed (in part) to decreased degradation of omeprazole in the stomach after multiple days of dosing because the gastric pH was increased by treatment, and omeprazole is acid labile (114). However, if this hypothesis were to completely explain the observations, time-dependent changes would be observed for both omeprazole enantiomers, and likely for all PPIs. Andersson et al., later concluded that "decreased hepatic metabolism of omeprazole might be responsible for the initial increase in AUC during repeated dosing" (115). Indeed, neither lansoprazole, pantoprazole, nor

rabeprazole pharmacokinetics are altered by multiple dosing (116-118). In contrast, the prescribing information for Nexium (esomeprazole) states “at repeated once-daily dosing with 40 mg, the systemic bioavailability is approximately 90% compared to 64% after a single dose of 40 mg. The mean exposure (AUC) to esomeprazole increases from 4.32 μmol*hr/L on Day 1 to 11.2 μmol*hr/L on Day 5 after 40 mg once daily dosing” (119). Because esomeprazole is metabolized mainly by CYP2C19 ($f_{mCYP2C19}$ ~ 0.87 – calculated from a comparison of AUC values in PMs and EMs (17)), this 2.6-fold increase in exposure with multiple dosing is strongly suggestive of metabolism-dependent autoinhibition, given the short half-life of esomeprazole (1 – 1.6 h).

Given omeprazole’s in vitro and clinical inhibitory effects on CYP2C19 in contrast to other PPIs, I set out to re-examine omeprazole and esomeprazole as metabolism-dependent inhibitors of CYP2C19. It was particularly noteworthy that none of the approximately 40 in vitro studies published prior to 2011 identified any PPI as a metabolism-dependent inhibitor of CYP2C19 (34) (See Chapter 4). After I identified omeprazole as an irreversible metabolism-dependent inhibitor of CYP2C19 in vitro (Chapters 4-5 and (34,111,120), 25 additional studies reported one or more PPIs as in vitro inhibitors of one or more drug-metabolizing enzymes, with eight studies examining inhibition of CYP2C19 by omeprazole, esomeprazole or its metabolites as inhibitors of CYP2C19 (27). Only four of these later studies specifically examined metabolism-dependent inhibition of CYP2C19 by omeprazole or esomeprazole or their metabolites (excluding my preliminary publications which will be covered in Chapters 5–6: (75,78,94,111,120,121).

Chapter 2. STATEMENT OF PURPOSE

2.1. Objectives and significance of the study

In 1991, the US Food & Drug Administration (FDA) approved ticlopidine as the first thienopyridine platelet aggregation inhibitor (or $P2Y_{12}$ inhibitor) indicated for secondary prevention of thrombotic strokes or primary prevention in patients at high risk of stroke. Because of its high risk for life-threatening blood dyscrasias such as agranulocytosis, aplastic anemia and thrombocytopenic purpura, this drug was reserved for use in high-risk patients who were intolerant of aspirin or had already failed aspirin or other anti-platelet therapy (e.g., cilostazol or dipyridamole). Clopidogrel was approved in the US in 1997 as the second thienopyridine platelet aggregation inhibitor and was initially indicated for reduction of atherosclerotic events including stroke and myocardial infarction in patients with atherosclerosis and a recent myocardial infarction (MI) or stroke, or in those with established peripheral artery disease. Clopidogrel therapy demonstrated much lower risk for the blood dyscrasias associated with ticlopidine therapy and it quickly supplanted ticlopidine as the primary therapeutic option for reducing atherothrombotic events. Due to the continued safety record of clopidogrel and completion of additional clinical trials, its use was expanded in 2002 to include FDA-approved indications for non-ST-segment acute coronary syndrome (e.g., unstable angina or non-Q-wave MI) and patients undergoing percutaneous coronary intervention or PCI (with or without stent placement). An indication for secondary prevention after ST-elevation MI was also added to US labeling in 2006. The FDA approved several generic formulations of clopidogrel in 2012. In spite of the FDA approval of new $P2Y_{12}$ inhibitors including prasugrel in 2009 and ticagrelor in 2011, clopidogrel remains the preferred treatment option for most indications, especially with regard to cost because it is now available in several generic formulations. A 2015 review of $P2Y_{12}$ inhibitors showed that the only cases when ticagrelor or prasugrel should be preferred over clopidogrel are in patients with carriage of known loss-of-function variants of CYP2C19 or in patients being treated concomitantly with proton pump inhibitors (PPIs) (see Chapter 1 for a

review of this topic) (122). As mentioned in Chapter 1, PPIs are coadministered with clopidogrel in up to two-thirds of patients after discharge from the hospital for acute coronary syndromes to decrease the incidence and severity of gastrointestinal bleeding.

In spite of the large number of publications discussing the interaction between PPIs and clopidogrel (reviewed in Chapter 1), the basis for the clinically relevant interaction between clopidogrel and omeprazole or esomeprazole but not other PPIs (in which the efficacy of clopidogrel is significantly reduced due to decreased formation of its active metabolite), has not yet been elucidated. A determination of the basis for this interaction would allow for clinically actionable recommendations to be made by regulatory agencies and professional medical societies (e.g., The American College of Cardiology, The American College of Gastroenterology) regarding the co-administration of clopidogrel with currently used and potentially future PPIs.

2.2. Specific aims

Specific Aim 1 tests the hypothesis that the major proton pump inhibitors in clinical use differ in their ability to inhibit CYP2C19 in a metabolism-dependent manner. This hypothesis was tested in *in vitro* systems including pooled human liver microsomes, cryopreserved hepatocytes and recombinant human CYP2C19, as well as in a physiological-based pharmacokinetic model to assess the clinical significance of the *in vitro* findings with omeprazole. The results of this specific aim are presented in Chapter 4.

Specific Aim 2 tests the hypothesis that the metabolism-dependent inhibition of CYP2C19 by omeprazole is enantioselective and also occurs due to formation of one or more of its major metabolites. This hypothesis was tested *in vitro* in pooled human liver microsomes. The results of this specific aim are presented in Chapters 4-5.

Specific Aim 3 tests the hypothesis that the metabolism-dependent inhibition of CYP2C19 by esomeprazole and its two inhibitory metabolites, omeprazole sulfone and 5-*O*-desmethyl omeprazole, is mechanism-based according to the following criteria: 1) inactivation of CYP2C19 occurs in a concentration-, time- and metabolism-dependent manner, 2) the efficiency of inactivation is not diminished by glutathione, superoxide dismutase nor catalase (exogenous scavengers), 3) the inactivation is irreversible (by ultracentrifugation and washing), 4) the inactivation is saturable with respect to inactivator concentration, 5) an alternate CYP2C19 substrate can protect the enzyme against inactivation, and 6) inactivation requires a catalytic event. The criteria for this hypothesis were tested *in vitro* in pooled human liver microsomes in multiple studies and the results presented in Chapters 4-6.

Specific aim 3A tests the hypothesis that the presence of a 5´-methyl substituent is necessary for metabolism-dependent inhibition of CYP2C19 by PPIs. This hypothesis was tested in pooled human liver microsomes with two clinically used PPIs (i.e., ilaprazole and rabeprazole) that lack a 5´-methyl substituent and one investigational PPI, tenatoprazole which, like omeprazole and esomeprazole, does have a 5´-methyl substituent. It was predicted that of the three, only tenatoprazole would cause metabolism-dependent inhibition of CYP2C19.

Studies proposed in *specific Aim 4* were designed to test the hypothesis that the inactivation of CYP2C19 by esomeprazole is the result of the formation of a reactive metabolite that binds covalently to the enzyme's heme prosthetic group. The rationale for these studies was based, in part, on the demonstration that the mechanism of CYP2C19 inactivation by esomeprazole could not be ascribed to formation of a metabolite-inhibitory complex (MIC) (presented in Chapter 6). Towards this end, HLM were incubated with esomeprazole or known heme-alkylating agents (1-aminobenzotriazole and gemfibrozil glucuronide) and formation of heme adducts analyzed by ultra-high performance liquid chromatography (UHPLC) with UV/VIS detection and high

resolution mass spectrometry (HRMS) (UHPLC-UV/HRMS) followed by post-acquisition mass-defect filtering. The results of this specific aim are presented in Chapter 7.

2.3. Innovation

The research proposed in this dissertation is innovative, because it examined and successfully identified the basis for the unexpected clinical interaction between the anti-platelet drug clopidogrel and some but not all proton pump inhibitors, which have long been recommended as a comedication to reduce the severity of upper gastrointestinal bleeding caused by clopidogrel. The novel finding stemming from my dissertation research is that omeprazole and esomeprazole, but not pantoprazole or lansoprazole, are irreversible inhibitors of CYP2C19, the major enzyme responsible for converting clopidogrel to its pharmacologically active metabolite. This discovery provides a mechanistic rationale for the FDA and EMA's decision to recommend against the coadministration of clopidogrel with omeprazole or esomeprazole but not other PPIs.

Chapter 3. EXPERIMENTAL MATERIALS AND METHODS

MATERIALS AND METHODS

Materials

1-Aminobenzotriazole, catalase, fexofenadine, glutathione, 4′-hydroxymephenytoin, omeprazole, superoxide dismutase and Trizma® base (for Tris buffer) were purchased from Sigma-Aldrich (St. Louis, MO). Esomeprazole, d_3-4′-hydroxymephenytoin, 5′-hydroxyomeprazole, 5-*O*-desmethylomeprazole, *S*-mephenytoin, lansoprazole, omeprazole sulfide and pantoprazole were purchased from Toronto Research Chemicals (North York, ON, Canada). *R*-Omeprazole and omeprazole sulfone were purchased from SynFine Research (Richmond Hill, ON, Canada) or Toronto Research Chemicals (North York, ON, Canada). Ilaprazole was purchased from Clearsynth Labs (Mumbai, India). Tenatoprazole was purchased from Santa Cruz Biotechnology, Inc. (Dallas, TX). Human liver microsomes (pooled from 16 donors) and human hepatocytes were prepared from non-transplantable livers and characterized as described previously (35,123), and recombinant CYP2C19 (Bactosomes) was obtained from Cypex (Dundee, Scotland). All other reagents were obtained from commercial sources, as detailed elsewhere (33-35,37,38).

CYP2C19 Inhibition: IC_{50} determinations

CYP2C19 activity in human liver microsomes (HLM) was determined according to previously published procedures (33-35,38,124). Briefly, incubations were conducted in 200-µL incubation mixtures (pH 7.4) containing high purity water, potassium phosphate buffer (50 mM), $MgCl_2$ (3 mM), EDTA (1 mM), NADP (1 mM), glucose-6-phosphate (5 mM), glucose-6-phosphate dehydrogenase (1 Unit/mL), *S*-mephenytoin (approximately equal to K_m, i.e., 40 µM, final) and HLM (0.1 mg protein/mL, except where otherwise noted). All incubations were conducted in duplicate at 37°C for 5 min (except where otherwise noted) and were terminated

by the addition of 200 µL acetonitrile containing an internal standard (d_3-4′-hydroxymephenytoin). Aliquots of the stock and/or working solutions of the inhibitors (i.e., omeprazole, esomeprazole, *R*-omeprazole, lansoprazole, pantoprazole, 5′-hydroxyomeprazole, omeprazole sulfide, omeprazole sulfone, 5-*O*-desmethylomeprazole, rabeprazole, ilaprazole or tenatoprazole; final concentrations ranging from 0.1 to 100 µM (or 70 µM for 5-*O*-desmethylomeprazole) in solvent were added to buffer mixtures containing the components described above, but prior to addition of the NADPH-generating system. For experiments in which stock solutions of inhibitors were not kept, the solvent was methanol (for a final incubation concentration of 1% v/v) or a mixture of methanol/DMSO/Tris buffer (at pH 9.0) at 70/20/10% v/v/v (0.7/0.2/0.1% v/v/v final incubation concentrations) for 5-*O*-desmethylomeprazole. For experiments in which stock solutions were to be saved for use in additional experiments (e.g., to decrease the amount of expensive PPIs or metabolites used), the solvent was a mixture of methanol and Tris buffer (pH 9.0 for greater stability) at 0.4/0.6% v/v final incubation concentration. To evaluate the potential for MDI, the inhibitors (at the same concentrations used to evaluate direct inhibition) were pre-incubated in HLM (0.1 mg/mL final) at 37°C with and without NADPH for approximately 30 min (or 60 min for ilaprazole and tenatoprazole). After the pre-incubation, *S*-mephenytoin (40 µM, final) was added, and the incubation was continued for 5 min to measure residual CYP activity. Precipitated protein was pelleted by centrifugation (920×*g* for 10 min at 10°C). Calibration and quality control (QC) standards (4′-hydroxymephenytoin) were prepared in zero-time incubations. IC_{50} determinations with recombinant human CYP2C19 (15 pmol/mL) were conducted in the same manner except that the incubation time was only 2 min to prevent over-metabolism of omeprazole. Metabolite formation (4′-hydroxymephenytoin) was analyzed by LC-MS/MS as described previously (33-35,37,38).

Incubations with cryopreserved human hepatocytes (pooled, n=3, 10^6 cells/mL) were conducted in 200-μL incubation mixtures at approximately 37°C in Krebs Henseleit Buffer (KHB), in triplicate. In all cases, the solvent or omeprazole was allowed to equilibrate for 10 min with hepatocytes prior to incubations. For samples with no pre-incubation with inhibitor, reactions were started by the addition of hepatocytes to pre-warmed KHB containing inhibitor and *S*-mephenytoin (40 μM, final concentration). For reactions with a pre-incubation, hepatocytes and inhibitor were incubated at 37°C for 30 minutes and reactions were started by addition of *S*-mephenytoin (40 μM, final). In all cases, marker substrate reactions were conducted for 60 min and terminated by the addition of an equal volume of acetonitrile and internal standard (d_3-4′-hydroxymephenytoin). Metabolite formation (4′-hydroxymephenytoin) was analyzed by LC-MS/MS as described previously (33-35,37,38).

Metabolic stability of omeprazole

The metabolic stability of omeprazole (10 μM), was determined at three concentrations of HLM (0.1, 1.0, and 2.5 mg/mL) under conditions similar to those described above for CYP2C19 inhibition experiments. Omeprazole was incubated for zero, 5, 10, 20, 30, 45, and 60 min, in triplicate. Reactions were terminated by the addition of an equal volume of acetonitrile and internal standard (pantoprazole). Precipitated protein was removed by centrifugation (920×*g* for 10 min at 10°C). Omeprazole disappearance was monitored by LC-MS/MS as described below. Calibration standards were prepared in zero-time incubations.

Microsomal binding of omeprazole

The binding of omeprazole to microsomal protein was determined by ultrafiltration with Millipore Amicon Centriplus centrifugal filter devices (15 mL, 30 kDa membrane) obtained from Fisher Scientific (Pittsburgh, PA). Omeprazole (2 and 10 μM), was incubated with pooled HLM

(zero, 0.1, 1.0, or 2.5 mg/mL), as described above, but in the absence of an NADPH-generating system at 37°C for 10 min. Aliquots (1.1 mL) were then removed and added to the ultrafiltration devices, and centrifuged at 1900×*g* in a Sorvall RC 5C centrifuge with a Sorvall SS-34 rotor at room temperature for 5 min. Aliquots of the ultrafiltrate (100 µL) were transferred to glass tubes and an equal volume of acetonitrile added and vortexed. Precipitated protein was removed by centrifugation (920 × *g* for 10 min at 10°C). Following centrifugation, an aliquot (100 µL) was transferred to an equal volume of acetonitrile (with pantoprazole as the internal standard) and analyzed for omeprazole concentration by LC-MS/MS.

K_I and k_{inact} determinations

To determine the K_I and k_{inact} values for the inactivation of CYP2C19, various concentrations of omeprazole (1 to 60 µM), esomeprazole (0.3 to 60), omeprazole sulfone (0.6-100 µM) or 5-*O*-desmethylomeprazole (0.6 – 70 µM) were pre-incubated at 37ºC for various times (i.e., 2.5 to 15 min for omeprazole; 3 – 30 min for esomeprazole, 3 – 30 min for omeprazole sulfone; and 3 – 30 min for 5-*O*-desmethylomeprazole) with pooled HLM (i.e., 0.1 and 2.5 mg/mL for omeprazole; 0.1, 0.5 and 1 mg/mL for esomeprazole and omeprazole sulfone and 0.5 mg/mL for 5-*O*-desmethylomeprazole). For the omeprazole experiments conducted at 0.1 mg/mL HLM (Chapter 4), after the pre-incubations, *S*-mephenytoin (40 or 400 µM final concentration [1× and 10×K_m]) was added and residual CYP2C19 activity determined as described above (i.e., no dilution). For experiments conducted at 2.5 mg/mL, after the pre-incubation, an aliquot (8 µL) was transferred to another incubation tube (final volume 200 µL) containing *S*-mephenytoin (400 µM [10×K_m]) and an NADPH-generating system in order to measure residual CYP2C19 activity as described above. The latter procedure diluted the microsomes to 0.1 mg/mL and diluted omeprazole to 1/25th its original concentration. For other K_I and k_{inact} determinations (i.e., esomeprazole, omeprazole sulfone and 5-*O*-desmethylomeprazole presented in Chapters 5-6) a 10-fold dilution was always utilized,

with a saturating concentration of *S*-mephenytoin (400 μM). Additional K_I and k_{inact} determinations for esomeprazole, omeprazole sulfone and 5-*O*-desmethylomeprazole presented in Chapters 6 were similarly carried out with the addition of glutathione (2 mM in pre-incubation), superoxide dismutase (500 U/mL in pre-incubation), catalase (1000 U/mL in pre-incubation) or pantoprazole (200 μM in pre-incubation). Reactions were carried out in triplicate.

CYP2C19 activity in cultured human hepatocytes

Cultured human hepatocytes were prepared, treated, and microsomes (0.02 mg/mL) isolated as described previously (38). Briefly, cultured human hepatocytes were treated for 72 h with 0.1% (v/v) DMSO (solvent control) or 100 μM omeprazole. Isolated microsomes were washed and incubated for 30 min with marker substrate (40 μM *S*-mephenytoin) to determine CYP2C19 activity as described above.

Assessment of MDI reversibility by ultracentrifugation

Omeprazole (100 μM), *R*-omeprazole (100 μM), esomeprazole (100 μM), omeprazole sulfone (100 μM) or 5-*O*-desmethyl omeprazole (70 μM) were incubated in triplicate with NADPH-fortified pooled HLM (0.1 mg/mL) at 37°C for 30 min in potassium phosphate buffer (50 mM, pH 7.4), $MgCl_2$ (3 mM), EDTA (1 mM, pH 7.4) and chemically reduced NADPH (1 mM), as described previously (34,35,111). Incubations (n=3) with solvent alone (1% methanol v/v, final) served as controls. Following the 30-min incubation, HLMs were (**1**) assayed directly for residual CYP2C19 activity, (**2**) re-isolated by ultracentrifugation and then assayed for residual CYP2C19 activity, or (**3**) treated with potassium ferricyanide, re-isolated by ultracentrifugation and then assayed for residual CYP2C19 activity. For samples in groups (2) and (3), microsomal protein was re-isolated by ultracentrifugation (100,000 × *g* for 30 min at 4ºC in a Beckman ultracentrifuge with a 70Ti rotor). The supernatant fraction was discarded and the resultant

microsomal pellets were rinsed three times with wash buffer (150 mM potassium chloride and 10 mM EDTA, pH 7.4) to remove residual omeprazole and/or any reversible inhibitory metabolites. Microsomal pellets were re-suspended in 250 mM sucrose and the microsomal protein concentration was determined by the Pierce BCA Protein Assay (Pierce, Rockford, IL). For samples in group (3), HLMs were incubated with potassium ferricyanide (2 mM) for 10 min at 37°C prior to re-isolation of microsomal protein by ultracentrifugation to disrupt nitrogen-based metabolite inhibitory complexes (MICs) (125). Residual CYP2C19 activity was assessed at a final concentration of 0.1 mg/mL HLM (supplemented with an NADPH regenerating system) with *S*-mephenytoin (400 µM, i.e., 10 × K_m) to reduce the inhibitory effects of any residual competitive inhibition.

Spectrophotometric Assessment of MI Complex Formation

Incubations were conducted in 1-mL incubation mixtures (pH 7.4) containing high purity water, potassium phosphate buffer (50 mM), $MgCl_2$ (3 mM), EDTA (1 mM), NADPH (1 mM), and either rhCYP2C19 (for esomeprazole or *S*-fluoxetine) or rhCYP3A4 (for troleandomycin) at 50 pmol/ml. Reactions were initiated by the addition of inhibitor (esomeprazole [100 µM final]; *S*-fluoxetine [200 µM final] or troleandomycin [75 µM final]) to the sample cuvettes. Solvent for each compound (methanol 1% v/v final for *S*-fluoxetine; acetonitrile 1% v/v final for troleandomycin or methanol/Tris (pH 9.0) at 0.4/0.6% v/v final) was added to the reference cuvettes. A Varian Cary 100 BIO UV/visible spectrophotometer (Agilent Technology, Santa Clara, CA) equipped with a circulating water bath (37°C) was set to scan 400–500 nm approximately every 30 seconds for up to approximately 31 min (esomeprazole), 16 min (*S*-fluoxetine) or 15 min (troleandomycin).

Isolation of heme from human liver microsomes or recombinant CYPs

Esomeprazole (100 μM), 1-aminobenzotriazole (2 mM – positive control for heme adduct formation that is undetectable at UV wavelengths), gemfibrozil glucuronide (100 μM – positive control for heme adduct formation that is detectable at UV wavelengths) were incubated in 3-mL incubation mixtures (pH 7.4) containing high purity water, potassium phosphate buffer (50 mM), $MgCl_2$ (3 mM), EDTA (1 mM), NADP (1 mM), glucose-6-phosphate (5 mM), glucose-6-phosphate dehydrogenase (1 Unit/mL), and HLM (1 mg protein/mL). Reactions were terminated after 60 min (gemfibrozil glucuronide) or 120 min (esomeprazole or 1-ABT), by the addition of 0.75 mL 1 N HCl and extracted with two volumes of dichloromethane. The organic fraction was evaporated to dryness and the residue reconstituted with acetonitrile prior to analysis of heme by UHPLC with UV and HRMS detection.

HPLC-MS/MS Analytical methods

LC-MS/MS methods for CYP marker metabolites were carried out as described previously (33-35,37,38). Omeprazole analysis was performed with an Applied Biosystems/ Sciex API2000 HPLC-MS/MS system equipped with an electrospray (TurboIonSpray) ionization source (Applied Biosystems, Foster City, CA), two LC-10ADvp pumps with an SCL-10Advp controller, SIL-HTA autosampler, and DGU-14 solvent degasser (Shimadzu, Columbia, MD). The HPLC column used was an Atlantis dC18, 5 μm, 100 x 2.0 mm column (Waters), which was preceded by a direct connection guard column with a C8, 4.0 mm x 2.0 mm cartridge (Waters). Masses were monitored in the multiple reaction monitoring mode (MRM): omeprazole, 345.9 →197.9 and internal standard, pantoprazole, 383.9 →199.9. Mobile phases were: A=0.2% formic acid in water, B=0.2% formic acid in methanol and omeprazole and pantoprazole were eluted with a linear gradient (25%B to 75%B) over 2.5 min.

UHPLC-UV/HRMS analytical methods

Heme and potential adducts were monitored by UHPLC-UV/HRMS with a Waters Synapt G2 quadrupole time of flight mass spectrometer equipped with a Waters Acquity LC system as described previously (126-129). Briefly, for chromatographic separation, 0.1% formic acid in water and acetonitrile were applied to an Agilent Zorbax 300 SB-C18 LC column (2.1 x 150 mm; 5 µm) with a gradient ranging from 2-98% organic mobile phase over 11 min, following an initial 1 min 2% hold. The mobile phase composition was held at 98% organic for an additional 2 min. The mass spectrometer was operated in positive, resolution MS^E mode with fexofenadine as a real-time mass calibrant. Data were acquired over the *m/z* range 50 – 1200 using a capillary voltage of 3.5 kV, sampling cone voltage of 20 V, source temperature of 120°C and desolvation temperature of 350°C. For the high energy scan function, a collision energy ramp of 15 – 45 eV was applied at the trap traveling wave ion guide. For product ion spectra acquisition (i.e., MS/MS), precursor ions were first selected with the quadrupole and a collision energy ramp of 15 – 45 eV was applied at the trap traveling wave ion guide. In-line UV/visible detection with a photodiode array detector scanning from 200 – 500 nm was incorporated.

Data Analyses and Simulations

All IC_{50}, half-life, K_I and k_{inact}, values were determined by nonlinear regression with GraFit (version 7.0.2; Erithracus Software Ltd., Horley, Surrey, UK), as detailed previously (33-35,37,38). Ninety percent confidence intervals for k_{inact} / K_I values were calculated about the arithmetic mean with Student's t-distribution.

Accurate mass data were acquired with MassLynx version 4.1 SCN 712 (Waters). Data were processed with the MetaboLynx XS subroutine of MassLynx for dynamic mass-defect filtering about the accurate mass defect of heme (±35 mDa). The structure-based *C*-heteroatom

dealkylation algorithm was employed to construct mass-defect filters for heme and possible heme-related components, similar to methods described previously (126-129).

In vitro-to-in vivo extrapolation of CYP2C19 inactivation data was performed using both a mechanistic static model (MSM) to calculate the AUC ratio (i.e., $\frac{AUC_i}{AUC}$ or simply AUCR, as defined by FDA) (31,94,130) and a mechanistic dynamic model (MDM) (131) in Chapter 4. The MSM was based on the following equation:

$$\frac{AUC_i}{AUC} = \frac{1}{\left(\frac{f_{m,CYP}}{1 + \left(\frac{k_{inact} \cdot [I]}{k_{deg} \cdot (K_I + [I])}\right)}\right) + \left(1 - f_{m,CYP}\right)} \qquad \textbf{Equation 3.1}$$

where ($f_{m,CYP}$) represents the fraction of a hypothetical concomitantly administered drug metabolized by a given P450 enzyme, [*I*] is the inactivator concentration, and k_{inact} and K_I are the in vitro inactivation parameters, and k_{deg} is the rate constant for enzyme degradation (which has not been determined experimentally in vivo for CYP2C19, but for which the average value was reported to be 0.000445 min^{-1} based on in vitro data (132,133). The unbound plasma C_{max} was previously found to be more predictive than total C_{max} for MDIs (130,134). Therefore, this value was used in the MSM (equation 1), and was based on the total omeprazole plasma C_{max} of 3.87 μM after 5 days of dosing (40 mg q.d.) in CYP2C19 EMs (135), coupled with its plasma protein binding of 95%, for an unbound plasma C_{max} of 0.19 μM. For the MSM analyses presented in Chapter 5, ($f_{m,CYP2C19}$) for H4 formation from clopidogrel was set equal to either 0.64 or 0.72 based on those reported by Boulenc et al. (94). Because a decrease in H4 was expected, data were presented as the H4 ratio (using parameters defined by Boulenc et al. (94)) or 1/AUCR (using conservative default parameters defined by the FDA (31)). Plasma

concentrations of omeprazole, esomeprazole, omeprazole sulfone or 5-ODM omeprazole were based on various sources for dosage regimens as discussed in Chapter 5.

The MDM simulations were carried out using Simcyp Population-Based Simulator (V10.2; Simcyp Limited, UK). The differential equations which make the basis of these simulations are described in detail elsewhere (131). Input parameters can be found in the supplemental data to the paper published in 2011 (34).

The purpose of the MDM simulations was to assess the time varying effect of repeated omeprazole administration (40 mg every 12 h) on the level of active CYP2C19 in liver. This included the self-inhibition effect as the deactivation of CYP2C19 led to lower clearance and higher concentrations of omeprazole itself. The simulations were carried out twice using the lower (1.7 μM) and upper (9.1 μM) boundaries of observed K_I values and taking into account an unbound fraction of 0.75 (i.e., the free fraction of omeprazole in HLM at 1-2.5 mg/mL). k_{inact} was assumed to be 0.045 min^{-1} and turn-over of CYP2C19 was the same as that assumed for the MSM.

Although the main purpose of the simulations was to assess the level of active enzyme, *S*-mephenytoin was simulated as a substrate on day 14 following simulated administration of omeprazole and the effect on AUC was simulated on day 7 following administration of omeprazole. The simulated omeprazole dose was continued until day 14 and the AUC for *S*-mephenytoin was assessed from day 7 until the end of simulation (day 14) and compared with AUC in the absence of an inactivator.

Chapter 4. OMEPRAZOLE (AND SELECTED METABOLITES), LANSOPRAZOLE AND PANTOPRAZOLE AS METABOLISM-DEPENDENT INHIBITORS (MDIs) OF CYP2C19

Abstract

As a direct-acting inhibitor of CYP2C19 *in vitro*, lansoprazole is more potent than omeprazole and other proton pump inhibitors (PPIs), and yet lansoprazole does not cause clinically significant inhibition of CYP2C19 whereas omeprazole does. To investigate this apparent paradox, omeprazole, esomeprazole, *R*-omeprazole, lansoprazole and pantoprazole were evaluated for their ability to function as direct-acting and metabolism-dependent inhibitors (MDIs) of CYP2C19 in pooled human liver microsomes (HLM), as well as in cryopreserved hepatocytes and recombinant CYP2C19. In HLM, all PPIs were found to be direct-acting inhibitors of CYP2C19 with IC_{50} values varying from 1.2 μM (lansoprazole; C_{max} = 2.2 μM) to 93 μM (pantoprazole; C_{max} = 6.5 μM). In addition, omeprazole, esomeprazole, *R*-omeprazole, and omeprazole sulfone were identified as MDIs of CYP2C19 (they caused IC_{50} shifts after a 30-min pre-incubation with NADPH-fortified HLM of 4.2-, 10-, 2.5-, and 3.2-fold, respectively), whereas lansoprazole and pantoprazole were not MDIs (IC_{50} shifts <1.5-fold). The MDI of CYP2C19 by omeprazole and esomeprazole was not reversed by ultracentrifugation, suggesting the inhibition was irreversible (or quasi-irreversible), whereas ultracentrifugation largely reversed such effects of *R*-omeprazole. Under various conditions, omeprazole inactivated CYP2C19 with K_I values of 1.7 – 9.1 μM and k_{inact} values (maximal rate of inactivation) of 0.041 – 0.046 min^{-1}. This study identified omeprazole, and esomeprazole, but not *R*-omeprazole, lansoprazole or pantoprazole, as irreversible (or quasi-irreversible) MDIs of CYP2C19. These results have important implications for the mechanism of the clinical interaction reported between omeprazole and clopidogrel, as well as other CYP2C19 substrates.

Introduction

Omeprazole and other proton pump inhibitors (PPIs, i.e., esomeprazole, lansoprazole, dexlansoprazole, rabeprazole, and pantoprazole) are well known for a relatively low incidence of adverse events and pharmacokinetic drug-drug interactions (DDIs). Nevertheless, PPIs are the perpetrators of interactions with cyclosporine (omeprazole and rabeprazole), diazepam (esomeprazole and omeprazole) and warfarin (esomeprazole, lansoprazole, omeprazole, and rabeprazole) (136). In addition, all drugs that increase gastric pH can affect the bioavailability of drugs such as ampicillin esters, iron salts and ketoconazole, among others (136). Omeprazole, the first approved PPI, decreases the clearance of drugs such as diazepam, moclobemide, escitalopram, carbamazepine, saquinavir, sibutramine, proguanil, etravirine, disulfiram, phenytoin, voriconazole, and clopidogrel, and, by inducing CYP1A2, increases the clearance of several antipsychotic drugs, such as imipramine, theophylline, and tacrine (27,84,136).

The inhibitory DDIs listed above have been attributed, at least in part, to inhibition of CYP2C19 by omeprazole. However, clinically relevant DDIs with omeprazole are generally of low magnitude (≤120% [2.2-fold] increase in plasma AUC of CYP2C19 substrates) (27). By way of comparison, there is up to a 14.6-fold increase in the AUC of omeprazole when CYP2C19 is completely absent as occurs in genetically determined CYP2C19 poor metabolizers (137). Over 60 *in vitro* studies examining PPIs as CYP inhibitors have been published (27). Only omeprazole, lansoprazole, (and their *S*-enantiomers) have been shown to inhibit CYP2C19 with IC50 or *K*i values ≤1.0 μM. Of particular interest is that none of these *in vitro* studies published prior to 2012 examined the PPIs as MDIs (a.k.a. time-dependent inhibitors) of P450 enzymes. Based on the lowest reported K_i values for CYP2C19 inhibition in the MTDI database (i.e., 0.45 μM for lansoprazole and 1 μM for omeprazole), and the reported plasma C_{max} for lansoprazole (30 mg, day 7) and omeprazole (40 mg, day 5) in CYP2C19 extensive

metabolizers (2.2 and 3.9 μM, respectively; (135,138), the so-called R1 values (i.e., 1 + $[I]_{total}/ K_i$) values for lansoprazole and omeprazole would be 5.9 and 4.9, respectively (calculated as recommended in the Draft FDA Guidance for Industry, 2012; (31)), which means that both drugs would be expected to cause clinically relevant direct inhibition of CYP2C19, but that lansoprazole would have a higher likelihood of doing so than would omeprazole. However, lansoprazole has been reported to cause no interaction with the CYP2C19 substrates diazepam, and phenytoin (27,136). The lack of clinically relevant direct inhibition of CYP2C19 by lansoprazole is likely explained by its relatively short half-life (1.1 hr; (138) and high plasma protein binding (~97%; (116)). However, omeprazole also has a short half-life (0.7 hr; (135) and high plasma protein binding (~95%; (139)), and yet, as described above, omeprazole does cause clinically significant inhibition of CYP2C19. This apparent discrepancy could be explained if omeprazole, but not lansoprazole, were an irreversible inhibitor of CYP2C19.

A large clinical study in 282 healthy subjects (84) demonstrated that omeprazole inhibited the CYP2C19-dependent activation of clopidogrel as evidenced by a 40-47% decrease in the formation of H4, the purported active antiplatelet metabolite of clopidogrel. Inhibition of clopidogrel activation was observed even when the two drugs were administered 12 hours apart. In the same subjects, no such interaction was observed between pantoprazole and clopidogrel. Additional clinical studies are reviewed in Chapter 1.

The interaction between clopidogrel and PPIs and the impact of the CYP2C19 poor metabolizer phenotype have prompted warnings from the FDA and EMA (109,140), although the FDA specifically warns against coadministration of clopidogrel and omeprazole and further specifically suggests that pantoprazole may be a safer alternative.

The identity of the enzyme(s) responsible for the multi-step activation of clopidogrel is controversial (45-49) (see Chapter 1 for additional review of this topic). Much of the

pharmacogenomic data strongly implicate CYP2C19 as the most important enzyme for clopidogrel activation, based on poor response to clopidogrel in carriers of reduced function CYP2C19 alleles (e.g., the *2 and *3 alleles), and also increased bleeding in carriers of the increased function CYP2C19*17 allele (141). The DDI between PPIs and clopidogrel is of particular importance because PPIs are co-prescribed in up to ~2/3 of patients after discharge from hospital because PPIs lessen the severity of the gastrointestinal hemorrhage associated with clopidogrel treatment (53).

In this study the *in vitro* inhibitory potential of omeprazole, its individual enantiomers and selected metabolites, as well as lansoprazole and pantoprazole (Figure 4.1) were examined in pooled HLM, pooled cryopreserved hepatocytes and rCYP2C19, with a special emphasis on the potential for these drugs to cause MDI of CYP2C19. The implications of our results were explored by dynamic simulations assessing the level of active CYP2C19 under multiple doses of omeprazole. This PBPK modeling and simulation provided additional insight into the ongoing debate surrounding the interaction between PPIs and clopidogrel.

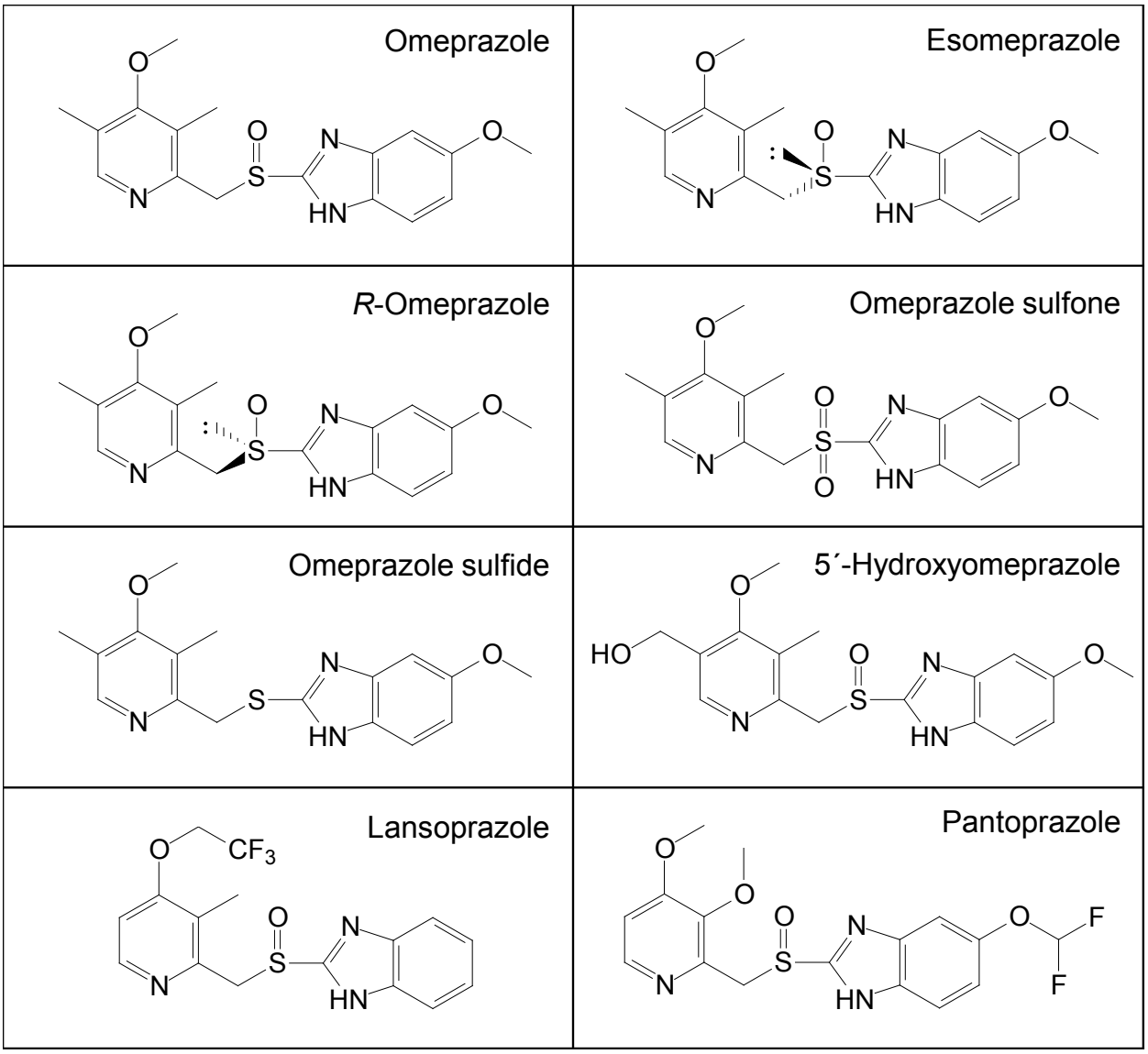

Figure 4.1. Structures of the PPIs and omeprazole metabolites examined.

Results

4.1. Inhibitory effect of omeprazole on *S*-mephenytoin 4´-hydroxylation in multiple test systems: IC_{50} determinations, metabolic stability and microsomal protein binding

Omeprazole was evaluated as a direct-acting and MDI of CYP2C19 activity (*S*-mephenytoin 4´-hydroxylation) in pooled human liver microsomes (n=16), recombinant CYP2C19 (Bactosomes®), and pooled, cryopreserved human hepatocytes (n=3), at a substrate concentration approximately equal to K_m (40 µM). The results are summarized in Figure 4.2a-d and Table 4.1. The results show that omeprazole caused MDI of CYP2C19 as evidenced by a left shift in IC_{50} curves following a 30-min pre-incubation with NADPH-fortified HLM, recombinant CYP2C19 and human hepatocytes (IC_{50} shifts of 4.1, 6.9 and 3.6-fold, respectively). A left shift of ≥1.5 fold is considered indicative of MDI (35). With no pre-incubation, omeprazole inhibited CYP2C19 in all three systems with similar IC_{50} values ranging from 4.7 to 9.6 µM, which decreased to approximately 1.5 µM in all three test systems after pre-incubation with NADPH. The experiment presented in Figure 4.2a also included an IC_{50} determination with a 30-min pre-incubation step without NADPH, to confirm that the IC_{50} shift was NADPH-dependent (Table 4.1 [for clarity, these data are not presented in Figure 4.2a]). Omeprazole was also examined as an inhibitor of CYP1A2, 2B6, 2C8, 2C9, 2D6, 3A4 and 2J2 and was found to be a weak direct inhibitor of these enzymes (IC_{50} values > approximately 100 µM), with no NADPH-dependent IC_{50} shift > 1.5 fold (supplemental data shown in Table 4.2).

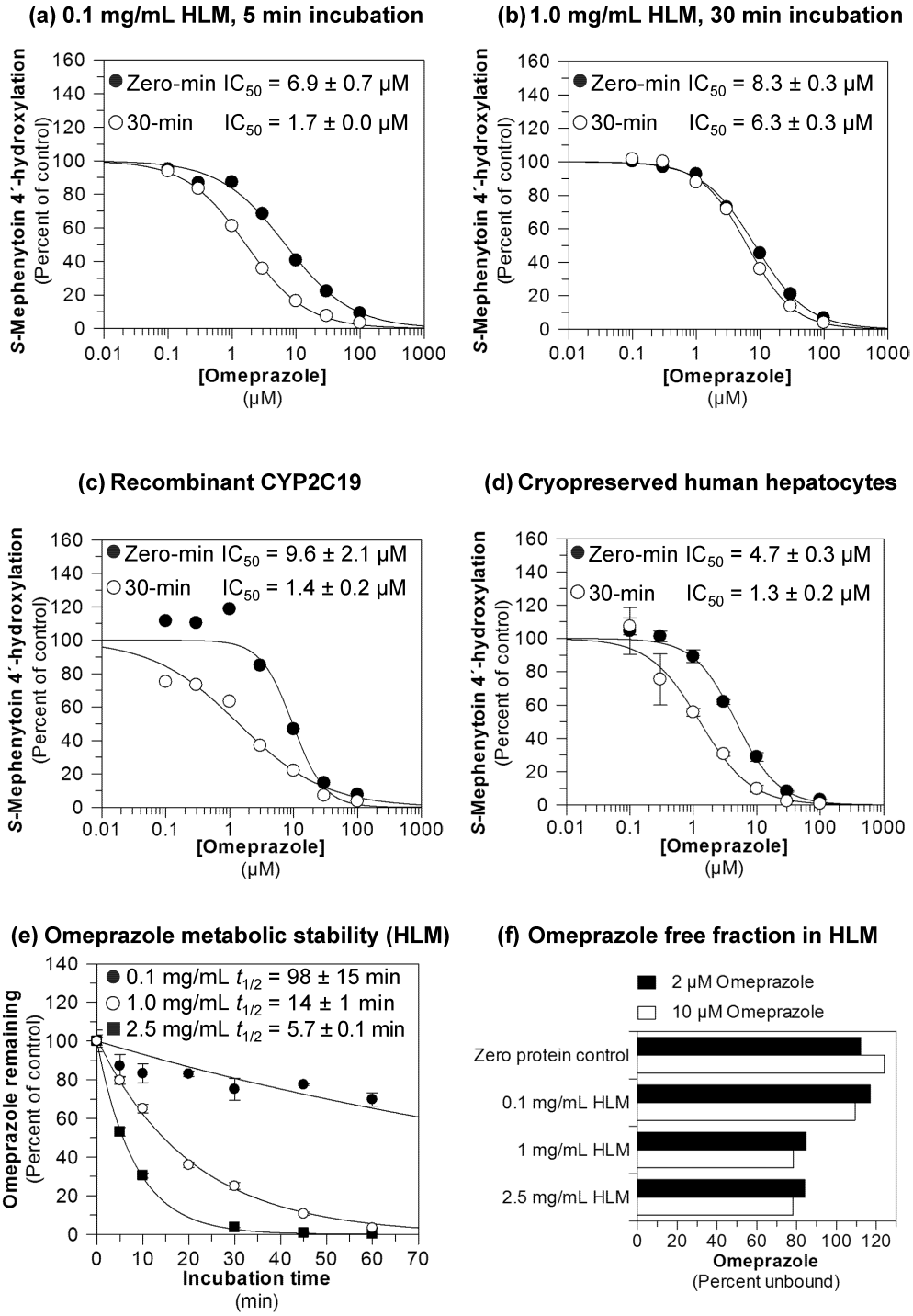

Figure 4.2. Evaluation of omeprazole as a direct-acting and MDI of CYP2C19.

Each symbol represents the average of duplicate determinations unless otherwise indicated. (a) Omeprazole inhibited CYP2C19 in pooled HLM with IC_{50} values as shown (*S*-mephenytoin 4´-hydroxylation control rates = 97.3 and 95.0 pmol/mg/min with and without pre-incubation, respectively). (b) Omeprazole inhibited CYP2C19 in pooled HLM with IC_{50} values as shown (*S*-mephenytoin 4´-hydroxylation control rates = 97.3 and 74.3 pmol/mg/min with and without

pre-incubation, respectively). (c) Omeprazole inhibited recombinant human CYP2C19 with IC_{50} values as shown (*S*-mephenytoin 4´-hydroxylation control rates = 0.690 and 0.828 min^{-1} with and without pre-incubation, respectively). (d) Omeprazole inhibited CYP2C19 cryopreserved human hepatocytes with IC_{50} values as shown (*S*-mephenytoin 4´-hydroxylation control rates = 24.7 and 24.8 pmol/million cells/min with and without pre-incubation, respectively). Each symbol represents the average of triplicate determinations and error bars represent the standard deviations. (e) The metabolic stability of omeprazole (10 μM) was evaluated in HLM at the protein concentrations utilized in this study (0.1, 1.0, and 2.5 mg/mL), as described in Chapter 3. Half-life values for the disappearance of omeprazole are as indicated. Each symbol represents the average of triplicate determinations and error bars represent the standard deviations; (f) The microsomal binding of omeprazole (2 and 10 μM) was evaluated as described in Chapter 3.

Table 4.1. Inhibition of CYP2C19 in human liver microsomes by omeprazole, its enantiomers or its major metabolites and lansoprazole and pantoprazole

Compound	IC_{50} (μM)[a]			IC_{50} shift (fold)[b]
	No pre-incubation	30 min pre-incubation (-NADPH)	30 min pre-incubation (+NADPH)	
Omeprazole	6.9 ± 0.7	8.7 ± 0.6	1.7 ± 0.0	**4.2**
Esomeprazole	15 ± 1	16 ± 1	1.5 ± 0.1	**10**
R-Omeprazole	8.1 ± 1.2	12 ± 1	3.3 ± 0.4	**2.5**
Omeprazole sulfide	9.7 ± 0.5	8.4 ± 2.7	9.6 ± 1.0	1.0
Omeprazole sulfone	18 ± 2	12 ± 3	5.6 ± 0.5	**3.2**
5-Hydroxyomeprazole	> 100	> 100	> 100	NA
Lansoprazole	1.2 ± 0.1	1.2 ± 0.1	1.2 ± 0.0	1.0
Pantoprazole	93 ± 7	>100	65 ± 4	1.4

[a] Values are displayed to two significant figures, ± standard error of the measurement

[b] Calculated from full precision values as (IC_{50} with no pre-incubation) ÷ (IC_{50} with 30 min pre-incubation + NADPH) and rounded to two significant figures. IC_{50} shifts > 1.5-fold appear in bold.

NA: Not applicable (i.e., IC_{50} values greater than the highest concentration examined)

Table 4.2. Summary of P450 inhibition in human liver microsomes by omeprazole

Enzyme (substrate)	IC_{50} (μM)[a]		
	No pre-incubation	30 min pre-incubation (+NADPH)	IC_{50} shift (fold)[b]
CYP1A2 (phenacetin)	> 100	> 100	NA
CYP2B6 (bupropion)	> 100	> 100	NA
CYP2C8 (Amodiaquine)	95 ± 5	78 ± 8	1.2
CYP2C9 (Diclofenac)	> 100	> 100	NA
CYP2D6 (Dextromethorphan)	> 100	> 100	NA
CYP3A4 (Midazolam)	> 100	69 ± 5	NA
CYP3A4 (Testosterone)	> 100	> 100	NA
CYP2J2 (Ebastine)	> 100	> 100	NA

[a] Values are displayed to two significant figures, ± standard error of the measurement

[b] Calculated from full precision values as (IC_{50} with no pre-incubation) ÷ (IC_{50} with 30 min pre-incubation + NADPH) and rounded to two significant figures.

NA: Not applicable (i.e., IC_{50} values greater than the highest concentration examined).

The data presented in Figure 4.2a were obtained under *"low microsomal protein−short incubation time*" conditions (i.e., 0.1 mg/mL HLM for 5 minutes). However, *S*-mephenytoin is a low turnover substrate in HLM, for which reason *S*-mephenytoin 4´-hydroxylation activity is frequently assessed by incubating *S*-mephenytoin with high concentrations of HLM (i.e., ≥ 0.2 mg/mL) for 20 - 40 min (e.g., (142,143). Because MDI of CYP2C19 by omeprazole had not been previously described, the ability of omeprazole to inhibit CYP2C19 under "*high microsomal protein−long incubation time*" conditions (i.e., 1 mg/mL HLM for 30 minutes) was also examined. Under such conditions no MDI of CYP2C19 by omeprazole (i.e., IC_{50} shift <1.5; Figure 4.2b) was detected.

Because of the difference in results between *"low microsomal protein−short incubation time*" and "*high microsomal protein−long incubation time*" conditions, the metabolic stability and non-specific binding of omeprazole in HLM was examined. In NADPH-fortified HLM at 0.1 mg/mL, omeprazole was relatively stable with a half-life of 98 min (Figure 4.2e). However, at 1.0 mg/mL and 2.5 mg/mL HLM (i.e., the concentration utilized in one of the k_{inact} determinations, see below) omeprazole rapidly disappeared from incubations, with half-life values of only 14 and 5.7 min, respectively. Non-specific binding of omeprazole to HLM was also examined (by ultrafiltration) as a possible cause of the discrepancy in results between *"low microsomal protein−short incubation time*" and "*high microsomal protein−long incubation time*" conditions. As shown in Figure 4.2f, however, >75% of omeprazole (2 and 10 μM) remained free in the incubation from 0.1 to 2.5 mg/mL.

4.2. Inhibitory effects of the major omeprazole metabolites and enantiomers on *S*-mephenytoin 4´-hydroxylation in human liver microsomes: IC_{50} determinations

Esomeprazole, *R*-omeprazole, omeprazole sulfide, omeprazole sulfone, and 5´-hydroxyomeprazole were evaluated as direct-acting and MDIs of CYP2C19 activity (*S*-mephenytoin 4´-hydroxylation) in pooled human liver microsomes (n=16, 0.1 mg/mL) at a substrate concentration approximately equal to the K_m (40 μM). The results are summarized in Table 4.1 and Figure 4.3. The results show that esomeprazole (Figure 4.3a), *R*-omeprazole (Figure 4.3b), and omeprazole sulfone (Figure 4.3d) caused MDI of CYP2C19 as evidenced by a left shift in IC_{50} curves (>1.5-fold) following a 30-min pre-incubation with NADPH-fortified HLM (10, 2.5 and 3.2-fold IC_{50} shifts, respectively), with similar "shifted" IC_{50} values ranging from 1.5 to 5.6 μM. The IC_{50} values following a 30-min pre-incubation in the absence of NADPH were higher than those in the presence of NADPH, suggesting that the time-dependent inhibition of CYP2C19 by these compounds was in fact metabolism-dependent (Table 4.1). The IC_{50} values for omeprazole sulfide after 30 min pre-incubation with or without NADPH remained similar to the value without pre-incubation (IC_{50} shift <1.5-fold), suggesting that omeprazole sulfide is only a direct-acting inhibitor of CYP2C19 (Figure 4.3c, Table 4.1). 5´-Hydroxyomeprazole, one of the major metabolites formed by CYP2C19, was a weak inhibitor of CYP2C19 (IC_{50} values > 100 μM) (Figure 4.3e). The experiments presented in Figure 4.3 also included an IC_{50} determination with a 30-min pre-incubation step without NADPH, to confirm that the IC_{50} shift was NADPH-dependent (Table 4.1 [for clarity, these data are not presented in Figure 4.3]).

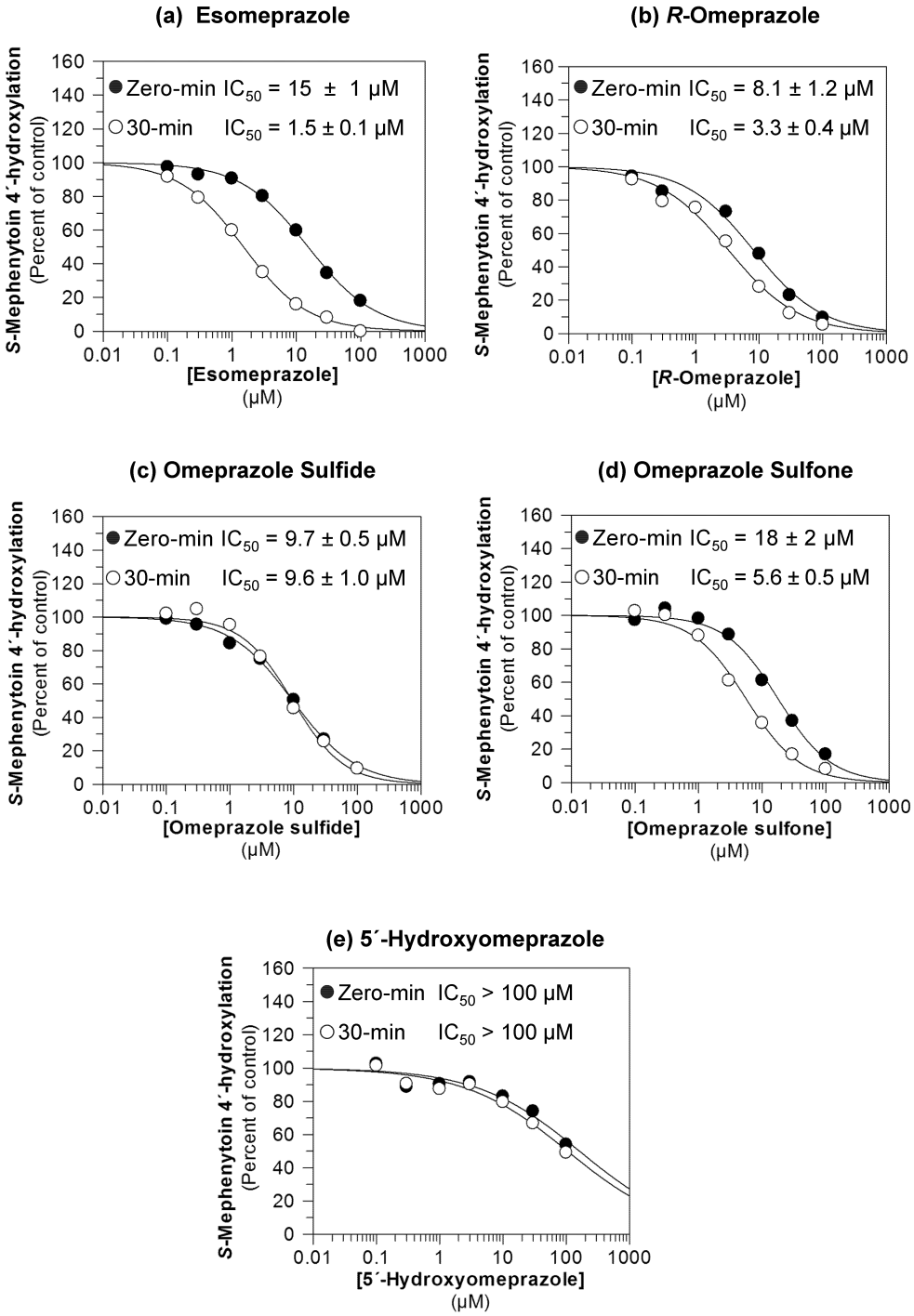

Figure 4.3. Evaluation of esomeprazole, *R*-omeprazole, omeprazole sulfone, and 5´-hydroxyomeprazole as direct-acting and MDIs of CYP2C19.

Each symbol represents the average of duplicate determinations unless otherwise indicated. (a) Esomeprazole inhibited CYP2C19 in pooled HLM with IC_{50} values as shown (*S*-mephenytoin 4´-hydroxylation control rates = 80.9 pmol/mg/min and 88.1 pmol/mg/min with pre-incubation). (b) *R*-Omeprazole inhibited CYP2C19 in pooled HLM with IC_{50} values as shown (*S*-mephenytoin 4´-hydroxylation control rates = 106 and 108 pmol/mg/min, with and without pre-incubation,

respectively). (c) Omeprazole sulfide inhibited CYP2C19 in pooled HLM with IC_{50} values as shown (*S*-mephenytoin 4´-hydroxylation control rates = 89.8 and 82.2 pmol/mg/min, with and without pre-incubation, respectively). (d) Omeprazole sulfone inhibited CYP2C19 in pooled HLM with IC_{50} values as shown (*S*-mephenytoin 4´-hydroxylation control rates = 85.4 and 84.7 pmol/mg/min, with and without pre-incubation, respectively). (e) 5´-Hydroxyomeprazole weakly inhibited CYP2C19 in HLM (*S*-mephenytoin 4´-hydroxylation control rates = 108 and 97.0 pmol/mg/min, with and without pre-incubation, respectively).

4.1.3. Inhibitory effects of lansoprazole and pantoprazole on *S*-mephenytoin 4´-hydroxylation in human liver microsomes and cryopreserved human hepatocytes: IC_{50} determinations

Lansoprazole and pantoprazole were evaluated as direct-acting and MDIs of CYP2C19 activity (*S*-mephenytoin 4´-hydroxylation) in pooled human liver microsomes (n=16) and pooled, cryopreserved human hepatocytes (n=3), at a substrate concentration approximately equal to the K_m (40 µM). The results are summarized in Table 4.1 and Figure 4.4. Neither lansoprazole nor pantoprazole caused MDI of CYP2C19 in either HLM or cryopreserved human hepatocytes (i.e., IC_{50} shifts <1.5-fold). Lansoprazole was a relatively potent (i.e., IC_{50} ≈1.0 µM), direct-acting inhibitor of CYP2C19 in both HLM and cryopreserved human hepatocytes (Figure 4.4a and b), whereas pantoprazole was a relatively weak inhibitor (Figure 4.4c and d). The experiments presented in Figure 4.4a and c also included an IC_{50} determination with a 30-min pre-incubation step without NADPH, to confirm that the IC_{50} shift was NADPH-dependent (Table 4.1 [for clarity, these data are not presented in Figure 4.4]).

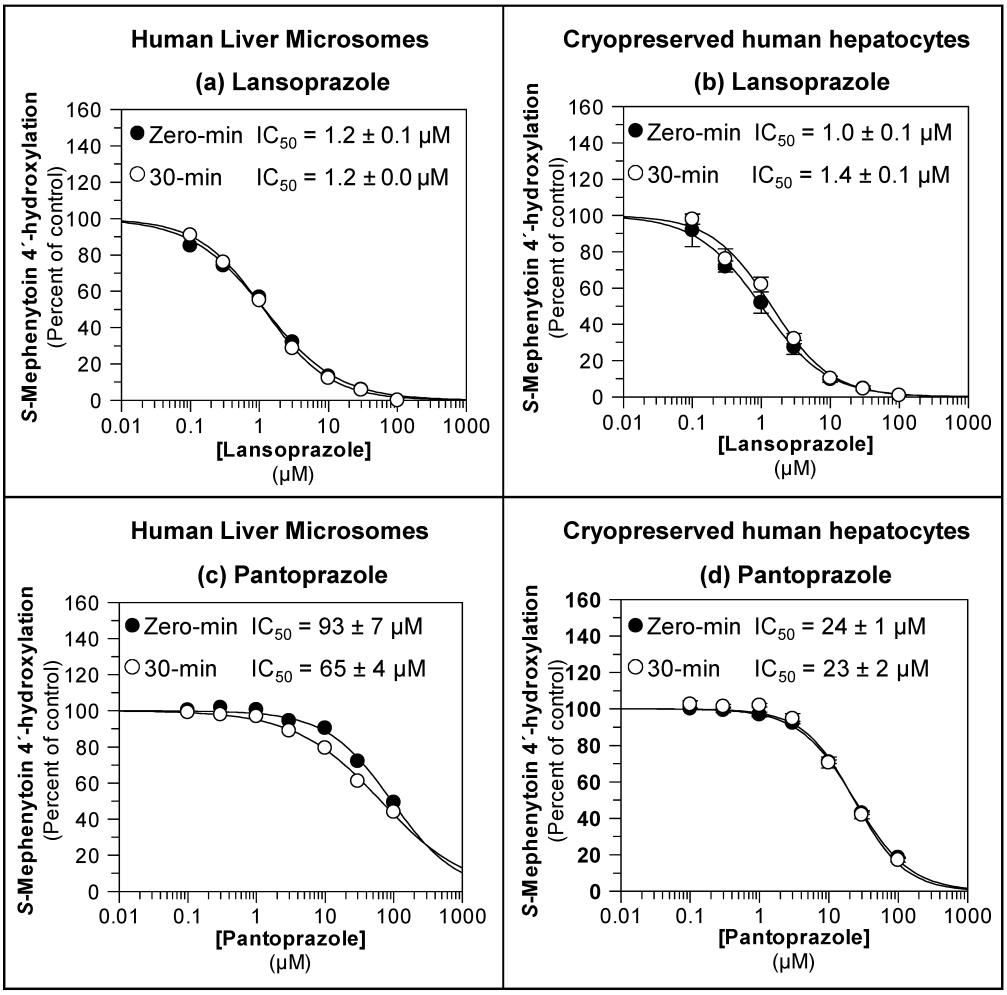

Figure 4.4. Evaluation of lansoprazole and pantoprazole as direct-acting and MDIs of CYP2C19

Each symbol represents the average of duplicate determinations unless otherwise indicated. (a) Lansoprazole inhibited CYP2C19 in HLM with IC_{50} values as shown (*S*-mephenytoin 4´-hydroxylation control rates = 83.8 and 79.6 pmol/mg/min, with and without pre-incubation, respectively). (b) Lansoprazole inhibited CYP2C19 in cryopreserved human hepatocytes with IC_{50} values as shown (*S*-mephenytoin 4´-hydroxylation control rates = 30.4 and 26.6 pmol/million cells/min, with and without pre-incubation, respectively). Each symbol represents the average of triplicate determinations and error bars represent the standard deviations; (c) Pantoprazole inhibited CYP2C19 in pooled HLM with IC_{50} values as shown (*S*-mephenytoin 4´-hydroxylation control rates = 61.7 and 71.0 pmol/mg/min, with and without pre-incubation, respectively). (d) Pantoprazole inhibited CYP2C19 in cryopreserved human hepatocytes with IC_{50} values as shown (*S*-mephenytoin 4´-hydroxylation control rates = 24.5 and 14.2 pmol/million cells/min, with and without pre-incubation, respectively). Each symbol represents the average of triplicate determinations and error bars represent the standard deviation.

4.3 Inactivation of CYP2C19 by omeprazole: K_I and k_{inact} determinations

The results in Figure 4.2 suggest that omeprazole is an MDI of CYP2C19. Accordingly, experiments were performed to determine K_I (the concentration of omeprazole supporting half maximal rate of CYP2C19 inactivation) and k_{inact} (the first order rate constant for CYP2C19 inactivation). The results from three different experiments are summarized in Figure 4.5. The three experimental conditions were (1) low HLM concentration with [S] = K_m with no dilution step (Figure 4.5a-b), (2) low HLM concentration with [S] = 10 × K_m (Figure 4.5c-d), and (3) high [HLM] with [S] = 10 × K_m with a 25-fold dilution step (Figure 4.5e-f). Under all three conditions, the inactivation of CYP2C19 was dependent on the concentration of omeprazole (over the full ranges examined) and the time course conformed to a first-order inactivation process (as indicated by the linearity of plots of the log of the residual enzyme activity against time; Figure 4.5a, c, and e). The K_I values differed depending on whether omeprazole was pre-incubated with human liver microsomes at 2.5 mg/mL (and subsequently diluted 25 fold to determine residual CYP2C19 activity with substrate = 10Km; Figure 4.5e-f) or 0.1 mg/mL (and not diluted to determine residual CYP2C19 activity, with substrate = 10Km or K_m; Figure 4.5a-d). The K_I value was approximately 9 μM in the former case, and approximately 2 μM in the latter cases. In all three cases, the k_{inact} values were approximately 0.04 min^{-1}, which means that, in the presence of saturating concentrations of omeprazole, 4% of CYP2C19 was inactivated every minute. The efficiency of CYP2C19 inactivation (k_{inact}/K_I) decreased by a factor of approximately five when the concentration of HLM was increased and a dilution step was used. Taken together, these data suggest that omeprazole is an irreversible inactivator of CYP2C19.

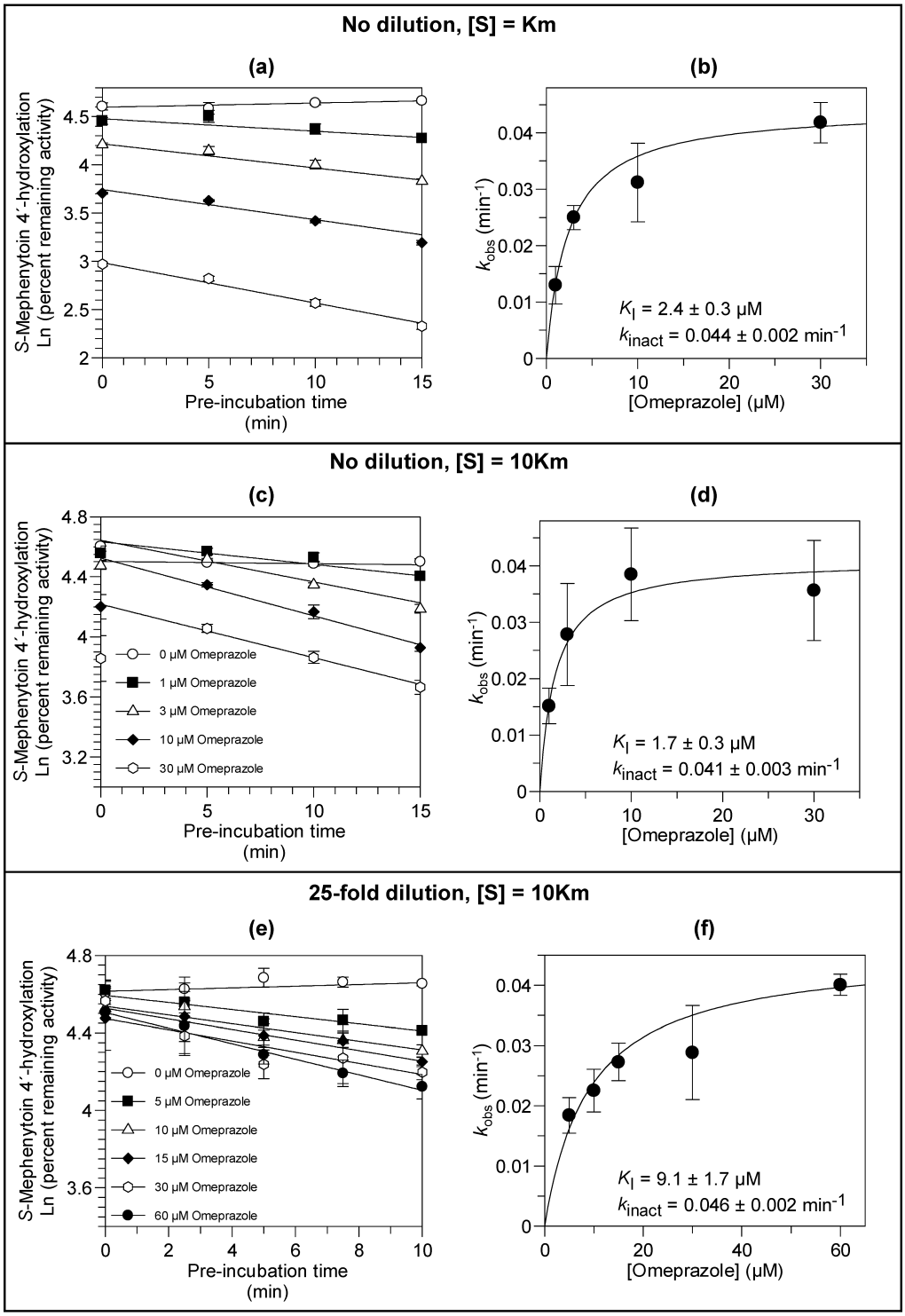

Figure 4.5. Determination of K_I and k_{inact} for the MDI of CYP2C19 by omeprazole

Individual points represent the average of triplicate determinations ± standard deviation, unless otherwise noted. For graphs in (a) and (c), omeprazole was pre-incubated (at concentrations indicated in the legend of panel c) and residual CYP2C19 activity determined as described in Chapter 3. For the graph in (e), omeprazole was pre-incubated (at concentrations indicated)

and residual CYP2C19 activity determined as described in Chapter 3 (after a 25-fold dilution). The graphs in (b), (d), and (f) represent the direct plots of the initial rates of inactivation of CYP2C19. Values are the slopes of the initial rates of inactivation (k_{obs}) at each concentration of omeprazole, shown ± standard error.

4.4. Effects of omeprazole on CYP2C19 activity in microsomes prepared from hepatocytes after three days of treatment

CYP2C19 activity (*S*-mephenytoin 4´-hydroxylation) was measured in microsomes isolated from fresh primary cultures of human hepatocytes treated with omeprazole (100 μM; three days). It should be noted that this concentration is approximately 19-times greater than the C_{max} in PMs (5.3 μM [(144)]; who can be neither induced nor inhibited with respect to CYP2C19), and 26-times greater than the C_{max} in EMs (135) after a 40 mg oral dose of omeprazole. Omeprazole treatment decreased microsomal CYP2C19 activity in hepatocytes that initially expressed high levels of CYP2C19, but increased microsomal CYP2C19 activity in hepatocytes that initially expressed low levels of CYP2C19 (Figure 4.6). This dual effect likely reflects the overall effect of two opposing actions of omeprazole; in hepatocytes with high CYP2C19 activity, the predominant effect of omeprazole was irreversible inactivation, but in hepatocytes with low CYP2C19 activity the predominant effect was induction via PXR activation (145). These data were obtained from many studies conducted to examine the potential for drug candidates to induce P450 enzymes, in which primary cultures of human hepatocytes were treated with 100 μM omeprazole, a well-known AhR activator and therefore positive control for CYP1A2 induction. Because the microsomes are obtained from these studies in a way that washes out residual inhibitor, these data provided additional evidence that omeprazole is an irreversible inactivator of CYP2C19.

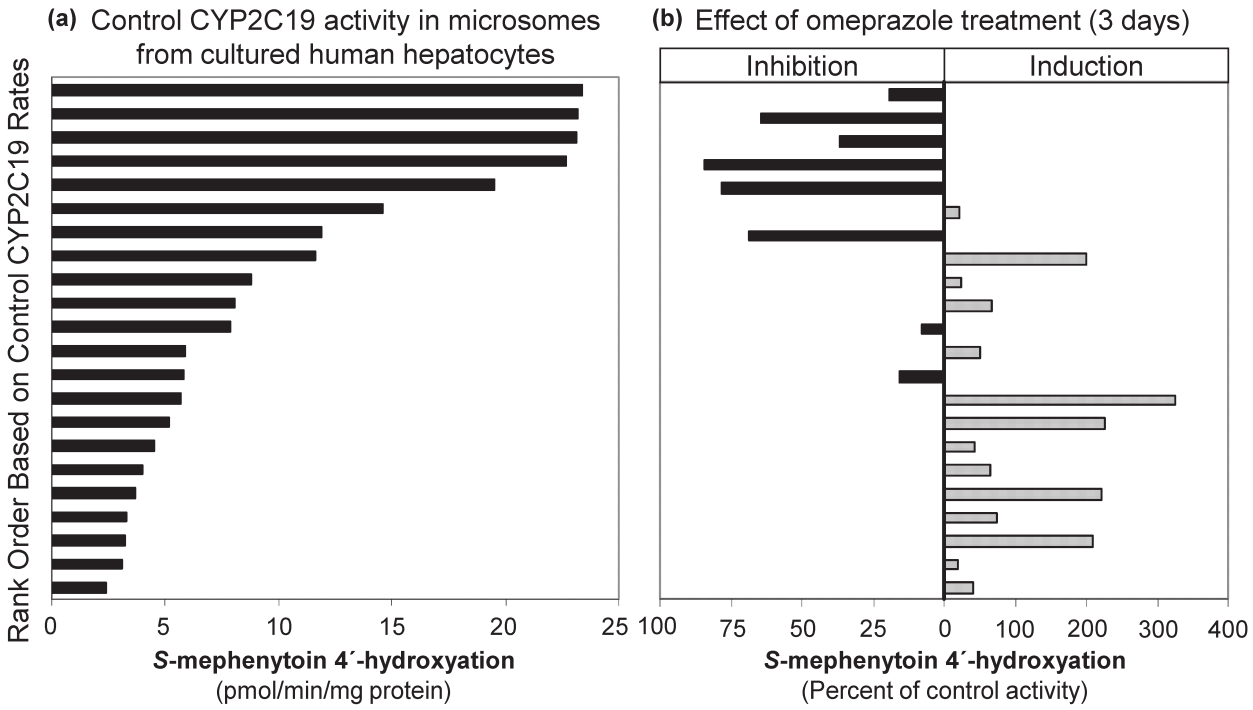

Figure 4.6. CYP2C19 activity (*S*-Mephenytoin 4'-hydroxylation) in microsomes isolated from fresh-plated hepatocytes treated with DMSO (control) or omeprazole

Primary cultures of human hepatocytes were treated for three consecutive days with DMSO or omeprazole (100 μM) and microsomes prepared from the hepatocytes 24-h after the last treatment. CYP2C19 activity was determined as described in Chapter 3. Activities were sorted in rank order from highest to lowest control rates (a) and the corresponding omeprazole-treated samples are displayed in panel (b) in terms of percent of control activity.

4.5 Irreversible or quasi-irreversible inhibition of CYP2C19 by omeprazole and esomeprazole, but not *R*-omeprazole: ultracentrifugation

Because esomeprazole was approximately 4-fold more effective as a MDI of CYP2C19 than *R*-omeprazole (Table 4.1, Figure 4.3a-b) with a 10-fold shift in IC_{50} value for the former and a 2.5-fold shift for the latter, omeprazole and its individual enantiomers were further examined to determine whether the inactivation of CYP2C19 involved irreversible or quasi-irreversible inhibition based on an ultracentrifugation method described in Chapter 3 and previously (35). A concentration of inhibitor that caused nearly complete (i.e., > ~95% inhibition) after 30-min pre-incubation with NADPH, but incomplete (< ~85%) inhibition after 30-min pre-incubation in the absence of NADPH was chosen (i.e., 100 μM for all). Pooled HLM were treated with inhibitor or solvent (methanol, 0.1% v/v) for 30 min in the presence of NADPH, and in the presence or absence of potassium ferricyanide (to reverse the formation of metabolite inhibitory complex associated with quasi-irreversible inactivation (125)) (Figure 4.7). Following the 30-min incubation, pooled HLM samples were either (1) assayed directly for residual CYP activity ("Pre-spin"), (2) re-isolated by ultracentrifugation and then assayed for residual CYP activity ("Post-spin"), or (3) treated with potassium ferricyanide, re-isolated by ultracentrifugation and then assayed for residual CYP activity ("Post-spin + $K_3[Fe(CN)_6]$"). As expected, substantial inhibition was observed after treatment with omeprazole, esomeprazole and *R*-omeprazole (Figure 4.7, "pre-spin"), in a rank-order consistent with the IC_{50} shifts: esomeprazole ≈ omeprazole > *R*-omeprazole. Surprisingly, centrifugation and re-isolation of HLM after pre-incubation largely reversed the inhibition caused by *R*-omeprazole (Figure 4.7, "Post-spin" and "Post spin + $K_3[Fe(CN)_6]$"). In contrast, centrifugation did not fully restore CYP2C19 activity after treatment with omeprazole or esomeprazole, which suggests that esomeprazole is the major contributor to the inactivation of CYP2C19 by omeprazole. Potassium ferricyanide treatment of the samples caused some additional restoration of activity after treatment with omeprazole and esomeprazole, but did not fully restore CYP2C19 activity. Taken together,

these results suggest that the MDI of CYP2C19 observed with racemic omeprazole is largely irreversible (due to covalent binding to the apoprotein, heme moiety or both). However, given the partial restoration of CYP2C19 activity with potassium ferricyanide, contribution of a quasi-irreversible mechanism (due to metabolite inhibitory complex [MIC] formation) cannot be completely ruled out. However, the results presented in Figure 4.7 show that the MDI of CYP2C19 caused by *R*-omeprazole is largely reversible after re-isolation of HLM, suggesting that one or more metabolites of this enantiomer is simply a more potent inhibitor of CYP2C19 than the parent, whereas metabolism of esomeprazole largely leads to irreversible inactivation of CYP2C19.

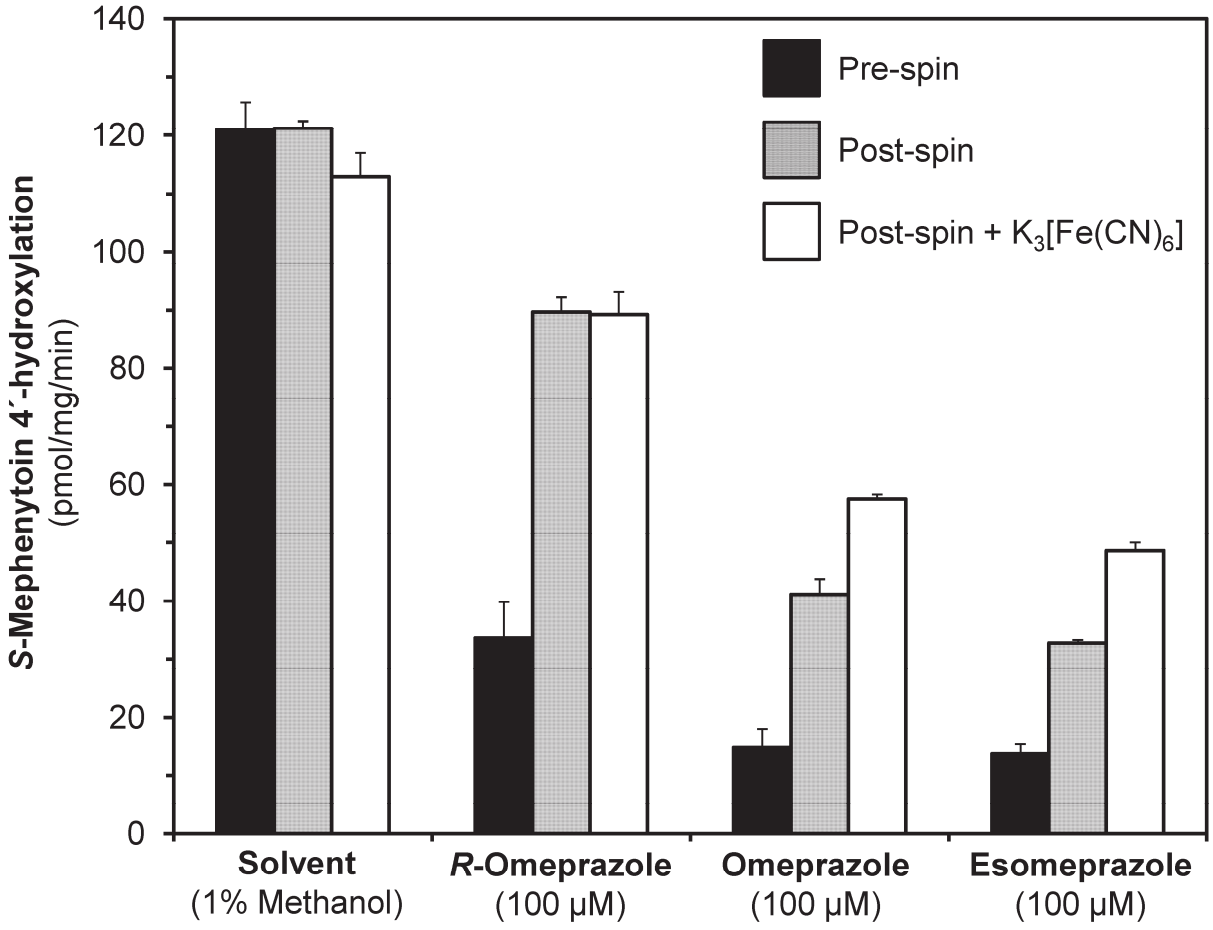

Figure 4.7. Reversibility assessment of the MDI of CYP2C19 by omeprazole and its enantiomers with the ultracentrifugation method

The potential reversibility of the MDI of CYP2C19 NADPH-fortified HLM (0.1 mg/mL) by omeprazole and its individual enantiomers (100 µM) was evaluated with the ultracentrifugation method, as described in Chapter 3. Incubations labeled "Pre-spin" were conducted similarly to analogous samples in the IC_{50} determinations (conduced in triplicate and displayed as the average rates of *S*-mephenytoin 4´-hydroxylation ± standard deviation). For incubations labeled "Post-spin" (conducted in triplicate *and* analyzed in triplicate), microsomal protein was isolated by ultracentrifugation after 30 min incubations with the inhibitor and NADPH, and analyzed in triplicate for residual CYP2C19 activity (*S*-mephenytoin 4´-hydroxylation) displayed as the average rates ± standard error, as described in Chapter 3. Half of the incubations from the "Post-spin" samples included potassium ferricyanide (2 mM, final concentration) as indicated. Samples treated with methanol (1% v/v, final) served as controls. All rates were normalized to final microsomal protein concentrations, as described in Chapter 3.

4.6 Simulation of time-dependent changes in active CYP2C19

Active levels of hepatic CYP2C19 in the presence of omeprazole (40 mg b.i.d. for 14 days) were simulated with Simcyp V10.2, as described in Chapter 3. Figure 4.8 shows the active CYP2C19 levels with time. Depending on the assumption regarding K_I (1.7 or 9.1 μM) the level of active enzyme could decrease to approximately 10 to 60% of the baseline which would be associated with a 1.4 to 10-fold increase in AUC of compounds mainly metabolized by CYP2C19. However, the simulated effect of omeprazole on *S*-mephenytoin AUC showed only a 1.45-fold increase when the K_I value was 9.1 μM, and a 5.46-fold increase when the K_I value was 1.7 μM, rather than a 10-fold increase, likely due to the contribution of other enzymes in its metabolism (e.g. CYP2B6 and CYP2C9 (146,147)).

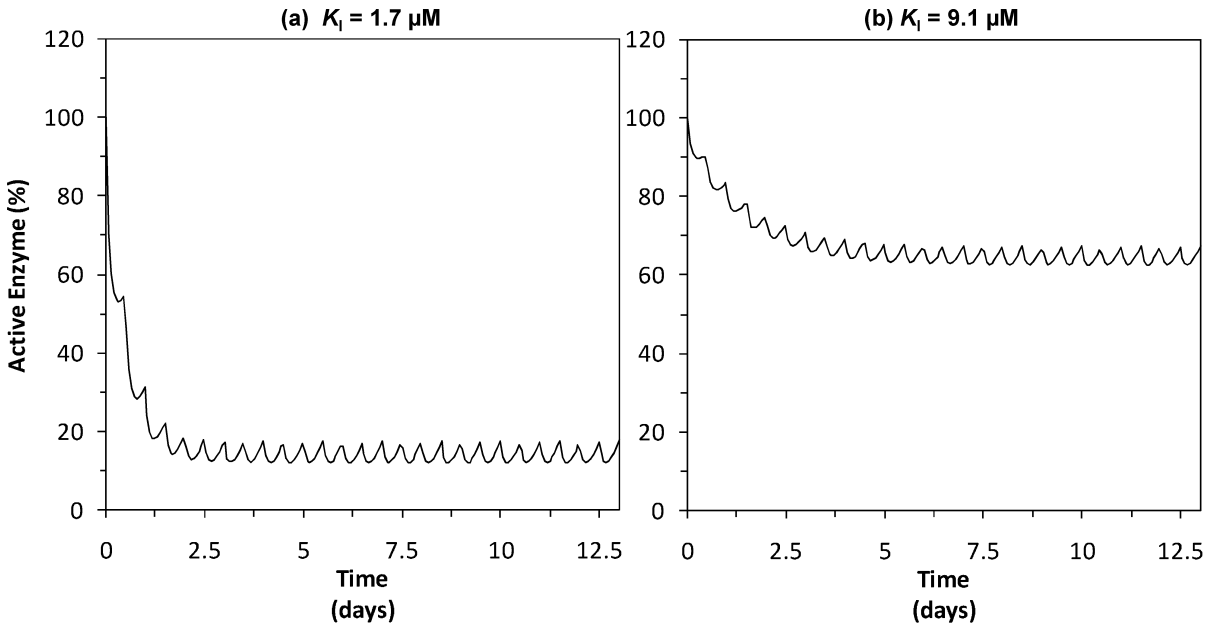

Figure 4.8. Simulation of time-dependent changes in active CYP2C19

Active levels of hepatic CYP2C19 in the presence of omeprazole (40 mg b.i.d. for 14 days) were simulated with the Simcyp Simulator V10.2, as described in Chapter 3. Panel (a) is based on a K_I value of 1.7 µM; panel (b) is based on a K_I value of 9.1 µM.

Discussion

Given the relatively few drugs that are metabolized extensively by CYP2C19, it is not surprising that few DDIs have been attributed to clinically relevant inhibition of CYP2C19. As noted in the Introduction to this chapter and in Chapter 1, there is evidence of clinically relevant inhibition of CYP2C19 by omeprazole, but direct competitive inhibition of CYP2C19 is an unlikely cause; if it were, lansoprazole would be expected to inhibit CYP2C19 more than omeprazole whereas the converse is observed clinically. It should be noted that the dose of lansoprazole versus omeprazole (which depends on indication) could partly explain this difference. For the lowest dose indications (i.e., GERD or maintenance of healing of erosive esophagitis), it is 20 mg q.d. for omeprazole ((139), and 15 mg q.d. for lansoprazole (116). For the highest dose indication (i.e., Zollinger–Ellison or other hypersecretory syndromes), the doses are equal (60 mg q.d. or up to 120 mg per day in divided doses). Based on this comparison alone, it seems unlikely that the slight difference in the low dose explains the differences in clinical DDIs. This supposition is borne out by clinical data in the MTDI: negative interactions were reported between lansoprazole (60 mg q.d., 10 days) and the CYP2C19 substrates diazepam and phenytoin (lansoprazole dose 60 mg q.d., 9 days with the latter drug) (27). No positive DDIs with CYP2C19 substrates have been reported in the MTDI with lansoprazole with the exception of a case report regarding a possible interaction with voriconazole in a CYP2C19 IM (27). On the other hand, with a low dose of omeprazole (20 mg q.d.) in various studies (8 to 23 days), the exposure (AUC) of the CYP2C19 substrates diazepam and escitalopram increased from 26 to 91% (27).

With the exception of the preliminary findings (148), in vitro evidence for MDI of CYP2C19 had not been described for any PPI prior to the publication of the data in this chapter in 2011 (34). In the current study, omeprazole, esomeprazole, *R*-omeprazole, and omeprazole

sulfone were identified as MDIs of CYP2C19 (IC_{50} shifts after a 30-min pre-incubation with NADPH of 4.2, 10, 2.5, and 3.2, respectively), whereas lansoprazole and pantoprazole were not MDIs (IC_{50} shifts <1.5). Furthermore, the MDI of CYP2C19 by omeprazole and esomeprazole was not reversed by ultracentrifugation, suggesting the inhibition was irreversible, whereas ultracentrifugation largely reversed such effects of *R*-omeprazole. Under various conditions, omeprazole inactivated CYP2C19 with K_I values of 1.7 – 9.1 μM and k_{inact} values (maximal rate of inactivation) of 0.041 – 0.046 min^{-1} (corresponding to k_{inact}/K_I values ranging from 5.1 to 24 $min^{-1} \cdot mM^{-1}$ depending on the experimental conditions used (Figure 4.5). The variation in K_I values, but not k_{inact} values, is generally consistent with previous reports investigating the impact of dilution (35,149). The quasi-irreversible or irreversible MDI of CYP2C19 by omeprazole (rather than reversible inhibition) likely explains, at least in part, the observed clinical interactions between omeprazole (and esomeprazole) and CYP2C19 substrates, including clopidogrel, notwithstanding the considerable debate surrounding the role of CYP2C19 in the activation of the latter drug (80,81) (see Chapter 1 for additional review of this topic).

Why did previous in vitro studies miss the MDI of CYP2C19 by omeprazole?

The IC_{50} or *K*i values for inhibition of CYP2C19 in HLM by omeprazole reported in the literature range from 150 μM to 1 μM in >40 studies (27). The lowest values (1 and ~4 μM) were reported with some of the longest substrate incubation periods (60 – 120 min; presumably used due to the low turnover of *S*-mephenytoin), and few (if any) studies specifically included a pre-incubation with NADPH-fortified HLM to examine the possibility of MDI of CYP2C19. Based on Fig. 4.5, 60 – 120 min would provide ample time for inactivation of CYP2C19 by omeprazole during the substrate incubation, therefore leading to "unintentional" MDI and artificially low IC_{50} or *K*i values, as reviewed previously (35). The data also show that the IC_{50} shift diminishes as higher protein concentrations and longer substrate incubation times are utilized (Figure 4.2b),

likely due to the combination of inhibitor depletion (Figure 4.2e) and the “unintentional” MDI during the long substrate incubation (35).

Would clinically relevant CYP2C19 inhibition by omeprazole be predicted on the basis of direct inhibition alone?

As noted in the introduction to this chapter, and in Chapter 1, clinically significant inhibition of CYP2C19 by omeprazole would not be predicted based on competitive inhibition alone. A thorough prediction of the impact of omeprazole on CYP2C19 substrates based on the experimentally determined K_I and k_{inact} values necessitated the use of physiologically based pharmacokinetic (PBPK) modeling to allow dynamic simulation of changes to both omeprazole (including self-inhibition), substrate concentrations as well as enzyme turnover (i.e., a so-called mechanistic dynamic model [MDM]), with the mechanistic static model (MSM, Equation 3.1) used as a comparator.

In the MDM under conditions where in vitro inhibitor depletion and microsomal protein binding of omeprazole were minimal (Figure 4.1e-f; i.e., K_I = 1.7 μM, Figure 4.5d) the level of active CYP2C19 is predicted to decrease to ~ 10% of baseline, after approximately 7 days of simulated omeprazole administration (Figure 4.8a) which could cause up to a 10-fold increase in the AUC of compounds predominantly metabolized by CYP2C19. When the higher estimate of K_I is used in the MDM (obtained with a 25-fold dilution, under conditions in which significant inhibitor depletion occurs, Figure 4.2e), the level of active CYP2C19 is predicted to decrease to ~60% of baseline, after approximately 12 days of simulated omeprazole administration (Figure 4.8b). Although *S*-mephenytoin is a model CYP2C19 probe substrate, only a 1.45 - 5.46-fold increase in its AUC (depending on K_I) is predicted by the MDM after 14 days of simulated omeprazole administration (40 mg b.i.d.), partly because of the contribution of other enzymes to

its metabolism (e.g. CYP2B6 and CYP2C9 (146,147)), and possibly due to less than complete inactivation of CYP2C19.

In the MSM, when the lowest value of K_I is used, omeprazole is predicted to cause a 2.85-fold increase in the AUC of a drug such as moclobemide which has an $f_{mCYP2C19}$ of 0.72 (112). The predicted AUC increase with moclobemide falls to 1.96-fold with the K_I value of 9.1 μM. If the $f_{mCYP2C19}$ were equal to 1.0, and the lowest K_I value used, omeprazole is predicted to cause up to a 10.4-fold increase in the AUC of such a hypothetical "perfect" CYP2C19 substrate. However, because there is up to a 14.6-fold increase in the AUC of omeprazole in CYP2C19 PMs relative to EMs, (137), this prediction suggests that omeprazole does not completely inactivate CYP2C19, which is consistent with either scenario in the MDM after several days of administration of omeprazole (Figure 4.8).

The clinical example of moclobemide ($f_{mCYP2C19}$ = 0.72) is generally in agreement with these predictions, with AUC_∞ increases averaging 2.21-fold (1.03 to 3.39-fold) in CYP2C19 EMs with omeprazole coadministration (112). The AUC increases predicted with the lowest K_I in the MSM value fall within this observed range. In addition, in order to achieve the reported 1.39-fold increase in AUC of clopidogrel with concomitant dosing of omeprazole (84), the $f_{mCYP2C19}$ for clopidogrel would need only to be approximately 0.31 according to the MSM.

Given the large difference in predicted active CYP2C19 after several days of simulated omeprazole administration in the MDM depending on which K_I value is used (Figure 4.8), the importance of determining the K_I value under conditions where microsomal protein binding and inhibitor depletion are minimized is underscored, similar to the case with IC_{50} values (35).

Is there clinical evidence of CYP2C19 inhibition by omeprazole?

In vivo evidence for MDI of CYP2C19 by omeprazole has already been reported (also reviewed in Chapter 1). For instance, Klotz reported that healing rates of GERD after 4 weeks' therapy with esomeprazole were not dependent on CYP2C19 status, as they are for lansoprazole (150). Based on the metabolite ratios of 5´-hydroxyomeprazole (formed by CYP2C19) to omeprazole sulfone (formed by CYP3A4), it was concluded that CYP3A4 plays the major role in the metabolism of esomeprazole after multiple dosing, consistent with autoinhibition of CYP2C19 and conversion of CYP2C19 EMs to IMs or PMs after repeat dosing (150). The changes in metabolite ratio suggests that the impact of multiple dosing on omeprazole reflects autoinhibition of CYP2C19, rather than increased stability due to higher gastric pH as originally suspected, especially because such time-dependent changes do not occur with other PPIs. On the other hand, the prescribing information for Nexium states "at repeated once-daily dosing with 40 mg, the systemic bioavailability is approximately 90% compared to 64% after a single dose of 40 mg" (119). In addition, Andersson and Weidolf (113) reported that when 15 mg of either omeprazole (i.e., the racemate), esomeprazole or *R*-omeprazole was administered orally for seven days, exposure to esomeprazole (plasma AUC) increased by approximately twofold over 7 days, whereas exposure to omeprazole increased by only 52%, and exposure to *R*-omeprazole actually decreased by 9%. These results are consistent with the in vitro results presented in this chapter showing that the inhibition of CYP2C19 by *R*-omeprazole appears to be largely reversible, whereas that of the racemate and esomeprazole are largely irreversible (Figure 4.7).

In vivo evidence for MDI of CYP2C19 by omeprazole also comes from clinical DDI studies with omeprazole as the perpetrator. For instance, in CYP2C19 extensive metabolizers (but not in poor metabolizers), the AUC of moclobemide increased by ~31% after a single 40 mg dose of omeprazole, but increased by 121% after 8 days of dosing with 40 mg omeprazole

(112). Such an apparent increase in the exposure of a victim drug with repeated dosing of the perpetrator drug is often apparent with MDIs. In addition, omeprazole (but not lansoprazole or pantoprazole) has long been known to inhibit the metabolism of diazepam in vivo, and this inhibition occurs in CYP2C19 EMs but not PMs, further suggesting the mechanism involves CY2C19 inhibition by omeprazole (151-153).

Does MDI of CYP2C19 by omeprazole explain the PPI-clopidogrel interaction?

The data and the predictions detailed above may explain, at least in part, the interaction between omeprazole (or esomeprazole) and clopidogrel. As noted in the introduction to this chapter, the FDA specifically warns against coadministration of clopidogrel and omeprazole (109). Given that the *in vivo* half-life of omeprazole (and other PPIs) is short, and plasma protein binding is high, it is remarkable that many publications attributed the clopidogrel-omeprazole interaction to *competitive* (reversible) inhibition of CYP2C19 by omeprazole, with some suggestion that separation of dosing can prevent the interaction (47,154,155). However, it should be noted that for clopidogrel, genetic differences in both the metabolism or transport of the drug and in the therapeutic target (the $P2Y_{12}$ receptor on platelets), as well as environmental factors (e.g., diet, disease, coadministered drugs) have been implicated in the variation in its clinical effect (47,154-156). As noted in Chapter 1, however, later pooled analysis of $P2Y_{12}$ receptor, CYP1A2, CYP2B6, CYP2C9, CYP2C19, CYP3A5, CYP2D6, and P-gp polymorphisms in nearly 400 subjects found that only CYP2C19 status had a significant impact on the antiplatelet effect of clopidogrel (68).

In addition, the interaction between omeprazole (or esomeprazole) and clopidogrel is particularly complex, as noted by Zhang et al. (157). These authors note that clopidogrel itself is an MDI of CYP2C19, increasing the ratio of 5´-hydroxyomeprazole to omeprazole by ~75% in CYP2C19 EMs (144,157) and that both clopidogrel and its 2-oxo metabolite (the precursor to

the active metabolite) also directly inhibit CYP2C19 with IC_{50} values ≤1 μM. The authors suggested that the "stronger" effect of omeprazole on CYP2C19 may be due to the "time-dependent" inhibition reported in the preliminary work (157). The finding of irreversible or quasi-irreversible inactivation of CYP2C19 by omeprazole, with up to a predicted 90% decrement in active CYP2C19 after approximately 7 days of simulated dosing (Figure 4.8a) is consistent with this hypothesis. The fact that the FDA warning applies only to omeprazole or esomeprazole (109) and not the other PPIs is consistent with a lack of MDI by the other PPIs examined in this study.

Given only minor inhibitory effects of omeprazole on other P450 enzymes (Table 4.2), the MDI of CYP2C19 by omeprazole and the reports of clinical interactions are consistent with a significant role for CYP2C19 in the metabolism of clopidogrel. In addition, as described in the introduction to this chapter, direct inhibition of CYP2C19 by other PPIs is not likely to be the cause of a clinically significant interaction with clopidogrel, which is consistent with the lack of in vitro MDI of CYP2C19 by lansoprazole and pantoprazole reported in this chapter, and a lack of clinically significant pharmacokinetic interactions between either lansoprazole or pantoprazole and clopidogrel (27).

Potential mechanisms of inactivation of CYP2C19 by omeprazole

Follow up studies to further elucidate the mechanism of inactivation of CYP2C19 by esomeprazole are covered in Chapters 5 – 7 of this dissertation. However, a few possibilities for the mechanism of CYP2C19 inactivation by omeprazole (or esomeprazole) were hypothesized at the time the work this was conducted based on the reported metabolism of the individual enantiomers of omeprazole (Figure 4.9, adapted from (113,158).

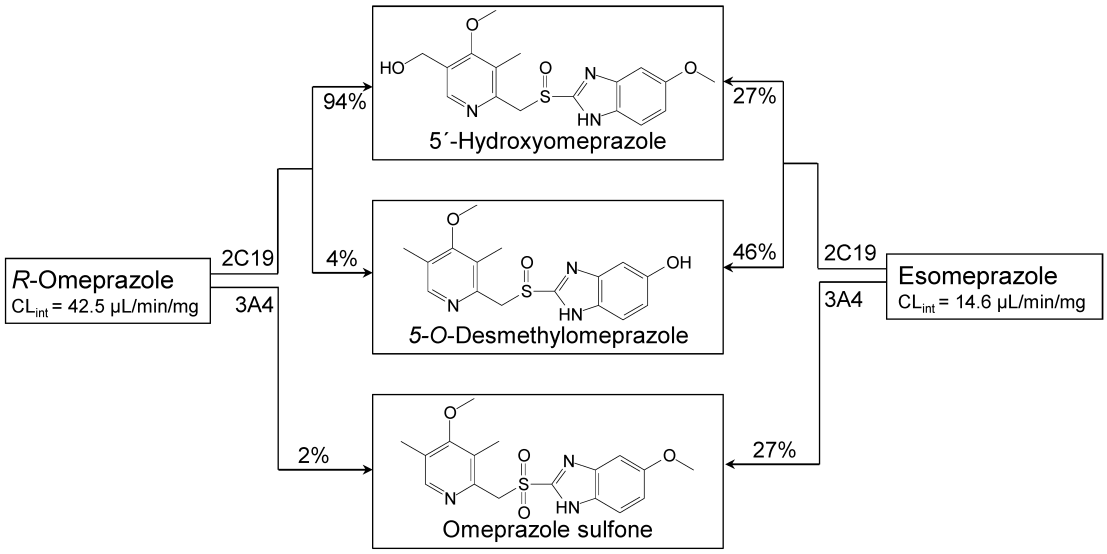

Figure 4.9. Metabolic scheme for omeprazole enantiomers

The conversion of each enantiomer of omeprazole to the major metabolites and enzymes responsible for each is shown. The scheme is adapted from that published by Andersson and Weidolf (113), which is in turn based on in vitro data published by Abelö et al. (158), which is the source of the CL_{int} values.

At the time the work presented in this chapter was published, it was hypothesized that methylhydroxylation of omeprazole to form 5´-hydroxyomeprazole could involve the intermediacy of a benzylic radical and heme alkylation, analogous to the inactivation of CYP2C8 by gemfibrozil glucuronide (33,159). The formation of 5-*O*-desmethylomeprazole (a *para*-aminophenol) could also lead to a reactive quinoneimine that could inactivate CYP2C19 if formed in its active site. The latter possibility may be unlikely given that the 5-hydroxylation of lansoprazole also leads to *para*-aminophenol formation (Figure 4.10; admittedly a tautomer of the analogous 5-*O*-desmethylomeprazole *para*-aminophenol), and yet lansoprazole is not an MDI of CYP2C19 (Figure 4.4a). Because the presence of glutathione could mitigate inhibition caused by such a mechanism, this possibility was followed up and will be presented in the following chapters.

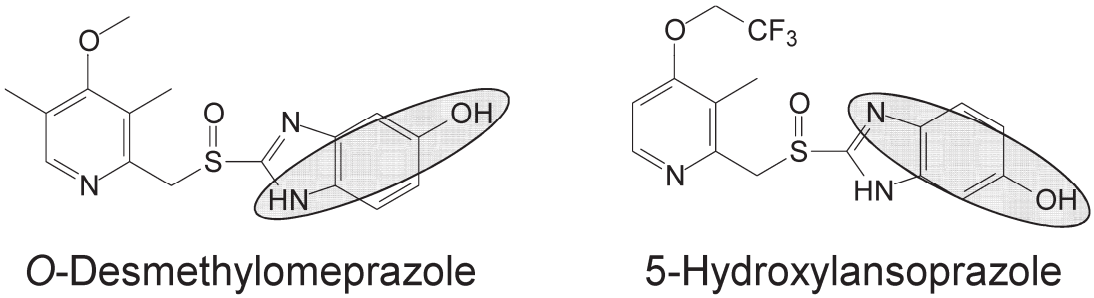

O-Desmethylomeprazole 5-Hydroxylansoprazole

Figure 4.10. Possible para-aminophenol formation from metabolites of omeprazole and lansoprazole

Major metabolites of omeprazole (*O*-desmethylomeprazole) and lansoprazole (5-hydroxylansoprazole) are shown. The highlighted area indicates the part of the molecules that are potentially reactive para-aminophenols.

However, the data presented in Figure 4.7 suggest that esomeprazole has a greater MDI effect on CYP2C19 than does *R*-omeprazole. These data are in fact consistent with clinical observations in which the plasma C_{max} of esomeprazole (40 mg q.d., oral solution) increases from 3.07 to 4.86 μM from day 1 to day 5, and that of omeprazole (40 mg q.d., oral solution) increases from 2.32 to 3.87 μM, while that of *R*-omeprazole (40 mg q.d., oral solution) only increases from 1.62 to 1.98 μM (135). In addition, published in vitro results in HLM suggest that the CL_{int} for esomeprazole sulfoxidation (catalyzed by CYP3A4) is 4.6-fold greater than that for *R*-omeprazole (158), even though the total CL_{int} for *R*-omeprazole is approximately threefold higher than for esomeprazole. This finding is even more apparent in the clinical data, which show an approximately 14-fold higher AUC for the sulfone when esomeprazole is administered for one day (20 or 40 mg) than for *R*-omeprazole; this ratio increases to nearly 40-fold after 5 days' dosing (158) because CYP3A4 plays a more important role in esomeprazole metabolism after multiple dosing (150). Because of the finding that omeprazole sulfone is also an MDI of CYP2C19, it seemed possible at the time these data were generated that the combination of effects from esomeprazole and its sulfone explain the much greater inactivation of CYP2C19 by esomeprazole than *R*-omeprazole, and this possibility is followed up on in Chapters 5-6.

At the same time, the CL_{int} for the 5′-hydroxylation of *R*-omeprazole is approximately 10-fold higher than for esomeprazole, which, along with the results presented in this chapter (Figure 4.7) suggest that, unless there is also a difference in the ultimate fate of *R*- vs. *S*-5′-hydroxyomeprazole (e.g., benzylic radical formation and oxygen rebound or other inactivating pathways), this pathway may not explain the formation of a reactive metabolite that inactivates CYP2C19. Enantiomer-enantiomer interactions at the active site of CYP2C19 when the racemate is used (as in some experiments in this study) could also complicate the interpretation of results with the single enantiomers as previously described (160), especially considering that the presence of *R*-omeprazole acts as an alternative substrate and offers

substrate-protection for the irreversible inactivation by esomeprazole or its sulfone. It is for this reason that primarily esomeprazole is investigated in later chapters.

In conclusion, in this study it was shown that omeprazole (but not pantoprazole or lansoprazole) is an MDI of CYP2C19 in HLM, cryopreserved human hepatocytes and recombinant human CYP2C19. Based on the K_I and k_{inact} values for the MDI of CYP2C19 by omeprazole in HLM, it was predicted that this inactivation is clinically significant. Furthermore, evidence was provided that esomeprazole is more likely to irreversibly inactivate CYP2C19 than is *R*-omeprazole. These findings have implications for the ongoing debate surrounding the interaction between clopidogrel (as well as other CYP2C19 substrates) and omeprazole and, in particular, esomeprazole, which is followed up on in the following chapters.

Chapter 5. ESOMEPRAZOLE AND TWO METABOLITES AS METABOLISM-DEPENDENT INHIBITORS (MDIs) OF CYP2C19

Abstract

As shown in the previous chapter, simulations of the effect of omeprazole on CYP2C19 did not predict complete inactivation of this enzyme. I hypothesized that the overall irreversible inhibitory effect of omeprazole (and esomeprazole in particular) on CYP2C19 may be due to a combination of effects of the parent drug and its sulfone (already established as a metabolism-dependent inhibitor of CYP2C19) as well as the 5-*O*-desmethyl metabolite. In an effort to characterize the potency with which esomeprazole and its major metabolites inactivate CYP2C19, experiments were undertaken in NADPH-fortified pooled human liver microsomes (HLM) under various conditions. 5-*O*-desmethyl omeprazole was first established as a metabolism-dependent inhibitor of CYP2C19 with an IC_{50} shift of 5.6-fold. Ultracentrifugation experiments subsequently established that, like esomeprazole, the MDI of CYP2C19 by omeprazole sulfone and 5-*O*-desmethyl omeprazole was largely irreversible. Depending on the experimental conditions used, K_I and k_{inact} values ranged from 3.23 – 13.9 μM and 0.048 – 0.068 min^{-1}, respectively for esomeprazole; 0.8 – 5.5 μM and 0.017 – 0.025 min^{-1}, respectively for omeprazole sulfone, and 10.3 – 11.9 μM and 0.025 – 0.028 min^{-1}, respectively for 5-*O*-desmethyl omeprazole. A mechanistic static drug-drug interaction model incorporating these values along with those for omeprazole or esomeprazole, was also employed in an attempt to rationalize the clinical interaction between omeprazole or esomeprazole and clopidogrel in terms of CYP2C19 inactivation. The model overpredicted (by a factor of ~2) the ability of omeprazole to block the conversion of clopidogrel to H4, but established that inactivation of CYP2C19 is the likely mechanism for the clinical interaction between omeprazole/esomeprazole and clopidogrel. The results of this study suggest that esomeprazole inactivates CYP2C19 at a rate similar to racemic omeprazole, and that omeprazole sulfone as well as 5-*O*-desmethyl omeprazole can also contribute to the overall *in vivo* inactivation of CYP2C19 by omeprazole and esomeprazole.

Introduction

In Chapter 4, I presented data showing that omeprazole (but not pantoprazole or lansoprazole) is an MDI of CYP2C19 in human liver microsomes (HLM), cryopreserved human hepatocytes and recombinant human CYP2C19 (34). I also presented evidence that esomeprazole is more likely to irreversibly inactivate CYP2C19 than is *R*-omeprazole. The major omeprazole metabolites, namely omeprazole sulfone, omeprazole sulfide and 5´-hydroxyomeprazole were also investigated as MDIs of CYP2C19 in pooled HLM, and only omeprazole sulfone was found to be an MDI (Chapter 4). Another major omeprazole metabolite, 5-*O*-desmethyl omeprazole, was not investigated in Chapter 4, and was therefore characterized as part of the studies presented in this chapter (for structure, see Figure 4.9). The studies presented in this chapter were undertaken as a further step toward characterizing the effect of esomeprazole and its metabolites on CYP2C19 pooled HLM with the ultimate goal of providing a basis for the clinically relevant interaction between esomeprazole and clopidogrel or other CYP2C19 substrates.

Results

5.1. Inhibitory effects of 5-*O*-desmethyl omeprazole on *S*-mephenytoin 4´-hydroxylation in human liver microsomes: IC_{50} shifts

5-*O*-Desmethyl omeprazole was not initially examined in the studies presented in Chapter 4, but as noted, is a major metabolite of esomeprazole and its formation (as a para-aminophenol) could lead to a reactive quinoneimine that could inactivate CYP2C19 if formed in its active site. Based on this possibility, IC_{50} determinations toward CYP2C19 activity as detailed in Chapter 3 were made. Once a commercial source of 5-*O*-Desmethyl omeprazole was found, qualitative solubility testing was undertaken, and this metabolite was found to have low solubility in the solvent used for the other compounds. Various combinations of solvents were attempted with the most successful being a mixture of methanol/DMSO/Tris buffer (at pH 9.0 to allow greater stability of the stock for longer storage) at 70/20/10% v/v/v, respectively, with an approximate stock concentration of 7 mM achieved. This combination of solvents was then used for additional experiments with this metabolite.

5-*O*-Desmethyl omeprazole was evaluated as a direct-acting and MDI of CYP2C19 activity (*S*-mephenytoin 4´-hydroxylation) in pooled human liver microsomes (n = 16, 0.1 mg/mL) at a substrate concentration approximately equal to the K_m for the marker reaction (40 µM). The results are summarized in Figure 5.1. The results show that 5-*O*-desmethyl omeprazole caused MDI of CYP2C19 as evidenced by a left shift in IC_{50} curves (44 → 8.2 µM or ~5.4-fold shift) following a 30-min pre-incubation with NADPH-fortified HLM. The IC_{50} value following a 30-min pre-incubation in the absence of NADPH (i.e., 93 µM) was higher than that in the presence of NADPH, suggesting that the time-dependent inhibition of CYP2C19 by these compounds was in fact also metabolism-dependent.

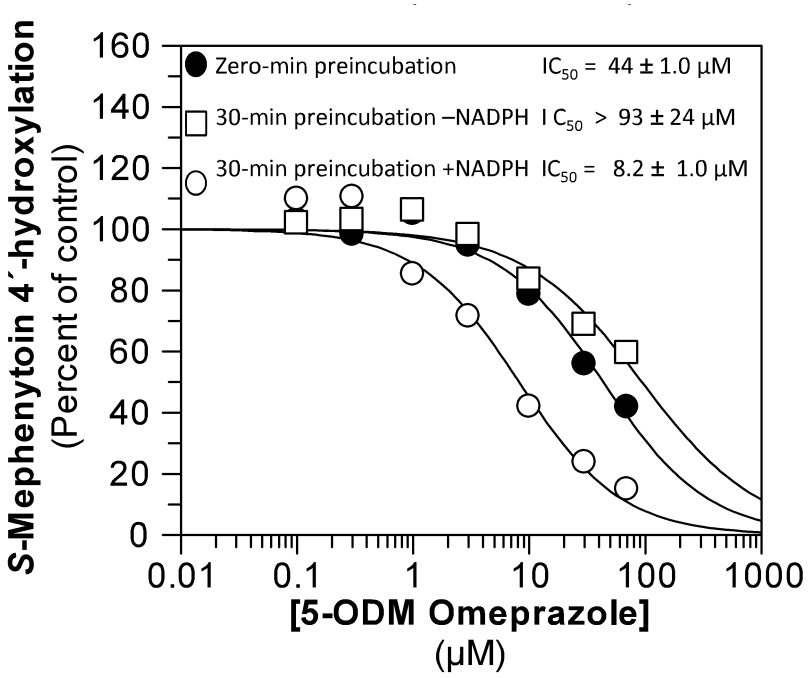

Figure 5.1. Evaluation of 5-*O*-desmethylomeprazole as a direct-acting and MDI of CYP2C19

Each symbol represents the average of duplicate determinations. 5-*O*-desmethyl omeprazole inhibited CYP2C19 in pooled HLM with IC50 values as shown (S-mephenytoin 4´-hydroxylation solvent control rates = 53.5, 58.8, and 45.8 pmol/mg/min for zero-min, 30-min –NADPH, and 30-min + NADPH pre-incubations, respectively).

5.2. Determination of irreversibility of MDI for omeprazole sulfone and 5-ODM omeprazole

Having established that omeprazole sulfone and 5-ODM omeprazole were metabolism-dependent inhibitors of CYP2C19 (Table 4.1 and Figure 5.1, respectively), these metabolites were further examined to determine whether the inactivation of CYP2C19 involved irreversible or quasi-irreversible inhibition based on the ultracentrifugation method described in Chapters 3 and 4 and previously (34,35). A concentration of omeprazole sulfone that caused nearly complete (i.e., >~90% inhibition) after 30-min pre-incubation with NADPH, but incomplete (<~85%) inhibition after 30-min pre-incubation in the absence of NADPH was chosen (i.e., 100 μM). Because the solubility of 5-ODM omeprazole was limiting, 70 μM was chosen as the concentration to be investigated, which caused ~40% inhibition after 30-min pre-incubation in the absence of NADPH but ~85% inhibition after 30-min pre-incubation in the absence of NADPH. Pooled HLM were treated with inhibitor or solvent for 30 min in the presence of NADPH, and in the presence or absence of potassium ferricyanide (to potentially reverse the formation of a metabolite inhibitory complex associated with quasi-irreversible inactivation) (Figure 5.2). Following the 30-min incubation, pooled HLM samples were either (1) assayed directly for residual CYP activity ("pre-spin"), (2) re-isolated by ultracentrifugation and then assayed for residual CYP activity ("post-spin"), or (3) treated with potassium ferricyanide, re-isolated by ultracentrifugation and then assayed for residual CYP activity ("post-spin + $K_3[Fe(CN)_6]$"). Substantial direct inhibition was observed after treatment with omeprazole sulfone and 5-ODM omeprazole (Figure 5.2, "pre-spin"), consistent with the results of the IC_{50} determinations. Centrifugation alone or with potassium ferricyanide did not restore CYP2C19 activity after treatment with omeprazole sulfone or 5-ODM omeprazole. Taken together, these results suggest that the MDI of CYP2C19 observed by omeprazole sulfone and 5-ODM omeprazole is largely irreversible (possibly due to covalent binding to the apoprotein, heme moiety or both).

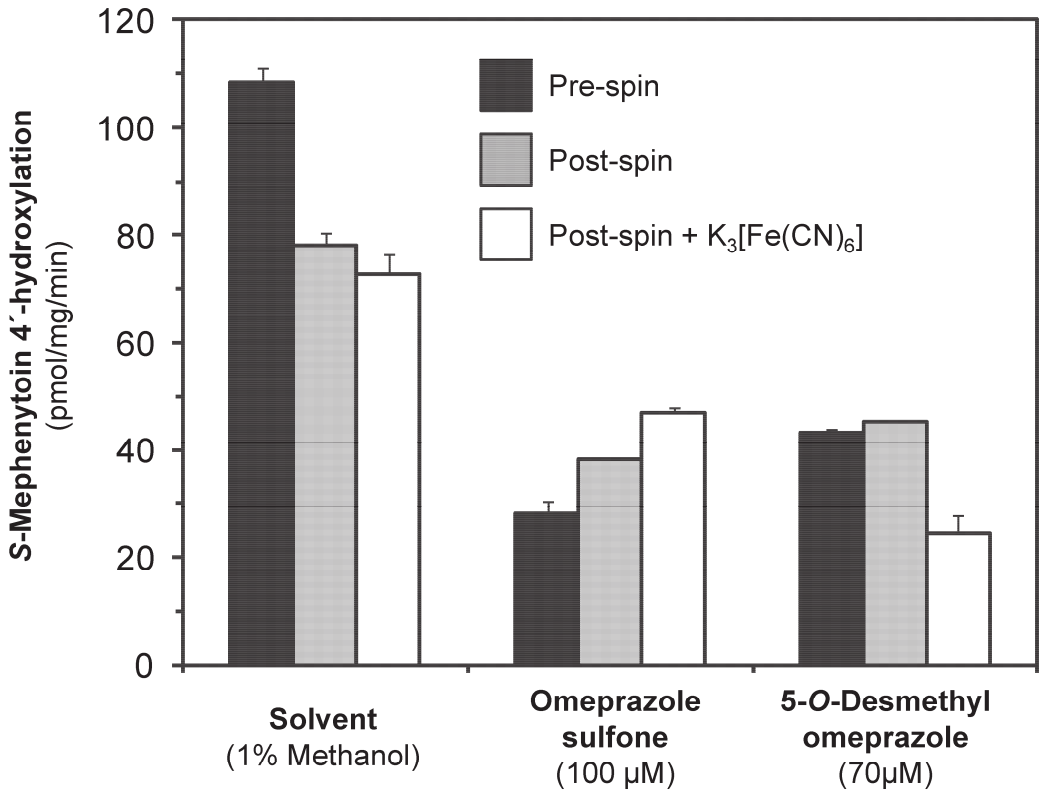

Figure 5.2. Reversibility assessment of the MDI of CYP2C19 by omeprazole sulfone and 5-ODM omeprazole with the ultracentrifugation method

The potential reversibility of the MDI of CYP2C19 NADPH-fortified HLM (0.1 mg/mL) by omeprazole sulfone and 5-ODM omeprazole (at concentrations shown) was evaluated with the ultracentrifugation method, as described in *Chapter 3*. Incubations labeled "Pre-spin" were conducted similarly to analogous samples in the IC_{50} determinations (conduced in triplicate and displayed as the average rates of *S*-mephenytoin 4´-hydroxylation ± standard deviation). For incubations labeled "Post-spin" (conducted in triplicate), microsomal protein was isolated by ultracentrifugation after 30 min incubations with the inhibitor and NADPH, and analyzed in triplicate for residual CYP2C19 activity (*S*-mephenytoin 4´-hydroxylation) displayed as the average rates ± standard error, as described in *Chapter 3*. Half of the incubations from the "Post-spin" samples included potassium ferricyanide (2 mM, final concentration) as indicated. Samples treated with methanol (1% v/v, final) served as controls. All rates were normalized to final microsomal protein concentrations, as described in *Chapter 3*.

5.3. Inactivation of CYP2C19 by esomeprazole: K_I and k_{inact} determinations

Because I had previously established that the MDI of CYP2C19 by esomeprazole was largely irreversible (Figure 4.7), I performed experiments to determine K_I (the concentration of esomeprazole supporting half maximal rate of CYP2C19 inactivation) and k_{inact} (the first order rate constant of enzyme inactivation). The results from three different experiments are summarized in Figure 5.3 and Table 5.1. The three experimental conditions were (1) "high" [HLM] (i.e., 1 mg/mL in pre-incubation) (Figure 5.3a - b), (2) "low" [HLM] (i.e., 0.1 mg/mL in pre-incubation) (Figure 5.3c-d), and (3) "medium" [HLM] (i.e., 0.5 mg/mL in pre-incubation) (Figure 5.3e-f). In all experiments, a 10-fold dilution step was utilized prior to the substrate incubation, which included *S*-mephenytoin (the marker substrate) at 10 × K_m. Under all three conditions, the inactivation of CYP2C19 was dependent on the concentration of esomeprazole (over the ranges examined) and the time course conformed to a first-order inactivation process (as indicated by the linearity of plots of the log of the residual enzyme activity against time; (Figure 5.3a, c, and e). However, because near-saturation of inactivation was not achieved in the first two experiments at esomeprazole concentrations up to 30 μM in pre-incubation, the final experiment used concentrations that were twice those used in the first two experiments. As with omeprazole (Chapter 4), the K_I values for esomeprazole generally decreased with microsomal protein concentration (Figure 5.3b and d). However, because of poor analytical sensitivity and a lack of saturation of inactivation under low protein conditions (Figure 5.3c-d), the K_I value actually decreased from this value at medium protein conditions (Figure 5.3e-f). Because of the acceptable analytical sensitivity at 0.05 mg/mL microsomal protein (final), the third experiment was considered definitive. However, in all three cases, the k_{inact} values ranged from approximately 0.048 – 0.068 min^{-1}, which means that, in the presence of saturating concentrations of esomeprazole, approximately 5 - 7% of CYP2C19 was inactivated every minute. The efficiency of CYP2C19 inactivation (k_{inact}/K_I) also increased by a factor of

approximately three when the concentration of HLM was decreased from 0.1 mg/mL (Figure 5.3b) to 0.05 mg/mL (Figure 5.3f) and saturating concentrations of esomeprazole were used. Taken together, these data further suggest that esomeprazole is an irreversible inactivator of CYP2C19.

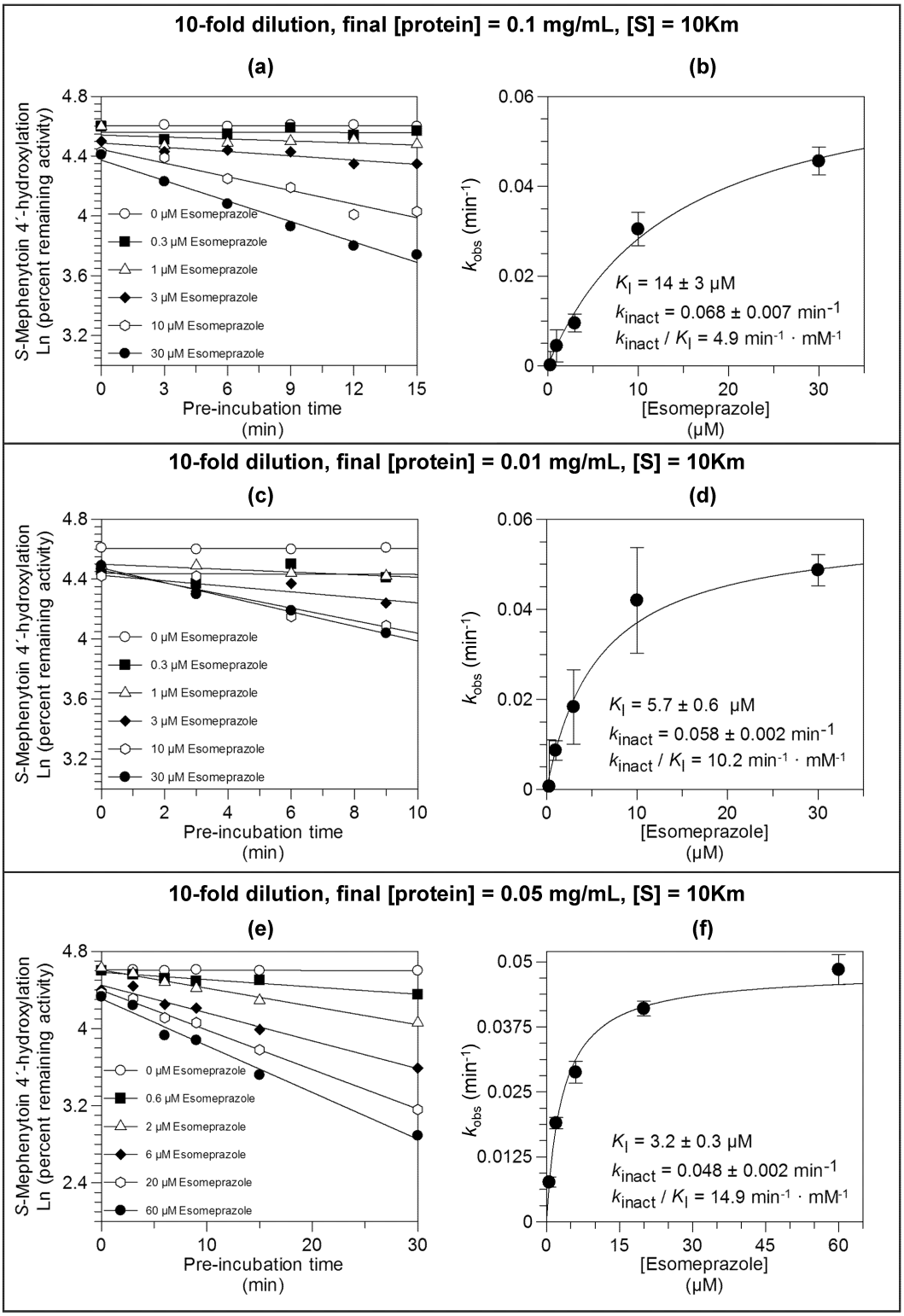

Figure 5.3. Determination of K_I and k_{inact} for the MDI of CYP2C19 by esomeprazole at various final protein concentrations

Individual points represent the average of triplicate determinations ± standard deviation, unless otherwise noted. For graphs in (a), (c), and (e) esomeprazole was pre-incubated (at concentrations indicated) and residual CYP2C19 activity determined (at final protein concentrations indicated) as described in *Chapter 3*. The graphs in (b), (d), and (f) represent the direct plots of the initial rates of inactivation of CYP2C19. Values are the slopes of the initial rates of inactivation (k_{obs}) at each concentration of esomeprazole, shown ± standard error.

5.4. Inactivation of CYP2C19 by omeprazole sulfone: K_I and k_{inact} determinations

Having shown that, like esomeprazole, the metabolism-dependent inhibition of CYP2C19 by omeprazole sulfone was largely irreversible (Figure 5.2), I also determined its K_I and k_{inact}, under the same three conditions used for esomeprazole (section 5.3). The results from these three experiments are summarized in Figure 5.4 and Table 5.1. As for esomeprazole, the three experimental conditions were (1) "high" [HLM] (i.e., 1 mg/mL in pre-incubation) (Figure 5.4a - b), (2) "low" [HLM] (i.e., 0.1 mg/mL in pre-incubation) (Figure 5.4c-d), and (3) "medium" [HLM] (i.e., 0.5 mg/mL in pre-incubation) (Figure 5.4e-f). In each experiment, a 10-fold dilution step was utilized prior to the substrate incubation. Under all three conditions, the inactivation of CYP2C19 was dependent on the concentration of omeprazole sulfone (over the ranges examined) and the time course conformed to a first-order inactivation process (as indicated by the linearity of plots of the log of the residual enzyme activity against time (Figure 5.4a, c, and e). However, because saturation of inactivation was achieved in the first two experiments (i.e., K_I values ≈ 1 – 4 μM) at omeprazole sulfone concentrations up to 100 μM in pre-incubation, the final experiment used lower concentrations and longer pre-incubations in an attempt to more accurately determine the K_I value. The apparent K_I values for the inactivation of CYP2C19 by omeprazole sulfone did not vary substantially between 0.1 and 0.05 mg/mL final microsomal protein concentration (Figure 5.4b and f). However, because of poor analytical sensitivity under low protein conditions (Figure 5.4c-d), the K_I value decreased by a factor of 5.5 from that at high protein conditions (Figure 5.4a-b). Because of the acceptable analytical sensitivity at 0.05 mg/mL microsomal protein (final), the third experiment was considered definitive, and further experiments were conducted under similar conditions. In spite of the variability in K_I values, the k_{inact} values spanned a relatively tight range from approximately 0.017 – 0.025 min^{-1}, which means that, in the presence of saturating concentrations of omeprazole sulfone, approximately 1.7 – 2.5% of CYP2C19 was inactivated every minute. The efficiency of

CYP2C19 inactivation (k_{inact}/K_I) remained within a factor of 1.5 when the final concentration of HLM was decreased from 0.1 mg/mL (Figure 5.4b) to 0.05 mg/mL (Figure 5.4f). These data provide additional evidence that omeprazole sulfone is an irreversible inactivator of CYP2C19.

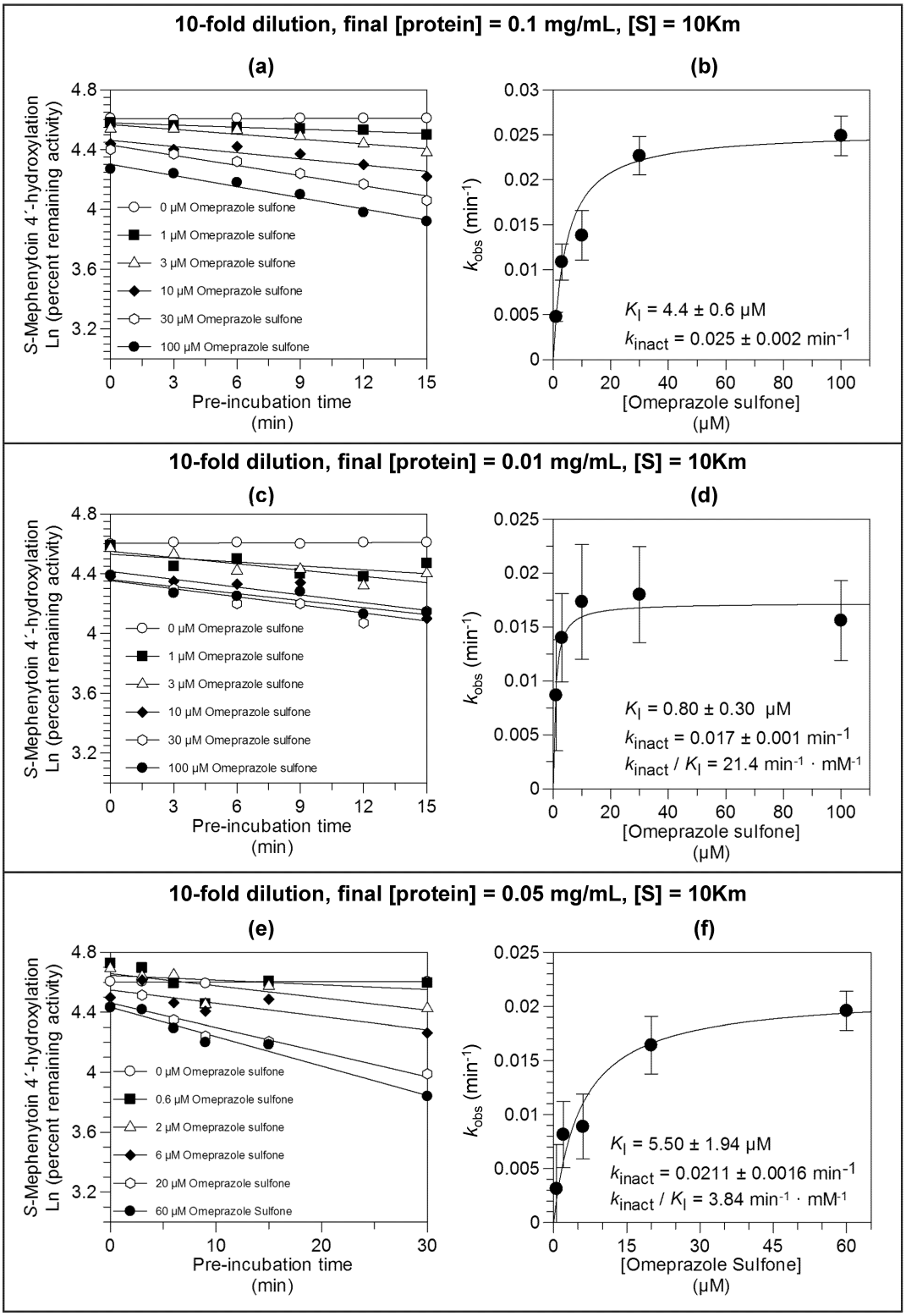

Figure 5.4. Determination of K_I and k_{inact} for the MDI of CYP2C19 by omeprazole sulfone at various final protein concentrations

Individual points represent the average of triplicate determinations ± standard deviation, unless otherwise noted. For graphs in (a), (c), and (e) omeprazole sulfone was pre-incubated (at concentrations indicated) and residual CYP2C19 activity determined (at final protein concentrations indicated) as described in *Chapter 3*. The graphs in (b), (d), and (f) represent the direct plots of the initial rates of inactivation of CYP2C19. Values are the slopes of the initial rates of inactivation (k_{obs}) at each concentration of omeprazole sulfone, shown ± standard error.

5.5. Inactivation of CYP2C19 by 5-*O*-desmethyl omeprazole: K_I and k_{inact} determinations

The experience gained in the experiments detailed in Figure 5.3 and Figure 5.4 allowed me to move forward with additional experiments under a single set of experimental conditions, namely 0.5 mg/mL pooled human liver microsomes in the pre-incubation with a 10-fold dilution, and marker substrate assay at 10 × K_m. Reproducibility under these conditions was explored in additional "quality control" assays which will be detailed in Chapter 6.

Having also shown that the metabolism-dependent inhibition of CYP2C19 by 5-ODM omeprazole was largely irreversible (Figure 5.2), I determined the K_I and k_{inact} values for this major metabolite of esomeprazole, but only under the "definitive" conditions (i.e., 0.5 mg/mL pooled human liver microsomes in pre-incubation with a 10-fold dilution and substrate at 10 × K_m). However, as noted previously, this metabolite was found to have poor solubility in standard solvents and a mixture of methanol/DMSO/Tris buffer (at pH 9.0 for greater stability of the stock) at 70/20/10%v/v, respectively, was used. However, the stock solution (7 mM) appeared to precipitate during the course of the first experiment, and I was concerned about the accuracy of any K_I value obtained with this preparation (Figure 5.5a-b). Because of this, I prepared a new stock solution with a top concentration of 6 mM and conducted a second experiment (Figure 5.5c-d).

The results from the two different experiments are summarized in Figure 5.5 and Table 5.1. In both experiments, the inactivation of CYP2C19 was dependent on the concentration of 5-ODM omeprazole (over the ranges examined) and the time course conformed to a first-order inactivation process (as indicated by the linearity of plots of the log of the residual enzyme activity against time (Figure 5.5a and c). In spite of solubility concerns in the first experiment, the K_I value in the first experiment (11.9 μM) was within approximately 15% of the second

(10.3 μM). Similarly, k_{inact} values were within approximately 10% of one another (0.0251 and 0.0278 min^{1}), which means that, in the presence of saturating concentrations of 5-ODM omeprazole, approximately 2.5 – 2.8% of CYP2C19 was inactivated every minute. These data provide additional evidence that 5-ODM omeprazole is an irreversible inactivator of CYP2C19.

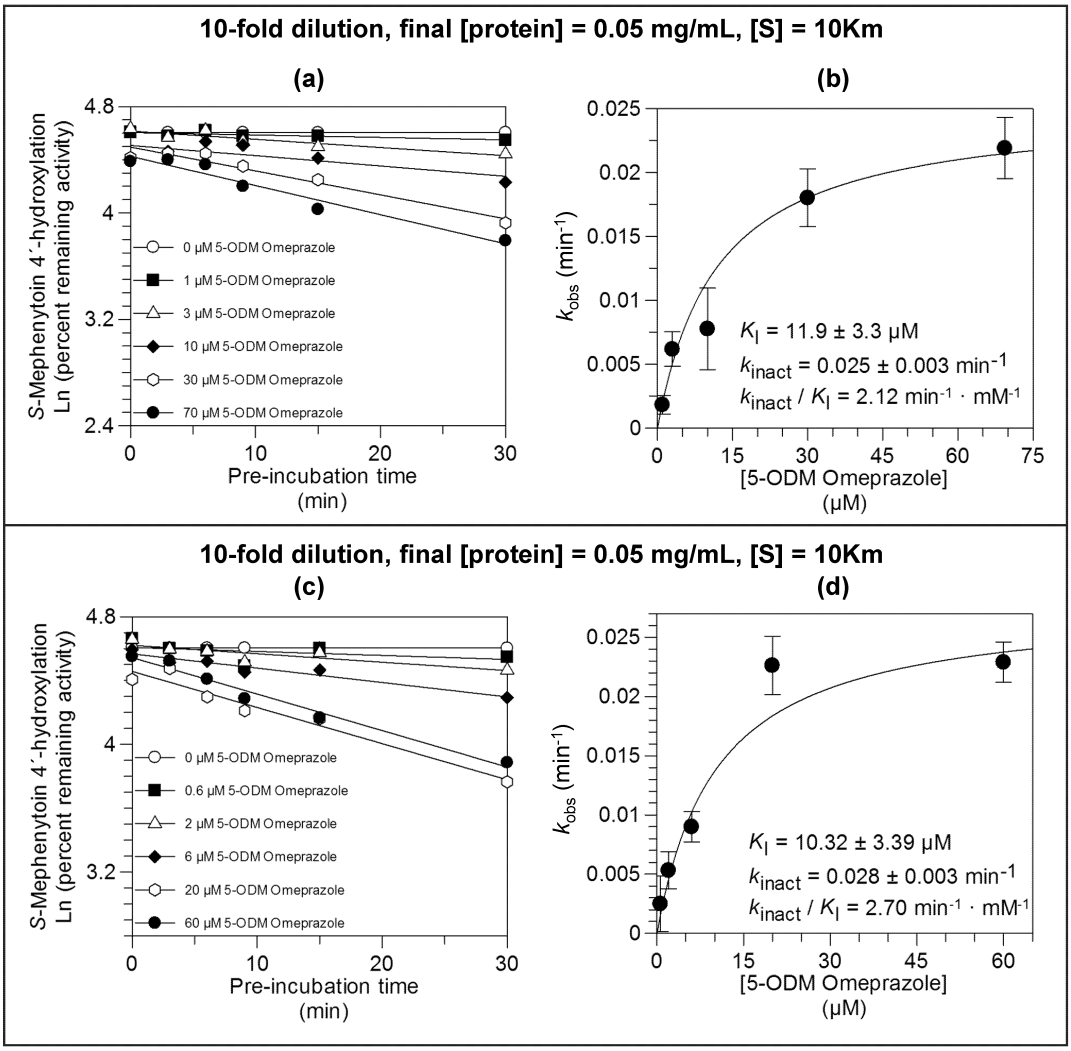

Figure 5.5. Determination of K_I and k_{inact} for the MDI of CYP2C19 by 5-ODM omeprazole on two different days

Individual points represent the average of triplicate determinations ± standard deviation, unless otherwise noted. For graphs in (a) and (c), 5-ODM omeprazole was pre-incubated (at concentrations indicated) and residual CYP2C19 activity determined as described in *Chapter 3*. The graphs in (b) and (d) represent the direct plots of the initial rates of inactivation of CYP2C19. Values are the slopes of the initial rates of inactivation (k_{obs}) at each concentration of 5-ODM omeprazole, shown ± standard error.

Table 5.1. Summary of K_I and k_{inact} determinations for esomeprazole, omeprazole sulfone and 5-*O*-desmethyl omeprazole

Compound	Final [Microsomal protein] (mg/mL)	K_I (μM) [a]	k_{inact} (min^{-1}) [a]	k_{inact} / K_I ($min^{-1} \cdot mM^{-1}$) [b]
Esomeprazole	0.1	13.9 ± 3.4	0.0677 ± 0.0072	4.86 ± 1.29
	0.01	5.73 ± 0.59	0.0582 ± 0.0018	10.2 ± 1.1
	0.05	**3.23 ± 0.35**	**0.0481 ± 0.0018**	**14.9 ± 1.7**
Omeprazole sulfone	0.1	4.43 ± 0.62	0.0254 ± 0.0015	5.73 ± 0.87
	0.01	0.803 ± 0.302	0.0172 ± 0.0009	21.4 ± 8.1
	0.05	**5.50 ± 1.94**	**0.0211 ± 0.0016**	**3.85 ± 1.39**
5-*O*-Desmethyl omeprazole	0.05 (Day 1)	11.9 ± 3.3	0.0251 ± 0.0027	2.12 ± 0.63
	0.05 (Day 2)	**10.3 ± 3.4**	**0.0278 ± 0.0033**	**2.70 ± 0.94**

[a] Values are displayed to three significant figures, ± standard error of the measurement.

[b] Calculated from full precision values and rounded to three significant figures.

Values in bold are considered the definitive values.

5.6. Estimation of the clinical impact of esomeprazole and its major metabolites on the decrease in H4 formation from clopidogrel

Based on the definitive K_I and k_{inact} values in Table 5.1, along with direct inhibition parameters presented in Figure 5.1 and Table 4.1 an attempt was made to estimate the in vivo impact that esomeprazole, omeprazole sulfone or 5-ODM omeprazole would have on the exposure to H4 upon coadministration of esomeprazole with clopidogrel under a number of scenarios as shown in Table 5.2 with two mechanistic static models, one with parameters as defined by Boulenc et al., (i.e., H4 ratio) and the other (i.e., 1/AUCR) with conservative default parameters defined by the FDA (31). Two $f_{m(CYP2C19)}$ values for the CYP2C19-dependent activation of clopidogrel to H4, reported by Boulenc et al. were used (94). The worst-case (i.e., most inhibitory) scenario for omeprazole (Figure 4.5e) was included as a comparator. The results in Table 5.2 are presented as reciprocal AUCR values (31) (because I was interested in a decrease in exposure to a metabolite, not an increase in AUC of the parent drug) and H4 AUC ratios following the method outlined by Boulenc and colleagues (94). Observed H4 ratios were included from two studies under similar omeprazole or esomeprazole dosing regimens (84,108) for comparison. The parameters used in the AUCR calculations, such as plasma protein binding, C_{max}, etc. for the metabolites were obtained from (75). The results of these simulations predict that omeprazole and esomeprazole would be expected to cause a significant decrease in exposure to H4. It should be noted that the effects of omeprazole metabolites were not added to the effects of omeprazole (because it worsened the over-prediction), but are modeled on their own for comparison.

Table 5.2. Predicted and observed impact on H4 formation after coadministration of either omeprazole or esomeprazole with clopidogrel

Perpetrator (dose and regimen)	Perpetrator C_{max} (μM)[a]	Predicted H4 ratio $f_{m(CYP2C19)}$ = 0.64[b]		Predicted H4 ratio $f_{m(CYP2C19)}$ = 0.72[b]		Observed H4 ratio
		1/AUCR[i]	H4 ratio[j]	1/AUCR[i]	H4 ratio[j]	
Omeprazole (20 mg single dose)[c]	0.660 (0.033)	0.46	0.59	0.40	0.54	NA
Omeprazole (20 mg 5 days)[d]	1.13 (0.057)	0.45	0.52	0.38	0.46	NA
Omeprazole (40 mg 5 days)[e]	3.87 (0.19)	0.40	0.42	0.32	0.35	NA
Omeprazole (80 mg 10 days)[f]	8.92 (0.45)	0.38	0.39	0.31	0.31	0.58[k]
Esomeprazole (20 mg single dose)[g]	1.32 (0.040)	0.44	0.63	0.37	0.59	NA
Esomeprazole (20 mg 5 days)[h]	2.1 (0.063)	0.43	0.57	0.36	0.51	0.62[l]
Esomeprazole (40 mg 5 days)[h]	4.7 (0.14)	0.40	0.47	0.32	0.41	0.63[l]
Omeprazole sulfone (20 mg omeprazole single dose)[c]	0.14 (0.0028)	NC	0.98	NC	0.98	NA
5-*O*-Desmethyl omeprazole (20 mg omeprazole single dose)[c]	0.030 (0.029)	NC	0.92	NC	0.91	NA

[a] Plasma C_{max} of drug or metabolite. Values in parentheses are the unbound plasma concentrations.

[b] From (94) where the two $f_{m(CYP2C19)}$ values for H4 were obtained from two clinical studies to determine the impact of CYP2C19 polymorphisms (68) or the effects of omeprazole or pantoprazole on H4 formation from clopidogrel (84).

[c] From (75). Value in parentheses is the unbound plasma concentration.

[d] From (161)

[e] From (135), used in Simcyp simulations presented in Chapter 4

[f] From (94)

[g] From (162)

[h] From Nexium (esomeprazole) prescribing information (119)

[i] 1/AUCR calculated based on (31)

[j] H4 ratio calculated based on (94)

[k] From (84)

[l] From (108)

NA: No studies found that match the perpetrator dose and regimen

NC: Not calculated for metabolites because the AUCR equations uses dose in mg.

Discussion

In my previous studies (Chapter 4) I presented evidence that omeprazole sulfone (formed by CYP3A4) was an MDI of CYP2C19 (Figure 4.3), and that esomeprazole was an irreversible MDI of CYP2C19 whereas *R*-omeprazole was not (Figure 4.7). Furthermore, because 5-*O*-desmethyl omeprazole is the major metabolite formed from esomeprazole based on in vitro intrinsic clearance (Figure 4.9), I speculated that that this metabolite also contributes to CYP2C19 inactivation (Figure 4.10), but it was not commercially available to examine at the time (34). These findings were followed up in this chapter, and I showed that 5-*O*-desmethyl omeprazole is in fact a metabolism-dependent inhibitor of CYP2C19 (Figure 5.1), and furthermore that both it and omeprazole sulfone irreversibly inactivate CYP2C19 (Figure 5.2).

The major metabolite formed from *R*-omeprazole based on in vitro intrinsic clearance is 5´-hydroxyomeprazole (Figure 4.9, (113)), which I previously showed was a weak direct inhibitor of CYP2C19 (i.e., IC_{50} > 100 μM) and not a metabolism-dependent inhibitor (Figure 4.3e). This finding is consistent with the nearly complete reversal of CYP2C19 inhibition by *R*-omeprazole upon centrifugation (Figure 4.7). The initial findings that both 5-*O*-desmethyl omeprazole and omeprazole sulfone were MDIs of CYP2C19 suggested the possibility that the clinically relevant CYP2C19 inhibition caused by omeprazole (reviewed in Chapter 1) is predominantly due to the combination of the presence of the *S*-enantiomer in the racemic drug, as well as formation of its major metabolites, 5-*O*-desmethyl omeprazole, mainly through CYP2C19, and omeprazole sulfone, mainly by CYP3A4. In an attempt to confirm or refute this hypothesis, I quantified the inactivation of CYP2C19 by each of these compounds.

K_I and k_{inact} values for esomeprazole, 5-*O*-desmethyl omeprazole and omeprazole sulfone were determined in order to attempt to predict the in vivo impact of esomeprazole and its inhibitory metabolites on CYP2C19, and clopidogrel in particular. Ideally, a PBPK model

would be used for this assessment as presented for omeprazole in Chapter 4. However, for a quantitative PBPK model to accurately predict the clinical impact of esomeprazole and its metabolites on clopidogrel, the kinetics of esomeprazole at steady-state, the formation-rate limited kinetics of 5-ODM omeprazole and the elimination rate-limited kinetics of omeprazole sulfone from both omeprazole and esomeprazole would be required (75,163). Most of these parameters are not currently available in the literature, although preliminary findings from my studies, including the K_I and k_{inact} values for esomeprazole, 5-*O*-desmethyl omeprazole and omeprazole sulfone, were previously presented (111,120). In spite of the lack of some experimentally determined parameters, the FDA collaborated with Simcyp to validate a PBPK model for the nonlinear pharmacokinetics of omeprazole enantiomers and the racemate (164), based in part on my previously published data (Chapter 4; (34). In addition, Sanofi-Aventis collaborated with Simcyp to validate a PBPK model for the sequential metabolism of clopidogrel (44). These latter two models combined with my K_I and k_{inact} values presented in this chapter may allow for an adequate PBPK model of the effect of omeprazole or esomeprazole on clopidogrel to be developed at some point in the future.

Because 5-ODM omeprazole and omeprazole sulfone are both direct-acting and MDIs of the enzymes that form them (i.e., CYP2C19 – above, and CYP3A4 – (75)), these inhibitor-inhibitor interactions would need to be accounted for over time in such a quantitative PBPK model of the impact of omeprazole or esomeprazole on clopidogrel (34,75,78,94,111,120,121). An additional complication in any PBPK modeling of the effect of esomeprazole or omeprazole and its metabolites on the two-step clopidogrel activation is the fact that clopidogrel and/ or its 2-oxo-metabolite are also MDIs of CYP2B6, 2C19 and 3A4 (three CYPs that are involved in activation of clopidogrel, two of which are involved in omeprazole and esomeprazole metabolism) (143,157,165-167). Therefore, as first hypothesized by Zhang et al. (157) clopidogrel coadministration with omeprazole or esomeprazole could potentially amplify the

impact that omeprazole or esomeprazole have on clopidogrel because they are metabolized by CYP2C19 and 3A4. For reasons listed above, the use of a PBPK model in this instance is much more complicated than that presented in Chapter 4, and is beyond the scope of this dissertation. Therefore, a modified mechanistic static model based on that described by Boulenc and colleagues was utilized (94).

The mechanistic static model I used in this chapter utilized the lowest and highest $f_{m(CYP2C19)}$ values for the conversion of clopidogrel to H4 as determined by Boulenc and colleagues in CYP2C19 EMs, namely 0.64 and 0.72 (94). The lower value is similar to the overall $f_{m(CYP2C19)}$ determined in vitro by Kazui and colleagues (0.45 for the conversion of clopidogrel to 2-oxo-clopidogrel and 0.21 for the subsequent conversion to H4, i.e., 0.66) (48). In addition, in a full PBPK model of the two-step activation of clopidogrel, CYP2C19 was predicted to contribute 49% to the first step and 21% to the second, for a total $f_{m(CYP2C19)}$ of 0.7 (44), again within the ranges I incorporated in my MSM. In spite of the agreement with the published $f_{m(CYP2C19)}$ values for clopidogrel activation to H4, I found that the MSM over-predicted the decrease in H4 formation by omeprazole (80 mg dose for 10 days) by approximately 1.5 - 1.9-fold (Table 5.2). For esomeprazole (20 mg for 5 days) the MSM was in closer agreement to observed values, with an over-prediction in the decrease in H4 formation of approximately 1.1 – 1.7-fold. For esomeprazole (40 mg for 5 days) the MSM over-predicted the decrease in H4 formation by approximately 1.3 – 1.9-fold. Because of the over-predictions with the parent drugs, the effects of the metabolites were not added to the MSM for either omeprazole or esomeprazole (which would only worsen the over-prediction), but are modeled on their own for comparison. Consistent with this over-prediction without consideration of the metabolites, Shirasaka and colleagues also found that the drug-drug interaction risk of omeprazole toward CYP2C19 was correctly identified (i.e., true positive) from their clinical and in vitro data on omeprazole without accounting for the contribution of metabolites (75). The modified MSM used

in this chapter also agrees relatively well with that proposed in Chapter 4 for the interaction between omeprazole (40 mg q.d. for for 5 days) and moclobemide (i.e. a predicted 2.85-fold increase in moclobemide AUC, $f_{mCYP2C19}$ of 0.72), with a predicted 2.73-fold increase in moclobemide caused by esomeprazole (40 mg q.i.d. for for 5 days). Although a clinical study has not been performed with esomeprazole and moclobemide, the observed moclobemide AUC_∞ increases averaged 2.21-fold (1.03 to 3.39-fold) in CYP2C19 EMs with omeprazole (112). On the basis of this comparison, the MSM appears to provide only a 1.3-fold over-prediction of the effect of esomeprazole on moclobemide, which has the same apparent $f_{mCYP2C19}$ as H4 formation from clopidogrel.

The over-predictions of the impact that omeprazole and esomeprazole have on H4 formation are likely due in part to the fact that I made use of a static model, and omeprazole and esomeprazole have short half-lives. The MSM is also relatively sensitive to small changes in K_I and k_{inact} values, which, as demonstrated in Chapter 4, can vary significantly with experimental conditions (34,35). Additionally, the activation of clopidogrel requires two sequential CYP-mediated steps and the MSM does not consider these, which is likely another source of error. In addition, Zvyaga and colleagues raised the possibility that K_I and k_{inact} values for the inactivation of CYP2C19 by omeprazole or esomeprazole may be substrate-dependent (78). Substrate-dependence for in vitro inhibition of CYP2C19 has previously been documented (168), and it is possible that a determination of K_I and k_{inact} with a different CYP2C19 marker substrate would yield better predictions. A seemingly obvious experimental design would utilize clopidogrel and 2-oxo-clopidogrel as the substrates and determine the K_I and k_{inact} values with omeprazole and esomeprazole as the inhibitors. However, as reviewed in Chapter 1, the analytical method to quantify H4 is particularly challenging and can lead to erroneous conclusions if metabolites other than H4 are inadvertently monitored. Ohbuchi and colleagues showed that omeprazole produces a 2-fold shift in IC_{50} upon pre-incubation in recombinant

human CYP2C19 (121) toward the formation of a putative clopidogrel active metabolite. However, the authors conceded that their analytical method detected three 3´-methoxyphenacyl bromide-derivatized metabolites, and the IC_{50} values for each were then averaged to determine the shift after pre-incubation.

In spite of the over-prediction (by a factor of ~2), the mechanistic static model does accurately predict that esomeprazole would be expected to decrease formation of H4 from clopidogrel. With recent advances in the PBPK modelling of omeprazole enantiomer pharmacokinetics (164) and the sequential metabolism of clopidogrel (44), more accurate PBPK models of the drug-drug interaction between these drugs should be possible in the future by incorporating the K_I and k_{inact} values for the inactivation of CYP2C19 by esomeprazole and its major metabolites that I presented in this chapter.

Chapter 6. MECHANISTIC STUDIES ON THE INACTIVATION OF CYP2C19 BY ESOMEPRAZOLE, 5-*O*-DESMETHYL OMEPRAZOLE, OMEPRAZOLE SULFONE AND INVESTIGATION OF ILAPRAZOLE, RABEPRAZOLE AND TENATOPRAZOLE AS METABOLISM-DEPENDENT INHIBITORS OF CYP2C19

Abstract

In Chapters 4 and 5, I presented evidence that esomeprazole, omeprazole sulfone and 5-*O*-desmethyl omeprazole, but not *R*-omeprazole, are irreversible metabolism-dependent inhibitors of CYP2C19. For esomeprazole, omeprazole sulfone and 5-*O*-desmethyl omeprazole, these studies established the following criteria for mechanism-based inhibition: 1) inactivation of CYP2C19 occurs in a concentration-, time- and metabolism-dependent manner, 2) the inactivation is largely irreversible (by ultracentrifugation and washing), and 3) the inactivation is saturable. Further studies were conducted to provide additional evidence that the irreversible MDI of CYP2C19 by esomeprazole and its inhibitory metabolites is in fact mechanism-based inactivation. Accordingly, near-complete substrate protection was achieved wtih the CYP2C19 substrate, pantoprazole (200 μM), for esomeprazole, omeprazole sulfone and 5-*O*-desmethyl omeprazole. Neither of the "protectants" glutathione (2 mM), superoxide dismutase (500 U/mL) nor catalase (1000 U/mL) significantly altered the efficiency of inactivation of CYP2C19 in pooled human liver microsomes by esomeprazole, omeprazole sulfone or 5-*O*-desmethyl omeprazole. In addition, quality control assays were performed to assess the robustness of the determination of efficiency of inactivation (i.e., k_{inact}/K_I) by each of these compounds from assay to assay in order to demonstrate that these protectants did not significantly affect inactivation of CYP2C19 by the three compounds. In addition, and as expected, esomeprazole did not form a metabolite inhibitory complex (MIC) under conditions in which the selective CYP2C19 inhibitor, *S*-fluoxetine, did, either in recombinant human CYP2C19 or in pooled human liver microsomes. Finally, to examine the hypothesis that the presence of a 5´-methyl substituent in PPIs is necessary for metabolism-dependent inhibition of CYP2C19, ilaprazole, rabeprazole and tenatoprazole were evaluated as direct-acting and MDIs of CYP2C19 activity. This study showed that tenatoprazole, the only PPI other than omeprazole and esomeprazole with a 5´-methyl substituent, is also an MDI of CYP2C19, whereas ilaprazole

and rabeprazole are not. The results of this study provide further evidence that esomeprazole, omeprazole sulfone and 5-O-desmethyl omeprazole inactivate CYP2C19 in a mechanism-based manner and suggest that the presence of a 5´-methyl substituent is necessary for metabolism-dependent inhibition of CYP2C19 by PPIs.

Introduction

The phrase “mechanism-based inhibition” is frequently used to refer to any irreversible or quasi-irreversible metabolism-dependent inhibition of CYP enzymes. However, by definition, the phrase “mechanism-based inhibition” excludes the formation of metabolites that are simply more potent direct-acting inhibitors than the parent, whereas the term “metabolism-dependent inhibition” includes this type of time-dependent inhibition. Simply put, mechanism-based inactivators are substrates for a CYP enzyme that, during catalysis by the enzyme, are converted to one or more products that immediately and irreversibly inactivate the enzyme and do not leave the active site (169). Strictly speaking, irreversible inhibitors that are affinity labeling agents, transition state analogs and slow, tight-binding inhibitors are not mechanism-based inhibitors because they do not require a metabolic event to exert their inhibitory effect (169). For a metabolism-dependent inhibitor of a CYP enzyme to be categorized as a mechanism-based inactivator, however, it must meet certain criteria that can be determined experimentally, according to Silverman, and as put in the context of CYP enzymes in later reviews (170-172), and further reviewed in my book chapter (16):

1. The CYP inhibition must be concentration-, NADPH-, and time-dependent. This was demonstrated for esomeprazole, omeprazole sulfone and 5-ODM omeprazole in Chapters 4 and 5.
2. Inactivation must occur prior to the release of the inhibitory metabolite. Any metabolite that is released from the active site cannot be the metabolite that inactivates the enzyme. (This criterion distinguishes mechanism-based inactivators from metabolism-dependent inhibitors that generate and release electrophilic metabolites. In such a case, inactivation may occur by binding to a site other than the active site, or by rearrangement of the metabolite prior to its return to the active site.) Furthermore, the addition of glutathione (GSH), radical scavengers, or other exogenous nucleophiles

cannot prevent inactivation in the case of true mechanism-based inhibition, but they often abrogate the inhibition observed with other types of metabolism-dependent inhibition. GSH, superoxide dismutase and catalase were examined in this chapter to meet this criterion for esomeprazole, omeprazole sulfone and 5-ODM omeprazole.

3. Mechanism-based inhibition should be irreversible. Dialysis, ultrafiltration, or ultracentrifugation and washing the protein (e.g., by isolating microsomes by centrifugation and resuspending them in drug-free buffer) will not restore enzyme activity. Evidence for this criterion was provided in Chapters 4 and 5 for esomeprazole, omeprazole sulfone and 5-ODM omeprazole with the use of ultracentrifugation. It should be noted, however, that some exceptions to irreversibility in spite of meeting most other criteria for MBI have been reported. For instance, the MBI of CYP2B4 by by *tert*-butyl acetylene is partially reversible upon overnight dialysis and the heme *N*-alkylation of chloroperoxidase by allylbenzene and 1-hexyne is transient (173,174).
4. Mechanism-based inhibition should be saturable. The rate of inactivation is proportional to the concentration of the inactivator until all enzyme molecules are saturated, in accordance with Michaelis-Menten kinetics. Additionally, the decrease in enzymatic activity over time should follow pseudo-first order kinetics. Again, evidence for this criterion was provided in Chapters 4 and 5 for esomeprazole, omeprazole sulfone and 5-ODM omeprazole.
5. Alternate substrates should protect against mechanism-based inhibition. The addition of an alternative substrate or competitive inhibitor with good affinity for the enzyme will prevent or at least decrease the rate of inactivation. The CYP2C19 substrate pantoprazole, which has an $f_{m(CYP2C19)}$ of 0.80, based on the change in AUC from genetically determined EMs to PMs (175) was utilized for this purpose in this chapter.
6. There should be stoichiometric (ideally one-to-one) binding of inactivator to enzyme. This was not attempted in this chapter, in part because of the complicating fact that two

inhibitory metabolites are also formed, namely 5-ODM omeprazole by CYP2C19 and omeprazole sulfone by CYP3A4.

7. CYP content is usually reduced by mechanism-based inhibitors. This criterion was not examined in this chapter, but evidence for a decrease in ~400 nm-detectable heme in the presence of esomeprazole will be presented in Chapter 7.
8. Enzyme inactivation should be preceded by a catalytic event that converts the mechanism-based inhibitor to the inactivating metabolite. Evidence was provided for this criterion in Chapters 4 and 5 in that enzyme inactivation required NADPH, the cofactor for CYP-dependent metabolism.

In the typical drug-development process for the evaluation of drug candidates that are irreversible MDIs of CYPs, only criteria 1, 3, 4 and 8 are established because the purpose of these evaluations is to decide if a drug candidate should be further investigated in a clinical DDI study. Establishment of criterion 4 is usually conducted as part of a K_I and k_{inact} determination such that mechanistic static models or PBPK models can be used to predict whether or not a drug candidate is likely to cause clinically relevant enzyme inactivation. Evidence that criteria 1, 3, 4 and 8 were met for esomeprazole, omeprazole sulfone and 5-ODM omeprazole were previously provided. Experiments conducted as part of this chapter were undertaken in an attempt to meet criteria 2 and 5 as well as to assess the robustness of the determination of efficiency of inactivation (i.e., k_{inact}/K_I) under the same set of experimental conditions. Additional experiments were conducted to provide further evidence that quasi-irreversible inhibition of CYP2C19 involving metabolite inhibitory complex formation by esomeprazole does not occur. Finally, to further probe the mechanism by which esomeprazole causes MDI of CYP2C19, it was hypothesized that the presence of a 5′-methyl substituent in PPIs is necessary for MDI of CYP2C19. To this end, two clinically used PPIs (i.e., ilaprazole and rabeprazole) that lack a 5′-methyl substituent and one investigational PPI, tenatoprazole which, like omeprazole and

esomeprazole, does have a 5´-methyl substituent, were examined as MDIs of CYP2C19 in HLM.

Results

As noted in Chapter 5, once "definitive" conditions were settled on, all additional experiments, including those detailed in this chapter were conducted under a single set of experimental conditions, namely (1) 0.5 mg/mL NADPH-fortified HLM in the pre-incubations, (2) a 10-fold dilution, and (3) 5-min incubation with the CYP marker substrate at 10 × K_m, in order to minimize membrane partitioning and direct-acting competitive inhibition, and to allow for comparisons when changing only a single variable, such as the addition of a "protectant" (i.e., glutathione, superoxide dismutase, catalase, or the alternate CYP2C19 substrate, pantoprazole). These methods are described in Chapter 3.

6.1. Effects of glutathione, superoxide dismutase, catalase, and the alternate CYP2C19 substrate, pantoprazole, on the inactivation of CYP2C19 by esomeprazole

Building on the evidence suggesting that esomeprazole is a metabolism-dependent inhibitor of CYP2C19 as described in Chapters 4 and 5, and to further test the hypothesis that esomeprazole is a mechanism-based inhibitor, I next performed experiments to determine K_I and k_{inact} values in the presence of the commonly used CYP enzyme "protectants", namely glutathione (GSH), superoxide dismutase, and catalase, as well as the alternative CYP2C19 substrate, pantoprazole. The results from four different experiments are summarized in Figure 6.1, Figure 6.5a and Table 6.1. As expected for a mechanism-based inhibitor, the inactivation of CYP2C19 by esomeprazole appeared to be largely unaffected by the presence of GSH, superoxide dismutase, or catalase and was dependent on the concentration of esomeprazole (over the concentration range examined) and the time course conformed to a first-order inactivation process (as indicated by the linearity of plots of the log of the residual enzyme activity against time) (Figure 6.1a, c, and e), and was saturable (Figure 6.1b, d, and f). The k_{inact} values ranged from 0.042 – 0.050 min^{-1} and K_I values ranged from 3.6 – 5.3 μM. The efficiency

of CYP2C19 inactivation (k_{inact}/K_I) ranged from 9.4 – 13.4 $min^{-1} \cdot mM^{-1}$. A more thorough comparison between treatment and control values will be described Section 6.5. In contrast, and as expected for a mechanism-based inactivator, the alternate CYP2C19 substrate, pantoprazole (200 μM), largely attenuated the ability of esomeprazole to inactivate CYP2C19, as summarized in Figure 6.1g-h and Table 6.1, with a loss of saturation, and inactivation only occurring to a small extent at 20 and 60 μM esomeprazole.

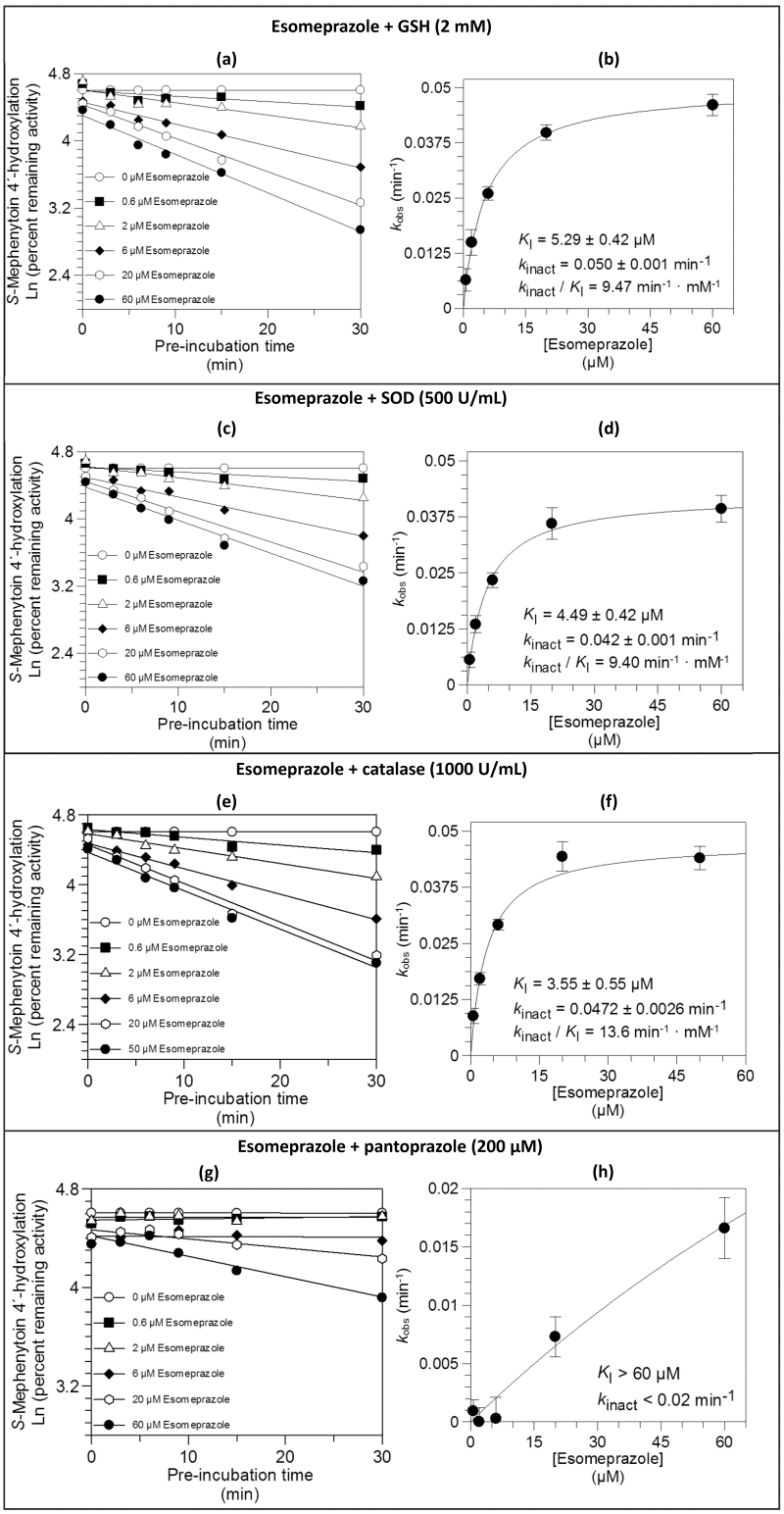

Figure 6.1. Determination of K_I and k_{inact} for the MDI of CYP2C19 in HLM by esomeprazole in the presence of glutathione, superoxide dismutase, catalase, and an alternate CYP2C19 substrate (pantoprazole)

Individual points represent the average of triplicate determinations ± standard deviation, unless otherwise noted. For graphs in (a), (c), (e), and (g) esomeprazole was pre-incubated (at concentrations indicated and at final protein concentrations indicated) and residual CYP2C19 activity determined as described in *Chapter 3*, in the presence of the additional component, as indicated. The graphs in (b), (d), (f), and (h) represent the direct plots of the initial rates of inactivation of CYP2C19. Values are the slopes of the initial rates of inactivation (k_{obs}) at each concentration of esomeprazole, shown ± standard error.

6.2. Effects of glutathione, superoxide dismutase, catalase, and the alternate CYP2C19 substrate, pantoprazole, on the inactivation of CYP2C19 by omeprazole sulfone

To further test the hypothesis that omeprazole sulfone is also a mechanism-based inhibitor of CYP2C19, I performed experiments to determine K_I and k_{inact} values in the presence of glutathione (GSH), superoxide dismutase, and catalase, as well as the alternative CYP2C19 substrate, pantoprazole. The results from four different experiments are summarized in Figure 6.2, Figure 6.5b and Table 6.1. As expected for a mechanism-based inhibitor, the inactivation of CYP2C19 by omeprazole sulfone appeared to be largely unaffected by the presence of GSH, superoxide dismutase, or catalase and was dependent on the concentration of omeprazole sulfone (over the concentration range examined) and the time course conformed to a first-order inactivation process (as indicated by the linearity of plots of the log of the residual enzyme activity against time) (Figure 6.2a, c, and e), and was saturable (Figure 6.2b, d, and f). The k_{inact} values ranged from 0.024 – 0.027 min^{-1} and K_I values ranged from 4.8 – 9.2 μM. The efficiency of CYP2C19 inactivation (k_{inact}/K_I) ranged from 2.9 – 5.0 $min^{-1} \cdot mM^{-1}$. A more thorough comparison between treatment and control values will be described Section 6.5. In contrast, and as expected for a mechanism-based inactivator, the alternate CYP2C19 substrate, pantoprazole (200 μM), largely attenuated the ability of omeprazole sulfone to inactivate CYP2C19, as summarized in Figure 6.2g-h and Table 6.1, with a loss of saturation, and inactivation only occurring to a small extent at 20 and 60 μM omeprazole sulfone.

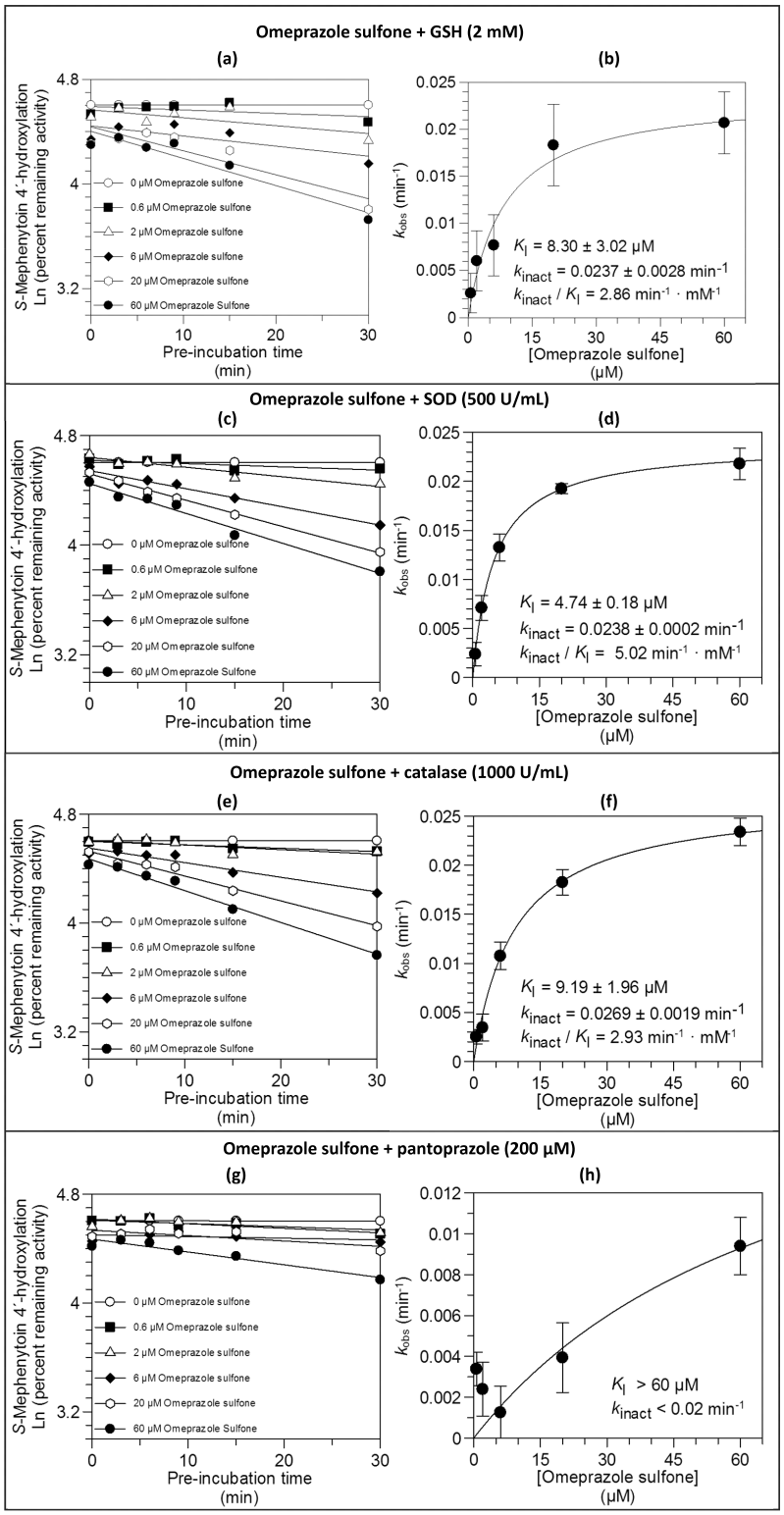

Figure 6.2. Determination of K_I and k_{inact} for the MDI of CYP2C19 in HLM by omeprazole sulfone in the presence of glutathione, superoxide dismutase, catalase, and an alternate CYP2C19 substrate (pantoprazole)

Individual points represent the average of triplicate determinations ± standard deviation. For graphs in (a), (c), (e), and (g) omeprazole sulfone was pre-incubated (at concentrations indicated) and residual CYP2C19 activity determined (at final protein concentrations indicated) as described in *Chapter 3*, in the presence of the additional component, as indicated. The graphs in (b), (d), (f), and (h) represent the direct plots of the initial rates of inactivation of CYP2C19. Values are the slopes of the initial rates of inactivation (k_{obs}) at each concentration of omeprazole sulfone, shown ± standard error.

6.3. Effects of glutathione, superoxide dismutase, catalase, and the alternate CYP2C19 substrate, pantoprazole, on the inactivation of CYP2C19 by 5-ODM omeprazole

To further test the hypothesis that 5-ODM omeprazole is also a mechanism-based inhibitor of CYP2C19 in HLM, I performed experiments to determine K_I and k_{inact} values in the presence of glutathione (GSH), superoxide dismutase, and catalase, as well as the alternative CYP2C19 substrate, pantoprazole. The results from four different experiments are summarized in Figure 6.3, Figure 6.5c and Table 6.1. As expected for a mechanism-based inhibitor, the inactivation of CYP2C19 by 5-ODM omeprazole appeared to be largely unaffected by the presence of GSH, superoxide dismutase, or catalase and was dependent on the concentration of 5-ODM omeprazole (over the concentration range examined) and the time course conformed to a first-order inactivation process (as indicated by the linearity of plots of the log of the residual enzyme activity against time) (Figure 6.3a, c, and e), and was saturable (Figure 6.3b, d, and f). The k_{inact} values ranged from 0.025 – 0.028 min^{-1} and K_I values ranged from 7.8 – 14 μM. The efficiency of CYP2C19 inactivation (k_{inact}/K_I) ranged from 2.1 – 3.7 $min^{-1} \cdot mM^{-1}$. A more thorough comparison between treatment and control values will be described Section 6.5. In contrast, but as expected for a mechanism-based inactivator, the alternate CYP2C19 substrate, pantoprazole (200 μM), completely attenuated the ability of 5-ODM omeprazole to inactivate CYP2C19, as summarized in Figure 6.3g-h and Table 6.1.

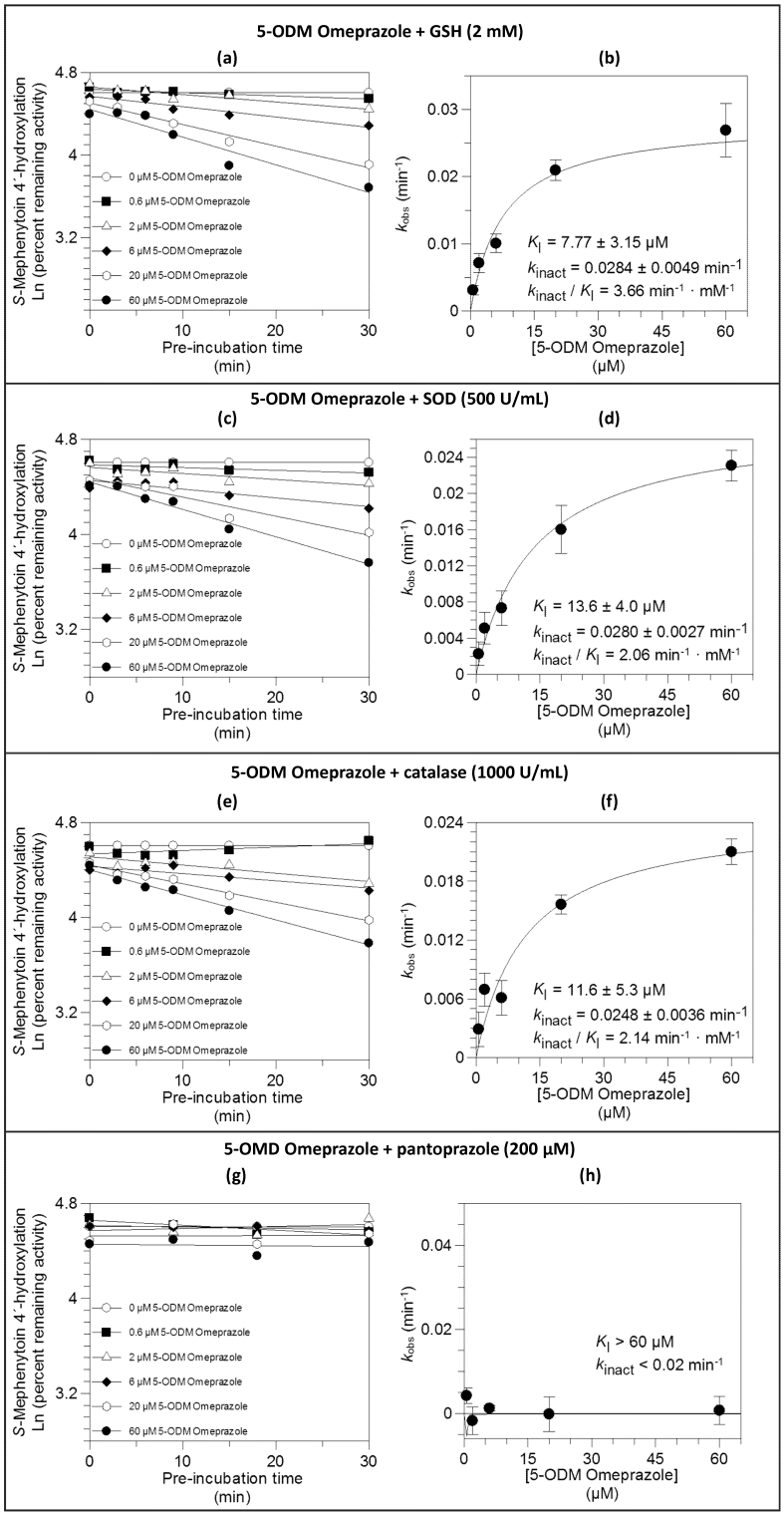

Figure 6.3. Determination of K_I and k_{inact} for the MDI of CYP2C19 in HLM by 5-ODM omeprazole in the presence of glutathione, superoxide dismutase, catalase, and an alternate CYP2C19 substrate (pantoprazole)

Individual points represent the average of triplicate determinations ± standard deviation, unless otherwise noted. For graphs in (a), (c), (e), and (g) 5-ODM omeprazole was pre-incubated (at concentrations indicated and at final protein concentrations indicated) and residual CYP2C19 activity determined as described in *Chapter 3*, in the presence of the protectants, as indicated. The graphs in (b), (d), (f), and (h) represent the direct plots of the initial rates of inactivation of CYP2C19. Values are the slopes of the initial rates of inactivation (k_{obs}) at each concentration of 5-ODM omeprazole, shown ± standard error.

Table 6.1. Summary of K_I and k_{inact} determinations for esomeprazole, omeprazole sulfone and 5-*O*-desmethyl omeprazole in the presence of glutathione, superoxide dismutase, catalase, or pantoprazole

Compound	Additive	K_I (μM)	k_{inact} (min^{-1})	k_{inact} / K_I ($min^{-1} \cdot mM^{-1}$)
Esomeprazole	GSH (2mM)	5.29 ± 0.42	0.0501 ± 0.0012	9.47 ± 0.79
	Superoxide dismutase (500 U/mL)	4.49 ± 0.42	0.0423 ± 0.0014	9.40 ± 0.94
	Catalase (1000 U/mL)	3.55 ± 055	0.0477 ± 0.0027	13.4 ± 2.2
	Pantoprazole (200 μM)	> 60	< 0.02	< 0.33
Omeprazole sulfone	GSH (2mM)	8.30 ± 3.02	0.0237 ± 0.0028	2.86 ± 1.09
	Superoxide dismutase (500 U/mL)	4.75 ± 0.18	0.0238 ± 0.0002	5.01 ± 0.20
	Catalase (1000 U/mL)	9.19 ± 1.96	0.0269 ± 0.0019	2.92 ± 0.66
	Pantoprazole (200 μM)	> 60	< 0.02	< 0.33
5-*O*-Desmethyl omeprazole	GSH (2mM)	7.77 ± 3.15	0.0284 ± 0.0049	3.66 ± 1.61
	Superoxide dismutase (500 U/mL)	13.6 ± 4.0	0.0280 ± 0.0027	2.06 ± 0.64
	Catalase (1000 U/mL)	11.6 ± 5.3	0.0248 ± 0.0036	2.14 ± 1.02
	Pantoprazole (200 μM)	> 60	< 0.02	< 0.33

6.4. Quality control assays

In Chapter 5, three microsomal protein concentrations were used to determine K_I and k_{inact} values for esomeprazole and omeprazole sulfone. The "medium concentration" of 0.5 mg/mL microsomal protein (pre-incubation concentration) appeared to be a good compromise with respect to the poor analytical sensitivity at 0.1 mg/mL and the higher membrane partitioning at 1 mg/mL (i.e., decreased free fraction of inhibitor). Therefore, additional experiments were conducted under these "standard conditions", namely 0.5 mg/mL NADPH-fortified HLM in the pre-incubation with a 10-fold dilution, and marker substrate assay at 10 × K_m. Some of the data in Chapter 5 also suggested the possibility that K_I values varied more than would be expected with changes in microsomal protein concentration. The efficiency of inactivation (i.e., k_{inact}/K_I), rather than the use of individual K_I or k_{inact} values, is a well-established parameter used to compare CYP inactivators with one another (35,134,176). In order to investigate the reproducibility of the efficiency of CYP2C19 inactivation under "standard conditions", abbreviated K_I and k_{inact} determinations in the absence of a "protectant" were conducted within at least three of the four assays for each compound (i.e., esomeprazole, omeprazole sulfone and 5-ODM omeprazole) presented in this chapter. These additional assays included five concentrations of each compound for four pre-incubation time points.

As in previous assays, the time course of CYP2C19 inactivation conformed to a first-order inactivation process, and was dependent on the concentration of inactivator (Figure 6.4). For convenience of comparison in Figure 6.4, the definitive direct plots for inactivation of CYP2C19 by esomeprazole, omeprazole sulfone and 5-ODM omeprazole are reproduced from Figure 5.3f, Figure 5.4f, and Figure 5.5d, respectively, and k_{inact} / K_I values are also summarized in Figure 6.4 and Table 6.2. The k_{inact} / K_I values for inactivation of CYP2C19 by esomeprazole in the absence of any protectants ranged from 10.5 to 14.9 $min^{-1} \cdot mM^{-1}$ (average = 11.8 ± 2.1 $min^{-1} \cdot mM^{-1}$); 3.85 to 5.20 $min^{-1} \cdot mM^{-1}$ (average = 4.45 ± 0.57 $min^{-1} \cdot mM^{-1}$) for omeprazole sulfone,

and 1.84 – 2.70 $min^{-1} \cdot mM^{-1}$ (average = 2.30 ± 0.35 $min^{-1} \cdot mM^{-1}$) for 5-ODM omeprazole. In all cases, individual values fell within the 90% confidence interval about the arithmetic mean of the four values for each compound.

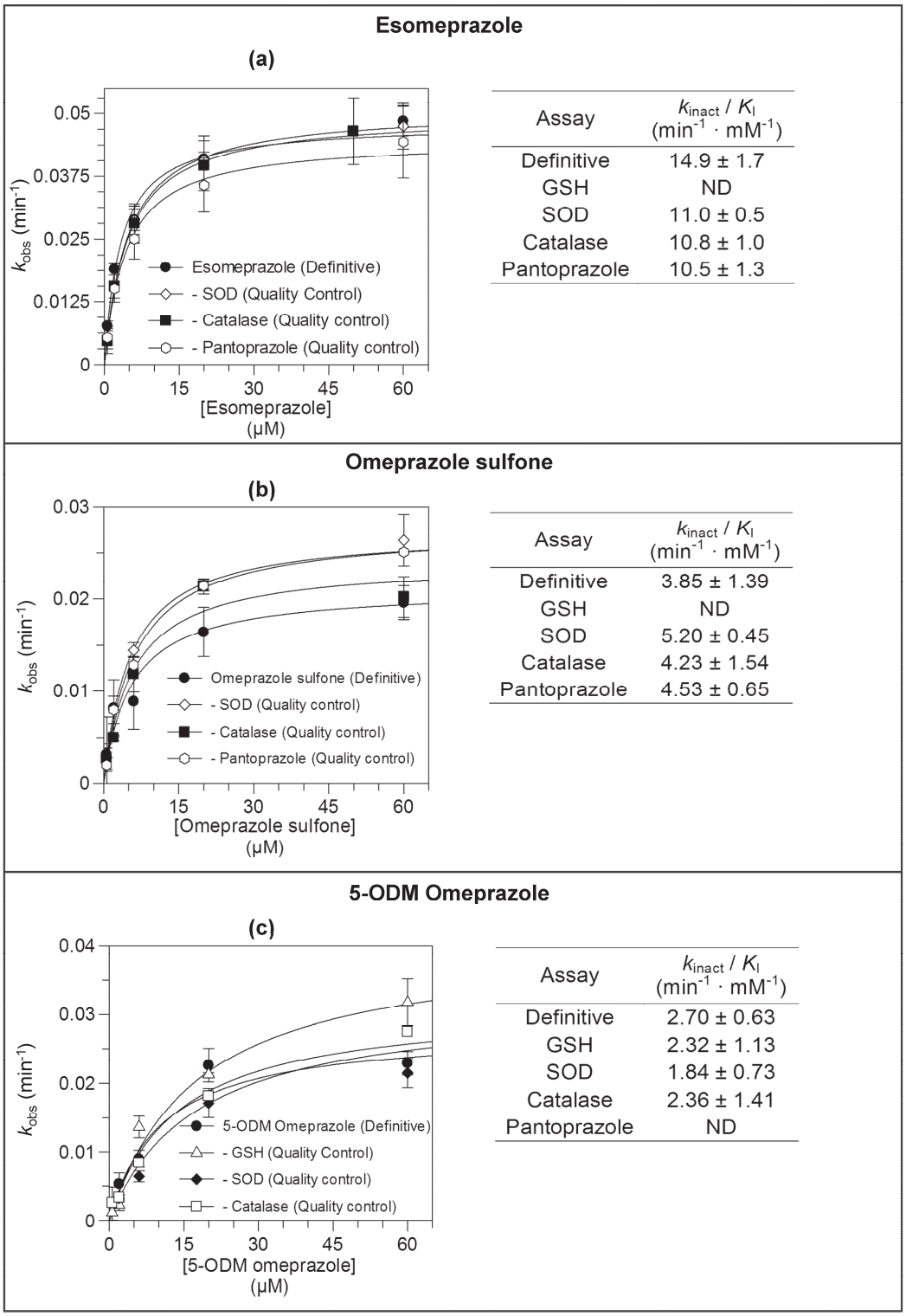

Assay	k_{inact} / K_I (min^{-1} · mM^{-1})
Definitive	14.9 ± 1.7
GSH	ND
SOD	11.0 ± 0.5
Catalase	10.8 ± 1.0
Pantoprazole	10.5 ± 1.3

Assay	k_{inact} / K_I (min^{-1} · mM^{-1})
Definitive	3.85 ± 1.39
GSH	ND
SOD	5.20 ± 0.45
Catalase	4.23 ± 1.54
Pantoprazole	4.53 ± 0.65

Assay	k_{inact} / K_I (min^{-1} · mM^{-1})
Definitive	2.70 ± 0.63
GSH	2.32 ± 1.13
SOD	1.84 ± 0.73
Catalase	2.36 ± 1.41
Pantoprazole	ND

Figure 6.4. Summary of quality control K_I and k_{inact} determinations for the MDI of CYP2C19 by esomeprazole, omeprazole sulfone and 5-ODM omeprazole in the *absence* of glutathione, superoxide dismutase, catalase, or pantoprazole

The graphs in (a), (b), and (c) represent the direct plots of the initial rates of inactivation of CYP2C19 with each inhibitor in the *absence* of glutathione, superoxide dismutase, catalase, or pantoprazole, in an abbreviated quality control assay. Values are the slopes of the initial rates of inactivation (k_{obs}) at each concentration, shown ± standard error.

Table 6.2 Summary of K_I and k_{inact} quality control assays for esomeprazole, omeprazole sulfone and 5-*O*-desmethyl omeprazole in the absence of glutathione, superoxide dismutase, catalase, or pantoprazole

Compound	QC Assay (in the absence of:)	K_I (μM)	k_{inact} (min^{-1})	k_{inact} / K_I ($min^{-1} \cdot mM^{-1}$)
Esomeprazole	GSH	ND	ND	ND
	Superoxide dismutase	4.65 ± 0.22	0.0509 ± 0.0007	11.0 ± 0.5
	Catalase	4.62 ± 0.4	0.0499 ± 0.0018	10.8 ± 1.0
	Pantoprazole	4.27 ± 0.49	0.0448 ± 0.0021	10.5 ± 1.3
Omeprazole sulfone	GSH	ND	ND	ND
	Superoxide dismutase	5.27 ± 0.43	0.0274 ± 0.0007	5.20 ± 0.45
	Catalase	5.68 ± 1.98	0.0240 ± 0.0024	4.23 ± 1.54
	Pantoprazole	6.10 ± 0.84	0.0276 ± 0.0011	4.53 ± 0.65
5-*O*-Desmethyl omeprazole	GSH	17.5 ± 7.7	0.0407 ± 0.0086	2.32 ± 1.13
	Superoxide dismutase	17.4 ± 6.3	0.0319 ± 0.0054	1.84 ± 0.73
	Catalase	13.3 ± 6.9	0.0314 ± 0.0095	2.36 ± 0.32
	Pantoprazole	ND	ND	ND

6.5. Comparison of k_{inact}/K_I values for the MDI of CYP2C19 by esomeprazole, omeprazole sulfone and 5-ODM omeprazole in the presence and absence of glutathione, superoxide dismutase or catalase

For visual comparison, k_{inact}/K_I values are displayed in Figure 6.5. The "control assays" represent the definitive values reported in Table 5.1 as well as the quality control values in Table 6.2 As noted previously, the four control k_{inact}/K_I values fell within the 90% confidence interval about the arithmetic mean for each compound. As such, a comparison was then made for k_{inact}/K_I values in the presence of each protectant (i.e., GSH, SOD or catalase) with each compound. The hypothesis being tested was that none of the protectants would significantly *decrease* the k_{inact}/K_I value compared with controls, consistent with mechanism-based inhibition. All of the k_{inact}/K_I values in the presence of the protectants fell within the 90% confidence interval about the arithmetic mean of the controls for each compound, with the exception of the GSH treatment with 5-ODM omeprazole (Figure 6.5c). However, in this case, the k_{inact}/K_I value in the presence of GSH fell within the lower bound of the 90% confidence interval, but *exceeded* the upper limit of the 90% confidence interval by approximately 9%.

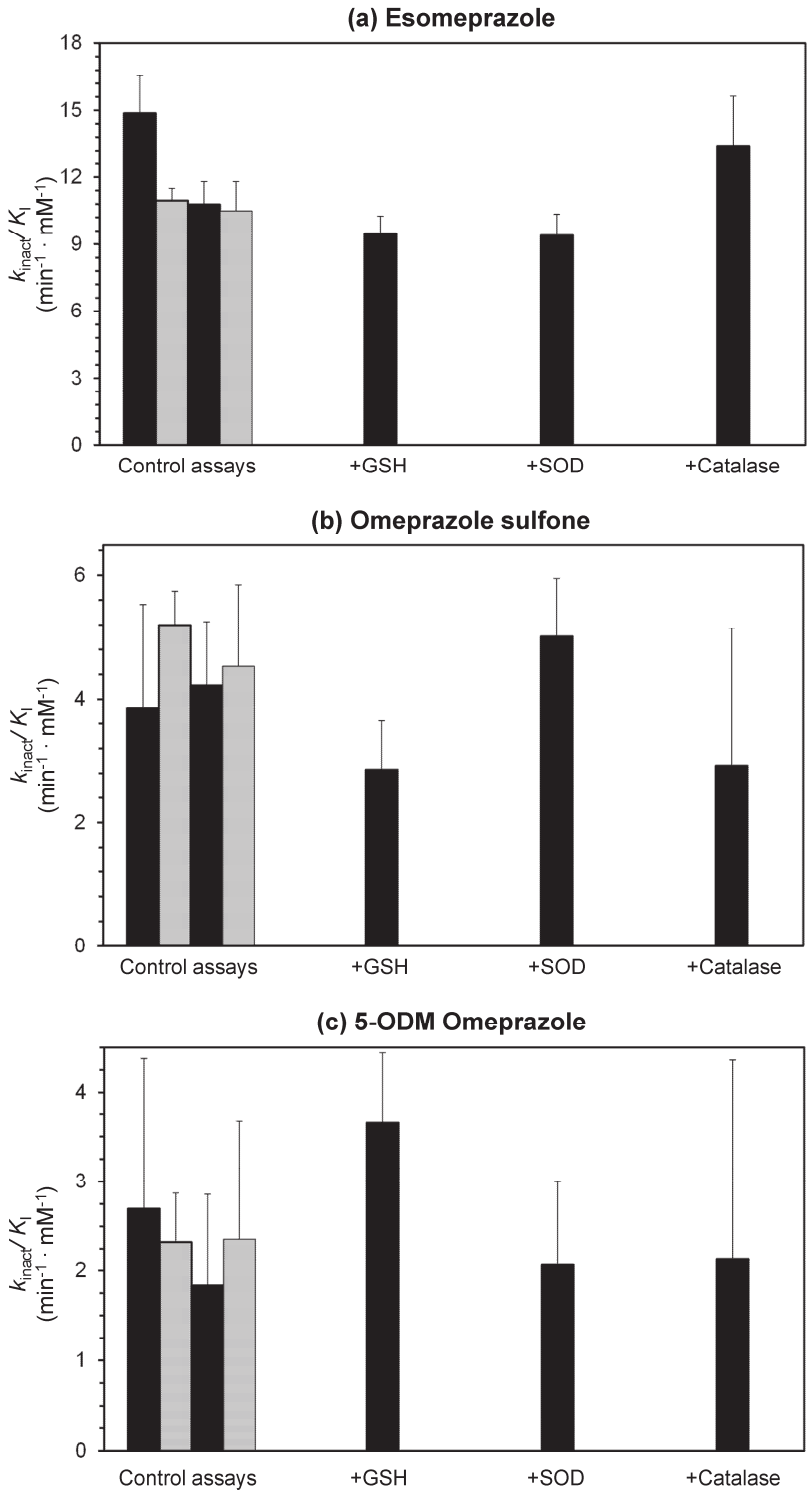

Figure 6.5. Graphical comparison of k_{inact}/K_I values for the MDI of CYP2C19 by esomeprazole, omeprazole sulfone and 5-ODM omeprazole in the presence and absence of glutathione, superoxide dismutase or catalase

Bars represent the efficiency of inactivation of CYP2C19 (k_{inact}/K_I values) ± standard error by (a) esomeprazole, (b) omeprazole sulfone, and (c) 5-ODM omeprazole. Data were compiled from Table 5.1, Table 6.1 and Table 6.2.

6.6. An investigation into the possibility that esomeprazole forms a metabolite-inhibitory complex with CYP2C19

As a further study into the investigation of the mechanism of inactivation of CYP2C19 by esomeprazole, spectral scans (400–500 nm) were measured over time to ascertain whether recombinant human CYP2C19 forms a metabolite-inhibitory complex (MIC) with esomeprazole (as described in Chapter 3). Treatment with potassium ferricyanide (which is well known to oxidize the ferrous iron to the ferric state and reverse the interaction between ferrous iron and the coordinately bound metabolite in the complex) previously had only a minor effect on the inhibition of CYP2C19 by esomeprazole as shown in Figure 4.7 (34). MICs typically absorb strongly around 455 nm, but some types (e.g., those formed by methylenedioxyphenyl-containing compounds) have maxima around 427 nm, and the latter MICs are not disrupted by potassium ferricyanide (125). Therefore, the studies presented in this section were undertaken in an attempt to more thoroughly rule out MIC formation as the mechanism of inactivation of CYP2C19 by esomeprazole.

Figure 6.6 shows a lack of formation of a peak near 427 or 455 when esomeprazole (100 μM) was incubated with recombinant human CYP2C19 (50 pmol/mL) for up to ~31 min. To further analyze these data, the change in absorbance between 427 or 455, and 490 nm (i.e., the isosbestic point) was also plotted vs. time as shown in Figure 6.7a-b. The lack of a time-dependent change the absorbance at these wavelengths provides further evidence that esomeprazole does not inactivate CYP2C19 through MIC formation.

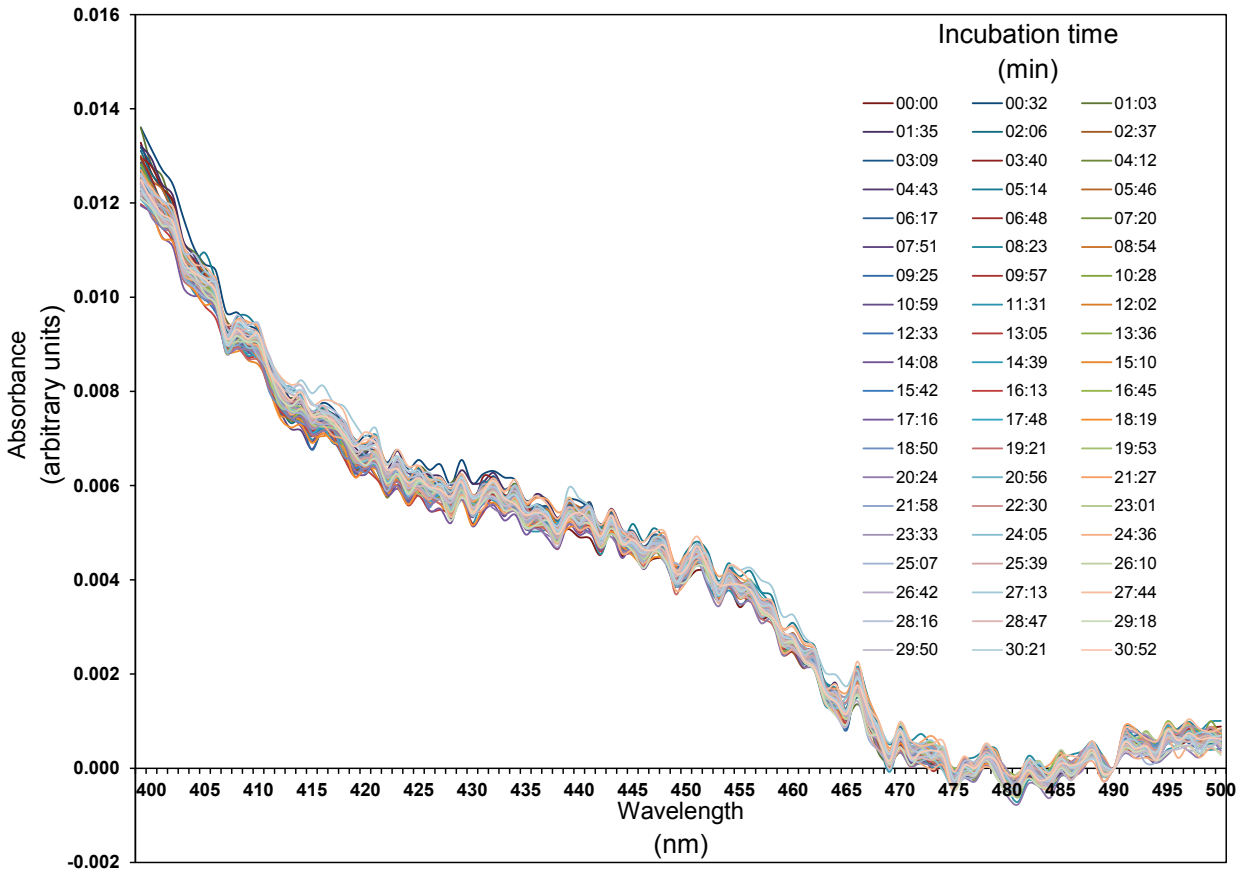

Figure 6.6. Difference spectra of the potential formation of a metabolite inhibitory complex by esomeprazole (100 µM) in rhCYP2C19 (50 pmol/mL)

The scan times are indicated after each line in the legend. The sample cuvette contained recombinant human CYP2C19 (50 pmol/mL), esomeprazole (100 µM), NADPH (1 mM) and other buffer components as indicated in *Chapter 3*. The reference cuvette contained the same components and the solvent used to dissolve esomeprazole as defined in *Chapter 3*. Absorbance was scanned from 400 – 500 nm approximately every 30 seconds up to approximately 31 min. The lines represent the absorbance recorded at each wavelength for each incubation time.

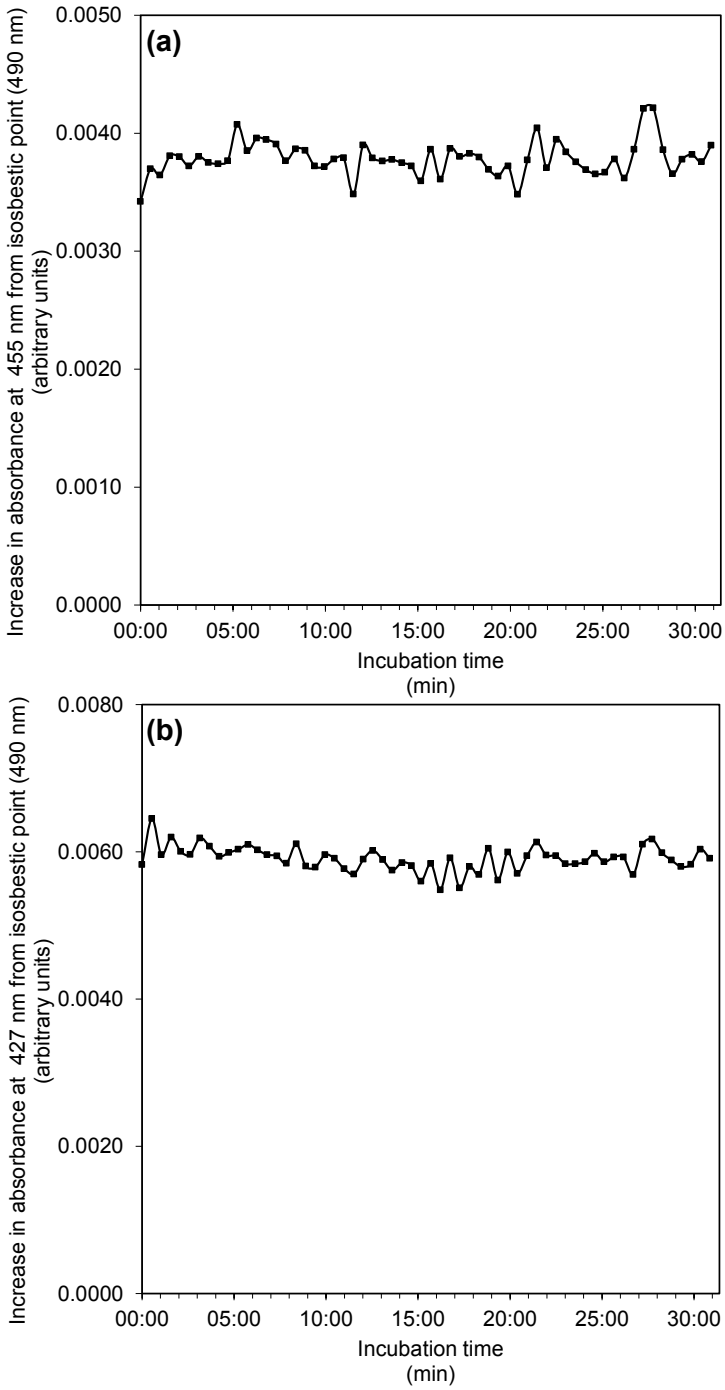

Figure 6.7. Lack of metabolite inhibitory complex formation by esomeprazole (100 μM) in rhCYP2C19 (50 pmol/mL)

Data are extracted from those presented in Figure 6.6, with points representing measurements of any absorbance increase at 455 (a) or 427 (b) nm relative to 490 nm (isosbestic point) over time.

6.7. Positive control assays

To provide additional evidence that the results in Figure 6.6 and Figure 6.7 were not false negatives, and that the test system could adequately detect an MIC with rhCYP2C19, the ability of *S*-fluoxetine to form an MIC under the same conditions was also examined (Figure 6.8). *S*-Fluoxetine was chosen because it has been shown previously to form an MIC in human liver microsomes (177,178). The concentration of *S*-fluoxetine chosen corresponds to approximately four-fold the total K_I value we previously determined in human liver microsomes (35). As shown in Figure 6.8 and Figure 6.9, a peak at approximately 455 nm formed immediately upon closing the spectrophotometer cover (i.e., 0 min), and continued to increase with time up to approximately 16 min of incubation. These experiments demonstrate that MICs formed by the CYP2C19 and 3A4 quasi-irreversible inhibitor, *S*-fluoxetine, can be detected in recombinant human CYP2C19.

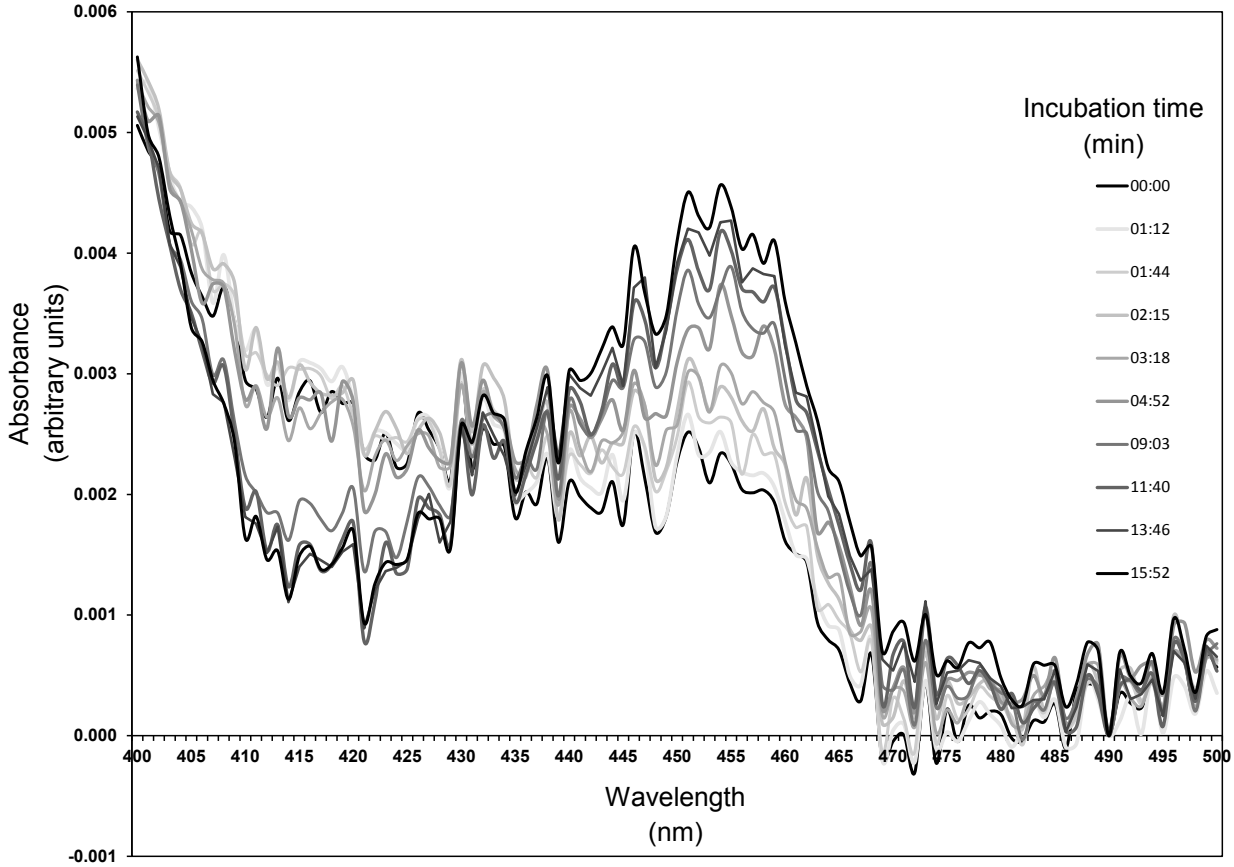

Figure 6.8. Difference spectra showing the formation of a metabolite inhibitory complex by *S*-fluoxetine (200 μM) in rhCYP2C19 (50 pmol/mL)

The scan times are indicated after each line in the legend. The sample cuvette contained recombinant human CYP2C19 (50 pmol/mL), *S*-fluoxetine (200 μM), NADPH (1 mM) and other buffer components as indicated in Chapter 3. The reference cuvette contained the same components and the solvent used to dissolve *S*-fluoxetine as defined in Chapter 3. Absorbance was scanned from 400 – 500 nm approximately every 30 seconds up to approximately 16 min. The lines represent the absorbance recorded at each wavelength.

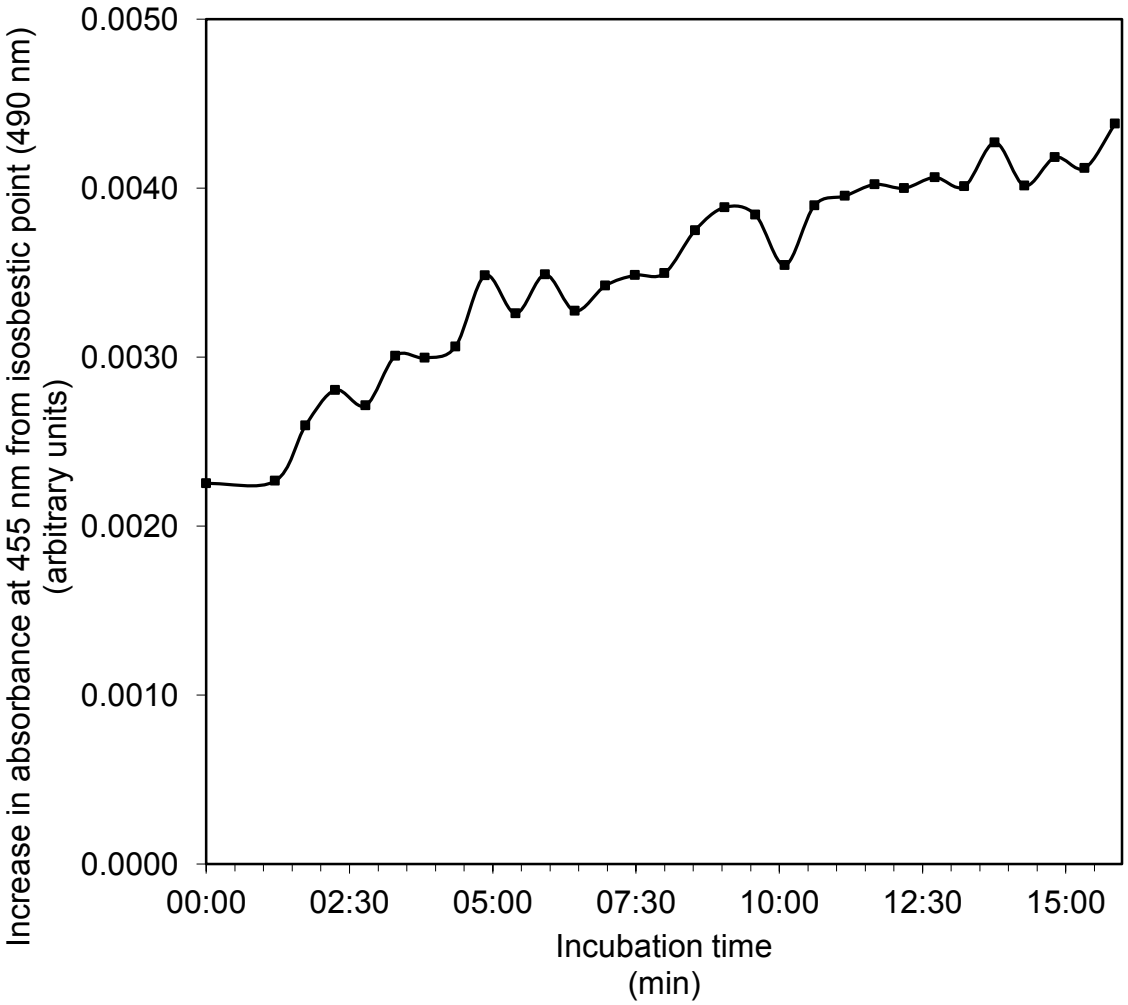

Figure 6.9. Metabolite inhibitory complex formation by *S*-fluoxetine (200 µM) with rhCYP2C19 (50 pmol/mL)

Data are extracted from those presented in Figure 6.8, with points representing measurements of the absorbance increase at 455 nm relative to 490 nm (isosbestic point) over time.

Finally, as an additional positive control, the ability of the well-known quasi-irreversible inhibitor of CYP3A4, troleandomycin, to form an MIC in recombinant human CYP3A4 was also demonstrated, as shown in Figure 6.10 and Figure 6.11. The time course of MIC formation in recombinant human CYP3A4 was similar to previous results in a human liver microsomal sample with high CYP3A4 content (16), with a rapid increase in MIC formation over the first few minutes followed by a slower increase to approximately 15 min.

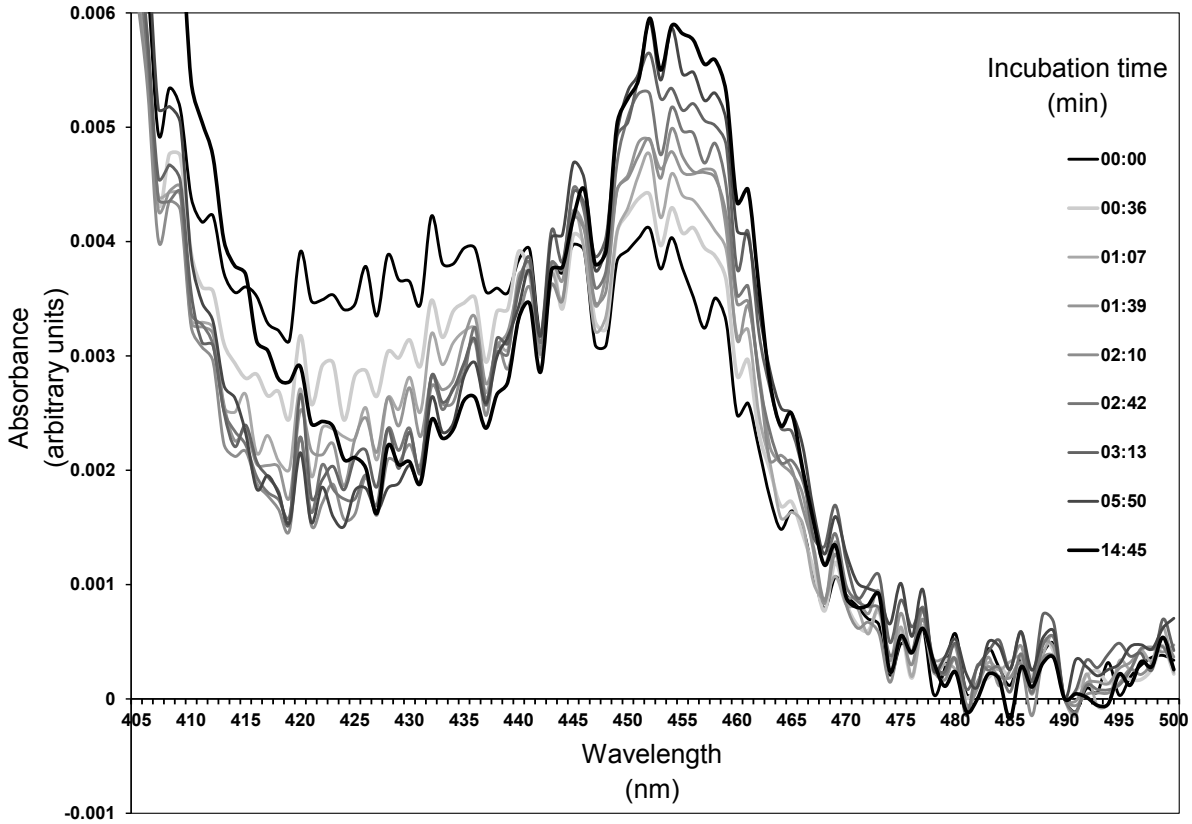

Figure 6.10. Difference spectra showing the formation of a metabolite inhibitory complex by troleandomycin (75 µM) in rhCYP3A4 (50 pmol/mL)

The scan times are indicated after each line in the legend. The sample cuvette contained recombinant human CYP3A4 (50 pmol/mL), troleandomycin (75 µM), NADPH (1 mM) and other buffer components as indicated in *Chapter 3*. The reference cuvette contained the same components and the solvent used to dissolve troleandomycin as defined in Chapter 3. Absorbance was scanned from 400 – 500 nm approximately every 30 seconds up to approximately 15 min. The lines represent the absorbance recorded at each wavelength.

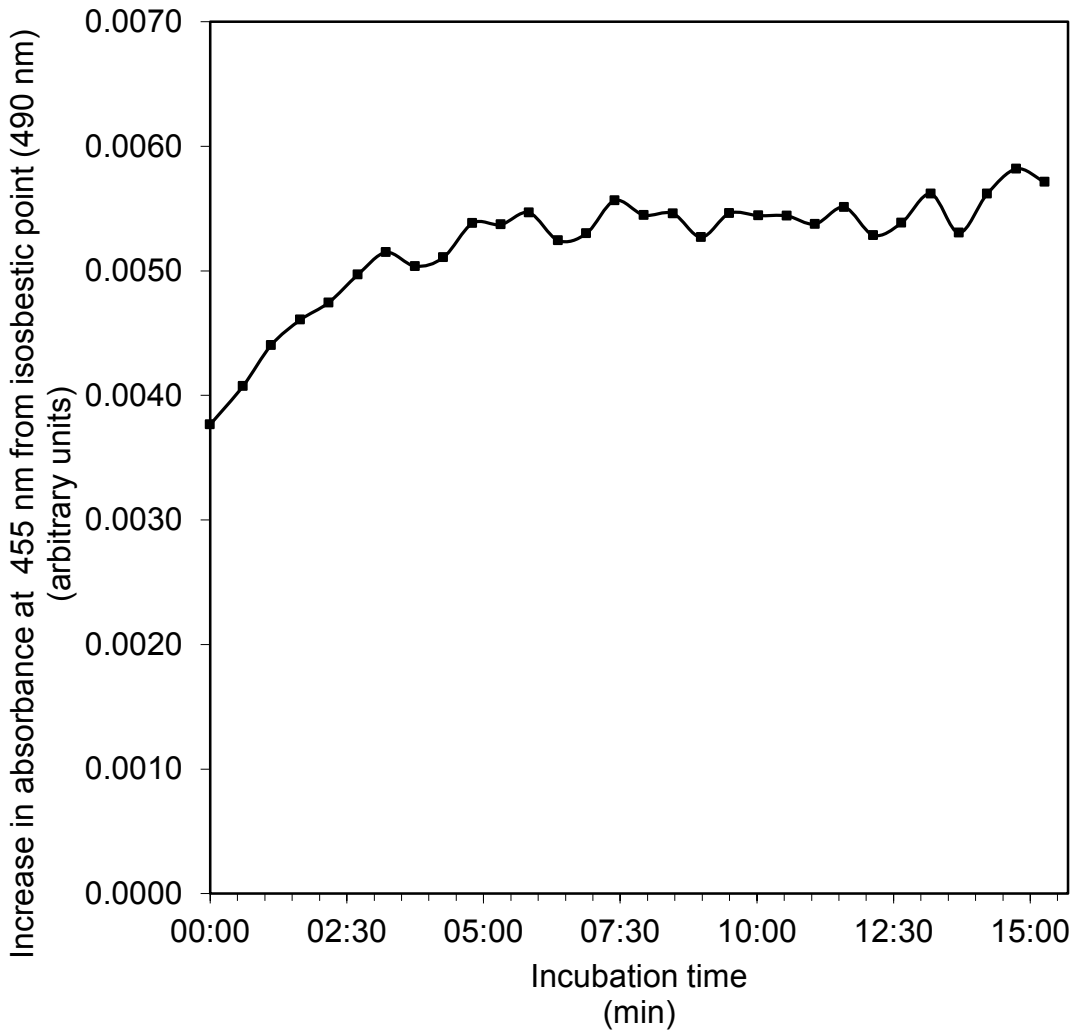

Figure 6.11. Metabolite inhibitory complex formation by troleandomycin (75 μM) in rhCYP3A4 (50 pmol/mL)

Data are extracted from those presented in Figure 6.10, with points representing measurements of the absorbance increase between 455 nm and 490 nm over time.

6.8. An investigation of additional proton pump inhibitors as metabolism-dependent inhibitors of CYP2C19

In Chapter 4 evidence that neither lansoprazole nor pantoprazole can cause metabolism-dependent inhibition of CYP2C19 (Table 4.1) was presented. It was also hypothesized that 5´-methylhydroxylation of omeprazole or esomeprazole (to form 5´-hydroxyomeprazole) could involve the intermediacy of a benzylic radical and heme alkylation, analogous to the inactivation of CYP2C8 by gemfibrozil glucuronide (33,148,159). Interestingly, of the PPIs, only omeprazole, esomeprazole and tenatoprazole have a 5´-methyl substituent (Table 1.1). In addition, conversion of omeprazole or esomeprazole to omeprazole sulfone or 5-ODM omeprazole leaves this substituent intact, and these metabolites are also MBIs of CYP2C19 (Table 6.1). In contrast, 5´-methylhydroxylation of esomeprazole or omeprazole leads to a metabolite that is not even a direct inhibitor of CYP2C19 (Table 4.1). It is also known that omeprazole sulfone can be further metabolized by CYP2C19 to 5´-hydroxyomeprazole sulfone (179) as shown in Figure 6.12. If hydroxylation at the 5´-position of omeprazole or esomeprazole and its inhibitory metabolites partitions between the formation of a non-inhibitory 5´-hydroxy metabolite by oxygen rebound and formation of an inhibitory benzylic radical, then this pathway would be common to esomeprazole and its inhibitory metabolites. This possibility is shown in Figure 6.13.

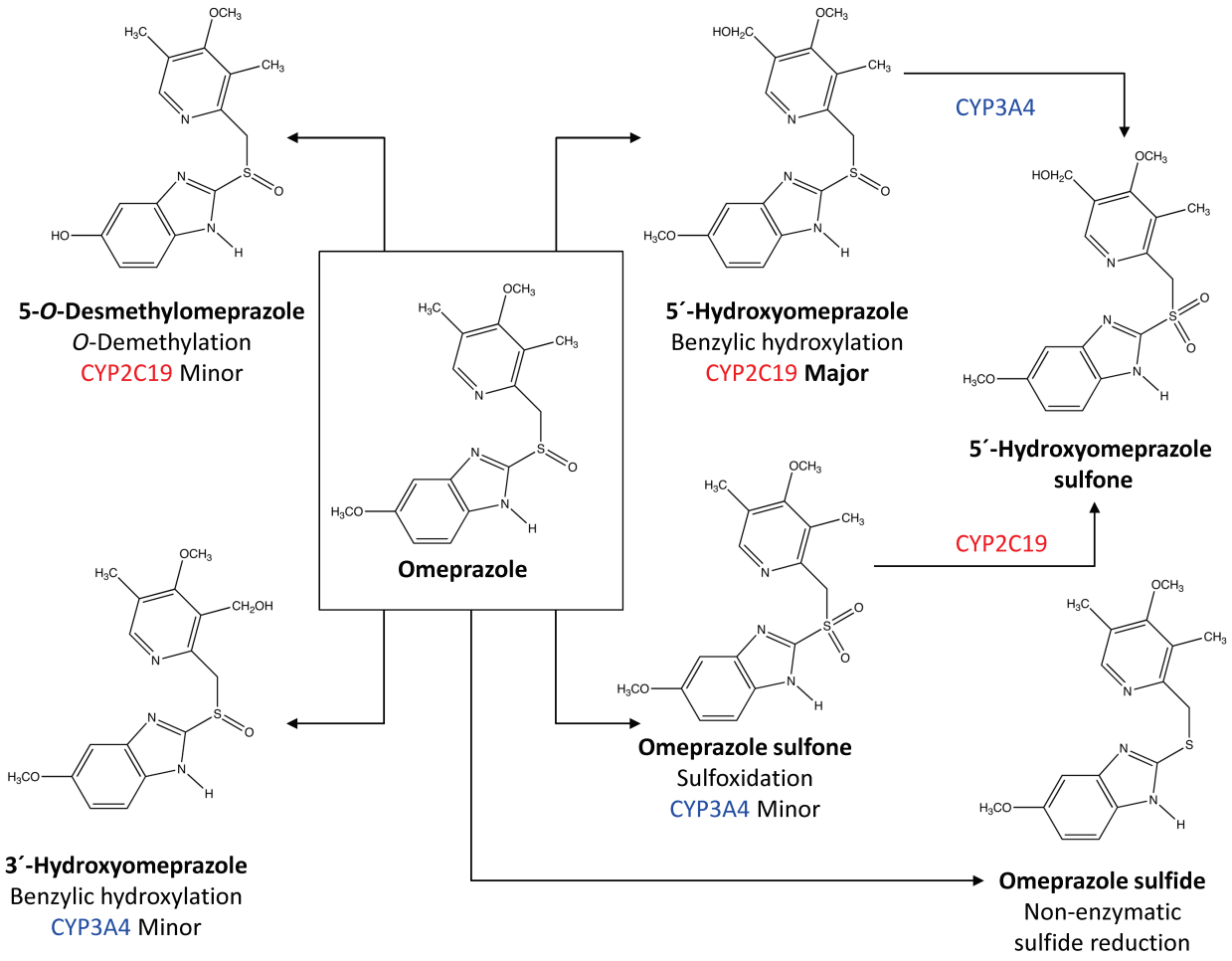

Figure 6.12. Metabolic scheme for omeprazole

The metabolism of omeprazole with CYP2C19-mediated reactions in red and CYP3A4-mediated reactions in blue. Adapted from (57,179).

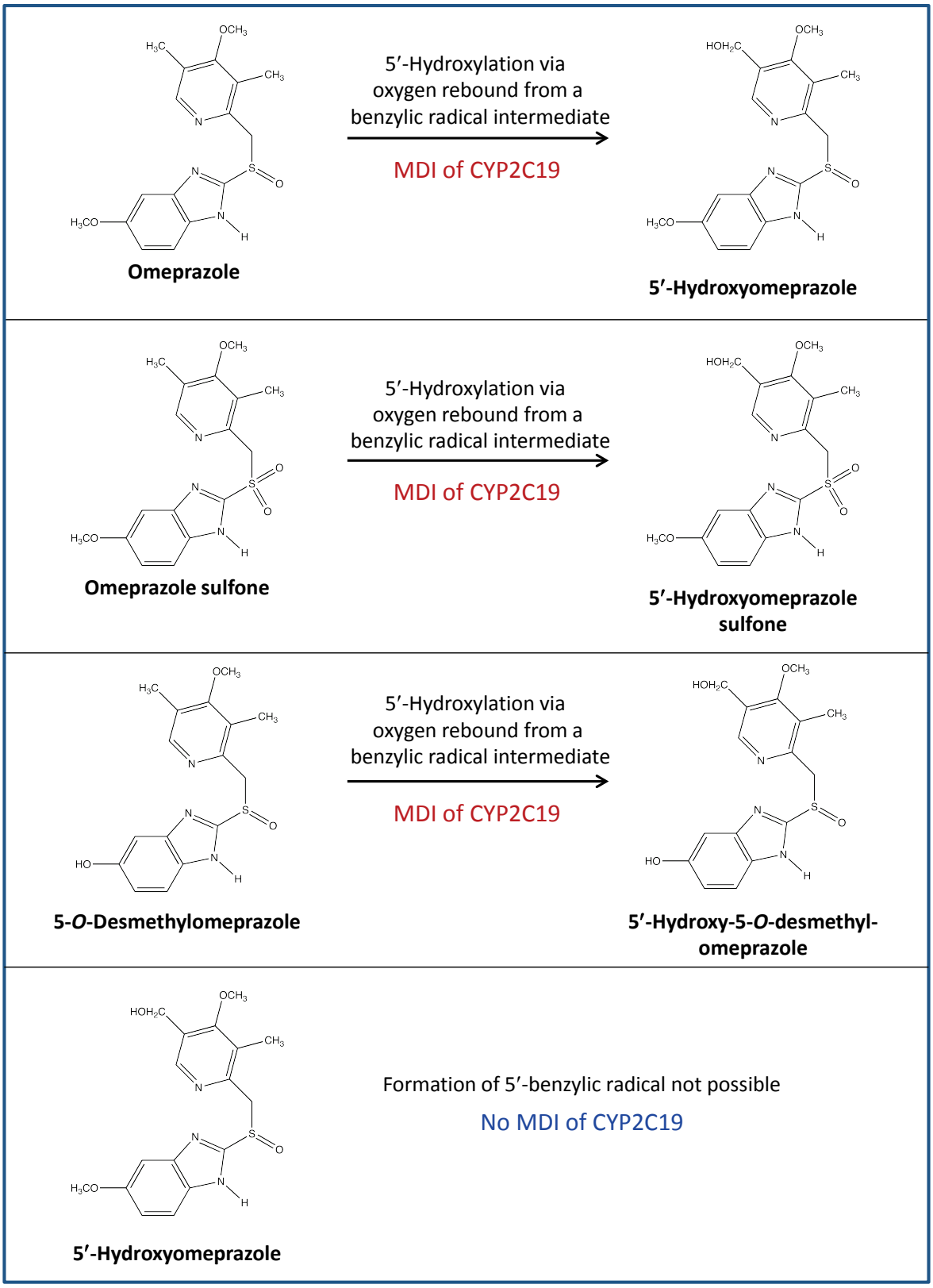

Figure 6.13. Omeprazole metabolites that can and cannot inactivate CYP2C19 and proposed mechanism

Three PPIs were not evaluated as CYP2C19 inhibitors in previous chapters, namely tenatoprazole, ilaprazole and rabeprazole (see Figure 6.14 for their structures; note that AGN201904 [Table 1.1] is excluded from this list because it is simply a prodrug of omeprazole). Tenatoprazole is unlike the other PPIs in that it is not a benzimidazole derivative, but an imidazopyridine derivative. However, like esomeprazole and its inhibitory metabolites, it does have a 5´-methyl substituent and was therefore predicted to cause metabolism-dependent inhibition of CYP2C19. The two remaining PPIs that had not been examined, namely ilaprazole and rabeprazole, like lansoprazole and pantoprazole, do *not* have a 5´-methyl substituent, and therefore were predicted not to cause MDI of CYP2C19.

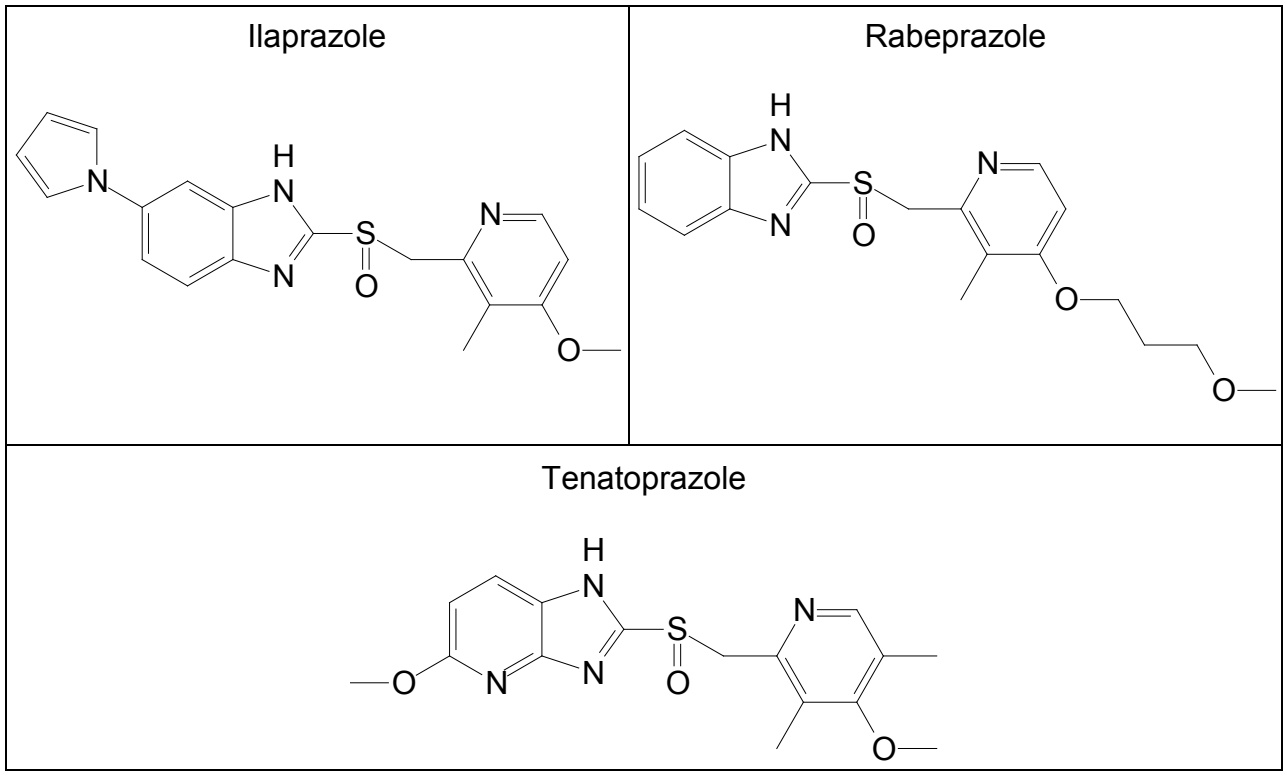

Figure 6.14. Structures of ilaprazole, rabeprazole and tenatoprazole

To test the hypothesis that the presence of a 5′-methyl substituent in PPIs is necessary for MDI of CYP2C19, ilaprazole, rabeprazole and tenatoprazole were evaluated as direct-acting and MDIs of CYP2C19 activity (*S*-mephenytoin 4′-hydroxylation) in pooled human liver microsomes as described in Chapter 3. Because no in vitro CYP inhibition results have been reported for ilaprazole or tenatoprazole (27), 60-min, rather than the previously used 30-min pre-incubations, were used to increase the chance of observing a shift in IC_{50} values. Rabeprazole has already been reported to directly inhibit CYP2C19 with *K*i values ranging from 10 – 20 μM (27). Rabeprazole is also non-enzymatically converted to its sulfide (or thioether) which directly inhibits CYP2C19 with a potency approximately 9-fold greater than the parent (138) (and is therefore and example of a reversible MDI). As shown in Figure 6.15, CYP-mediated metabolism of rabeprazole plays a relatively minor role in its metabolism (57), and the standard pre-incubation time of 30 min was used. The results are summarized in Figure 6.16 and Table 6.3.

As in previous chapters, a zero-min pre-incubation IC_{50} determination was also included in these experiments. For lansoprazole, pantoprazole, omeprazole, *R*-omeprazole and esomeprazole, all IC_{50} values with a pre-incubation in the *absence* of NADPH were greater than or equal to those with a zero-min pre-incubation (Table 4.1). In contrast, for ilaprazole, rabeprazole and tenatoprazole the IC_{50} values with a pre-incubation in the *absence* of NADPH were *less* than those determined with a zero-min pre-incubation (for clarity, these data are not presented in Figure 6.16). These results suggest that, as described for rabeprazole, and unlike the other PPIs and metabolites, ilaprzole and tenatoprazole may be more prone to non-enzymatic reduction to their sulfides or conversion to other inhibitory degradation products. Because of this observation, IC_{50} shifts were based on a comparison of the IC_{50} values for the samples pre-incubated with and without NADPH as presented in Table 6.3. This approach allowed any increase in inhibition upon pre-incubation with to be attributed to the presence of

NADPH (i.e., MDI). The results show that, as predicted, only tenatoprazole caused MDI of CYP2C19 as evidenced by a 4.2-fold shift in IC_{50} value of following a 60-min pre-incubation with NADPH-fortified HLM.

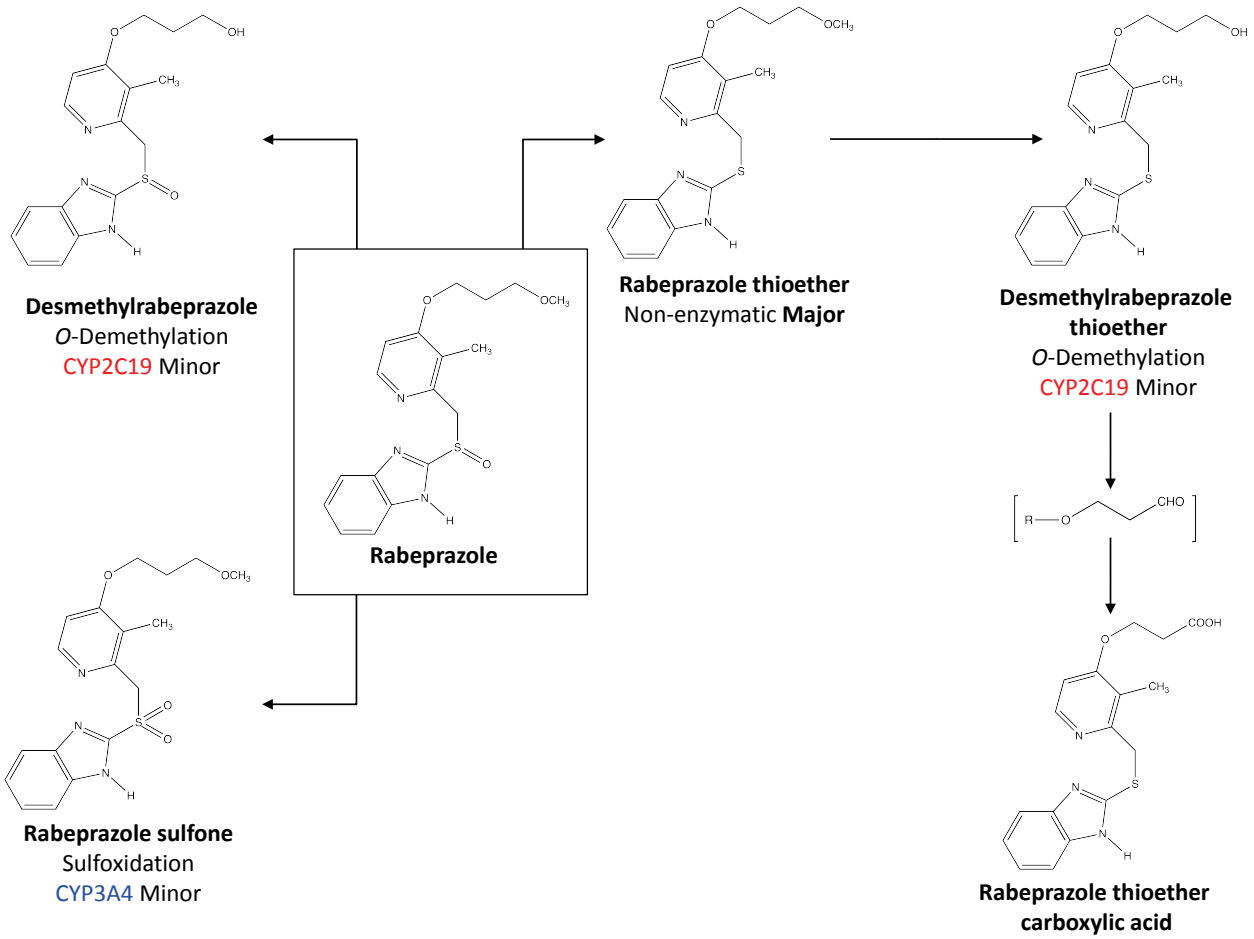

Figure 6.15. Metabolic scheme for rabeprazole

The metabolism of rabeprazole with CYP2C19-mediated reactions in red, CYP3A4-mediated reactions in blue and non-enymatic degradation in black. Adapted from (57).

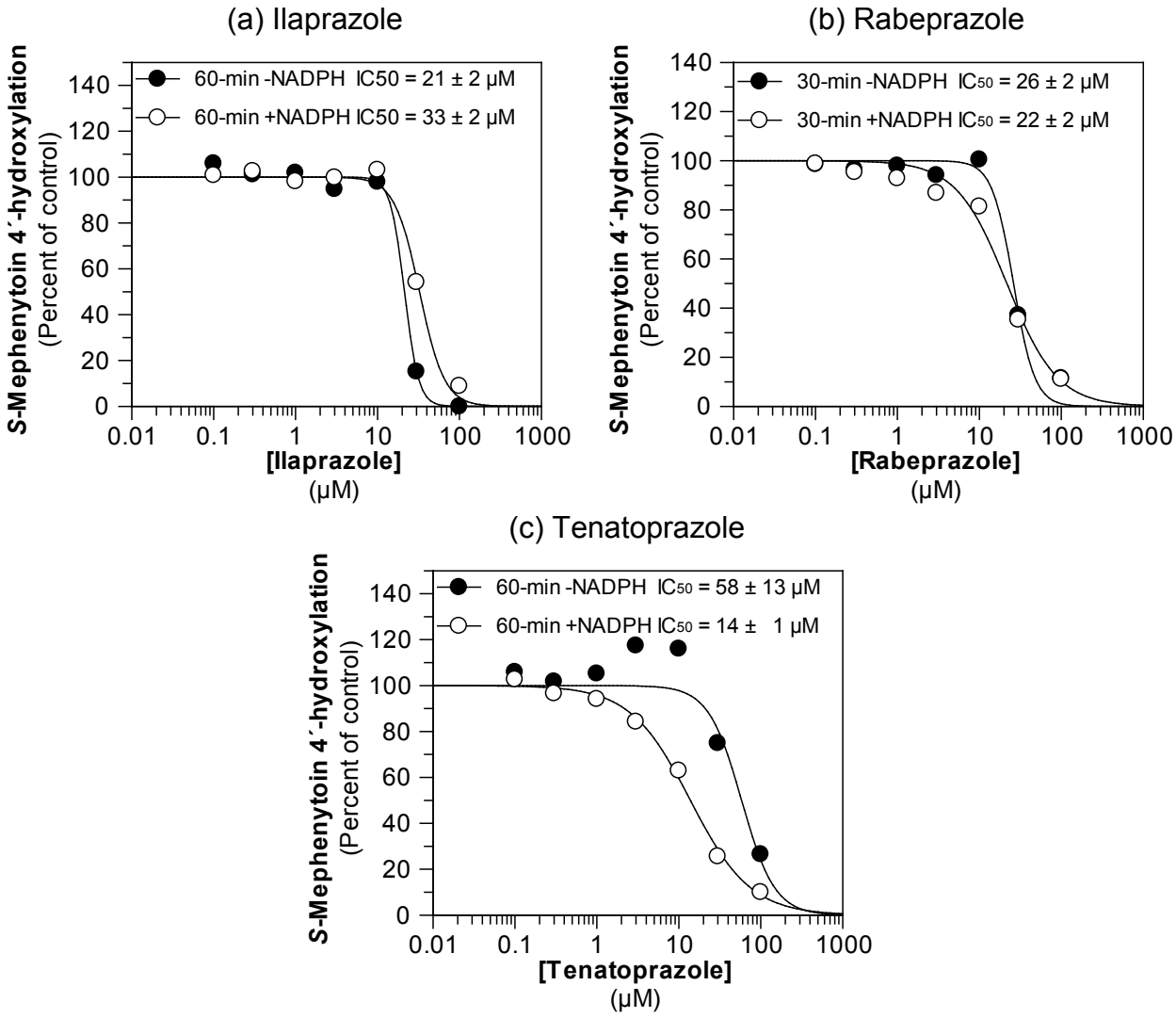

Figure 6.16. Evaluation of ilaprazole, rabeprazole and tenatoprazole as direct-acting and MDIs of CYP2C19

Each symbol represents the average of duplicate determinations. (a) Ilaprazole inhibited CYP2C19 in pooled HLM with IC_{50} values as shown (*S*-mephenytoin 4´-hydroxylation solvent control rates = 44.4 and 67.5 pmol/mg/min for 60-min –NADPH, and 60-min + NADPH pre-incubations, respectively). (b) Rabeprazole inhibited CYP2C19 in pooled HLM with IC_{50} values as shown (*S*-mephenytoin 4´-hydroxylation solvent control rates = 70.1 and 87.3 pmol/mg/min for 30-min –NADPH, and 30-min + NADPH pre-incubations, respectively). (c) Tenatoprazole inhibited CYP2C19 in pooled HLM with IC_{50} values as shown (*S*-mephenytoin 4´-hydroxylation solvent control rates = 44.9 and 64.9 pmol/mg/min for 60-min –NADPH, and 60-min + NADPH pre-incubations, respectively).

Table 6.3. Inhibition of CYP2C19 in human liver microsomes by ilaprazole, rabeprazole and tenatoprazole

Proton pump inhibitor	IC_{50} (μM)[a]			IC_{50} shift (fold)[b]
	5´-methyl substituent	Pre-incubation without NADPH[c]	Pre-incubation with NADPH[c]	
Ilaprazole	No	21 ± 2	33 ± 2	0.66
Rabeprazole	No	26 ± 2	22 ± 2	1.2
Tenatoprazole	**Yes**	58 ± 13	14 ± 1	**4.2**

[a] Values are displayed to two significant figures, ± standard error of the measurement

[b] Calculated from full precision values as (IC_{50} from pre-incubation without NADPH) ÷ (IC_{50} from pre-incubation with NADPH) and rounded to two significant figures. IC_{50} shifts > 1.5-fold appear in bold.

[c] Pre-incubation time is 60 min for ilaprazole and tenatoprazole and 30 min for rabeprazole.

Discussion

As described in the introduction to this chapter, mechanism-based inhibition (MBI) is a subset of time- or metabolism-dependent inhibition, but experiments to provide evidence that meet all of the criteria for MBI as described by Silverman (169) are rarely performed in the typical course of drug development. Taken together, the data presented in Chapter 5 and in this chapter (Table 6.1, Figure 6.5) are consistent with several of the criteria for mechanism-based inhibition of CYP2C19 by esomeprazole, 5-ODM omeprazole and omeprazole sulfone (i.e., criteria 1, 2, 3. 4. 5, and 8 as outlined in the introduction to this chapter and (16). Neither glutathione, superoxide dismutase, nor catalase, had a significant impact on the inactivation of CYP2C19 by esomeprazole, 5-ODM omeprazole or omeprazole sulfone (criterion 2). In addition, data presented in this chapter showed that the efficiency of inactivation of CYP2C19 by esomeprazole, 5-ODM omeprazole and omeprazole could be robustly determined in various experiments, providing more certainty that the effects of these "protectants" did not have a significant impact on CYP2C19 inactivation. Particularly strong evidence for MBI was shown by the alternate CYP2C19 substrate, pantoprazole, which provided significant enzyme protection against the inactivation of CYP2C19 by these compounds (criterion 5 – a hallmark of MBI). Evidence for criterion 7 (i.e., reduction of CYP content) will be presented in Chapter 7 for esomeprazole.

Are there structural features within omeprazole, esomeprazole or their metabolites that suggest possible mechanisms of inactivation of CYP2C19?

As for gemfibrozil glucuronide (33,159), there are no particularly obvious structural moieties within esomeprazole associated with MBI of CYPs (170,171). As hypothesized in Chapter 4, however, methylhydroxylation of esomeprazole to form 5´-hydroxyomeprazole could involve the intermediacy of a benzylic radical and heme alkylation, analogous to the inactivation

of CYP2C8 by gemfibrozil glucuronide as illustrated in Figure 6.17 (33,148,159). In this case, gemfibrozil glucuronide appears to partition between the formation (and non-inhibitory release) of 4′-hydroxygemfibrozil glucuronide and the formation of the reactive benzylic radical that adducts to heme (159).

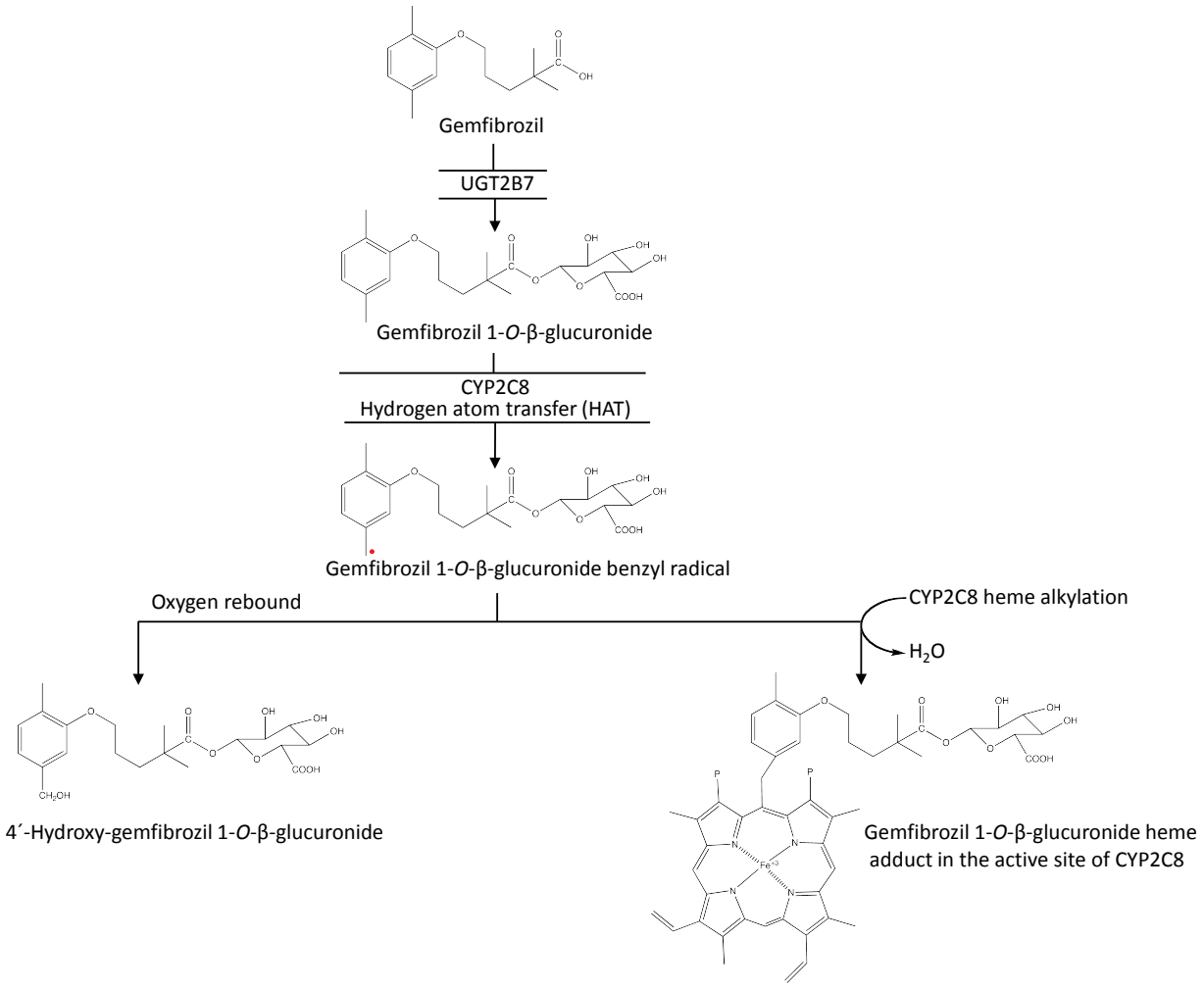

Figure 6.17. Benzylic radical formation as the mechanism of the irreversible metabolism-dependent inhibition of CYP2C8 by gemfibrozil

The metabolism-dependent inhibition of CYP2C8 by gemfibrozil involves the conversion of gemfibrozil to an acyl glucuronide which is then metabolized by CYP2C8 to a benzylic radical that covalently binds to the heme moiety and irreversibly inhibits the enzyme (33,148,159).

In such a case, benzylic radical formation as a potential cause of CYP2C19 inactivation by esomeprazole would also be a precursor to the formation of 5′-hydroxyomeprazole. This benzylic radical would form *prior* to formation and release of 5′-hydroxyomeprazole, not after, explaining why 5′-hydroxyomeprazole does not inhibit CYP2C19 (Figure 4.3). In this scenario, as in the case of CYP2C8 inactivation by gemfibrozil glucuronide, esomeprazole would be converted to a benzylic radical that has one of two fates: 1) it could alkylate the heme moiety and inactivate CYP2C19 or 2) undergo oxygen rebound to form 5′-hydroxyomeprazole. However, 5-ODM omeprazole is also an MBI of CYP2C19. The second possibility for inactivation of CYP2C19 raised in Chapter 4 was that formation of 5-*O*-desmethylomeprazole (a *para*-aminophenol) could lead to a reactive quinoneimine that could inactivate CYP2C19 if formed in its active site, but the data presented in this chapter showing that inactivation of CYP2C19 by 5-ODM omeprazole is not decreased by the addition of GSH argues against this possibility. Another remote possibility based on the presence of secondary and tertiary amines was that esomeprazole formed a MIC with CYP2C19. Evidence against this mechanism was provided by the lack of reversal of inactivation in the presence of potassium ferricyanide (Figure 4.7). In the studies presented in this chapter there was no evidence that esomeprazole formed an MIC with rhCYP2C19 based on the spectrophotometric studies depicted in Figure 6.6 under conditions where *S*-fluoxetine did form an MIC with rhCYP2C19 and troleandomycin formed an MIC with rhCYP3A4 (Figure 6.8 and Figure 6.10).

Do the metabolic pathways of omeprazole suggest that benzylic radical formation is a possible mechanism of CYP inactivation?

In spite of the lack of any obvious structural moiety known to be associated with MBI of CYPs, the results implicating esomeprazole as an MBI of CYP2C19 are not surprising on their own given that it is a well-known substrate of CYP2C19, and could therefore be activated to a reactive species that inactivates the enzyme prior to leaving the active site. Likewise,

5-ODM omeprazole is formed by CYP2C19, and additional oxidation of this metabolite once formed in the active site of CYP2C19 could conceivably give rise to a reactive intermediate that inactivates CYP2C19. For omeprazole sulfone, the situation is more complex, because CYP3A4 is the main enzyme involved in the formation of this metabolite from esomeprazole (113). For omeprazole sulfone to also be a MBI of CYP2C19, omeprazole sulfone would need to leave the active site of CYP3A4, and then be further oxidized by CYP2C19 to a reactive intermediate that inactivates this enzyme.

There is in fact evidence that omeprazole sulfone is further metabolized to 5´-hydroxyomeprazole sulfone by CYP2C19 and CYP3A4, with CYP2C19 acting as the high affinity enzyme (K_m = 7.6 μM) and contributing approximately 70% to this conversion (179). The known metabolic pathways for omeprazole and its metabolites are shown in Figure 6.12. Andersson et al., also showed that omeprazole sulfone inhibits the CYP2C19-dependent formation of 5´-hydroxyomeprazole and 5-ODM omeprazole from omeprazole with an apparent Ki value of approximately 10 μM (179). These in vitro experiments were conducted at 1 mg/mL HLM for 30 min and, as discussed in Chapter 4, these conditions would have allowed ample time for MDI to occur, leading to the reasonable conclusion that the inhibition was competitive, without a specific examination of time-dependence. It is also of interest that the estimated K_m for formation of 5´-hydroxyomeprazole sulfone by CYP2C19 (i.e., 7.6 μM (179)) is similar to the K_I value of 5.5 μM in the definitive K_I and k_{inact} determination for omeprazole sulfone toward CYP2C19 (Figure 5.4f). A similar value for the inactivation of CYP2C19 by omeprazole sulfone was reported by Shirasaka et al., with a K_I value of 5.7 μM (75). The concordance in these values is notable because the K_I value (i.e., the concentration that provides half-maximal inactivation) is analogous to K_m (i.e., the concentration that provides half-maximal catalysis). The secondary metabolism of 5-ODM omeprazole has not been examined, but if, like omeprazole sulfone, it could also be hydroxylated at the 5´-position by CYP2C19, then the

possibility remains that oxidation at this position within the active site *prior* to release of a further metabolite could be a common pathway for the inactivation of CYP2C19 by esomeprazole, omeprazole and 5´-ODM omeprazole, as proposed in Figure 6.13.

Why wouldn't other PPIs potentially form benzylic radicals and inactivate CYP2C19?

As shown in Table 1.1, of the PPIs, only omeprazole, esomeprazole and tenatoprazole have a 5´-methyl substituent. In addition, omeprazole sulfone and 5-ODM omeprazole can inactivate CYP2C19, and conversion of either esomeprazole or omeprazole to these metabolites leaves the 5´-methyl substituent intact. As described in Chapter 4, neither lansoprazole nor pantoprazole, which lack a 5´-methyl substituent can cause MDI of CYP2C19, and, based on their metabolic schemes (Figure 6.18), their metabolites are also not amenable to methylhydroxylation at the 5´-position.

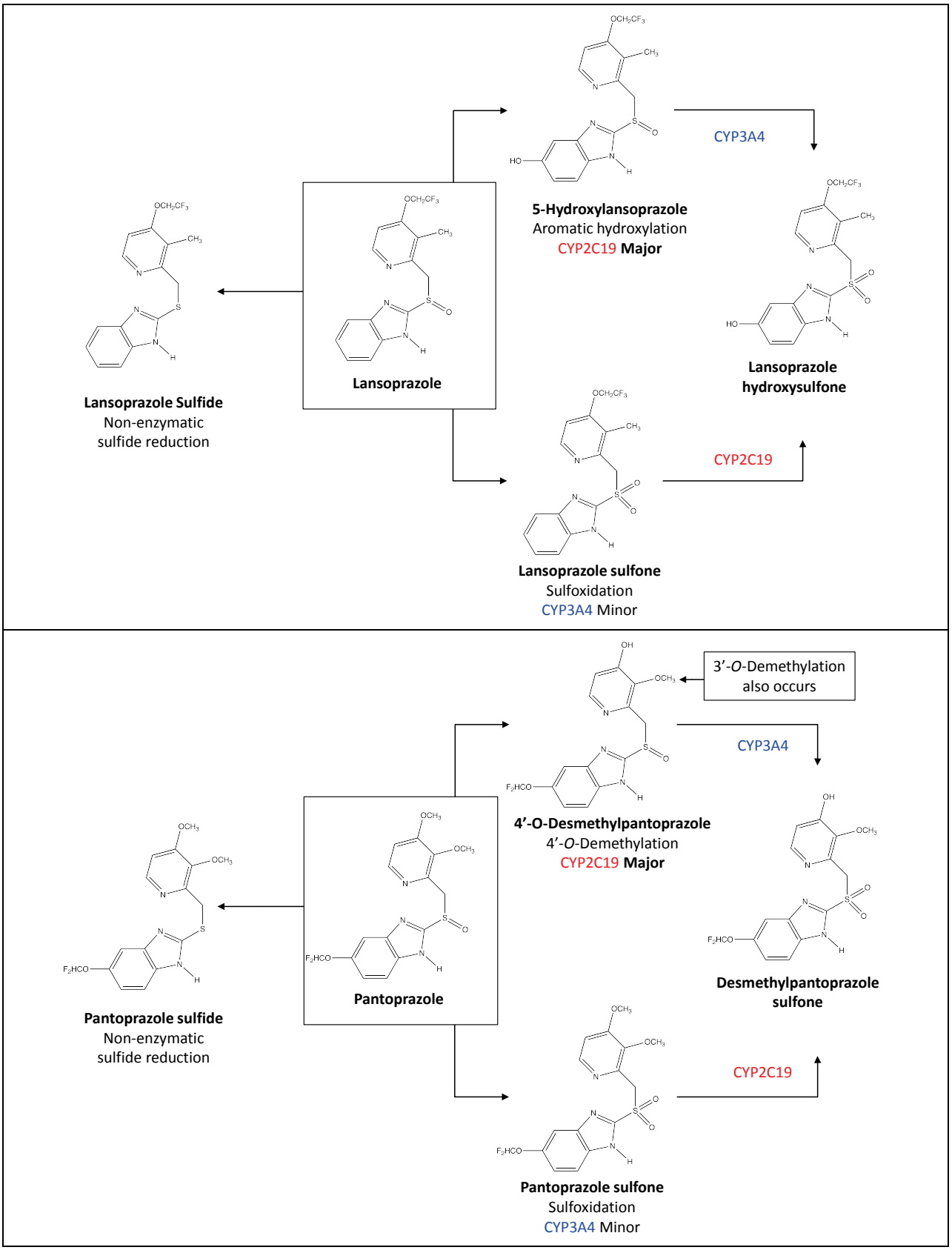

Figure 6.18. Metabolic schemes for lansoprazole and pantoprazole

The metabolism of lansoprazole and pantoprazole with CYP2C19-mediated reactions in red, CYP3A4-mediated reactions in blue and non-enymatic degradation in black. Adapted from (57).

The data presented in this chapter for rabeprazole and ilaprazole, which also lack a 5′-methyl substituent, show that these PPIs do not cause MDI of CYP2C19 (Figure 6.16, Table 6.3). In contrast, tenatoprazole caused a 4.2-fold shift in IC_{50} value when pre-incubated with NADPH-fortified HLM, which is the same as that observed for omeprazole (Table 4.1). However, as for esomeprazole (113), the clinical pharmacokinetics of tenatoprazole are consistent with MDI of CYP2C19 (the enzyme largely responsible for its metabolism). The accumulation ratios of tenatoprazole AUC from day 1 to day 20 range from 1.4 – 2.2 over the dose range 10 – 120 mg (61). Taken together with the data presented in Chapter 4 for lansoprazole and pantoprazole, all of these findings appear to be consistent with the hypothesis that the presence of a 5′-methyl substituent in a PPI is necessary for MDI of CYP2C19. It should also be remembered that, as discussed in Chapter 4, *R*-omeprazole does not appear to be an irreversible MDI of CYP2C19 (Figure 4.7). This suggests that the particular stereochemistry of the PPIs may also play a role in the ability of a PPI with a 5′-methyl substituent to inactivate CYP2C19. The fact that conversion of *R*-omeprazole to the non-inhibitory 5′-hydroxyomeprazole by CYP2C19 comprises more than 94% of the intrinsic clearance of this enantiomer (Figure 4.9) seems counter-intuitive to the hypothesis that this metabolite is produced by oxygen rebound after benzylic radical formation. However, the results taken as a whole would suggest that if the “benzylic radical hypothesis” is true, then the partition ratio (i.e., the number of productive catalytic events per inactivation event) for *R*-omeprazole must be very high compared to esomeprazole (because a lower partition ratio means that more inactivation events occur than productive catalytic events). This in turn suggests that the stereochemistry of esomeprazole may allow for a more favorable positioning of the theoretical 5′-hydroxy benzyl radical near the heme moiety than *R*-omeprazole. This difference is reminiscent of the reportedly more favorable positioning of the *ortho* benzylic methyl group of gemfobrozil glucuronide within 3.0 – 4.0 Å of the γ-meso position of CYP2C8 heme than the *meta* benzylic methyl group (159,180). The stereoselectivity of the inactivation of

CYP2C19 by esomeprazole and its metabolites needs to be investigated further, and will be discussed in Chapter 8. Finally, the fact tenatoprazole, esomeprazole, and the esomeprazole and omeprazole metabolites, namely omeprazole sulfone and 5-ODM omeprazole, can inactivate CYP2C19, whereas 5´-hydroxyomeprazole cannot (Figure 6.13), suggests the possibility that, analogous to the proposed mechanism of inactivation of CYP2C8 by gemfibrozil glucuronide, formation of a reactive benzylic radical within the active site of CYP2C19 may be the common mechanism of inactivation for these compounds.

In conclusion, further evidence for mechanism-based inhibition of CYP2C19 by esomeprazole, omeprazole sulfone and 5-ODM omeprazole was provided in this chapter in that neither glutathione, superoxide dismutase, nor catalase was found to have a significant impact on the inactivation of CYP2C19 by these three compounds. In contrast, the alternate CYP2C19 substrate, pantoprazole, provided significant enzyme protection. I obtained no spectrophotometric evidence to suggest that esomeprazole forms a MIC with CYP2C19 under conditions where positive controls did. The data presented in this chapter also showed that tenatoprazole, the only PPI other than omeprazole and esomeprazole with a 5´-methyl substituent, is also an MDI of CYP2C19, whereas ilaprazole and rabeprazole are not. The possibility of heme alkylation through the formation of a benzylic radical as a common pathway of inactivation of CYP2C19 by esomeprazole, omeprazole sulfone, 5-ODM omeprazole and tenatoprazole was also discussed. Additional experimental approaches to further investigate the mechanism of inactivation of CYP2C19 by esomeprazole will be discussed in Chapter 8.

Chapter 7. AN INITIAL EVALUATION OF THE ABILITY OF ESOMEPRAZOLE TO BIND TO THE HEME OF CYP2C19 BY UHPLC/UV/HRMS

Abstract

Studies were undertaken to test the hypothesis that the inactivation of CYP2C19 by esomeprazole is the result of the formation of a reactive metabolite that binds covalently to the heme moiety. The results described in this chapter provide tentative support for this hypothesis but, perhaps more interestingly, they revealed the potential for an unusual artifact that can result when heme-adducts potentially formed from a sulfur-containing drug are analyzed by high-resolution mass spectrometry with mass-defect filtering. When incubated with NADPH-fortified human liver microsomes (1 mg/mL) for 120 min, esomeprazole (100 μM) caused a ~50% loss of heme (relative to NADPH-fortified HLM in the absence of substrate) as measured by both ultra-high performance liquid chromatography (UHPLC) with UV/VIS detection at 398 nm and by high resolution mass spectrometry (HRMS). Although this finding supported the heme-alkylation hypothesis, no new 398 nm-absorbing chromatographic peak could be detected, suggesting the missing heme was either covalently cross-linked to the apoprotein (and hence lost during protein precipitation) or the heme adduct did not absorb light at 398 nm, or heme was fragmented or destroyed, which has been reported for other CYP inactivators. To investigate the possibility that an isolable heme adduct was formed but not detectable at 398 nm, heme was extracted from esomeprazole-incubated samples and analyzed by UHPLC-UV with HRMS and post-acquisition mass-defect filtering. Mass-defect filtered HRMS identified an apparent heme-associated component (observed *m/z* = 723.2266) that appeared to have an isotopic distribution pattern characteristic of the intact heme if the absence of certain low abundance isotopes were attributed to background noise. However, subsequent analysis established that the putative heme adduct identified by mass-defect filtering with *m/z* = 723.2266 and a theoretical elemental composition of $C_{41}H_{39}FeN_4O_5$ was in fact a dimer of esomeprazole sulfone, which has a theoretical *m/z* = 723.2271 and an elemental composition of $C_{34}H_{39}N_6O_8S_2$. Compared with the abundance of the monoisotope (set to 100%), the +1, +2 and +3 isotopes of omeprazole sulfone

dimer were 40%, 9% and 3%, respectively, which were similar to the relative abundance of the +1, +2 and +3 isotopes of heme, namely, 40%, 7% and 1%, respectively. A distinguishing feature was the absence (<1%) of −1 and −2 isotopes in the mass spectrum of omeprazole sulfone dimer and their presence at a relative abundance of 2% and 6%, respectively, in the mass spectrum of heme. Analysis of a reference standard solution of omeprazole sulfone resulted in the detection of a component within the accurate *m/z* range of both the theoretical dimer and the potential heme adduct at the same retention time of the component observed in the esomeprazole-incubation samples.

In summary, the results presented in this chapter provide tentative support for the possibility that, based on the loss of 398 nm-detectable heme, esomeprazole inactivates CYP2C19 by alkylating the heme moiety. Analysis of the putative heme adduct by high resolution mass spectrometry with mass-defect filtering did not identify a heme adduct but instead revealed an interesting artifact whereby a dimer of omeprazole sulfone had mass spectral characteristics remarkably similar to a heme adduct, which should be taken into consideration when such studies are performed with other sulfur-containing drugs.

Introduction

In chapters 4-6, I presented evidence that esomeprazole, omeprazole sulfone and 5-*O*-desmethyl omeprazole, but not *R*-omeprazole, are mechanism-based inhibitors of CYP2C19. These studies established that esomeprazole, omeprazole sulfone and 5-*O*-desmethyl omeprazole meet the following criteria for mechanism-based inhibition (MBI) of CYP2C19: 1) inactivation of CYP2C19 occurs in a concentration-, time- and metabolism-dependent manner, 2) the efficiency of inactivation is not diminished by glutathione, superoxide dismutase nor catalase (exogenous scavengers), 3) the inactivation is irreversible (by ultracentrifugation and washing), 4) the inactivation is saturable with respect to inactivator concentration, 5) the alternate CYP2C19 substrate pantoprazole protects the enzyme against inactivation, and 6) inactivation requires a catalytic event in that it does not occur in the absence of the CYP co-factor NADPH.

In Chapter 6, MIC formation was ruled out as the mechanism of inactivation of CYP2C19 by esomeprazole. This suggests the inactivation of CYP2C19 by esomeprazole involves formation of a metabolite that alkylates the apoprotein, alkylates the heme prosthetic group or cross links these two moieties in a manner that blocks further catalytic activity. The studies described in this chapter were designed to test the hypothesis that esomeprazole inactivates by CYP2C19 by alkylating the heme moiety. It is worth noting that studies to investigate the possible binding of esomeprazole to the apoprotein moiety of CYP2C19 were not investigated because radioactive esomeprazole is not commercially available and because purified CYP2C19 (as opposed to cDNA-expressed CYP2C19) was prohibitively expensive. Purified CYP2C19 is a more optimal test system than an expressed form of CYP2C19 (e.g., Supersomes) because mass spectral analysis of proteins produces an envelope of multiply charged ions that must be deconvoluted in order to detect a small change in protein mass due

to adduction of a small molecule to the apoprotein. With the many proteins present in expressed recombinant CYP2C19, the protein "envelope" would be particularly difficult to deconvolute.

As noted above, MBI of a CYP enzyme can involve alkylation of the apoprotein or cross-linking of the heme to the apoprotein. In the former case (protein alkylation) there is no loss of extractable heme and no formation of a new 398 nm-absorbing chromatographic peak indicative of a heme adduct. In the latter case (cross-linking), there is loss of extractable heme but there is no formation of new 398 nm-absorbing heme peak. On the other hand, MBI could involve heme alkylation without cross linking to the apoprotein. In this case, it is possible – but not inevitable – that a new 398 nm-absorbing peak will be detected by analysis of the extracted heme by HPLC with UV/VIS detection. In order to observe a new peak, the heme adduct must be chromatographically distinct from heme and it must absorb light at ~400 nm. Heme adducts have been shown to have extinction coefficients at ~400 nm that are essentially zero (they do not absorb light at ~400 nm) or are much lower than that of intact heme. For example, 1-aminobenzotriazole (1-ABT), an MBI that alkylates the heme of numerous CYP enzymes, appears to have an extinction coefficient at 398 nm of zero; hence, heme alkylation by 1-ABT does not lead to the appearance of a new 398 nm-absorbing chromatographic peak. In the case of gemfibrozil glucuronide, a selective MBI of CYP2C8, the heme adduct has an extinction coefficient that is approximately 12% of that for intact heme (159). From these examples it is apparent that, when examining the mechanism of CYP inactivation, failure to detect a new 398 nm-absorbing chromatographic peak does not rule out the possibility that a heme adduct formed, as in the case of 1-ABT. In some cases, such as the cumene hydroperoxide-mediated inactivation of CYP3A4, or inactivation of one or more CYPs in rat or human liver microsomes by parathion or carbamazepine, heme may be completely destroyed and reactive fragments of heme can subsequently bind irreversibly to the apoprotein (181,182). However, the loss of

heme (as evidenced by a decrease in absorbance at 398 nm) is evidence of heme adduct formation, cross-linking of heme to apoprotein, or heme destruction.

In previous studies conducted to examine the mechanism of inactivation of CYP by various compounds that modify the prosthetic heme, heme was extracted from cytochrome P450 with a strong acid followed by extraction into an organic solvent such as dichloromethane or acetone (159,181,183-187). Strong acids are used in the initial step because heme-protein bonds are completely broken at pH≤1.0 (188). As discussed in Chapter 1, PPIs become protonated under acidic conditions, and the resulting cyclic sulfenamide can covalently bind to cysteine residues (Figure 1.2). Omeprazole is rapidly and nearly completely converted to the cyclic sulfenamide within 10 to 100 milliseconds at pH 1-4 (189,190). Free omeprazole and omeprazole bound to heme at the benzylic position would also be expected to undergo conversion to the cyclic sulfenamide at low pH. Because the addition of a strong acid (i.e., 1N HCl) to facilitate heme extraction catalyzes this rearrangement, UHPLC-UV/HRMS combined with post-acquisition mass-defect filtering (MDF) was used to detect the formation of a heme-associated adduct with an unexpected mass (i.e., an adduct that was not a simple addition of esomeprazole or a known inhibitory metabolite to heme, but a rearranged product). The accurate mass defect is the difference between the accurate mass and the nearest whole integer mass of the combined elements with a specific molecular formula (126). For example, the accurate mass defect for heme (*m*/*z* of $C_{34}H_{32}FeN_4O_4$ = 616.1773) is +0.1773. MDF is an *in silico* data filter that screens out all mass spectral peaks that are not associated with the accurate mass defect for the analyte of interest, in this case heme. By constructing a mass-defect filter within 35 mDa of the mass defect for heme, only heme-associated small-molecule components should be detected (126). UHPLC-UV/HRMS combined with mass-defect filtering (MDF) was used to investigate the mechanism of inactivation of CYP2C19 by esomeprazole, based on the hypothesis that a *lack* of detection of a new heme-associated peak by HRMS-

MDF would suggest that the mechanism of inactivation was covalent modification of the apoprotein or cross linking of the heme to the apoprotein.

For simplicity, the term ‘esomeprazole-incubated sample’ is used throughout this chapter to describe in vitro incubations of esomeprazole with human liver microsomes in the presence of NADPH. A corresponding term is used for incubations of gemfibrozil glucuronide or 1-ABT with NADPH-fortified human liver microsomes. In addition, for convenience when discussing isotopic distributions, the terms ‘lighter’ and ‘heavier’ are used to denote isotopes with less and more mass than the monoisotopic mass, respectively. Finally, for UV-detectable, the term 398 nm-detectable will be used, even though 398 nm is within the UV spectrum.

Results

7.1. Loss of 398 nm-detectable heme from esomeprazole-treated and 1-ABT-treated HLM

In an initial attempt to determine if the mechanism-based inhibition of CYP2C19 involved heme modification, the heme extracted from esomeprazole-incubated samples was analyzed by UHPLC-UV/HRMS). The initial hypotheses being tested in these experiments were 1) that 398 nm-detectable heme would decrease relative to the control if heme were modified or cross linked to apoprotein, and 2) that an additional chromatographic peak detectable at 398 nm would be evidence of heme modification. To generate sufficient heme adduct for detection at 398 nm, a relatively high concentration of HLM (1 mg/mL) supplemented with NADPH was incubated for 120 min with a high concentration of esomeprazole (100 μM) or solvent (negative control). Chromatograms of 398 nm-detectable heme from a solvent control and esomprazole-incubated sample (both containing NADPH) are shown in Figure 7.1a and b, respectively. Under the conditions tested, approximately 50% of the 398 nm-detectable heme was lost when HLM were incubated with esomeprazole. However, no new 398 nm-absorbing chromatographic peak was observed. It is possible that not all of the heme was extracted from the control sample, such that the amount of heme lost may be an over-estimate.

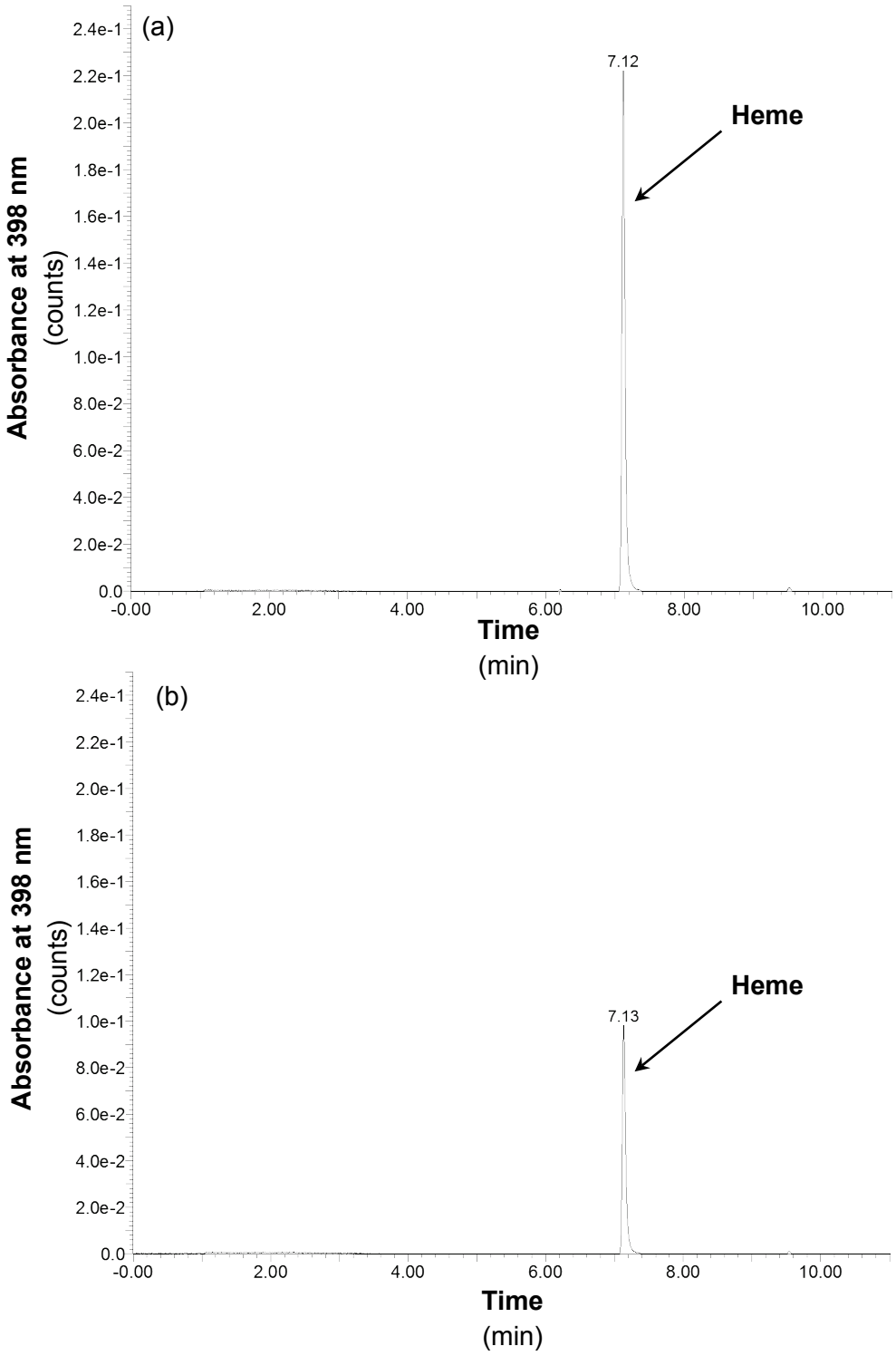

Figure 7.1. UV chromatograms (λ = 398 nm) showing the heme extracted from control and esomeprazole-treated human liver microsomes

The chromatograms show the UV peak for heme extracted from NADPH-fortified human liver microsomes (1 mg/mL) incubated for 120 min with solvent (i.e., methanol/Tris (pH 9.0) at 0.4/0.6% v/v final) (chromatogram a) or 100 µM esomeprazole (chromatogram b).

As a positive control for the loss of 398 nm-detectable heme, the ubiquitous CYP inactivator 1-ABT (2 mM) was incubated with NADPH-fortified HLM (1 mg/mL) for 120 min. As shown in Figure 7.2, 1-ABT decreased the amount of 398 nm-detectable heme by more than 95%. It is possible that not all of the heme was extracted from the control sample, such that the amount of heme lost may be an over-estimate. No new 398 nm-absorbing chromatographic peak was observed, as previously reported by others (183,186,191,192).

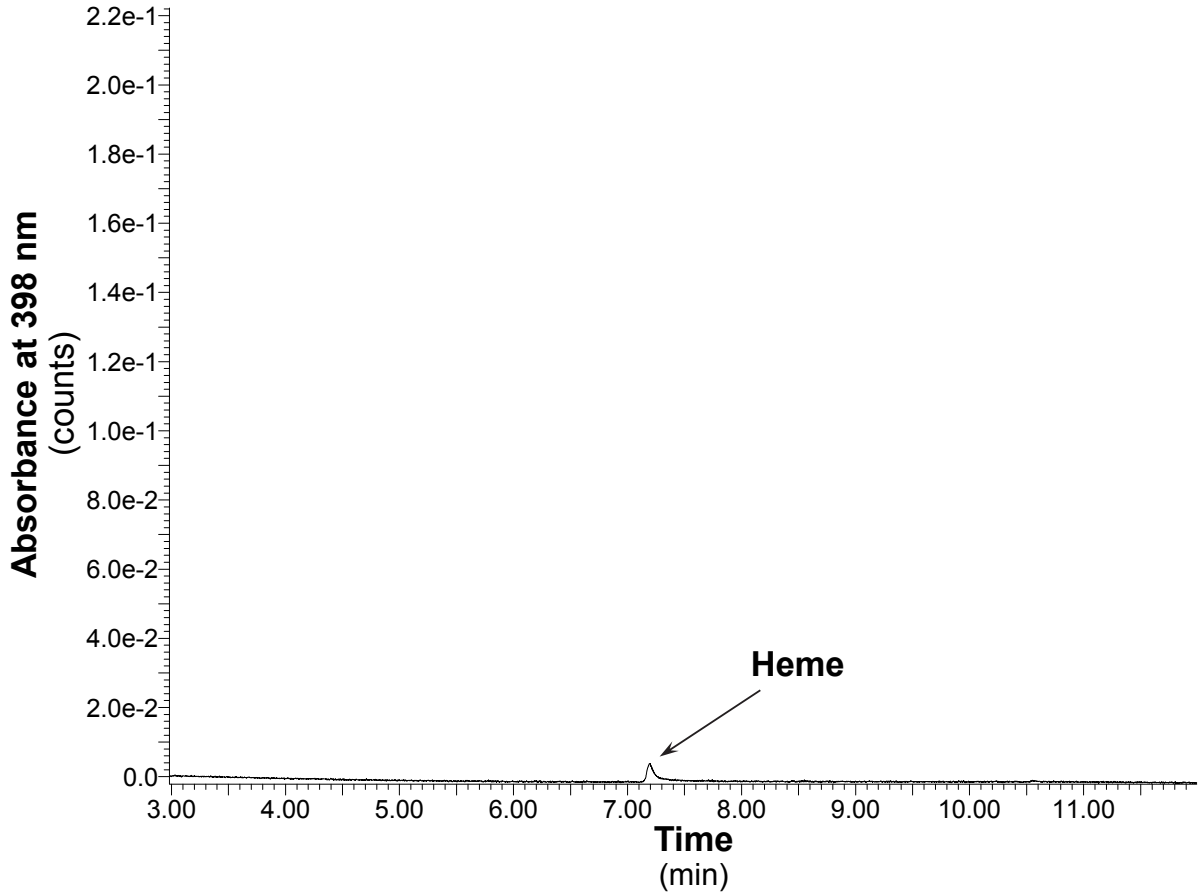

Figure 7.2. UV chromatograms (λ = 398 nm) showing the heme extracted from 1-aminobenzotriazole- treated human liver microsomes

The chromatogram shows the UV peak for heme extracted from an incubation of NADPH-fortified human liver microsomes (1 mg/mL) for 120 min with 1-ABT-treated (2 mM). The corresponding control sample is shown in Figure 7.1a.

The heme extracted from esomeprazole- and 1-ABT-incubated samples was also quantified by accurate mass spectrometry (*m*/*z* = 616.1773 ± 20 mDa) from the in-line analysis and chromatographic peaks were integrated and compared against the control. The results are shown in Figure 7.3. The results were in agreement with the 398 nm-detectable loss of heme, with approximately 50% of the heme lost from esomeprazole-incubated samples and >95% lost from 1-ABT-incubated samples. No additional mass spectral peaks within 20 mDa of the exact mass for heme or small-molecule heme adducts were detected in either the esomeprazole- or 1-ABT-incubated sample, which is also consistent with the analysis of heme based on UV absorbance. Ion chromatograms were processed by mass-defect filtering for a non-targeted evaluation of the heme and associated adducts, as well as by extraction of specific *m/z* values of interest for heme and predicted heme/esomeprazole adducts (data not shown).

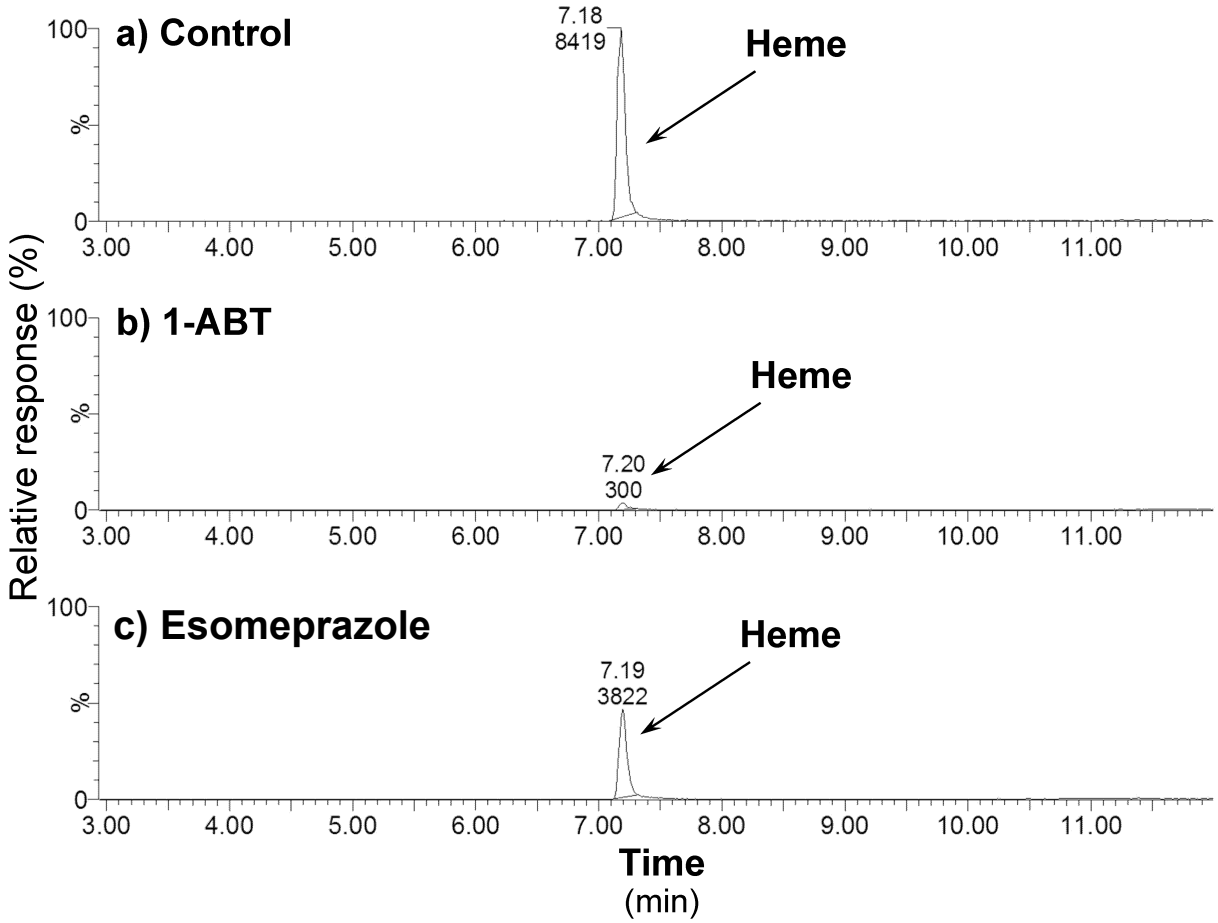

Figure 7.3. Integrated extracted accurate mass chromatograms of heme extracted from incubations of 1-aminobenzotriazole or esomeprazole with human liver microsomes

The chromatograms show the integrated extracted accurate mass (*m*/*z* = 616.1773 ± 20 mDa) for heme extracted from NADPH-fortified human liver microsomes (1 mg/mL) incubated for 120 min with solvent (chromatogram a), 1-ABT (chromatogram b) or esomeprazole (chromatogram c). The results are expressed relative to the solvent control (i.e., NADPH-fortified HLM in the absence of substrate). Values of integrated peak areas for the heme peak at ~7.2 min are shown below the retention time in each figure.

7.2. The use of mass-defect filtering to examine the potential for heme-associated components in treated human liver microsomes

Figure 7.4 shows the total ion chromatograms (TIC) acquired with the MS^E scan type across the *m/z* 50-1200 for heme extracted from solvent-incubated samples (i.e., NADPH-fortified HLM in the absence of substrate) (chromatogram a) and esomeprazole-incubated samples (chromatogram b). A notable difference between the two chromatograms is the large peak at ~ 5 min in the TIC for the esomeprazole-incubated sample, which was attributed in part to esomeprazole metabolites. The TIC was searched for specific ions with masses corresponding to adducts between heme and either esomeprazole (~*m/z* 960) or its known metabolites (such as ~ *m/z* 976 for heme + hydroxy-omeprazole and ~*m/z* 946 for heme + desmethylomeprazole). No such adducts were detected. Screening for heme adducts based on a search for diagnostic fragments of heme was not attempted because, as shown in Figure 7.5, the product ion spectrum (PIS) for intact heme revealed no suitably diagnostic fragments. Therefore, in an attempt to find a heme-associated peak with an unanticipated mass, a *C*-heteroatom mass-defect filter (dynamic with mass range) (127,193) was constructed ±35 mDa around the mass defect of heme (theoretical *m*/*z* of intact heme = 616.1773) and potential small molecule heme adducts, as described below.

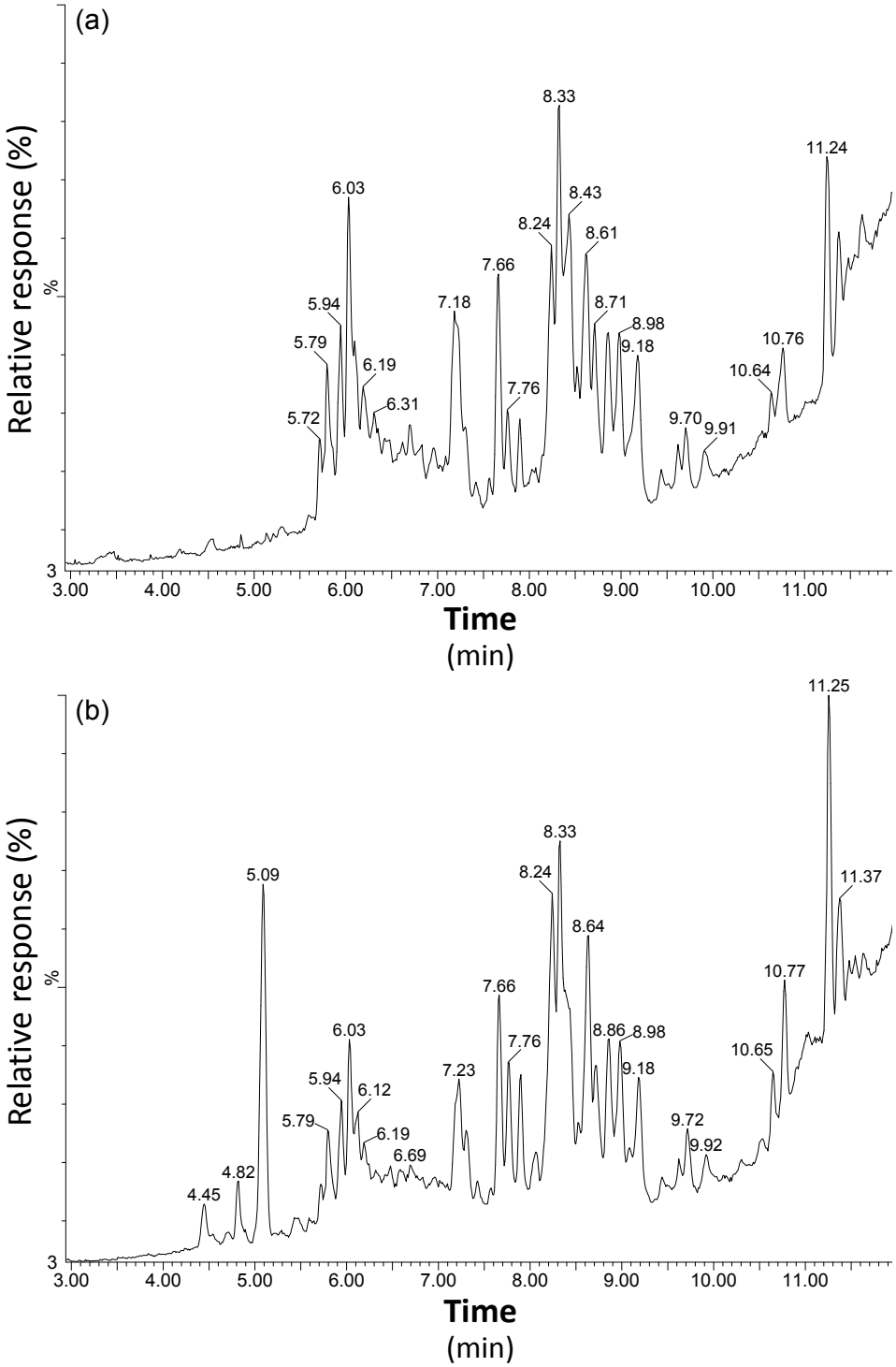

Figure 7.4. Total ion chromatogram for heme extracted from control and esomeprazole-treated human liver microsomes

Total ion chromatograms (TICs) are shown for extracts from NADPH-fortified human liver microsomes (1 mg/mL) following a 120-min incubation with solvent (i.e., methanol/Tris (pH 9.0) at 0.4/0.6% v/v final) (chromatogram a) or 100 μM esomeprazole (chromatogram b). The

prominent peak at ~ 5 min in chromatogram b was subsequently identified as omeprazole sulfone, the major metabolite formed by CYP3A4.

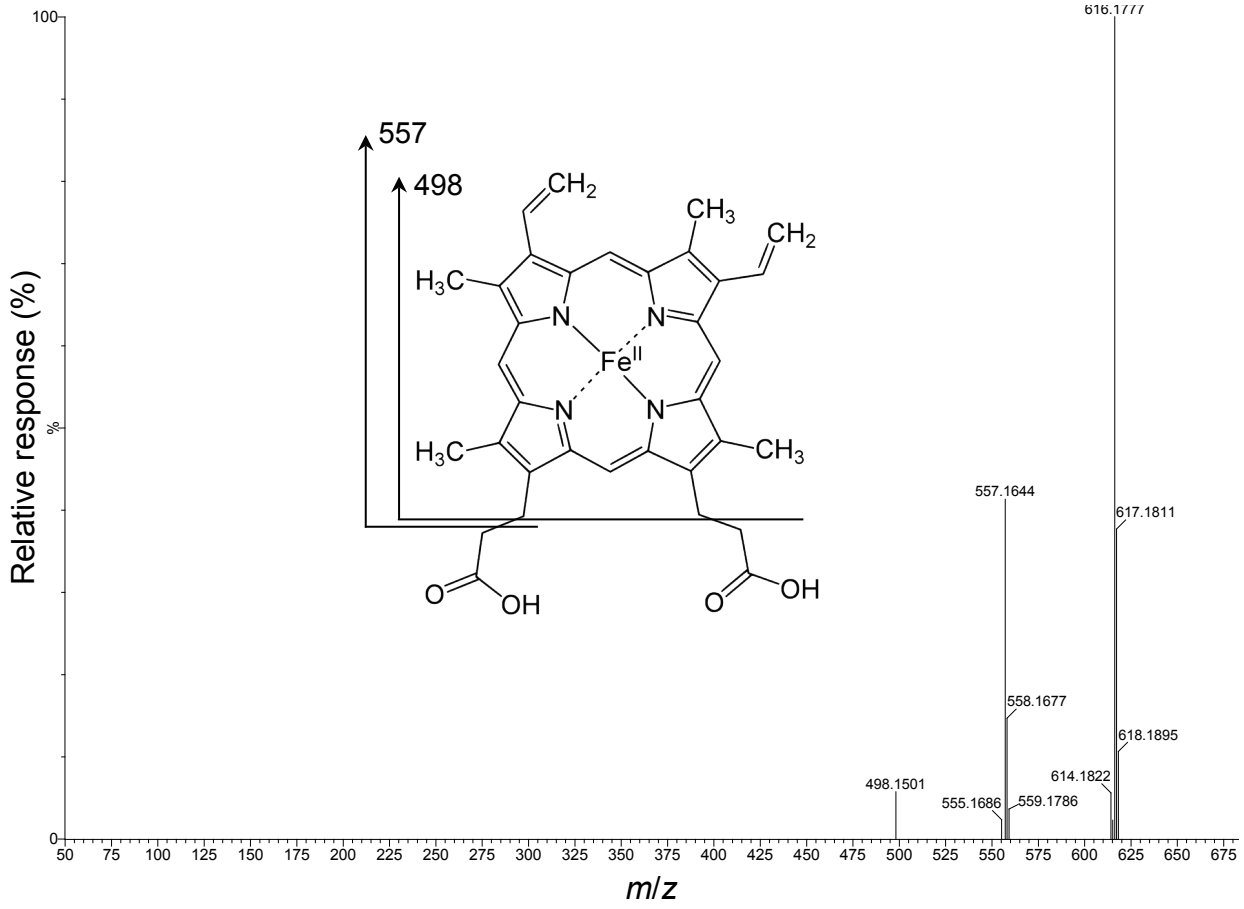

Figure 7.5. Product ion spectrum for heme extracted from esomeprazole-treated human liver microsomes

The product ion spectrum of heme was based on an analysis of intact heme extracted from incubations of esomeprazole (100 μM) with NADPH-fortified human liver microsomes (1 mg/mL).

Figure 7.6 shows the accurate mass-defect filtered chromatograms obtained following a 120-min incubation of NADPH-fortified HLM (1 mg/ML) with solvent (chromatogram a), 2 mM 1-ABT (chromatogram b) or 100 μM esomeprazole (chromatogram c). The marked and partial loss of heme following incubation with 1-ABT and esomeprazole, respectively, were similar to those shown in Figure 7.1 and Figure 7.2 (based on UV absorbance) and Figure 7.3 (based on *m*/*z* = 616.1773). The mass-defect filtered chromatograms show only peaks with a mass defect within ±35 mDa of the range of the mass defect for heme and heme-related components. Because the *C*-heteroatom dealkylation algorithm was used to construct the mass filter, at the low end of the examined mass range, the specific high and low values of the mass defect filter vary to bracket the mass defects of possible fragments of heme (i.e., within 35 mDa). At the high end of the examined mass range, the intact mass defect of heme (+0.1773) is the central mass of the filter range. In theory, the majority of component masses not filtered out should be related to the heme structure.

Based on mass-defect filtering, the loss of heme from esomeprazole-treated HLM was similar to that in Figure 7.3, but an additional peak was observed at a retention time of approximately 5 min. This additional peak was not detected in the 1-ABT-incubated sample and appeared to correspond to a protonated molecule of *m*/*z* = 723.2266 (mass error = -0.6 ppm). A heme-containing ion of this *m/z* would correspond to the mass of intact heme (616.1773) + a mass of 107.0493 amu. The additional mass (theoretically caused by the addition of C_7H_7O, with a theoretical mass of 107.0497 amu) does not correspond to the mass of esomeprazole or any of its known metabolites, but it seemed possible that the apparent adduct was a fragment of esomeprazole (or a metabolite) formed by acid-catalyzed rearrangement during the extraction of heme with hydrochloric acid. An extracted accurate mass chromatogram from esomeprazole-treated HLM at *m*/*z* = 723.2270 ± 20 mDa (Figure 7.7) showed two peaks with retention times of 4.82 min (minor) and 5.09 min (major). Both components were obscured by other ions in the

TIC shown in Figure 7.4b, including those within the large peak at approximately the same retention time.

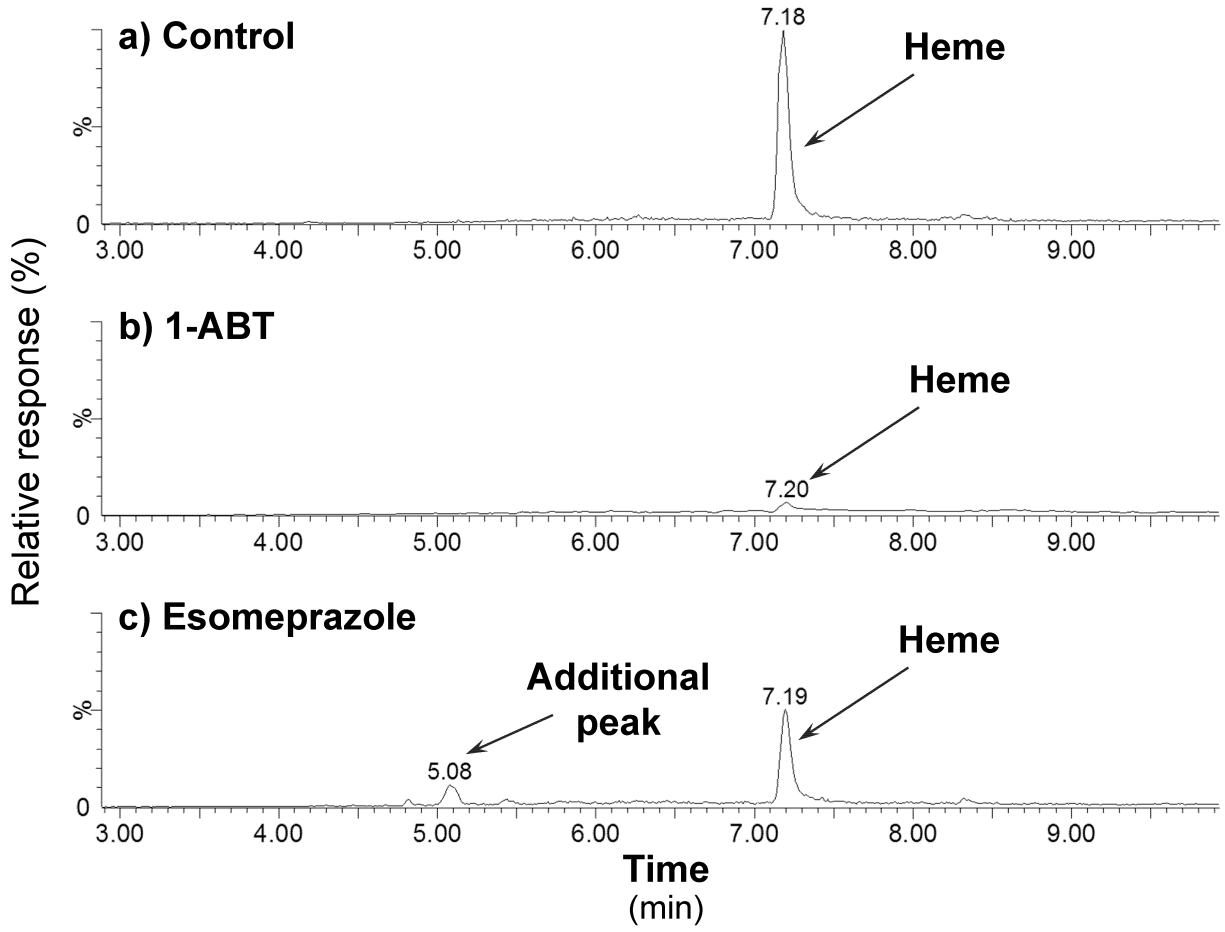

Figure 7.6. *C*-Heteroatom accurate mass-defect filtered chromatograms from incubations of human liver microsomes with solvent, 1-aminobenzotriazole or esomeprazole

The mass-defect filter was constructed ±35 mDa around the theoretical accurate mass of heme (*m*/*z* = 616.1773) to search for heme-associated components in 120-min incubations of NADPH-fortified human liver microsomes (1 mg/mL) with solvent (chromatogram a), 2 mM 1-aminobenzotriazole (chromatogram b) or 100 μM esomeprazole (chromatogram c).

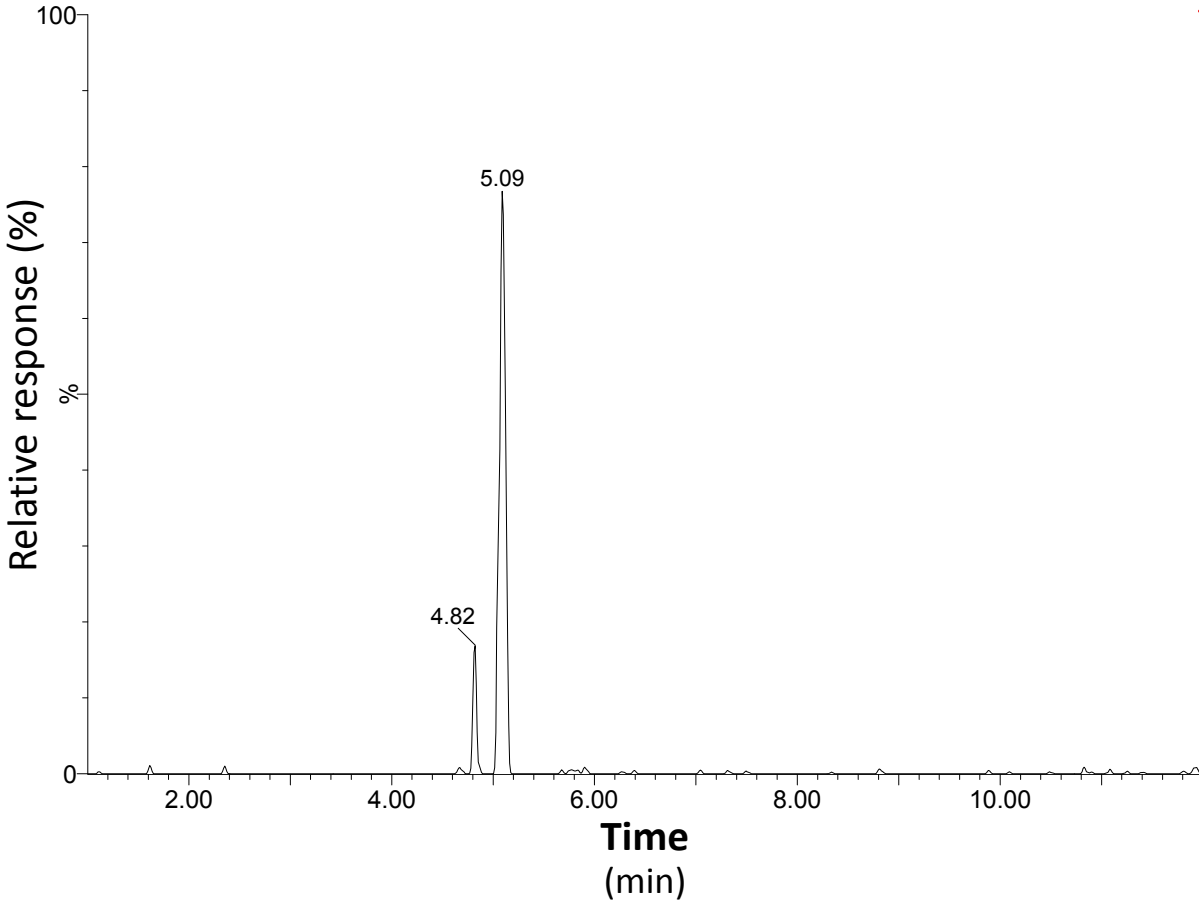

Figure 7.7. Extracted accurate mass chromatogram of components with m/z = 723.2270 ± 20 mDa in esomeprazole-treated human liver microsomes

The total response is 1000 x relative to the total ion chromatogram shown in Figure 7.4.

7.2. Low energy full scan MS^E mass spectra for heme extracted from control and esomeprazole-treated human liver microsomes

Isotopic distribution was used to evaluate whether the additional peaks identified in esomeprazole-incubated samples by mass-defect filtering were actually associated with heme. Isotopic distribution was examined in low energy full scan MS^E spectra for intact heme from a control sample and the additional peaks found in esomeprazole-incubated samples, and the results are shown in Figure 7.8 and Figure 7.9, respectively. The isotopic distribution of intact heme showed the typical pattern for iron-, oxygen- and nitrogen-containing organic compounds (discussed later in Section 7.5). Three peaks containing heavier isotopes than the protonated monoisotopic molecule and two peaks containing lighter isotopes were evident in the mass spectrum of heme, as shown in Figure 7.8. Relative to the monoisotope with an observed m/z = 616.1772 (100%), the -2, -1, +1, +2 and +3 isotopes have an abundance of approximately 6, 2, 40, 7 and 1%, respectively. As shown in Figure 7.9, the additional peak found in esomeprazole-incubated samples by mass-defect filtering, and more so its sodium and potassium adducts, showed 3 heavier isotopes but no lighter isotopes; the relative abundance of the +1, +2 and +3 isotopes were approximately 40, 9 and 3% of the monoisotope.

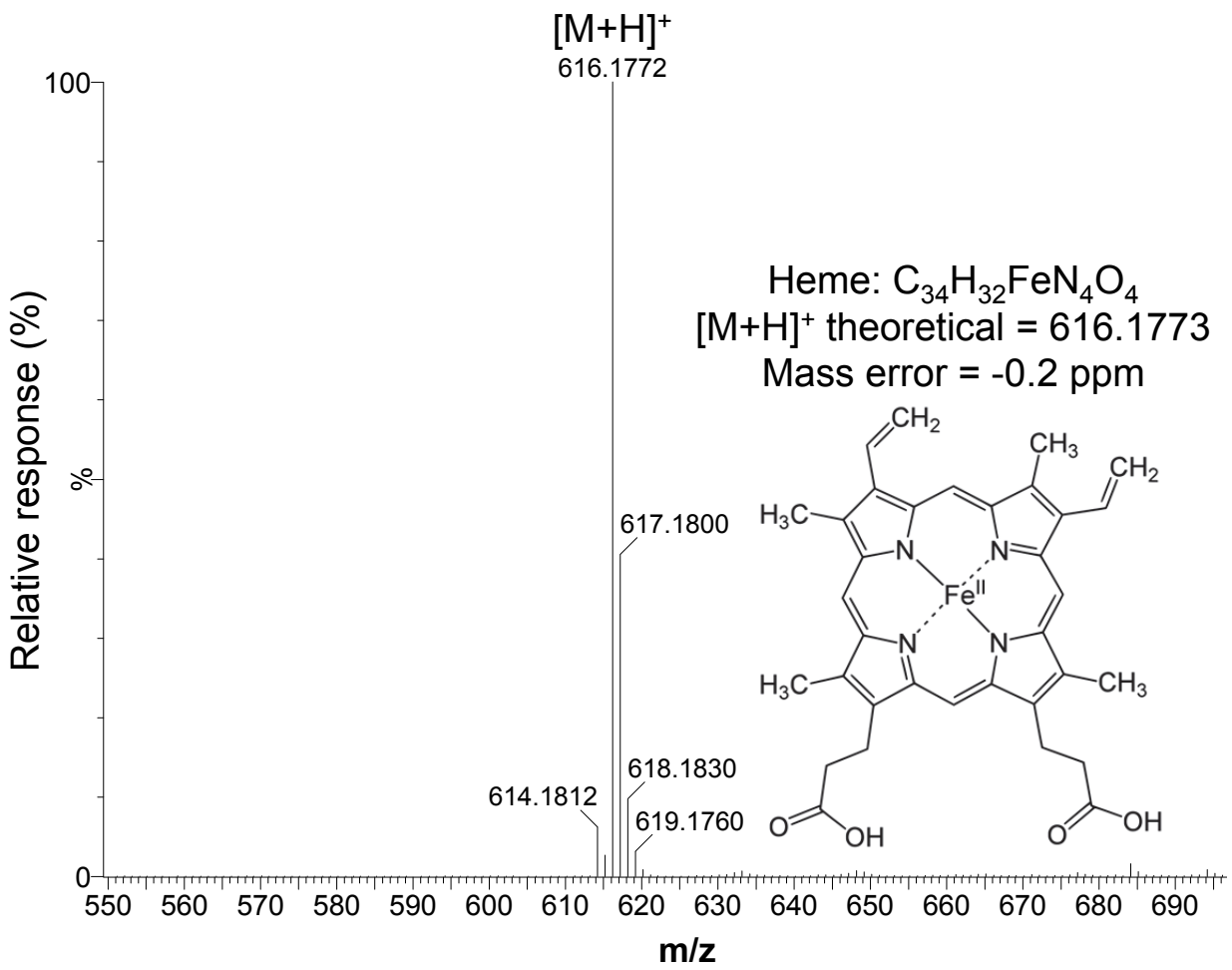

Figure 7.8. Low energy full scan MS^E mass spectrum of intact heme extracted from control human liver microsomes

The chromatogram shows a protonated molecule of *m/z* = 616.1772, which is within 0.2 ppm of the theoretical value for heme. Relative to the monoisotope (100%), the -2, -1, +1, +2 and +3 isotopes have an abundance of approximately 6, 2, 40, 7 and 1%, respectively.

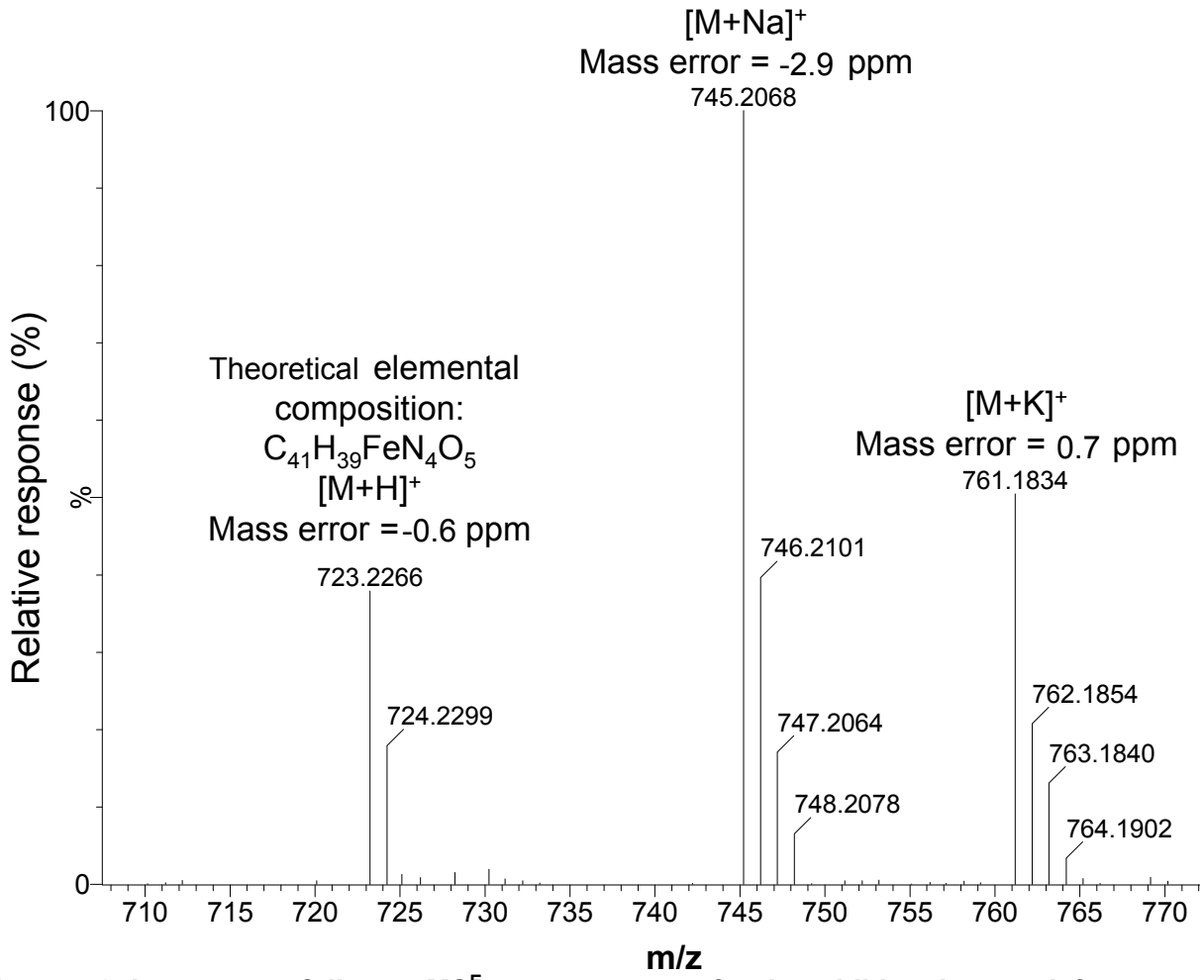

Figure 7.9. Low energy full scan MS^E mass spectrum for the additional mass-defect filtered peak found in esomeprazole-treated human liver microsomes

The chromatogram shows a protonated molecule of *m/z* = 723.2266 (mass error = -0.6 ppm). A heme-containing ion with this *m/z* would correspond to the mass of intact heme (616.1773) + a mass of 107.0493 amu consistent with the proposed elemental composition indicated in the figure). Corresponding sodium and potassium adducts were also detected, as indicated. Relative to the monoisotope (100%), the abundance of the +1, +2 and +3 isotopes were approximately 40, 9 and 3%, respectively.

7.3. Gemfibrozil glucuronide as a positive control for the use of mass-defect filtering to detect heme adducts

Gemfibrozil glucuronide was chosen as an additional positive control for heme-related mass-defect filtering because Baer and colleagues published compelling evidence that the mechanism of CYP2C8 inactivation by this glucuronide involved formation of a benzylic radical that alkylates the CYP2C8 heme, creating a 398 nm-detectable adduct with an approximate *m/z* of 1040.7, as shown in Figure 6.17 (159). NADPH-fortified HLM (1 mg/mL) were incubated with gemfibrozil glucuronide (100 μM) for 60 minutes, and the heme was extracted and analyzed as described in Chapter 3. Based on the structure of the gemfibrozil glucuronide-heme adduct proposed by Baer et al., (159) the protonated molecule would have a theoretical *m/z* = 1040.3506. A UV-absorbing peak corresponding to gemfibrozil glucuronide heme adduct was detected at 7.91 min, slightly later than the retention time of intact heme (7.33 min) (Figure 7.10). This UV-absorbing peak was very small relative to the remaining intact heme, which is attributable to three factors. First, gemfibrozil glucuronide is highly selective for CYP2C8, which comprises only 5-8% of the total drug-metabolizing CYP enzymes in human liver microsomes (1,33) and SimCYP. Second, the intact heme remaining in the microsomal incubations with gemfibrozil glucuronide is derived not only from the CYP enzymes that were not inactivated but also from cytochrome b_5, which accounts for approximately 50% of the heme in human liver microsomes (123). Third, as reported by Baer et al. (159), the absorbance of the gemfibrozil glucuronide heme adduct at 407 nm with are consistent with an extinction coefficient that is approximately 12% of that of intact heme. Accordingly, when HLM are used as the source of CYP2C8, the 398-nm absorbing peak corresponding to gemfibrozil glucuronide-heme adduct is predicted to be 0.5% or less of the peak corresponding to intact heme.

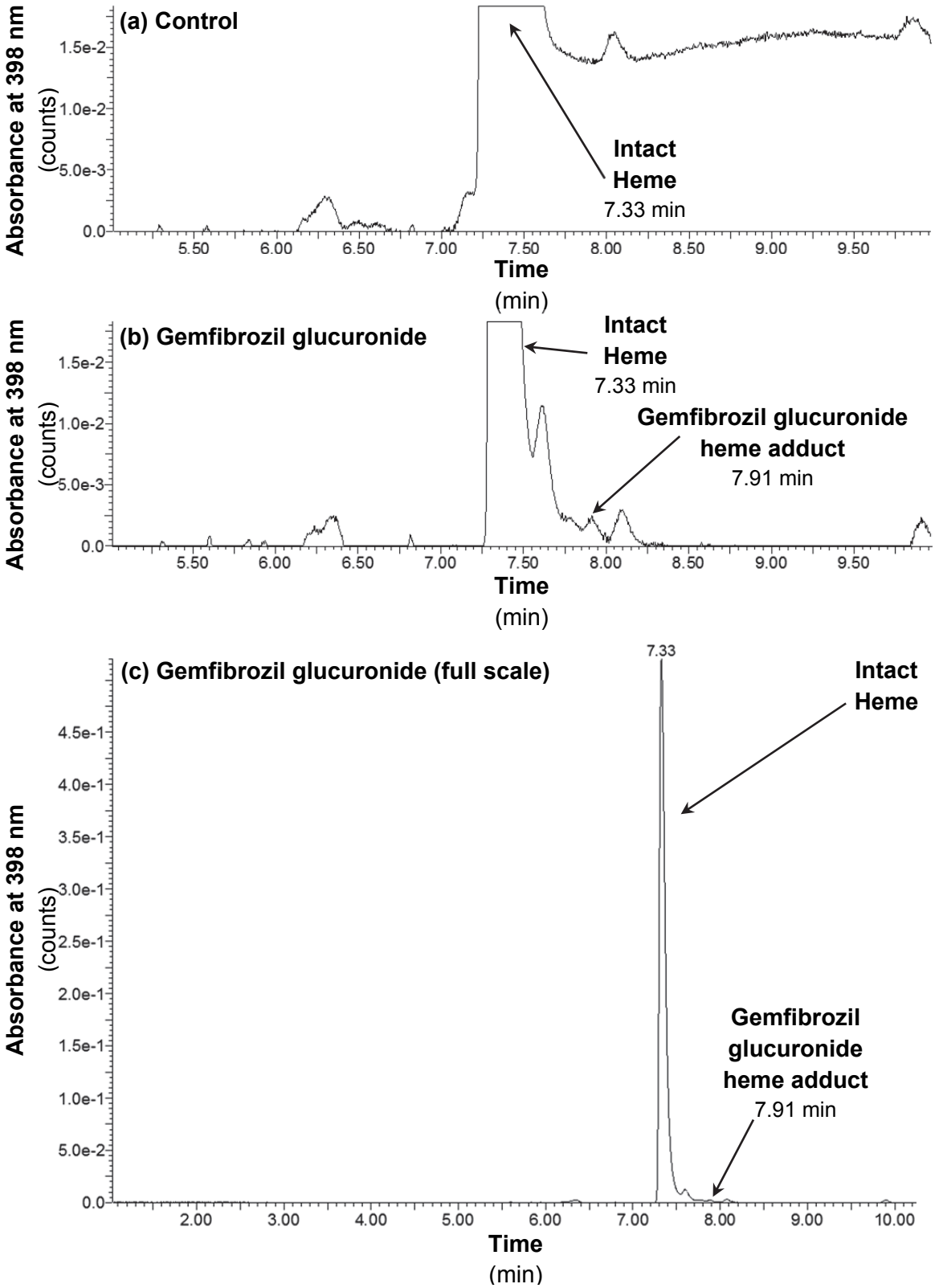

Figure 7.10. UV chromatograms (λ = 398 nm) of the heme extracted from control and gemfibrozil glucuronide-treated pooled human liver microsomes

The chromatograms show the 398 nm-absorbing peaks of heme extracted from NADPH-fortified human liver microsomes (1 mg/mL) incubated for 60 min with solvent (chromatogram a) or 100 μM gemfibrozil glucuronide (chromatogram b). Chromatogram c is a full-scale version of chromatogram b.

The microsomal samples incubated with gemfibrozil glucuronide were analyzed by essentially the same mass-defect filtering procedure described previously for microsomal samples incubated with esomeprazole, The mass-defect filter was constructed ± 35 mDa around the theoretical mass of gemfibrozil glucuronide-heme adduct (*m/z* = 1040.3506) using the same *C*-heteroatom dealkylation algorithm. As shown in Figure 7.11, the extracted accurate mass chromatogram, based on *m/z* = 1040.3506 ± 20 mDa, identified a heme-containing ion at 7.9 min, the same retention time as the 398 nm-absorbing peak (chromatogram b in Figure 7.10). As shown in Figure 7.12, a low energy full scan MS^E spectrum of the 7.9-min peak revealed an isotopic distribution characteristic of heme (Figure 7.12), with two lighter (-2 and -1) and three heavier (+1, +2 and +3) isotopes that were present with a relative abundance of approximately 10, 5, 65, 22 and 7%, respectively. The results demonstrated that the heme adduct with gemfibrozil glucuronide could be identified by mass-defect filtering, and the adduct identified had the expected accurate mass (within -1.2 ppm) and an isotopic distribution characteristic of a heme-containing adduct.

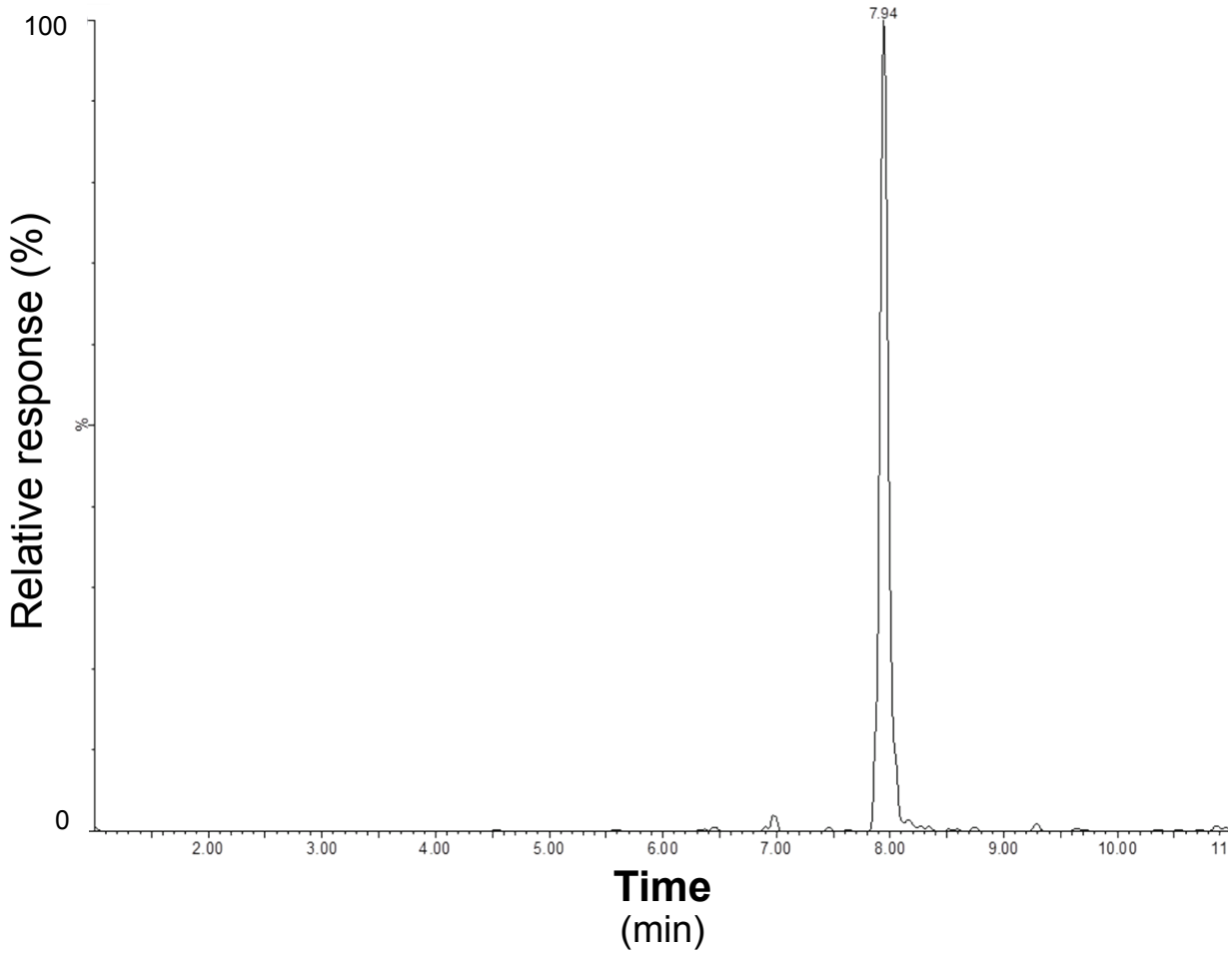

Figure 7.11. Extracted accurate mass chromatogram of *m*/*z* = 1040.3506 ± 20 mDa for gemfibrozil glucuronide-treated human liver microsomes

The mass-defect filter was constructed ±35 mDa around the theoretical gemfibrozil glucuronide heme adduct (*m*/*z* = 1040.3506).

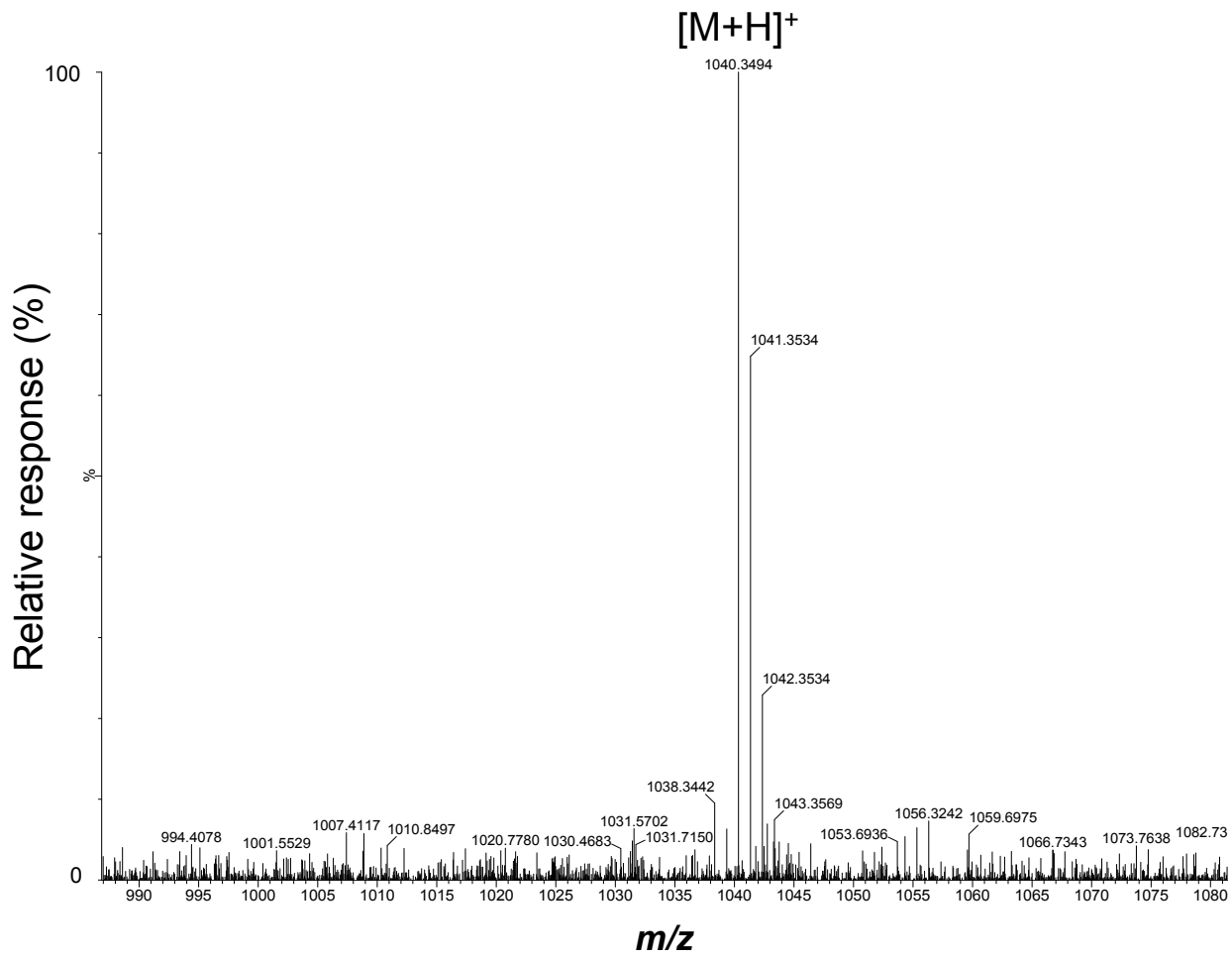

Figure 7.12. Low energy full scan MS^{E} mass spectrum of gemfibrozil glucuronide heme adduct extracted from incubations of gemfibrozil glucuronide with NADPH-fortified human liver microsomes

The spectrum shows a protonated monoisotopic molecule of *m/z* = 1040.3494, which is within -1.2 ppm of theoretical, with an isotopic distribution similar to that of intact heme (Figure 7.8).

7.4. Evidence that the apparent esomeprazole-heme adduct is an unusual artifact

Because the MS/MS acquisition in the first experiment with heme extracted from either control or esomeprazole-treated NADPH-fortified HLM did not provide any useful diagnostic fragments, the experiment was repeated. Similar UV results were obtained (i.e., ~ 50% loss, not shown), and MS/MS analysis of control heme again did not show diagnostic fragments (not shown). Mass-defect filtering was employed again to look for possible heme-associated peaks (i.e., heme mass defect of 0.1773 ± 35 mDa). As shown in Figure 7.13, the extracted accurate mass chromatogram (based on m/z = 723.2270 ± 20 mDa) revealed a major peak at 5.09 min and a minor peak at 4.78 min when esomeprazole was incubated with HLM in the presence of NADPH but not in the absence of NADPH. As before, because these peaks were dependent on the presence of NADPH, and were only detected after mass-defect filtering based on the heme mass defect of +0.1773, they were presumed to be associated with both metabolism and heme. Accordingly, the 4.78 and 5.09 min peaks were considered candidates for an esomeprazole-heme adduct.

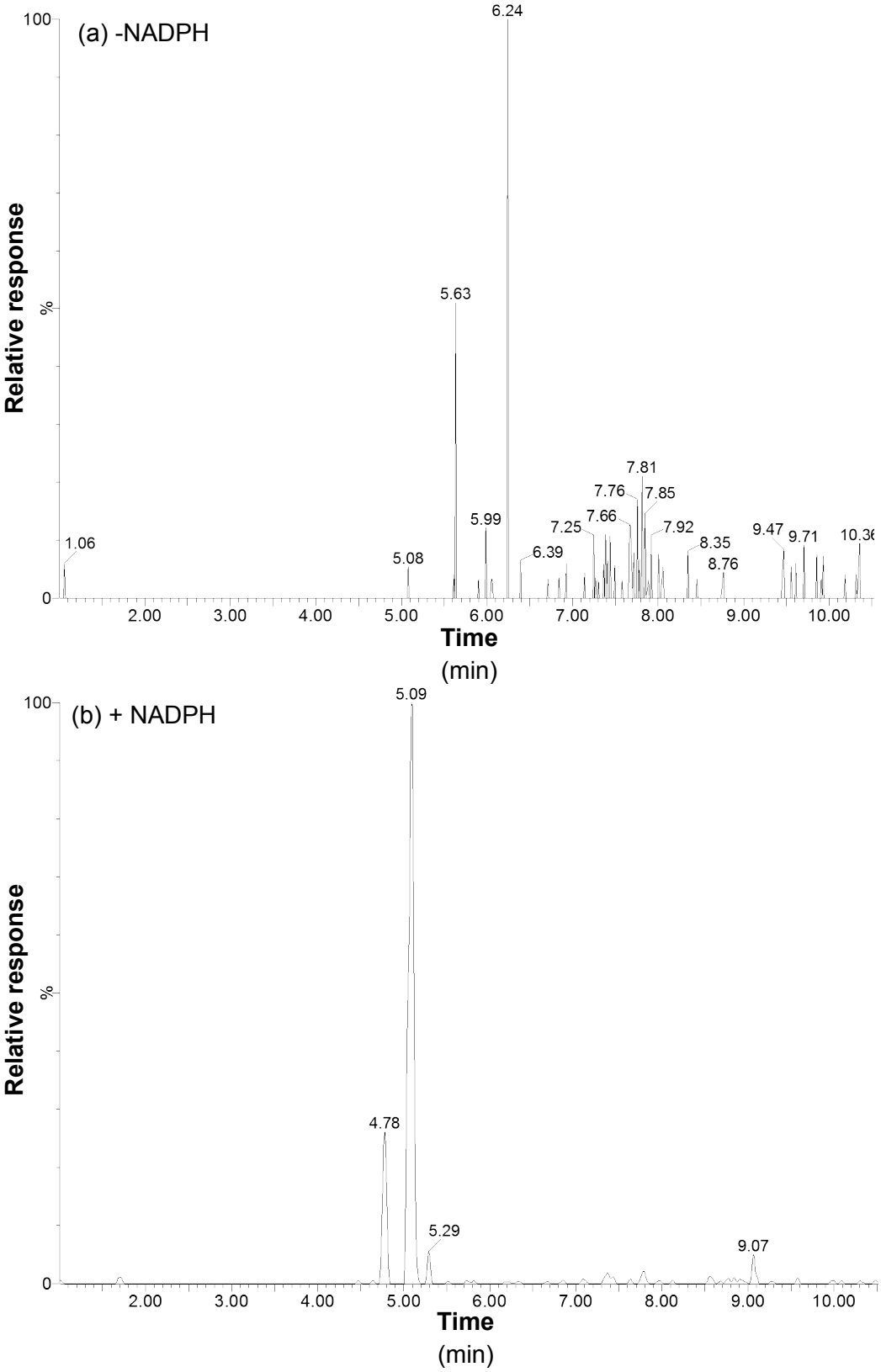

Figure 7.13. Extracted accurate mass chromatogram showing additional peaks from esomeprazole-treated HLM (a) –NADPH, and (b) +NADPH, at m/z = 723.2270 ± 20 mDa

No significant peaks were detected by mass-defect filtering at *m/z* = 723.2270 ± 35 mDa in the NADPH-free sample (chromatogram a) (maximum scale = 370 counts). The peaks found by mass-defect filtering in the NADPH-supplemented sample (chromatogram b) are similar to those in Figure 7.7 (maximum scale = 1110 counts).

In an attempt to find diagnostic fragments from the peaks detected by mass-defect filtering at *m/z* = 723.2270 ± 35 mDa (Figure 7.13), product ion spectra of the *m/z* 723 ions were acquired for the heme extracts from esomeprazole-incubated samples. The major product ion was observed at *m/z* = 362.1172 (Figure 7.14), which is half the parent ion mass and which corresponds to the exact mass of omeprazole sulfone and 5´-hydroxyomeprazole (*m*/*z* =362.1175) reported by Boix et al. (194). In other words, if $[M_2H]^+$ =723.2270, then M =361.1093 and $[MH]^+$ = 362.1172. In addition, less intense product ions were observed at *m/z* 298.1548, 214.0522, and 150.0895, which are diagnostic for the structure of omeprazole sulfone. Because this was a product ion spectrum for a peak found by mass-defect filtering based on the heme mass defect of +0.1773 (and formed only in the presence of NADPH), such a finding was entirely unexpected; it seemed remarkable that a heme adduct would fragment exactly in half. Accordingly, it was hypothesized that the proposed heme-associated component shown in Figure 7.9, with an observed *m/z* = 723.2266 and theoretical elemental composition of $C_{41}H_{39}FeN_4O_5$ was actually a monoprotonated dimer of omeprazole sulfone, which would have a theoretical *m/z* of 723.2271 and an elemental composition of $C_{34}H_{39}N_6O_8S_2$. The observed *m/z* = 723.2266 was within -0.1 ppm of such a theoretical dimer. Relatively large amounts of omeprazole sulfone would have formed in the 120-min incubation of esomeprazole with NADPH-fortified HLM (it is the major metabolite formed by CYP3A4), but the potential for its dimerization was not known. However, dimerization of omeprazole and esomeprazole has been previously reported, (195,196). The product ion spectrum in Figure 7.14 is consistent with predominant fragmentation of the labile dimer of omeprazole sulfone to the more stable monomer, given the presence of the strong signal at *m/z* = 362.1172, which is within 0.8 ppm of the theoretical *m/z* for the protonated monomer of omeprazole sulfone of 362.1175. The absence of the quadrupole-selected precursor ion of *m/z* ≈ 723 in the spectrum is consistent with fragmentation patterns for labile dimers. It should also be noted that it is possible that the

dimer does not exist in aqueous solution, but rather forms “post-column” during the de-solvation phase of electrospray ionization, and this possibility cannot be ruled out.

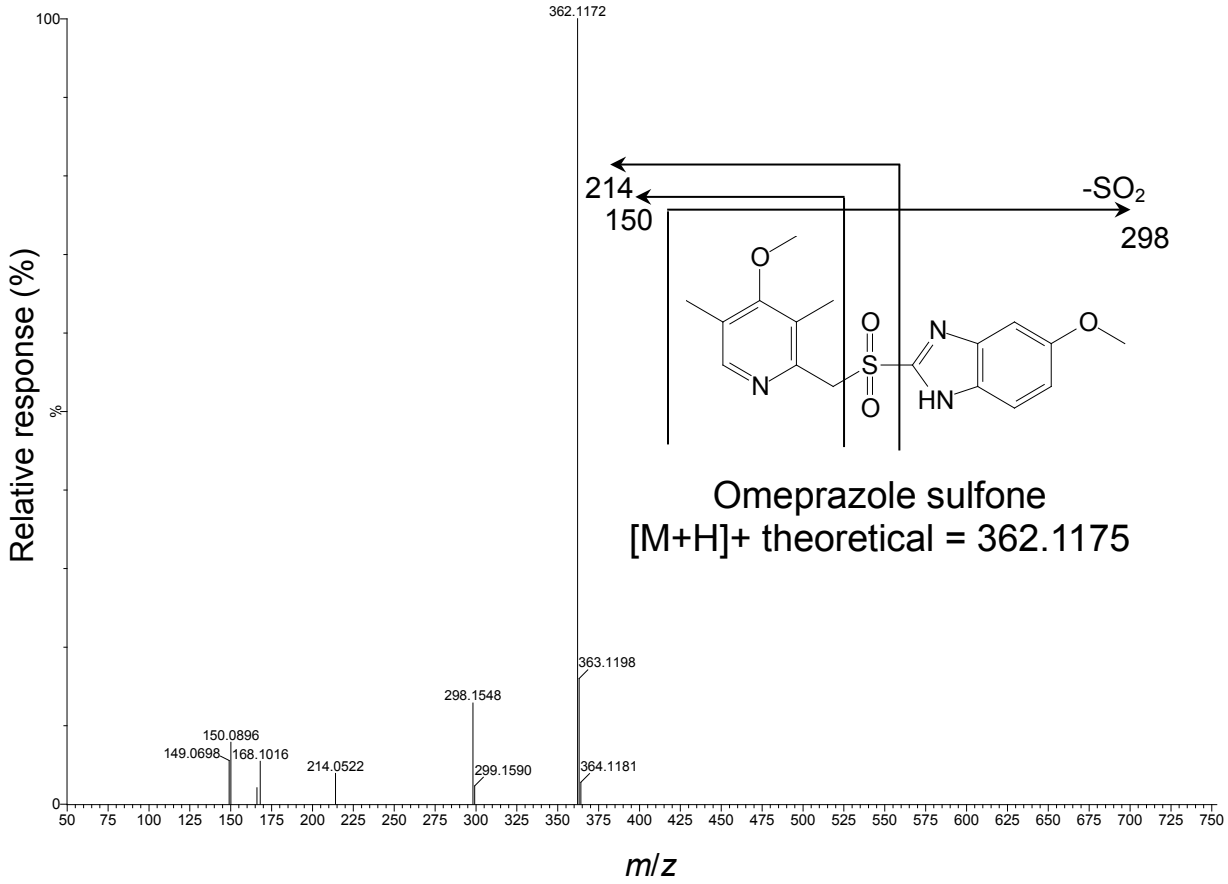

Figure 7.14. Product ion spectrum for the peak at *m/z* = 723 extracted from esomeprazole-treated NADPH-fortified human liver microsomes

The product ion at *m/z* = 362.1172 corresponds to omeprazole sulfone (i.e., *m/z* = 362.1175 theoretical, structure shown) within -0.83 ppm.

To test the hypothesis that omeprazole sulfone could dimerize in the matrix as reported for omeprazole and esomeprazole, a reference standard solution of omeprazole sulfone (6 mM in methanol / Tris buffer, pH 9.0, 60:40 v/v, stored at -20°) was analyzed by MS/MS. As in Figure 7.7 and Figure 7.13, an extracted accurate mass chromatogram at m/z = 723.2270 ± 20 mDa again revealed a peak at 5.09 min, as shown in Figure 7.15a, consistent with the presence of a dimer of omeprazole sulfone. Furthermore, an extracted accurate mass chromatogram at m/z = 362.1175 ± 20 mDa from the solution of omeprazole sulfone also showed a peak at 5.09 min, as shown in Figure 7.15b, consistent with the presence of monomeric omeprazole sulfone. Given the relative abundance of the two chromatographic peaks in the sample when analyzed under low energy conditions, the vast majority of the omeprazole sulfone present appeared to exist as the dimer. Importantly, the retention time of omeprazole sulfone is the same as that of the predominant peak found in Figure 7.6c and Figure 7.7 in the original experiment.

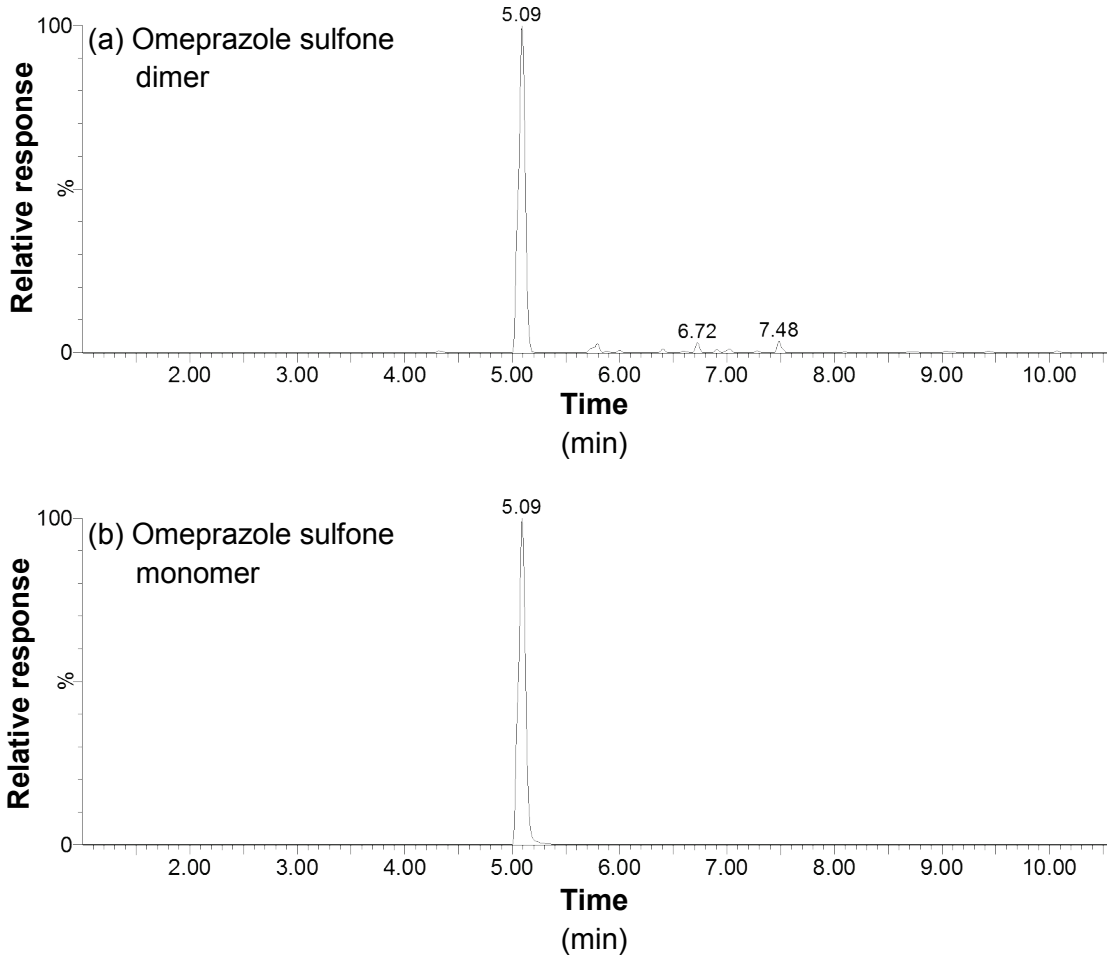

Figure 7.15. Extracted accurate mass chromatograms for a reference standard solution of omeprazole sulfone for *m/z* 723.2270 ± 20 mDa (a) and 362.1172 ± 20 mDa (b), showing a peak at 5.09 min

(a) Maximum scale = 941,000 counts; (b) Maximum scale = 2900 counts.

The peak found by mass-defect filtering at *m*/*z* = 723.2270 ± 35 mDa with a retention time of approximately 5 min in the reference solution of omeprazole sulfone was examined by MS/MS, as described in Chapter 3. The results are shown in Figure 7.16. The product ion spectrum obtained by MS/MS (with quadrupole precursor ion selection at *m*/*z* = 723) showed a large peak at *m*/*z* ≈ 362.12, with less intense product ions observed at *m/z* 298.1548, ~214, and 150.0896, which were diagnostic for the structure of omeprazole sulfone. Importantly, no peaks with *m*/*z* between 362.12 and 723.24 were observed, consistent with complete dissociation of a labile dimer of omeprazole sulfone to the monomer due to the collision energy applied to acquire the product ion spectrum. The low-energy MS^E scan in Figure 7.17 shows the isotopic distribution of the protonated monoisotopic molecule at *m/z* = 723.2277 and its sodium and potassium adducts (Figure 7.17), which displayed 3 peaks containing heavier isotopes than the protonated monoisotopic molecule; relative to the monoisotope (100%), the abundance of the +1, +2 and +3 isotopes was approximately 40, 15 and 2%, respectively. The similarity in the MS/MS spectra between Figure 7.14 (from esomeprazole-incubated samples) and Figure 7.16 (a reference standard of omeprazole sulfone), along with the similarity in isotopic distribution of the component found by mass-defect filtering in the esomeprazole-incubated samples (Figure 7.9) and the solution of omeprazole sulfone (Figure 7.17) provide additional evidence that the apparent heme-associated peak found by mass-defect filtering in esomeprazole-incubated samples was actually due to the metabolic conversion of esomeprazole to the sulfone by CYP3A4, and its subsequent dimerization, rather than formation of an adduct with heme.

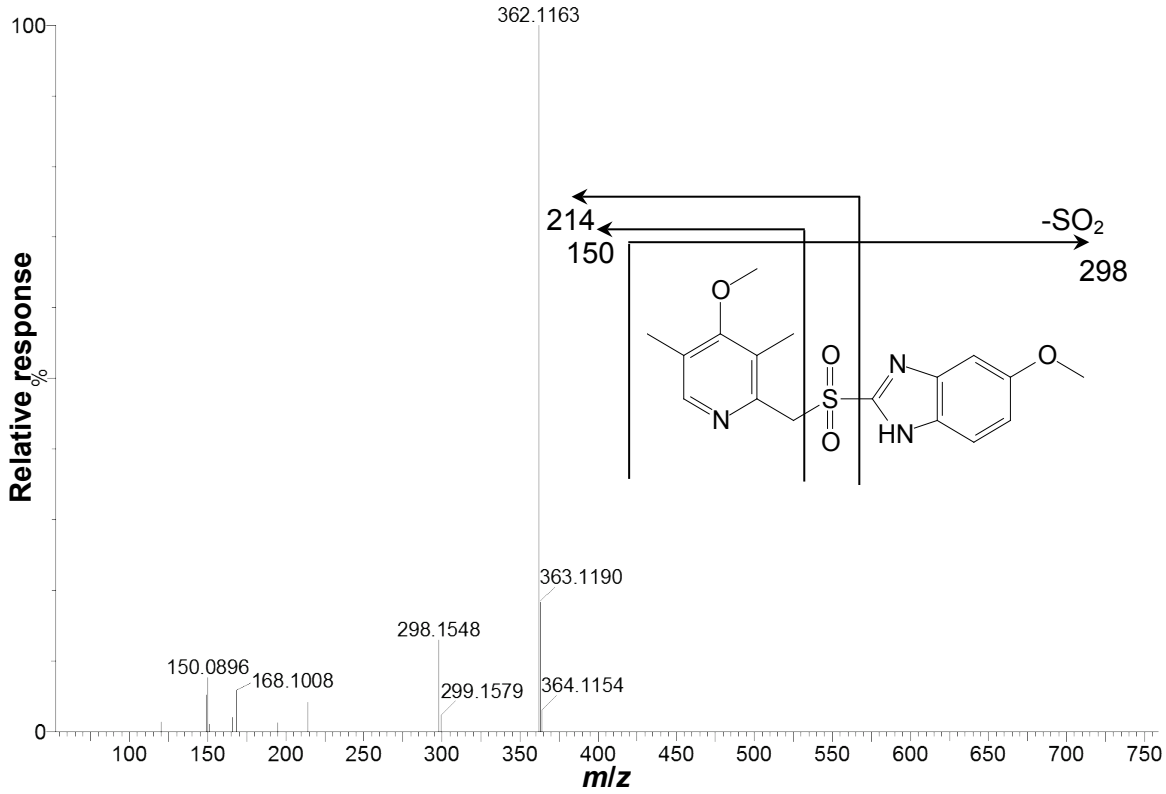

Figure 7.16. Product ion spectrum for the peak at m/z = 723 extracted from a solution of omeprazole sulfone

The ion at 362.1163 corresponds to omeprazole sulfone (theoretical *m/z* = 362.1175) within -3.3 ppm.

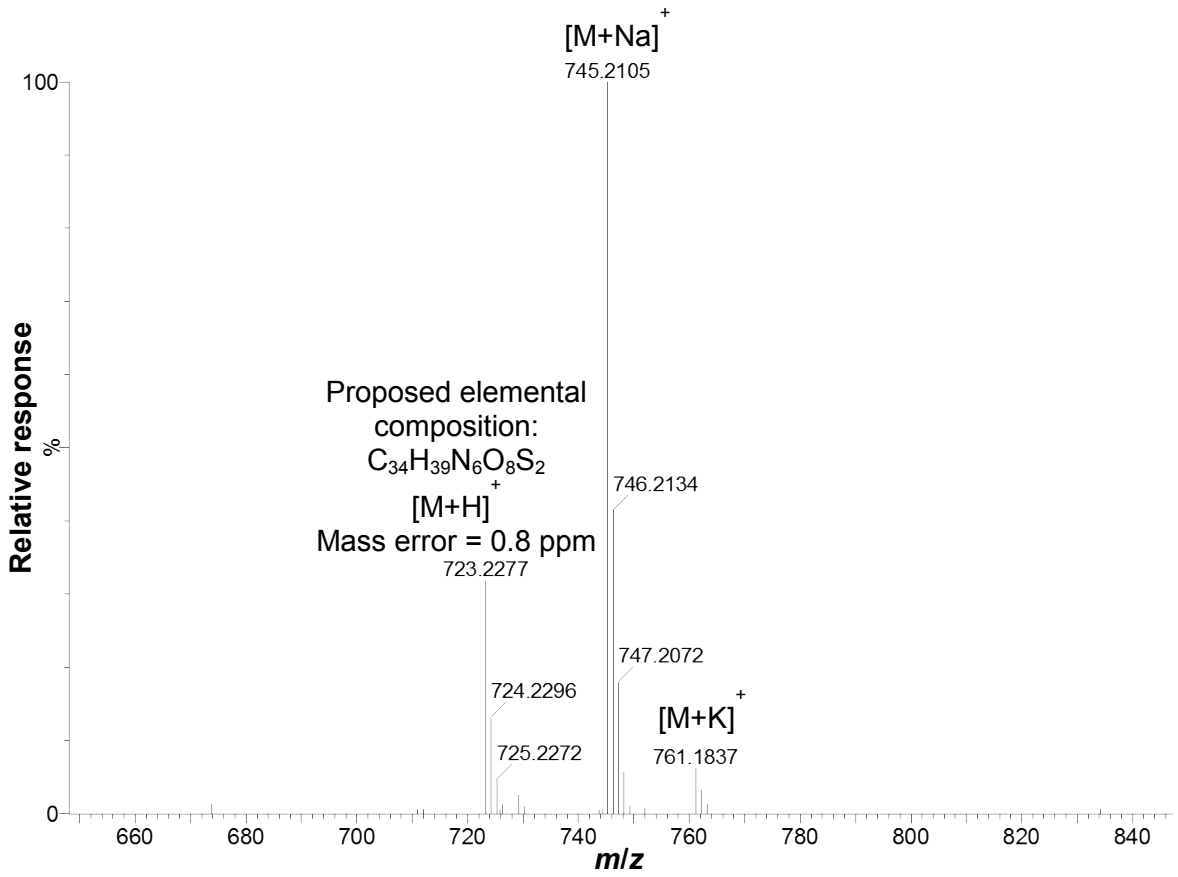

Figure 7.17. Low energy full scan MS^E mass spectrum for a proposed omeprazole sulfone dimer and its sodium and potassium adducts in a reference standard

The spectrum shows a protonated monoisotopic molecule of *m/z* = 723.2277 (mass error from the theoretical omeprazole sulfone dimer is 0.8 ppm). The mass error from the protonated monoisotopic molecule of *m/z* = 723.2266 shown in Figure 7.9 is 1.5 ppm. Corresponding sodium and potassium adducts were also detected, as indicated.

7.5. Theoretical accurate mass isotopic distributions for various iron-, oxygen- nitrogen- or sulfur-containing organic compounds

The initial evidence for an esomeprazole-heme adduct relied not only on the discovery of an unexpected protonated molecule at *m/z* = 723.2266 upon mass-defect filtering with the heme-based *C*-heteroatom mass-defect filter, but also the isotopic distribution of the putative adduct and its sodium and potassium adducts (Figure 7.9). The putative esomeprazole-heme adduct displayed 3 peaks containing heavier isotopes than the protonated monoisotopic molecule but it did not contain peaks with lighter isotopes. It was initially assumed that these lighter isotopes were of such low abundance that they were obscured by background noise, a common occurrence for lower abundance isotope peaks in high resolution mass spectrometry. Given the unexpected finding that a dimer of omeprazole sulfone had many of the mass spectral features of a heme adduct, and was initially mistaken as such, a theoretical investigation was undertaken to examine the effects of the presence or absence of iron and/or sulfur in various compounds on their accurate mass spectra.

To illustrate the effect of iron on the mass spectrum of heme, theoretical full scan accurate mass spectra were constructed for both heme (with iron) and protoporphyrin IX (without iron), focusing on peaks with a relative response > 1% of the monoisotope. The theoretical accurate mass spectrum of heme shown in Figure 7.18a is very similar to the experimentally determined heme spectrum shown in Figure 7.8. Relative to the monoisotope (100%), the abundance of the −2, −1, +1, +2 and +3 isotopes was 6, 2, 40, 7 and 1%, respectively (Figure 7.18a). In contrast, the theoretical accurate mass spectrum of protoporphyrin IX lacks the two peaks containing lighter isotopes due to the absence of iron, as shown in Figure 7.18b. The abundance of the +1, +2, and +3 isotopic peaks for protoporphyrin IX (40, 7 and 1%, respectively) is identical to their abundance in heme (i.e., these peaks are independent of iron). A theoretical full scan accurate mass spectrum was also constructed for

the heme adduct with gemfibrozil glucuronide, as shown in Figure 7.19, which again shows an isotopic distribution similar to that of the experimentally obtained spectrum of gemfibrozil glucuronide-heme adduct (Figure 7.12) and both the theoretical spectrum (Figure 7.18a) and experimentally determined spectrum of heme (Figure 7.8).

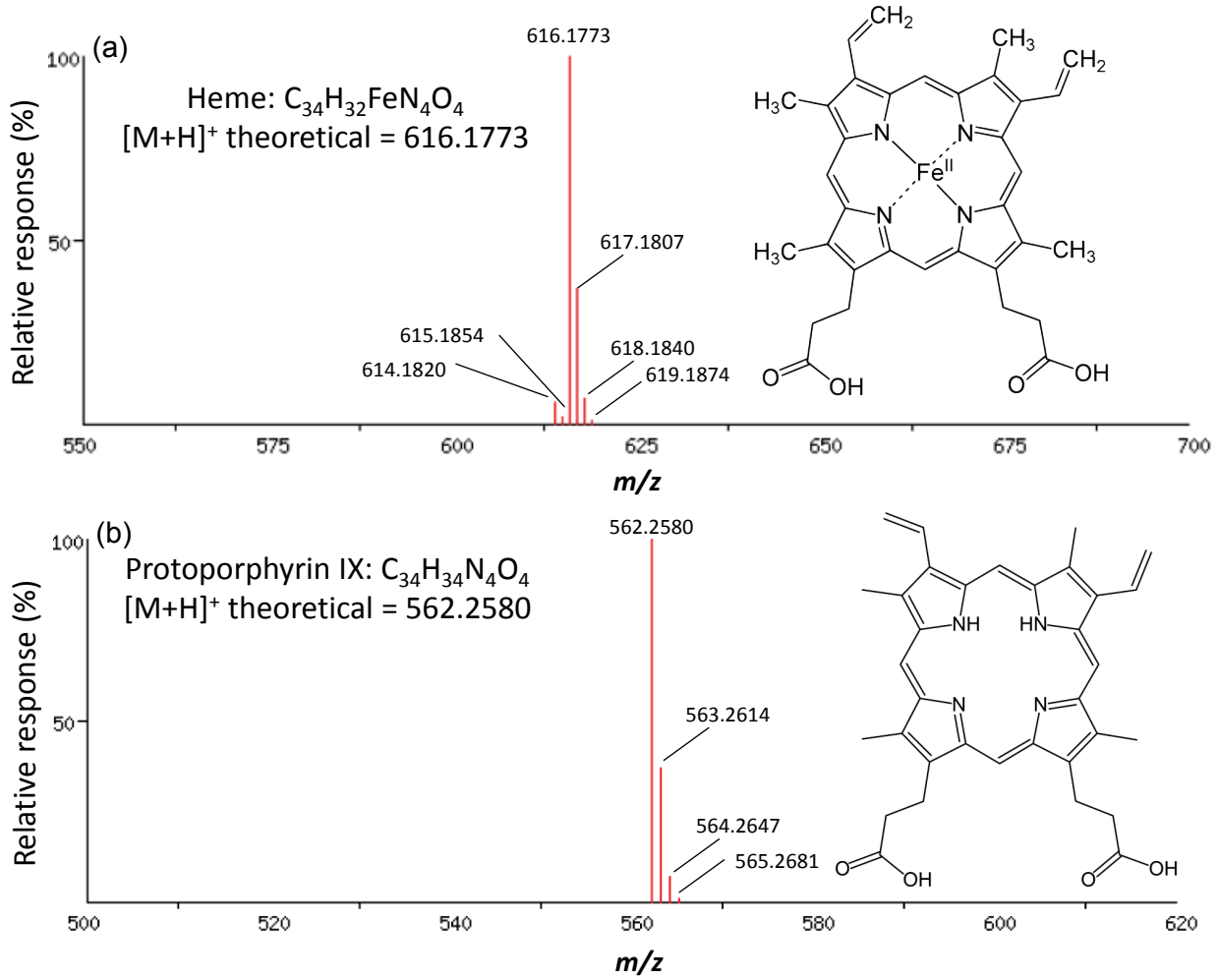

Figure 7.18. Theoretical full scan accurate mass spectra for heme and protoporphyrin IX

The theoretical *m/z* for intact heme = 616.1773 (a), differs from the observed protonated molecule of *m/z* = 616.1772 shown in Figure 7.8 by 0.2 ppm. The theoretical full scan accurate mass spectrum for protoporphyrin IX (i.e., iron-depleted heme) is shown in (b).

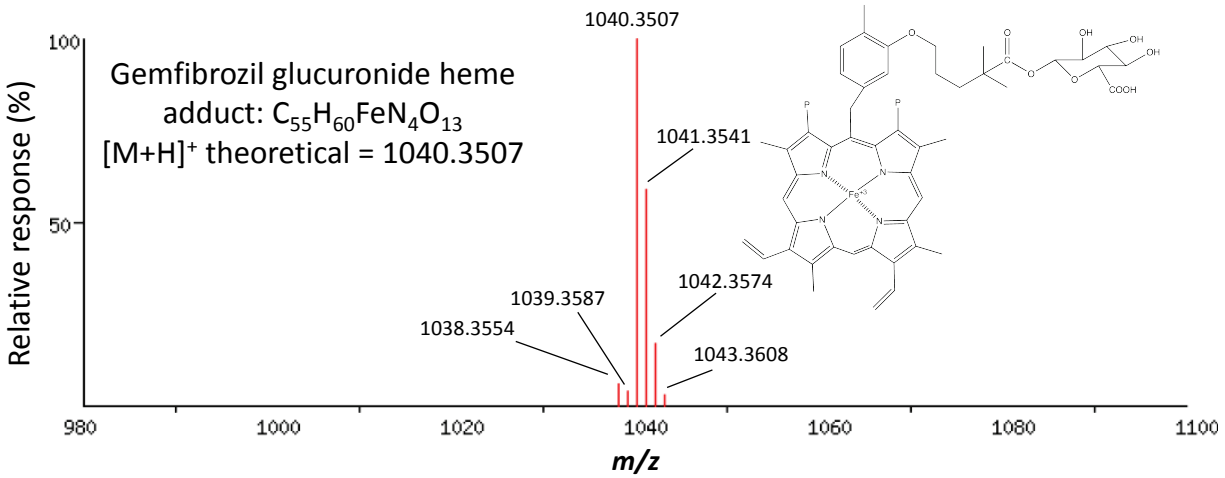

Figure 7.19. Theoretical full scan accurate mass spectrum for the heme adduct with gemfibrozil glucuronide

The theoretical *m/z* for the gemfibrozil glucuronide heme adduct = 1040.3507 (structure proposed by Baer and colleagues (159)) differs from the observed protonated molecule of *m/z* = 1040.3494 shown in Figure 7.12 by 1.3 ppm.

A theoretical full scan accurate mass spectrum was constructed for ferricrocin iron ($C_{28}H_{44}FeN_9O_{13}$) (197), an iron-containing but not a heme-containing organic compound. The theoretical spectrum is shown in Figure 7.20. As with heme, two peaks containing lighter isotopes and three peaks containing heavier isotopes than the protonated monoisotopic molecule are evident with relative abundance values similar to those in heme.

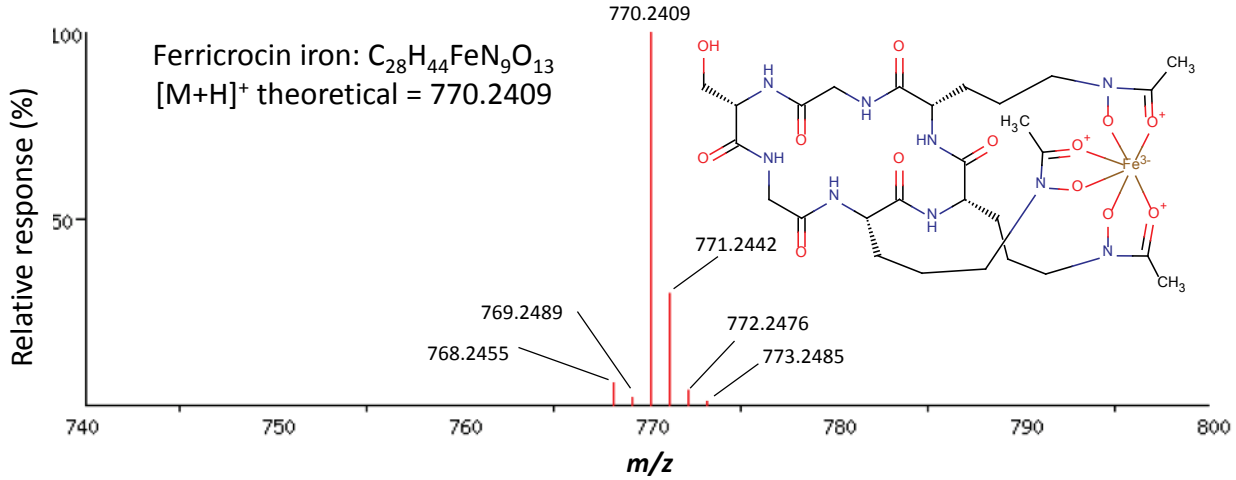

Figure 7.20. Theoretical full scan accurate mass spectrum and structure for ferricrocin iron

The 5.09-min peak in esomeprazole-incubated samples that was initially mistaken as a heme adduct was predicted to have the elemental composition $C_{41}H_{39}FeN_4O_5$. A theoretical full scan accurate mass spectrum was constructed for a compound with this elemental composition. As shown in Figure 7.21, the theoretical accurate mass spectrum of this proposed heme adduct would indeed have two lighter peaks at *m/z* 721.2317 and 722.2351, which are notably lacking from the experimentally determined mass spectrum of the 5.09-min peak, as shown in Figure 7.9.

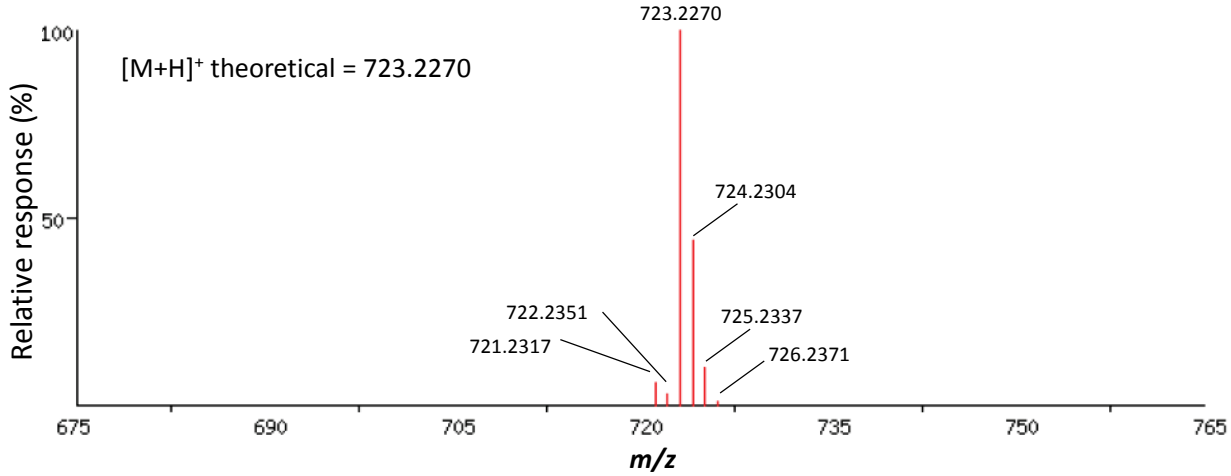

Figure 7.21. Theoretical full scan accurate mass spectrum for the proposed elemental composition of the additional mass-defect filtered peak found in esomeprazole-treated human liver microsomes

The theoretical *m/z* for the additional mass-defect filtered peak = 723.2270 differs from the observed protonated molecule of *m/z* = 723.2266 (consistent with the proposed elemental composition of $C_{41}H_{39}FeN_4O_5$) shown in Figure 7.9 by -0.6 ppm.

To show how the full scan accurate mass spectrum for a dimer of omeprazole sulfone should appear, a theoretical accurate mass spectrum was constructed for a protonated molecule with the formula $C_{34}H_{39}N_6O_8S_2$, as shown in Figure 7.22. The spectrum shows three peaks containing heavier isotopes than the protonated monoisotope, but none with lighter isotopes. Relative to the monoisotope (100%), the abundance of the +1, +2, and +3 isotopes was approximately 40, 9 and 3%, respectively (compared with 40, 7 and 1% for heme). The proposed structure of the omeprazole sulfone dimer is based on that described for omeprazole and esomeprazole dimers (195,196). The dimer is proposed to form based on the formation of hydrogen bonds between one of the sulfone oxygen atoms (i.e., the proton acceptor) on one molecule of omeprazole sulfone and the protonated benzimidazole nitrogen (i.e., the proton donor) on the other molecule (195,196). Importantly, the theoretical *m/z* for the proposed dimer differs from the observed protonated molecule of *m/z* = 723.2266 shown in Figure 7.9 by only 0.7 ppm.

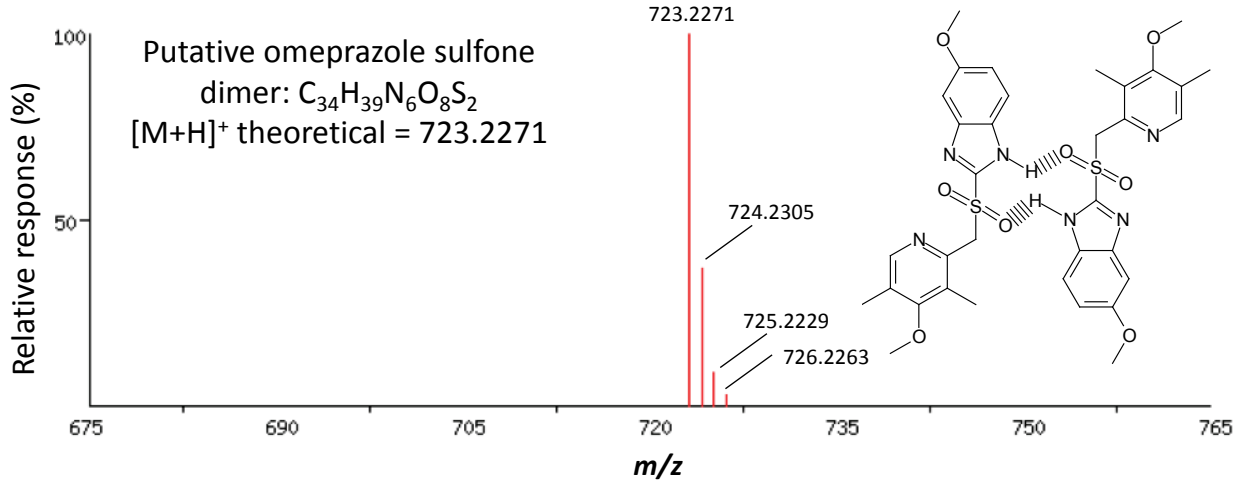

Figure 7.22. Theoretical full scan accurate mass spectrum and proposed structure for omeprazole sulfone dimer

The theoretical *m/z* for a dimer of omeprazole sulfone = 723.2271, which differs from the observed protonated molecule of *m/z* = 723.2266 shown in Figure 7.9 by -0.7 ppm. The structure shown is based on that proposed for the omeprazole and esomeprazole dimers by Baciocchi et al. and Marom et al. (195,196) with the dashed bonds representing hydrogen bonding between the two molecules.

Finally, to show how a lack of sulfur affects the full scan accurate mass spectrum for an omeprazole-related compound, a theoretical accurate mass spectrum was constructed for a protonated molecule of an environmental degradation product of omeprazole that lacks sulfur, namely OTP3, with the formula $C_{17}H_{19}N_3O_4$ (194). The spectrum (Figure 7.23) shows only two peaks containing heavier isotopes than the protonated monoisotopic molecule and no peaks containing lighter ones. This differs from the theoretical isotopic distribution of the proposed omeprazole sulfone dimer in that the latter has three peaks containing heavier isotopes (Figure 7.22). Importantly, the three peaks at approximately +1, +2, and +3 mass units from the monoisotopic mass for the proposed omeprazole sulfone dimer have an abundance of approximately 40, 9 and 3% that of the monoisotopic mass (respectively) (Figure 7.22). In contrast the two peaks at approximately +1, +2 mass units from the monoisotopic mass for OTP3 (Figure 7.23) have an abundance of only approximately 20, and 2% that of the monoisotopic mass, respectively.

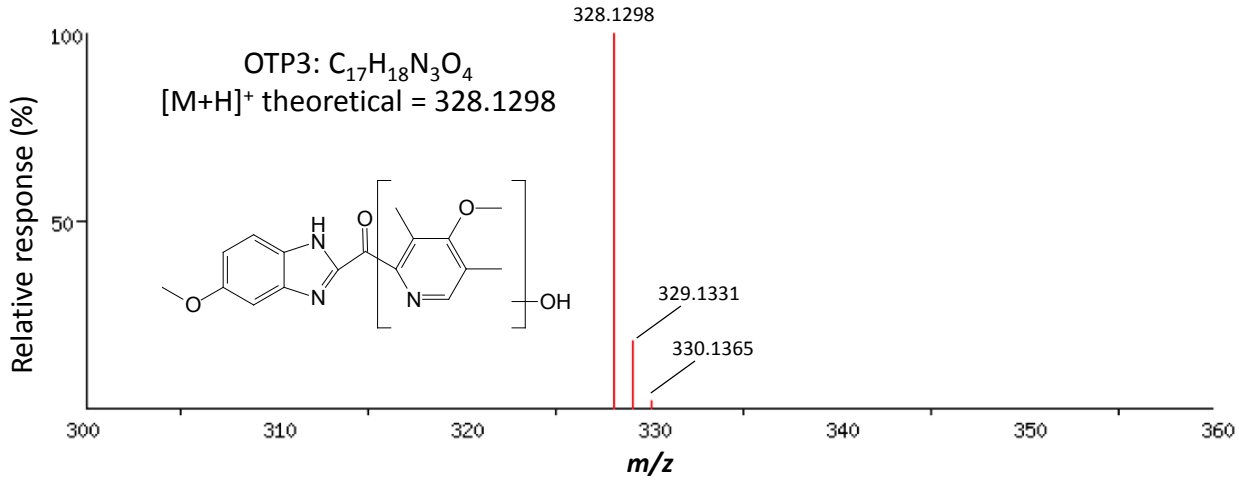

Figure 7.23. Theoretical full scan accurate mass spectrum and proposed structure of omeprazole environmental degradation product OTP3

The theoretical *m/z* for OTP3 = 328.1298, which differs from the reported protonated molecule of *m/z* = 328.1313 by 4.6 ppm (*m/z* and proposed structure reported by Boix et al. (194)).

Discussion

From the studies presented in this chapter, it can be concluded that esomeprazole causes a ~50% loss of heme as measured by both ultra-high performance liquid chromatography (UHPLC) with UV/VIS detection at 398 nm and by high resolution mass spectrometry (HRMS) in NADPH-fortified pooled human liver microsomes (relative to NADPH-fortified HLM in the absence of substrate). Under these conditions, 1-ABT caused more than a 95% loss of heme and the CYP2C8-selective inactivator gemfibrozil glucuronide formed a new 398 nm- and HRMS-detectable heme adduct with minimal loss (<1%) of total heme. In addition to the criteria for MBI that esomeprazole was shown to meet in Chapter 6, the loss of 398 nm- and HRMS-detectable heme caused by esomeprazole in the presence of NADPH provides indirect evidence that CYP holoenzyme content is also reduced (criterion 7 in Chapter 6). Because CYP2C19 makes up only approximately 1 to 3 % of the total drug metabolizing CYPs in human liver (1) and SimCYP), the 50% loss of heme strongly suggests that CYPs other than CYP2C19 were inactivated, likely including CYP3A through the formation of 5-*O*-desmethyl omeprazole, which has been reported to be a metabolism-dependent inhibitor of CYP3A4/5 (75) and / or that a portion of the lost heme was also covalently cross-linked to the apoprotein (and hence lost during protein precipitation). The experimental conditions used were selected to maximize the possibility of finding a heme adduct in human liver microsomes. Under such conditions, omeprazole was found to have a half-life of 14 min (Figure 4.2). Furthermore, when incubating NADPH-fortified HLM with esomeprazole, formation of 5-ODM omeprazole contributes nearly 50% to its clearance (Figure 4.9), suggesting that significant amounts of this CYP2C19 and CYP3A4 inactivator would be formed. The loss of 398 nm-detectable heme without the formation of a new 398 nm-absorbing chromatographic peak suggests esomeprazole inactivates CYP2C19 and/or CYP3A4 by cross-linking the heme prosthetic group

to the apopotein moiety or by forming a heme adduct that does not absorb light at 398 nm, as is the case with 1-ABT.

When heme is directly modified by a CYP inactivator, the heme adducts may give rise to new 398 nm-absorbing chromatographic peaks, as described for heme adducts with gemfibrozil glucuronide (159), secobarbital (184,198) and tert-butyl 1-methyl-2-propynyl ether (199). However, loss of the heme chromophore due to its fragmentation during CYP inactivation has also been previously described, and depending on the exact mechanism, is referred to as heme bleaching or destruction (181,200). 1-ABT was used as a positive control for a compound that causes extensive loss of 398 nm-detectable heme from pooled human liver microsomes without causing the formation of new 398 nm-detectable peaks. The results of the experiments with 1-ABT were consistent with those reported by several groups (183,186,191). The mechanism of inactivation of CYPs by 1-ABT has been elucidated, and involves the formation of a highly reactive metabolite, namely benzyne, upon incubation with CYP enzymes and NADPH, which adds directly across two nitrogen atoms within the heme moiety to form an *N*,*N*-bridged heme. This bridged heme entity can either auto-oxidize to release the *N*,*N*-bridged, iron-depleted porphyrin, or it can first add to a nitrogen and the iron in the heme, followed by rearrangement to the *N*,*N*-bridged porphyrin (186,191). This mechanism is shown in Figure 7.24.

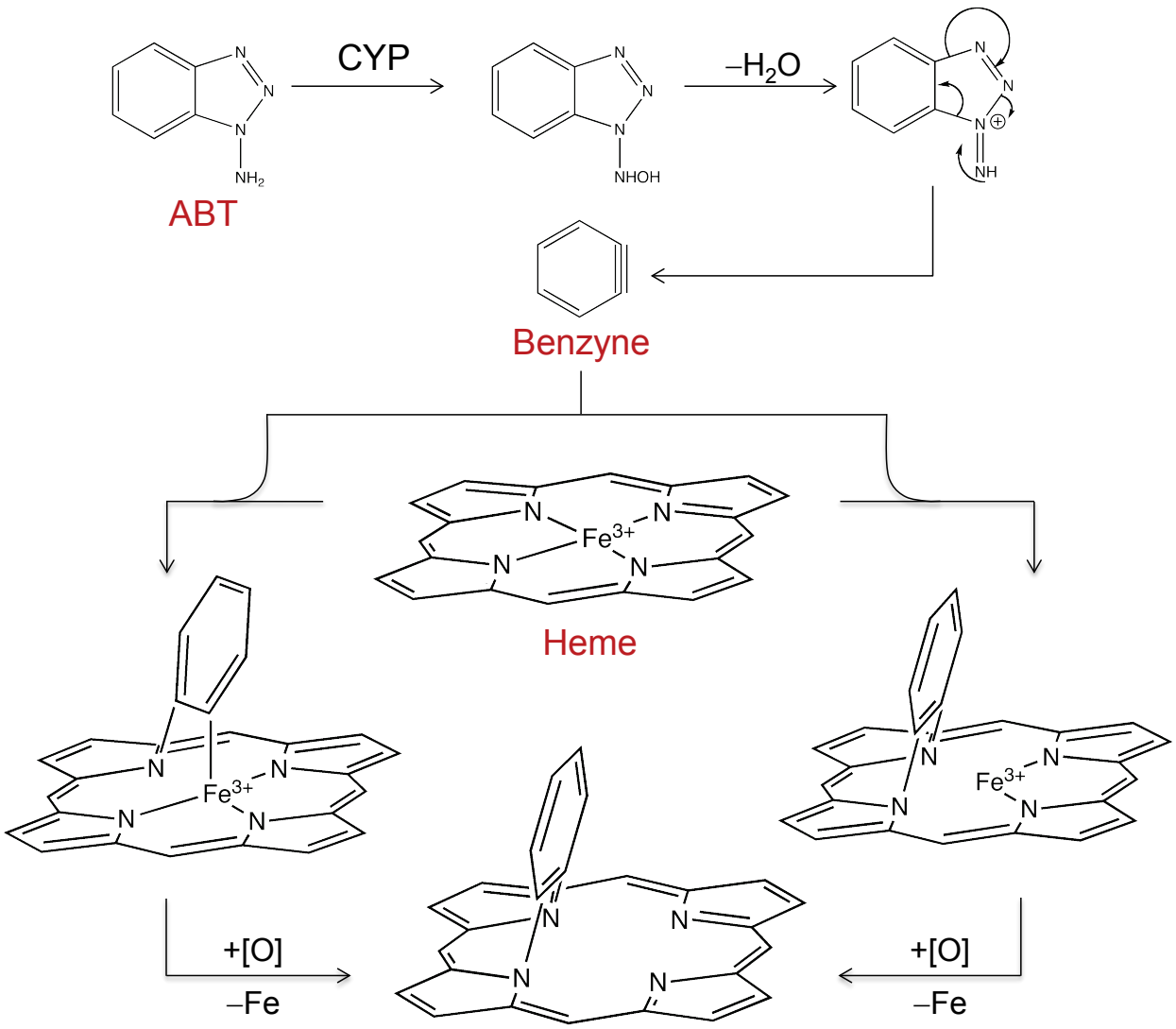

Figure 7.24. Mechanism of 1-aminobenzotriazole activation and alternative pathways to heme adduct formation by benzyne

Note that for clarity the peripheral heme substituents have been omitted. Adapted from (16,182,201).

In the case of the positive control for formation of a 398 nm-detectable heme adduct, namely gemfibrozil glucuronide, a new, albeit small, 398 nm-absorbing chromatographic peak was detected; one that eluted shortly after intact heme (Figure 7.10b). The UV peak was small relative to that described by Baer et al., who used purified CYP2C8, rather than HLM that I used because 1) gemfibrozil glucuronide is highly selective for CYP2C8, which comprises only 5-8% of the total drug-metabolizing CYP enzymes, 2) a significant portion of the total heme in HLM derives from cytochrome b5, and 3) the extinction coefficient (at ~400 nm) of the heme adduct with gemfibrozil glucuronide is ~ 12% of intact heme (159). In spite of the relatively small amount of adduct formed, the use of mass-defect filtering around the mass proposed by Baer et al. (159), provided strong evidence for the formation of the gemfibrozil glucuronide heme adduct in human liver microsomes (Figure 7.11) which was bolstered by the isotopic pattern in the full scan accurate mass spectrum (Figure 7.12), which closely resembled the isotopic distribution of intact heme (Figure 7.8).

In the case of esomeprazole, no new 398 nm-absorbing chromatographic peak was identified after incubating a high concentration of esomeprazole (100 μM) with a high concentration of HLM (1 mg/mL) in the presence of NADPH for 120 min. Dynamic mass-defect filtering within 35 mDa of the heme mass defect (i.e., +0.1773) appeared to demonstrate the formation of a heme-associated component with a protonated molecule of m/z = 723.2266. Low energy full scan MS^E showed that this component (and its sodium and potassium adducts) had an isotopic distribution with three peaks containing heavier isotopes than the protonated monoisotopic molecule (see Figure 7.9). Although the peaks containing lighter isotopes observed in intact heme were not found in the putative heme adduct with esomeprazole (see Figure 7.8), it seemed reasonable to conclude that these peaks were of such low abundance that they were obscured by background noise, as commonly occurs in high resolution mass spectrometry. In addition, in the esomeprazole-incubated sample, the isotopic peaks observed

at approximately +1, +2 and +3 mass units from the monoisotopic mass had an abundance of approximately 40, 9 and 3% that of the monoisotopic mass, respectively, which was similar but not identical to the abundance of the corresponding peaks observed in intact heme (namely 40, 7 and 1%). Subsequent analysis provided evidence that the putative esomeprazole-heme adduct found by mass-defect filtering was actually a dimer of omeprazole sulfone. Dimerization of omeprazole and esomeprazole has been previously reported (195,196), and it seems likely given the data presented in this chapter that omeprazole sulfone can also dimerize. Evidence for the presence of omeprazole sulfone dimer was found not only in microsomal incubations with esomeprazole, but also in a solution of omeprazole sulfone (reference standard). In hindsight, the reason that this dimer was not found in NADPH-free microsomal incubation samples is obvious: the CYP3A4-mediated formation of omeprazole sulfone from esomeprazole simply could not occur in the absence of NADPH.

The reason that the putative omeprazole sulfone dimer was not excluded by the mass-deficit filter constructed within 35 mDa around the mass defect for heme is not as obvious. False positives rarely occur with mass-defect filtering. However, because the mass-defect filtering algorithm employed is dynamic rather than linear across the mass range of interest, false positive and negative results are minimized because of the relatively large mass changes (and therefore mass defects) that occur with xenobiotic metabolism such as heteroatom dealkylation, hydrolysis or conjugation, etc. In addition, the dynamic nature of the mass-defect filtering algorithm allows a relatively narrow accurate mass defect window to be maintained across the mass range of interest (129). Inspection of the isotopic distribution of the filtered component (as described in this chapter) can typically screen out any additional false positives. Table 7.1 shows the isotopic masses and natural abundances of carbon, hydrogen, oxygen, nitrogen, sulfur and iron.

Table 7.1. Isotopic masses and natural abundances of stable isotopes of hydrogen, carbon, oxygen, nitrogen, sulfur and iron

Element	Symbol	Mass of atom (amu)	Representative isotopic composition (mole fraction × 100)
Hydrogen	^{1}H	1.0079	99.989
	^{2}H	2.0141	0.012
Carbon	^{12}C	12.0000	98.930
	^{13}C	13.0034	1.070
Oxygen	^{16}O	15.9949	99.757
	^{17}O	16.9991	0.038
	^{18}O	17.9992	0.205
Nitrogen	^{14}N	14.0031	99.636
	^{15}N	15.0001	0.364
Sulfur	^{32}S	31.9721	94.990
	^{33}S	32.9715	0.750
	^{34}S	33.9679	4.250
	^{36}S	35.9671	0.010
Iron	^{54}Fe	53.9396	5.845
	^{56}Fe	55.9349	91.754
	^{57}Fe	56.9354	2.119
	^{58}Fe	57.9333	0.282

Sources: (202,203).

Although the isotopic distribution of the apparent heme adduct (Figure 7.9) did not exactly correspond with that of intact heme (Figure 7.8), it was much more similar than a typical organic molecule that lacks sulfur or iron (e.g., OTP3, Figure 7.23), which have only two peaks containing heavier isotopes than the protonated monoisotopic molecule and no peaks containing lighter isotopes. The experimentally determined (Figure 7.17) and the theoretical (Figure 7.22) isotopic distribution for the sulfur-containing dimer of omeprazole sulfone both revealed three peaks containing heavier isotopes than the protonated monoisotopic molecule. Importantly, because of the presence of sulfur in the molecule, the peaks at approximately +1 and +2 mass units from the monoisotopic mass for the proposed omeprazole sulfone dimer are present at approximately 40 and 9% the abundance of the protonated monoisotopic molecule, whereas the corresponding theoretical peaks are present at only approximately 20 and 2% that of the protonated monoisotopic OTP3 (Figure 7.23). The effect of iron on the isotopic distribution is even more dramatic than the effect of sulfur, with at least two peaks containing lighter isotopes and three peaks containing heavier isotopes than the protonated monoisotopic molecule (see Figures 7.18a – 7.21). However, the effects of the presence of sulfur on the isotopic distribution observed in full scan accurate mass spectra (Figure 7.9) coupled with the low signal intensity led to the mistaken identification of the component found by mass-deficit filtering in esomeprazole-incubated samples- as a heme adduct because it was assumed that the absence of the two lighter peaks was a consequence of background noise If the component found by MDF were to have been OTP3, for instance, inspection of the isotopic distribution would led to its rapid identification as a false positive due to the lack of sulfur.

As discussed in Chapters 1 and 6, of the PPIs, only omeprazole, esomeprazole and tenatoprazole have a 5´-methyl substituent (Table 1.1), and these PPIs are all MDIs of CYP2C19, whereas those lacking this substituent are not (Table 4.1 and Table 6.3). The conversion of omeprazole or esomeprazole to omeprazole sulfone or 5-ODM omeprazole

leaves this substituent intact, and these metabolites are also MBIs of CYP2C19 (and possibly CYP3A4 in the case of 5-ODM omeprazole). As discussed in Chapter 6, it is known that omeprazole sulfone can be further metabolized by CYP2C19 to 5´-hydroxyomeprazole sulfone (179). If hydroxylation at the 5´-position partitions between the formation of a non-inhibitory 5´-hydroxy metabolite by oxygen rebound and a benzylic radical (analogous to that shown for gemfibrozil glucuronide, Figure 6.17), then this mechanism would be common to esomeprazole and its inhibitory metabolites. However, a 398 nm-detectable peak was not detected that would corroborate this mechanism (as it was for gemfibrozil glucuronide). An alternative to heme alkylation that must be considered is that activation of esomeprazole (by the HCl used to extract heme) caused an artificial loss of heme. I considered this possibility when first designing experiments to extract heme from HLM, but hypothesized that mass-defect filtering presented a novel approach to the problem because it would allow for the detection of a heme-associated adduct with an unexpected mass (i.e., an adduct that was not a simple addition of esomeprazole to heme accompanied by the loss of two hydrogen atoms, as is the case for gemfibrozil glucuronide (159)).

Under acidic conditions, PPIs become protonated to form a sulfenic acid which then hydrolyzes to the active cyclic sulfenamide form of the drug that covalently binds to cysteine residues, which is the basis for their pharmacological activity. Heme was extracted from esomeprazole-treated HLM with 1N HCl. If esomeprazole did form an adduct with heme, perhaps involving formation of a benzylic radical, it is possible that, following treatment with HCl, the adduct would have rearranged and possibly cross-linked the heme to the apoprotein by alkylation of a cysteine residue within the active site of the CYP enzyme. This cross-linking of heme to the apoprotein would presumably prevent the extraction of heme. The cross-linked heme adduct would end up in the pellet of precipitated protein, making it undetectable by UHPLC with either UV of MS analysis. However, it is important to note that the metabolites of

omeprazole or esomeprazole are inactive, and reportedly cannot rearrange to a reactive cyclic sulfenamide (57). Whether this would apply to omeprazole bound to heme via its 5′-methyl group is not known. Given the high concentration of HLM (1 mg/mL) and long incubation times (60 – 120 min) used in the current study, it is highly likely that most of the esomeprazole that did not inactivate CYPs was converted to these inactive metabolites that cannot be converted to an active cyclic sulfenamide. In addition, such cross-linking could only occur if this reaction occurred more quickly than the heme itself was extracted from the apoprotein upon addition of HCl. Nevertheless, the potential for any esomeprazole bound to the heme of CYPs in HLM to cross-link to active site cysteine residues is a possibility that needs to be followed up and will be discussed in Chapter 8.

In conclusion, the use of high-resolution mass spectrometry coupled with mass-defect filtering appeared to identify an esomeprazole-heme adduct that was subsequently revealed to be a dimer of omeprazole sulfone. This artifact should be taken into consideration by others using mass-defect filtering to investigate the inactivation of CYP enzymes by sulfur-containing compounds. Although compelling evidence for the formation of a heme adduct with esomeprazole was not found, under conditions where 1-ABT destroyed >95% of 398 nm-and HRMS-detectable heme and gemfibrozil glucuronide formed the expected heme adduct in NADPH-fortified HLM, esomeprazole was found to cause a ~50% loss of the 398 nm- and HRMS detectable heme (with no new peaks found), consistent with mechanism-based inhibition of CYP through covalent binding to the apoprotein, cross-linking of the heme prosthetic group to the apoprotein moiety, or heme destruction.

Chapter 8. CONCLUSIONS AND FUTURE DIRECTIONS

8.1. Summary and conclusions

In 2008, the American College of Cardiology Foundation, the American College of Gastroenterology and the American Heart Association recommended that certain high risk patients prescribed the anti-platelet drug clopidogrel (Plavix) also take a proton pump inhibitor (PPI), such as omeprazole, esomeprazole, lansoprazole, rabeprazole or pantoprazole, to suppress the production of gastric acid and thereby lessen the severity of upper gastrointestinal bleeding commonly associated with clopidogrel therapy (56). In response to numerous but often contradictory reports that PPIs had the unexpected effect of reducing the therapeutic effectiveness of clopidogrel, regulatory agencies in Europe (EMA) and America (FDA) cautioned against the use of PPIs with clopidogrel. The FDA and EMA narrowed their recommended restrictions to omeprazole and esomeprazole when it was discovered that these PPIs, but not lansoprazole or pantoprazole, decreased the anti-platelet effect of clopidogrel (109,140).

Clopidogrel is a prodrug. It is converted to its pharmacologically active metabolite H4, which covalently binds to the $P2Y_{12}$ receptor on platelets, by two sequential reactions that are catalyzed mainly by CYP2C19. PPIs are also metabolized by CYP2C19. in spite of their relatively short plasma half-lives, it seemed reasonable to assume, therefore, that PPIs could reduce the therapeutic effectiveness of clopidogrel by inhibiting its conversion to H4 by CYP2C19. With the exception of omeprazole and lansoprazole (and their *S*-enantiomers), which have *K*i values ≤1.0 μM for direct inhibition of CYP2C19, PPIs are weak inhibitors of CYP2C19; hence, direct inhibition of CYP2C19 seemed an unlikely explanation for the clinical observation that only certain PPIs compromised the therapeutic effectiveness of clopidogrel.

For my dissertation research, I tested the hypothesis that omeprazole and esomeprazole, but not lansoprazole or pantoprazole, are metabolism-dependent inhibitors of CYP2C19 and the selective inactivation of CYP2C19 by omeprazole and esomeprazole is the mechanism by which these two PPIs reduce the therapeutic effectiveness of clopidogrel. The

results of my dissertation research provide compelling support for the proposed mechanism and provide a scientific rationale for the FDA and EMA's recommendation that patients prescribed clopidogrel should avoid taking omeprazole and esomeprazole and reduce the severity of gastrointestinal bleeding by taking other PPIs.

The key findings of my dissertation research can be summarized as follows.

As shown in *Chapter 4*, omeprazole (a racemic mixture of *R*- and *S*-enantiomers) and esomeprazole (the *S*-enantiomer) were identified as metabolism-dependent inhibitors (MDIs) of CYP2C19 in human liver microsomes (HLM), human hepatocytes and recombinant CYP2C19. In contrast, lansoprazole and pantoprazole did not cause MDI of CYP2C19. In addition to its clinical relevance, these observations are important because they underscore the importance of using a low concentration of enzyme and a short incubation with the CYP marker substrate in order to detect MDI of CYP enzyme in vitro. In ALL previous studies of CYP2C19 inhibition by PPIs, the concentration of HLM was too high and/or the substrate incubation time was too long to detect metabolism-dependent inhibition. The kinetic parameters for CYP2C19 inactivation by omeprazole, namely k_{inact} the maximum rate of inactivation, and K_I, the concentration of inhibitor supporting half the maximum rate of inactivation, were used in a physiologically based pharmacokinetic (PBPK) model to predict the degree of CYP2C19 inactivation under clinical conditions. Omeprazole and esomeprazole were subsequently shown to be *irreversible* MDIs, which also explained the clinical observation that the loss of clopidogrel's therapeutic effectiveness cannot be prevented by separating the doses of clopidogrel and omeprazole or esomeprazole.

In *Chapter 5,* I demonstrated that, like the parent drug, two of the three major metabolites of omeprazole are also irreversible inactivators of CYP2C19. The kinetic parameters for CYP2C19 inactivation were determined and, along with those for omeprazole and esomeprazole, used in a mechanistic static model to predict the reduction of H4 formation

from clopidogrel under clinical conditions. The model slightly overpredicted (by a factor of 2) the ability of omeprazole to block the conversion of clopidogrel to H4, its pharmacologically active metabolites, but otherwise established that inactivation of CYP2C19 is the likely mechanism for the clinical interaction between omeprazole/esomeprazole and clopidogrel.

In *Chapter 6*, I established that esomeprazole and its two inhibitory metabolites, namely omeprazole sulfone and 5-*O*-desmethylomeprazole, meet the so-called Silverman criteria for mechanism-based inhibition (a special case of irreversible MDI). In this chapter I initiated studies to test the hypothesis that the mechanism of CYP2C19 inactivation by esomeprazole and its metabolites involves the formation of a benzylic radical (on the 5′-methyl group) that binds covalently to the heme moiety. This hypothesis was based on the observation that the 5′-methyl group is present on the pyridine ring of those compounds that irreversibly inactivate CYP2C19, namely omeprazole, esomeprazole, omeprazole sulfone and 5-*O*-desmethylomeprazole, but absent from those compounds that did not inactivate CYP2C19, namely lansoprazole, pantoprazole and 5′-hydroxyomeprazole. (The latter compound contains a 5′-methyl group but it is hydroxylated and, hence, cannot be converted to a benzylic radical.) Based on this hypothesis, I correctly predicted that tenatoprazole, which contains a 5′-methyl group, does cause MDI of CYP2C19 whereas ilaprazole and rabeprazole, which lack a 5′-methyl group, do not cause MDI of CYP2C19. Tenatoprazole and ilaprazole have not been approved by the FDA for use in the USA but ilaprazole has been approved in other countries. The results presented in Chapter 6 suggest that the investigational drug, tenatoprazole, but not the clinically used ilaprazole or rabeprazole, will compromise the therapeutic effectiveness of clopidogrel and should be added to the list of PPIs to avoid in patients taking clopidogrel, if it is approved.

Chapter 7 describes studies that were performed to provide direct evidence for the proposed mechanism of inactivation of CYP2C19 by esomeprazole, namely the formation of a

heme adduct. These studies would have been performed with ^{14}C-labeled omeprazole or esomeprazole had they been commercially available, but they are not. Therefore, formation of a heme adduct in incubations of esomeprazole in HLM was evaluated by UHPLC analysis with UV/VIS detection (to measure heme at ~400 nm) and by high resolution mass spectrometry (HRMS) with post-acquisition mass-defect filtering to identify heme and heme-containing adducts. The results in Chapter 7 show that incubating HLM with esomeprazole results in a substantial decrease in the amount of heme detectable by UHPLC coupled with either UV absorbance or HRMS and *appeared* to show the formation of a heme adduct based on mass-defect filtering. However, the putative heme adduct was subsequently identified as a dimer of esomeprazole sulfone (a metabolite of esomeprazole formed by CYP3A4/5). Chapter 7 did not identify an adduct between heme and a metabolite of esomeprazole but it did reveal the potential for an unusual artifact; namely, that sulfur-containing drugs can be converted to metabolites that closely resemble a heme adduct based on mass-defect filtering and isotopic distribution.

Overall, the results of my dissertation research support the hypothesis that irreversible inactivation of CYP2C19 is the mechanism by which omeprazole and esomeprazole reduce the therapeutic effectiveness of clopidogrel. This property is not shared by lansoprazole, pantoprazole, rabeprazole or ilaprazole. These findings support the FDA's recommendation that, in order to reduce the risk of gastrointestinal bleeding, clopidogrel should not be coadministered with omeprazole or esomeprazole but should be coadministered with other PPIs.

8.2. Future directions

The results of my dissertation research suggest that PPIs containing a 5′-methyl group on the pyridine ring, such as omeprazole and esomeprazole, can be converted to a benzylic radical that binds covalently to the heme moiety of CYP2C19 leading to irreversible loss of enzyme activity. In the future, this proposed mechanism could be evaluated by testing the prediction that changing the 5′-methyl group in esomeprazole to a 5′-trifluoromethyl group would block the formation of a 5′-benzylic radical and, hence, prevent the irreversible inactivation of CYP2C19. Trifluoromethyl-omeprazole, especially trifluoromethyl-*R*-omeprazole, represents a possible new PPI, one that would be (1) metabolized slower than *R*-omeprazole or esomeprazole (because the trifluoromethyl group would block 5′-hydroxylation by CYP2C19), (2) suitable for coadministration with clopidogrel (provided it did not, as predicted, inactivate CYP2C19), and (3) less susceptible to pharmacokinetic variation due to genetic polymorphisms of CYP2C19.

Future experiments could also be undertaken to investigate the mechanism of CYP2C19 inactivation by esomeprazole. Such studies would be greatly assisted by custom-synthesizing ^{14}C-esomeprazole to establish whether a metabolite of esomeprazole binds to the heme prosthetic group or apoprotein moiety of CYP2C19 (or cross-links the heme to the apoprotein). Future studies of the mechanism of CYP2C19 inactivation by esomeprazole would also be assisted by the availability of purified CYP2C19, which could be used to detect the covalent binding of esomeprazole metabolites to the apoprotein by whole-protein mass spectrometry (with suitable deconvolution software).

An intriguing finding from my dissertation research is the difference between the *R*- and *S*-enantiomers of omeprazole. Only esomeprazole (the *S*-enantiomer) inactivated CYP2C19, which is surprising because the *R*-enantiomer not only contains a 5′-methyl group but this position is extensively metabolized by CYP2C19 (more so than esomeprazole). The

5′-hydroxylation of *R*-omeprazole presumably involves the intermediacy of a benzylic radical, which begs the question: Why doesn't *R*-omeprazole inactivate CYP2C19? Stereoselective inhibition of CYP2C19 has been reported for fluoxetine. Both the *R*- and *S*-enantiomers are metabolism-dependent inhibitors but only *S*-fluoxetine causes *irreversible* metabolism-dependent inhibition due to formation of a metabolite that coordinates with the heme iron of CYP2C19 (to form a metabolite inhibitory complex or MIC) (as shown in Figure 6.8) (177,178). Stereoselective metabolism of mesantoin (racemic mephenytoin) is of historical interest because it led to the discovery of CYP2C19, which was identified as the enzyme responsible for genetic polymorphisms in the metabolism of *S*-mephenytoin that had no effect on the disposition of *R*-mephenytoin (1). Even though mesantoin was withdrawn from the market, *S*-mephenytoin continues to be widely used as a selective in vitro, and even clinical, probe substrate for CYP2C19.

Although stereoselective metabolism and inhibition of CYP2C19 are not unprecedented, future studies could be undertaken to explain why esomeprazole irreversibly inactivates CYP2C19 and *R*-omeprazole does not. CYP2C19 has been crystallized, allowing mapping of its substrate-binding site (204). Future docking experiments might compare the binding of esomeprazole and *R*-omeprazole in the same orientation (with the 5′-methyl group adjacent to the heme moiety) to evaluate whether differences in binding can explain why only esomeprazole inactivates CYP2C19. An alternative explanation is that the inactivation of CYP2C19 by esomeprazole is not due to the formation of 5′-benzylic radical but is due to *O*-demethylation of methoxy group on the benzimidazole ring (with possible formation of a reactive quinoneimine). However, if *O*-demethylation were responsible for the inactivation of CYP2C19 by esomeprazole, then such inactivation would be expected to occur with lansoprazole. Nevertheless, future experiments with structural modifications of the methoxy group on the

benzimidazole ring of esomeprazole (such as its replacement with a trifluoromethyl group to block metabolism) could be conducted to examine this possibility.

My dissertation research provided a clinically relevant example of the importance of in vitro incubation conditions on the ability to detect metabolism-dependent inhibition of CYP enzymes. Numerous studies of the inhibitory potential of omeprazole failed to detect its ability to inactivate CYP2C19, and this can be attributed to the use of high concentrations of HLM and/or inappropriately long substrate incubation times. It is possible that the ability of other drugs to inactivate CYP enzymes in vitro has also been missed due the use of inappropriate incubation conditions. In light of the potential importance of benzylic radicals in the inactivation of CYP2C19 by omeprazole, esomeprazole and tenatoprazole, as well as the known role of a benzylic radical in the inactivation of CYP2C8 by gemfibrozil glucuronide, it would be of interest in the future to evaluate other drugs that undergo benzylic hydroxylation for their ability to cause metabolism-dependent inhibition of CYP enzymes under appropriate in vitro conditions. Such drugs include amitriptyline, *celecoxib*, debrisoquine, desloratadine, *glibornuride*, *gliclazide*, metoprolol, nortryptyline, salmeterol, reparixin, terodiline, *tolazamide*, *tolbutamide*, *tolmetin*, *torasemide*, tripelennamine, sitaxsentan, and warfarin (those shown in italics are hydroxylated at an unsubstituted benzylic methyl group).

My dissertation research identified tenatoprazole but not ilaprazole or rabeprazole as metabolism-dependent inhibitors of CYP2C19. As such, tenatoprazole (but not ilaprazole or rabeprazole) is predicted to inhibit the CYP2C19-dependent conversion of clopidogrel to its pharmacologically active metabolite H4. Tenatoprazole and ilaprazole are not approved PPIs in the USA. Nevertheless, it would be of clinical interest to conduct studies in human subjects to examine the potential of tenatoprazole and ilaprazole to inhibit the formation of H4 and thereby reduce the therapeutic effectiveness of clopidogrel.

Providing a mechanistic rationale for the clinically important interaction between clopidogrel and omeprazole and esomeprazole, and the lack of interaction with lansoprazole and pantoprazole, and identifying tenatoprazole as a new PPI with the same drug interaction potential as omeprazole and esomeprazole are major highlights of my dissertation research.

REFERENCES

1. Parkinson, A., Ogilvie, B. W., Buckley, D. B., Kazmi, F., Czerwinski, M., and Parkinson, O. (2013) Biotransformation of xenobiotics. in *Casarett and Doull's Toxicology: The Basic Science of Poisons* (Klaassen, C. D. ed.), 8th Ed., McGraw-Hill Medical Pub. Division, New York. pp 185-367

2. Wilkinson, G. R. (2005) Drug metabolism and variability among patients in drug response. *N Engl J Med* **352**, 2211

3. Tomalik-Scharte, D., Lutjohann, D., Doroshyenko, O., Frank, D., Jetter, A., and Fuhr, U. (2009) Plasma 4β-hydroxycholesterol: an endogenous CYP3A metric? *Clin Pharmacol Ther* **86**, 147-153

4. Paine, M. F., Hart, H. L., Ludington, S. S., Haining, R. L., Rettie, A. E., and Zeldin, D. C. (2006) The human intestinal cytochrome P450 "pie". *Drug Metab Dispos* **34**, 880-886

5. Aronson, J. K., and Ferner, R. E. (2003) Joining the DoTS: new approach to classifying adverse drug reactions. *BMJ* **327**, 1222-1225

6. Aronson, J. K. (2009) Medication errors: what they are, how they happen, and how to avoid them. *QJM* **102**, 513-521

7. Wiffen, P. (2001) *Evidence-based pharmacy*, Radcliffe Medical Press, Abingdon, Oxon

8. Lazarou, J., Pomeranz, B. H., and Corey, P. N. (1998) Incidence of adverse drug reactions in hospitalized patients: a meta-analysis of prospective studies. *JAMA* **279**, 1200-1205

9. Gurwitz, J. H., Field, T. S., Avorn, J., McCormick, D., Jain, S., Eckler, M., Benser, M., Edmondson, A. C., and Bates, D. W. (2000) Incidence and preventability of adverse drug events in nursing homes. *Am J Med* **109**, 87-94

10. Schappert, S. M., and Burt, C. W. (2006) Ambulatory care visits to physician offices, hospital outpatient departments, and emergency departments: United States, 2001-02. *Vital Health Stat* **13**, 1-66

11. The Henry J. Kaiser Family Foundation. (2014) Total Number of Retail Prescription Drugs Filled at Pharmacies. http://kff.org/other/state-indicator/total-retail-rx-drugs/#. Accessed: January 14, 2015.

12. Jacubeit, T., Drisch, D., and Weber, E. (1990) Risk factors as reflected by an intensive drug monitoring system. *Agents Actions Suppl* **29**, 117-125

13. Winterstein, A. G., Hatton, R. C., Gonzalez-Rothi, R., Johns, T. E., and Segal, R. (2002) Identifying clinically significant preventable adverse drug events through a hospital's database of adverse drug reaction reports. *Am J Health Syst Pharm* **59**, 1742-1749

14. Smith, D. A., and Obach, R. S. (2005) Seeing through the MIST: abundance versus percentage. Commentary on metabolites in safety testing. *Drug Metab Dispos* **33**, 1409-1417

15. Smith, D. A., Obach, R. S., Williams, D. P., and Park, B. K. (2009) Clearing the MIST (metabolites in safety testing) of time: The impact of duration of administration on drug metabolite toxicity. *Chem Biol Interact* **179**, 60-67

16. Ogilvie, B. W., Usuki, E., Yerino, P., and Parkinson, A. (2008) In vitro approaches for studying the inhibition of drug-metabolizing enzymes and identifying the drug-metabolizing enzymes responsible for the metabolism of drugs (Reaction Phenotyping) with emphasis on cytochrome P450. in *Drug-Drug Interactions* (Rodrigues, A. D. ed.), 2nd Ed., Informa Healthcare USA Inc., New York, NY. pp 231-358

17. Ogilvie, B. W., and Parkinson, A. (2014) Drugs as victims and perpetrators and the pharmacokinetic concept of maximum exposure. in *Handbook of Metabolic Pathways of Xenobiotics* (Prakash, C., Gan, L. S., Zhong, D., Aizawa, H., and Lee, P. eds.), 2nd Ed., John Wiley & Sons, Hoboken, NJ. pp 103-123

18. Tamargo, J. (2000) Drug-induced torsade de pointes: from molecular biology to bedside. *Jpn J Pharmacol* **83**, 1-19

19. Eaton, D. L., and Gilbert, S. G. (2013) Principles of toxicology. in *Casarett & Doull's Toxicology: The Basic Science of Poisons* (Klaassen, C. D. ed.), 8th Ed., McGraw-Hill, Inc., New York. pp 13-48

20. Scott, S., and Thompson, J. (2011) Adverse drug reactions. *Anaesth Intensive Care Med* **12**, 319-323

21. Rangan, G. K., Nguyen, T., Mainra, R., Succar, L., Schwensen, K. G., Burgess, J. S., and Ho, K. O. (2009) Therapeutic role of sirolimus in non-transplant kidney disease. *Pharmacol Ther* **123**, 187-206

22. Province, M. A., Goetz, M. P., Brauch, H., Flockhart, D. A., Hebert, J. M., Whaley, R., Suman, V. J., Schroth, W., Winter, S., Zembutsu, H., Mushiroda, T., Newman, W. G., Lee, M. T., Ambrosone, C. B., Beckmann, M. W., Choi, J. Y., Dieudonne, A. S., Fasching, P. A., Ferraldeschi, R., Gong, L., Haschke-Becher, E., Howell, A., Jordan, L. B., Hamann, U., Kiyotani, K., Krippl, P., Lambrechts, D., Latif, A., Langsenlehner, U., Lorizio, W., Neven, P., Nguyen, A. T., Park, B. W., Purdie, C. A., Quinlan, P., Renner, W., Schmidt, M., Schwab, M., Shin, J. G., Stingl, J. C., Wegman, P., Wingren, S., Wu, A. H., Ziv, E., Zirpoli, G., Thompson, A. M., Jordan, V. C., Nakamura, Y., Altman, R. B., Ames, M. M., Weinshilboum, R. M., Eichelbaum, M., Ingle, J. N., and Klein, T. E. (2014) CYP2D6 genotype and adjuvant tamoxifen: meta-analysis of heterogeneous study populations. *Clin Pharmacol Ther* **95**, 216-227

23. Bluet, G., Blankenstein, J., Brohan, E., Prévost, C., Chevé, M., Schofield, J., and Roy, S. (2014) Synthesis of the stabilized active metabolite of clopidogrel. *Tetrahedron* **70**, 3893-3900

24. US FDA - Center for Drug Evaluation and Research. (2014) Adderall XR Prescribing Information and Medication Guide.

http://www.accessdata.fda.gov/drugsatfda_docs/label/2014/021303s027lbl.pdf. Accessed: November 21, 2014.

25. US FDA - Center for Drug Evaluation and Research. (2013) Plavix Prescribing Information and Medication Guide. http://www.accessdata.fda.gov/drugsatfda_docs/label/2013/020839s058lbl.pdf. Accessed: November 21, 2014.

26. US FDA - Center for Drug Evaluation and Research. (2013) Codeine Sulfate Prescribing Information. http://www.accessdata.fda.gov/drugsatfda_docs/label/2013/022402s006lbl.pdf. Accessed: November 21, 2014.

27. University of Washington. (2015) Metabolism and Transport Drug Interaction Database. http://www.druginteractioninfo.org/. Accessed: April 2, 2015.

28. Cubeddu, L. X. (2009) Iatrogenic QT abnormalities and fatal arrhythmias: Mechanisms and clinical significance. *Curr Cardiol Rev* **5**, 166-176

29. Kalvass, J. C., Polli, J. W., Bourdet, D. L., Feng, B., Huang, S. M., Liu, X., Smith, Q. R., Zhang, L. K., and Zamek-Gliszczynski, M. J. (2013) Why clinical modulation of efflux transport at the human blood-brain barrier is unlikely: the ITC evidence-based position. *Clin Pharmacol Ther* **94**, 80-94

30. Neuvonen, P. J., Niemi, M., and Backman, J. T. (2006) Drug interactions with lipid-lowering drugs: mechanisms and clinical relevance. *Clin Pharmacol Ther* **80**, 565-581

31. US FDA - Center for Drug Evaluation and Research. (2012) Guidance for Industry: Drug Interaction Studies — Study Design, Data Analysis, Implications for Dosing, and Labeling Recommendations. http://www.fda.gov/downloads/drugs/guidancecomplianceregulatoryinformation/guidances/ucm292362.pdf. Accessed: November 21, 2014.

32. European Medicines Agency. (2012) Guideline on the Investigation of Drug Interactions. http://www.ema.europa.eu/docs/en_GB/document_library/Scientific_guideline/2012/07/WC500129606.pdf. Accessed: January 3, 2015.

33. Ogilvie, B. W., Zhang, D., Li, W., Rodrigues, A. D., Gipson, A. E., Holsapple, J., Toren, P., and Parkinson, A. (2006) Glucuronidation converts gemfibrozil to a potent, metabolism-dependent inhibitor of CYP2C8: implications for drug-drug interactions. *Drug Metab Dispos* **34**, 191-197

34. Ogilvie, B. W., Yerino, P., Kazmi, F., Buckley, D. B., Rostami-Hodjegan, A., Paris, B. L., Toren, P., and Parkinson, A. (2011) The proton pump inhibitor, omeprazole, but not lansoprazole or pantoprazole, is a metabolism-dependent inhibitor of CYP2C19: implications for coadministration with clopidogrel. *Drug Metab Dispos* **39**, 2020-2033

35. Parkinson, A., Kazmi, F., Buckley, D. B., Yerino, P., Paris, B. L., Holsapple, J., Toren, P., Otradovec, S. M., and Ogilvie, B. W. (2011) An evaluation of the dilution method for identifying metabolism-dependent inhibitors of cytochrome P450 enzymes. *Drug Metab Dispos* **39**, 1370-1387

36. Nagar, S., and Korzekwa, K. (2012) Commentary: nonspecific protein binding versus membrane partitioning: it is not just semantics. *Drug Metab Dispos* **40**, 1649-1652

37. Paris, B. L., Ogilvie, B. W., Scheinkoenig, J. A., Ndikum-Moffor, F., Gibson, R., and Parkinson, A. (2009) In vitro inhibition and induction of human liver cytochrome P450 enzymes by milnacipran. *Drug Metab Dispos* **37**, 2045-2054

38. Nassar, A. E., King, I., Paris, B. L., Haupt, L., Ndikum-Moffor, F., Campbell, R., Usuki, E., Skibbe, J., Brobst, D., Ogilvie, B. W., and Parkinson, A. (2009) An in vitro evaluation of the victim and perpetrator potential of the anticancer agent laromustine (VNP40101M), based on reaction phenotyping and inhibition and induction of cytochrome P450 enzymes. *Drug Metab Dispos* **37**, 1922-1930

39. Cheng, Y., and Prusoff, W. H. (1973) Relationship between the inhibition constant (Ki) and the concentration of inhibitor which causes 50 per cent inhibition (IC_{50}) of an enzymatic reaction. *Biochem Pharmacol* **22**, 3099-3108

40. Honkalammi, J., Niemi, M., Neuvonen, P. J., and Backman, J. T. (2012) Gemfibrozil is a strong inactivator of CYP2C8 in very small multiple doses. *Clin Pharmacol Ther* **91**, 846-855

41. Honkalammi, J., Niemi, M., Neuvonen, P. J., and Backman, J. T. (2011) Mechanism-based inactivation of CYP2C8 by gemfibrozil occurs rapidly in humans. *Clin Pharmacol Ther* **89**, 579-586

42. Backman, J. T., Honkalammi, J., Neuvonen, M., Kurkinen, K. J., Tornio, A., Niemi, M., and Neuvonen, P. J. (2009) CYP2C8 activity recovers within 96 hours after gemfibrozil dosing: estimation of CYP2C8 half-life using repaglinide as an in vivo probe. *Drug Metab Dispos* **37**, 2359-2366

43. Tornio, A., Niemi, M., Neuvonen, M., Laitila, J., Kalliokoski, A., Neuvonen, P. J., and Backman, J. T. (2008) The effect of gemfibrozil on repaglinide pharmacokinetics persists for at least 12 h after the dose: evidence for mechanism-based inhibition of CYP2C8 in vivo. *Clin Pharmacol Ther* **84**, 403-411

44. Djebli, N., Fabre, D., Boulenc, X., Fabre, G., Sultan, E., and Hurbin, F. (2015) Physiologically based pharmacokinetic modeling for sequential metabolism: effect of CYP2C19 genetic polymorphism on clopidogrel and clopidogrel active metabolite pharmacokinetics. *Drug Metab Dispos* **43**, 510-522

45. Savi, P., Combalbert, J., Gaich, C., Rouchon, M. C., Maffrand, J. P., Berger, Y., and Herbert, J. M. (1994) The antiaggregating activity of clopidogrel is due to a metabolic activation by the hepatic cytochrome P450-1A. *Thromb Haemost* **72**, 313-317

46. Clarke, T. A., and Waskell, L. A. (2003) The metabolism of clopidogrel is catalyzed by human cytochrome P450 3A and is inhibited by atorvastatin. *Drug Metab Dispos* **31**, 53-59

47. Abraham, N. S., Hlatky, M. A., Antman, E. M., Bhatt, D. L., Bjorkman, D. J., Clark, C. B., Furberg, C. D., Johnson, D. A., Kahi, C. J., Laine, L., Mahaffey, K. W., Quigley, E. M., Scheiman, J., Sperling, L. S., and Tomaselli, G. F. (2010) ACCF/ACG/AHA 2010 expert

consensus document on the concomitant use of proton pump inhibitors and thienopyridines: a focused update of the ACCF/ACG/AHA 2008 expert consensus document on reducing the gastrointestinal risks of antiplatelet therapy and NSAID use. A report of the American College of Cardiology Foundation Task Force on Expert Consensus Documents. *J Am Coll Cardiol* **56**, 2051-2066

48. Kazui, M., Nishiya, Y., Ishizuka, T., Hagihara, K., Farid, N. A., Okazaki, O., Ikeda, T., and Kurihara, A. (2010) Identification of the human cytochrome P450 enzymes involved in the two oxidative steps in the bioactivation of clopidogrel to its pharmacologically active metabolite. *Drug Metab Dispos* **38**, 92-99

49. Zahno, A., Brecht, K., Bodmer, M., Bur, D., Tsakiris, D. A., and Krahenbuhl, S. (2010) Effects of drug interactions on biotransformation and antiplatelet effect of clopidogrel in vitro. *Br J Pharmacol* **161**, 393-404

50. Dansette, P. M., Levent, D., Hessani, A., Bertho, G., and Mansuy, D. (2013) Thiolactone sulfoxides as new reactive metabolites acting as bis-electrophiles: implication in clopidogrel and prasugrel bioactivation. *Chem Res Toxicol* **26**, 794-802

51. Hariharan, S., Southworth, M. R., and Madabushi, R. (2014) Clopidogrel, CYP2C19 and proton pump inhibitors: what we know and what it means. *J Clin Pharmacol* **54**, 884-888

52. Dansette, P. M., Rosi, J., Bertho, G., and Mansuy, D. (2012) Cytochromes P450 catalyze both steps of the major pathway of clopidogrel bioactivation, whereas paraoxonase catalyzes the formation of a minor thiol metabolite isomer. *Chem Res Toxicol* **25**, 348-356

53. Ho, P. M., Maddox, T. M., Wang, L., Fihn, S. D., Jesse, R. L., Peterson, E. D., and Rumsfeld, J. S. (2009) Risk of adverse outcomes associated with concomitant use of clopidogrel and proton pump inhibitors following acute coronary syndrome. *JAMA* **301**, 937-944

54. Brunton, L., Chabner, B., and Knollman, B. (2011) *Goodman and Gilman's The Pharmacological Basis of Therapeutics*, 12th ed., McGraw-Hill Education, New York

55. Hsu, P. I., Lai, K. H., and Liu, C. P. (2011) Esomeprazole with clopidogrel reduces peptic ulcer recurrence, compared with clopidogrel alone, in patients with atherosclerosis. *Gastroenterology* **140**, 791-798

56. Bhatt, D. L., Scheiman, J., Abraham, N. S., Antman, E. M., Chan, F. K., Furberg, C. D., Johnson, D. A., Mahaffey, K. W., Quigley, E. M., Harrington, R. A., Bates, E. R., Bridges, C. R., Eisenberg, M. J., Ferrari, V. A., Hlatky, M. A., Kaul, S., Lindner, J. R., Moliterno, D. J., Mukherjee, D., Schofield, R. S., Rosenson, R. S., Stein, J. H., Weitz, H. H., and Wesley, D. J. (2008) ACCF/ACG/AHA 2008 expert consensus document on reducing the gastrointestinal risks of antiplatelet therapy and NSAID use: a report of the American College of Cardiology Foundation Task Force on Clinical Expert Consensus Documents. *J Am Coll Cardiol* **52**, 1502-1517

57. Roche, V. F. (2006) The chemically elegant proton pump inhibitors. *Am J Pharm Educ* **70**, 101

58. Hunt, R. H., Armstrong, D., Yaghoobi, M., James, C., Chen, Y., Leonard, J., Shin, J. M., Lee, E., Tang-Liu, D., and Sachs, G. (2008) Predictable prolonged suppression of gastric acidity with a novel proton pump inhibitor, AGN 201904-Z. *Aliment Pharmacol Ther* **28**, 187-199

59. Shin, J. S., Lee, J. Y., Cho, K. H., Park, H. L., Kukulka, M., Wu, J. T., Kim, D. Y., and Park, S. H. (2014) The pharmacokinetics, pharmacodynamics and safety of oral doses of ilaprazole 10, 20 and 40 mg and esomeprazole 40 mg in healthy subjects: a randomised, open-label crossover study. *Aliment Pharmacol Ther* **40**, 548-561

60. Emerson, C. R., and Marzella, N. (2010) Dexlansoprazole: A proton pump inhibitor with a dual delayed-release system. *Clin Ther* **32**, 1578-1596

61. Domagala, F., Ficheux, H., Houin, G., and Barre, J. (2006) Pharmacokinetics of tenatoprazole, a newly synthesized proton pump inhibitor, in healthy male Caucasian volunteers. *Arzneimittelforschung* **56**, 33-39

62. Shin, J. M., and Sachs, G. (2008) Pharmacology of proton pump inhibitors. *Curr Gastroenterol Rep* **10**, 528-534

63. McQuaid, K. R. (2012) Drugs used in the treatment of gastrointestinal diseases. in *Basic & Clinical Pharmacology* (Katzung, B. G., Masters, S. B., and Trevor, A. J. eds.), 12th Ed., The McGraw-Hill Companies, New York, NY. pp 1067–1101

64. Hulot, J. S., Bura, A., Villard, E., Azizi, M., Remones, V., Goyenvalle, C., Aiach, M., Lechat, P., and Gaussem, P. (2006) Cytochrome P450 2C19 loss-of-function polymorphism is a major determinant of clopidogrel responsiveness in healthy subjects. *Blood* **108**, 2244-2247

65. Hirota, T., Eguchi, S., and Ieiri, I. (2013) Impact of genetic polymorphisms in CYP2C9 and CYP2C19 on the pharmacokinetics of clinically used drugs. *Drug Metab Pharmacokinet* **28**, 28-37

66. Furuta, T., Iwaki, T., and Umemura, K. (2010) Influences of different proton pump inhibitors on the anti-platelet function of clopidogrel in relation to CYP2C19 genotypes. *Br J Clin Pharmacol* **70**, 383-392

67. Sorich, M. J., Polasek, T. M., and Wiese, M. D. (2013) Challenges and limitations in the interpretation of systematic reviews: making sense of clopidogrel and CYP2C19 pharmacogenetics. *Clin Pharmacol Ther* **94**, 376-382

68. Simon, T., Bhatt, D. L., Bergougnan, L., Farenc, C., Pearson, K., Perrin, L., Vicaut, E., Lacreta, F., Hurbin, F., and Dubar, M. (2011) Genetic polymorphisms and the impact of a higher clopidogrel dose regimen on active metabolite exposure and antiplatelet response in healthy subjects. *Clin Pharmacol Ther* **90**, 287-295

69. Farid, N. A., Payne, C. D., Small, D. S., Winters, K. J., Ernest, C. S., 2nd, Brandt, J. T., Darstein, C., Jakubowski, J. A., and Salazar, D. E. (2007) Cytochrome P450 3A inhibition by ketoconazole affects prasugrel and clopidogrel pharmacokinetics and pharmacodynamics differently. *Clin Pharmacol Ther* **81**, 735-741

70. Ford, N. F., and Taubert, D. (2013) Clopidogrel, CYP2C19, and a black box. *J Clin Pharmacol* **53**, 241-248

71. Ford, N. F. (2014) Clopidogrel: what is a cardiologist to do? *J Clin Pharmacol* **54**, 881-883

72. Angiolillo, D. J., Ferreiro, J. L., Price, M. J., Kirtane, A. J., and Stone, G. W. (2013) Platelet function and genetic testing. *J Am Coll Cardiol* **62**, S21-31

73. Leeder, J. S. (2015) Meaningful use and clinical utility of preemptive pharmacogenetic testing: (Re)View from a CYP2D6 poor metabolizer. *Clin Pharmacol Ther* **97**, 119-121

74. Soons, P. A., van den Berg, G., Danhof, M., van Brummelen, P., Jansen, J. B., Lamers, C. B., and Breimer, D. D. (1992) Influence of single- and multiple-dose omeprazole treatment on nifedipine pharmacokinetics and effects in healthy subjects. *Eur J Clin Pharmacol* **42**, 319-324

75. Shirasaka, Y., Sager, J. E., Lutz, J. D., Davis, C., and Isoherranen, N. (2013) Inhibition of CYP2C19 and CYP3A4 by omeprazole metabolites and their contribution to drug-drug interactions. *Drug Metab Dispos* **41**, 1414-1424

76. Dixit, R. K., Chawla, A. B., Kumar, N., and Garg, S. K. (2001) Effect of omeprazole on the pharmacokinetics of sustained-release carbamazepine in healthy male volunteers. *Methods Find Exp Clin Pharmacol* **23**, 37-39

77. Ogawa, R., and Echizen, H. (2010) Drug-drug interaction profiles of proton pump inhibitors. *Clin Pharmacokinet* **49**, 509-533

78. Zvyaga, T., Chang, S. Y., Chen, C., Yang, Z., Vuppugalla, R., Hurley, J., Thorndike, D., Wagner, A., Chimalakonda, A., and Rodrigues, A. D. (2012) Evaluation of six proton pump inhibitors as inhibitors of various human cytochromes P450: focus on cytochrome P450 2C19. *Drug Metab Dispos* **40**, 1698-1711

79. Holmberg, M. T., Tornio, A., Neuvonen, M., Neuvonen, P. J., Backman, J. T., and Niemi, M. (2014) Grapefruit juice inhibits the metabolic activation of clopidogrel. *Clin Pharmacol Ther* **95**, 307-313

80. Bouman, H. J., Schomig, E., van Werkum, J. W., Velder, J., Hackeng, C. M., Hirschhauser, C., Waldmann, C., Schmalz, H. G., ten Berg, J. M., and Taubert, D. (2011) Paraoxonase-1 is a major determinant of clopidogrel efficacy. *Nat Med* **17**, 110-116

81. Sibbing, D., Koch, W., Massberg, S., Byrne, R. A., Mehilli, J., Schulz, S., Mayer, K., Bernlochner, I., Schomig, A., and Kastrati, A. (2011) No association of paraoxonase-1 Q192R genotypes with platelet response to clopidogrel and risk of stent thrombosis after coronary stenting. *Eur Heart J* **32**, 1605-1613

82. Oh, J., Shin, D., Lim, K. S., Lee, S., Jung, K. H., Chu, K., Hong, K. S., Shin, K. H., Cho, J. Y., Yoon, S. H., Ji, S. C., Yu, K. S., Lee, H., and Jang, I. J. (2014) Aspirin decreases systemic exposure to clopidogrel through modulation of P-glycoprotein but does not alter its antithrombotic activity. *Clin Pharmacol Ther* **95**, 608-616

83. Tuffal, G., Roy, S., Lavisse, M., Brasseur, D., Schofield, J., Delesque Touchard, N., Savi, P., Bremond, N., Rouchon, M. C., Hurbin, F., and Sultan, E. (2011) An improved method for specific and quantitative determination of the clopidogrel active metabolite isomers in human plasma. *Thromb Haemost* **105**, 696-705

84. Angiolillo, D. J., Gibson, C. M., Cheng, S., Ollier, C., Nicolas, O., Bergougnan, L., Perrin, L., LaCreta, F. P., Hurbin, F., and Dubar, M. (2011) Differential effects of omeprazole and pantoprazole on the pharmacodynamics and pharmacokinetics of clopidogrel in healthy subjects: randomized, placebo-controlled, crossover comparison studies. *Clin Pharmacol Ther* **89**, 65-74

85. Gong, I. Y., Crown, N., Suen, C. M., Schwarz, U. I., Dresser, G. K., Knauer, M. J., Sugiyama, D., DeGorter, M. K., Woolsey, S., Tirona, R. G., and Kim, R. B. (2012) Clarifying the importance of CYP2C19 and PON1 in the mechanism of clopidogrel bioactivation and in vivo antiplatelet response. *Eur Heart J* **33**, 2856-2464a

86. Dansette, P. M., Rosi, J., Bertho, G., and Mansuy, D. (2011) Paraoxonase-1 and clopidogrel efficacy. *Nat Med* **17**, 1040-1041

87. Bouman, H. J., Schomig, E., van Werkum, J. W., Velder, J., Hackeng, C. M., Hirschhauser, C., Waldmann, C., Schmalz, H. G., Ten Berg, J. M., and Taubert, D. (2011) Reply to: "Paraoxonase-1 and clopidogrel efficacy". *Nat Med* **17**, 1042-1044

88. Gurbel, P. A., Bergmeijer, T. O., Tantry, U. S., ten Berg, J. M., Angiolillo, D. J., James, S., Lindahl, T. L., Svensson, P., Jakubowski, J. A., Brown, P. B., Duvvuru, S., Sundseth, S., Walker, J. R., Small, D., Moser, B. A., Winters, K. J., and Erlinge, D. (2014) The effect of CYP2C19 gene polymorphisms on the pharmacokinetics and pharmacodynamics of prasugrel 5-mg, prasugrel 10-mg and clopidogrel 75-mg in patients with coronary artery disease. *Thromb Haemost* **112**, 589-597

89. Karazniewicz-Lada, M., Danielak, D., Rubis, B., Burchardt, P., Oszkinis, G., and Glowka, F. (2014) The influence of genetic polymorphism of CYP2C19 isoenzyme on the pharmacokinetics of clopidogrel and its metabolites in patients with cardiovascular diseases. *J Clin Pharmacol* **54**, 874-880

90. Horenstein, R. B., Madabushi, R., Zineh, I., Yerges-Armstrong, L. M., Peer, C. J., Schuck, R. N., Figg, W. D., Shuldiner, A. R., and Pacanowski, M. A. (2014) Effectiveness of clopidogrel dose escalation to normalize active metabolite exposure and antiplatelet effects in CYP2C19 poor metabolizers. *J Clin Pharmacol* **54**, 865-873

91. Kim, H. S., Cho, D. Y., Park, B. M., Bae, S. K., Yoon, Y. J., Oh, M., Ghim, J. L., Kim, E. Y., Kim, D. H., and Shin, J. G. (2014) The effect of CYP2C19 genotype on the time course of platelet aggregation inhibition after clopidogrel administration. *J Clin Pharmacol* **54**, 850-857

92. Hulot, J. S., Collet, J. P., Cayla, G., Silvain, J., Allanic, F., Bellemain-Appaix, A., Scott, S. A., and Montalescot, G. (2011) CYP2C19 but not PON1 genetic variants influence clopidogrel pharmacokinetics, pharmacodynamics, and clinical efficacy in post-myocardial infarction patients. *Circ Cardiovasc Interv* **4**, 422-428

93. Kelly, R. P., Close, S. L., Farid, N. A., Winters, K. J., Shen, L., Natanegara, F., Jakubowski, J. A., Ho, M., Walker, J. R., and Small, D. S. (2012) Pharmacokinetics and pharmacodynamics following maintenance doses of prasugrel and clopidogrel in Chinese carriers of CYP2C19 variants. *Br J Clin Pharmacol* **73**, 93-105

94. Boulenc, X., Djebli, N., Shi, J., Perrin, L., Brian, W., Van Horn, R., and Hurbin, F. (2012) Effects of omeprazole and genetic polymorphism of CYP2C19 on the clopidogrel active metabolite. *Drug Metab Dispos* **40**, 187-197

95. Hobl, E. L., Stimpfl, T., Ebner, J., Schoergenhofer, C., Derhaschnig, U., Sunder-Plassmann, R., Jilma-Stohlawetz, P., Mannhalter, C., Posch, M., and Jilma, B. (2014) Morphine decreases clopidogrel concentrations and effects: a randomized, double-blind, placebo-controlled trial. *J Am Coll Cardiol* **63**, 630-635

96. Gurbel, P. A., Bliden, K. P., Logan, D. K., Kereiakes, D. J., Lasseter, K. C., White, A., Angiolillo, D. J., Nolin, T. D., Maa, J. F., Bailey, W. L., Jakubowski, J. A., Ojeh, C. K., Jeong, Y. H., Tantry, U. S., and Baker, B. A. (2013) The influence of smoking status on the pharmacokinetics and pharmacodynamics of clopidogrel and prasugrel: the PARADOX study. *J Am Coll Cardiol* **62**, 505-512

97. Delavenne, X., Magnin, M., Basset, T., Piot, M., Mallouk, N., Ressnikoff, D., Garcin, A., Laporte, S., Garnier, P., and Mismetti, P. (2013) Investigation of drug-drug interactions between clopidogrel and fluoxetine. *Fundam Clin Pharmacol* **27**, 683-689

98. Hartter, S., Sennewald, R., Schepers, C., Baumann, S., Fritsch, H., and Friedman, J. (2013) Pharmacokinetic and pharmacodynamic effects of comedication of clopidogrel and dabigatran etexilate in healthy male volunteers. *Eur J Clin Pharmacol* **69**, 327-339

99. Pinheiro, L. F., França, C. N., Izar, M. C., Barbosa, S. P., Bianco, H. T., Kasmas, S. H., Mendes, G. D., Povoa, R. M., and Fonseca, F. A. H. (2012) Pharmacokinetic interactions between clopidogrel and rosuvastatin: Effects on vascular protection in subjects with coronary heart disease. *Int J Cardiol* **158**, 125-129

100. Lau, W. C., Welch, T. D., Shields, T., Rubenfire, M., Tantry, U. S., and Gurbel, P. A. (2011) The effect of St John's Wort on the pharmacodynamic response of clopidogrel in hyporesponsive volunteers and patients: increased platelet inhibition by enhancement of CYP3A4 metabolic activity. *J Cardiovasc Pharmacol* **57**, 86-93

101. Farid, N. A., Small, D. S., Payne, C. D., Jakubowski, J. A., Brandt, J. T., Li, Y. G., Ernest, C. S., Salazar, D. E., Konkoy, C. S., and Winters, K. J. (2008) Effect of atorvastatin on the pharmacokinetics and pharmacodynamics of prasugrel and clopidogrel in healthy subjects. *Pharmacotherapy* **28**, 1483-1494

102. US FDA - Center for Drug Evaluation and Research. (2012) Eliquis (apixaban) Drug Approval Package. http://www.accessdata.fda.gov/drugsatfda_docs/nda/2012/202155Orig1s000TOC.cfm. Accessed: January 12, 2015.

103. US FDA - Center for Drug Evaluation and Research. (2009) Effient (prasugrel) Drug Approval Package.

http://www.accessdata.fda.gov/drugsatfda_docs/nda/2009/022307s000TOC.cfm. Accessed: January 12, 2015.

104. Funck-Brentano, C., Szymezak, J., Steichen, O., Ducint, D., Molimard, M., Remones, V., Azizi, M., and Gaussem, P. (2013) Effects of rabeprazole on the antiplatelet effects and pharmacokinetics of clopidogrel in healthy volunteers. *Arch Cardiovasc Dis* **106**, 661-671

105. Wu, J., Jia, L. T., Shao, L. M., Chen, J. M., Zhong, D. D., Xu, S., and Cai, J. T. (2013) Drug-drug interaction of rabeprazole and clopidogrel in healthy Chinese volunteers. *Eur J Clin Pharmacol* **69**, 179-187

106. Frelinger, A. L., 3rd, Lee, R. D., Mulford, D. J., Wu, J., Nudurupati, S., Nigam, A., Brooks, J. K., Bhatt, D. L., and Michelson, A. D. (2012) A randomized, 2-period, crossover design study to assess the effects of dexlansoprazole, lansoprazole, esomeprazole, and omeprazole on the steady-state pharmacokinetics and pharmacodynamics of clopidogrel in healthy volunteers. *J Am Coll Cardiol* **59**, 1304-1311

107. Harmsze, A. M., van Werkum, J. W., Taubert, D., Hackeng, C. M., and Deneer, V. H. (2011) Esomeprazole but not pantoprazole is associated with lower plasma concentrations of clopidogrel's active metabolite. *Ann Pharmacother* **45**, 542-543

108. Andersson, T., Nagy, P., Niazi, M., Nylander, S., Galbraith, H., Ranjan, S., and Wallentin, L. (2014) Effect of esomeprazole with/without acetylsalicylic acid, omeprazole and lansoprazole on pharmacokinetics and pharmacodynamics of clopidogrel in healthy volunteers. *Am J Cardiovasc Drugs* **14**, 217-227

109. US FDA - Center for Drug Evaluation and Research. (2010) FDA reminder to avoid concomitant use of Plavix (clopidogrel) and omeprazole. http://www.fda.gov/drugs/drugsafety/ucm231161.htm. Accessed: January 12, 2015.

110. Johnson, D. A., Chilton, R., and Liker, H. R. (2014) Proton-pump inhibitors in patients requiring antiplatelet therapy: new FDA labeling. *Postgrad Med* **126**, 239-245

111. Ogilvie, B. W., Toren, P., Kazmi, F., and Parkinson, A. (2011) Esomeprazole and omeprazole sulfone are in vitro metabolism-dependent inactivators of CYP2C19: Determination of K_I and k_{inact} values. *Drug Metab Rev* **43(S2)**, 145

112. Yu, K. S., Yim, D. S., Cho, J. Y., Park, S. S., Park, J. Y., Lee, K. H., Jang, I. J., Yi, S. Y., Bae, K. S., and Shin, S. G. (2001) Effect of omeprazole on the pharmacokinetics of moclobemide according to the genetic polymorphism of CYP2C19. *Clin Pharmacol Ther* **69**, 266-273

113. Andersson, T., and Weidolf, L. (2008) Stereoselective disposition of proton pump inhibitors. *Clin Drug Investig* **28**, 263-279

114. Andersson, T., Andren, K., Cederberg, C., Lagerstrom, P. O., Lundborg, P., and Skånberg, I. (1990) Pharmacokinetics and bioavailability of omeprazole after single and repeated oral administration in healthy subjects. *Br J Clin Pharmacol* **29**, 557-563

115. Andersson, T., Bergstrand, R., and Cederberg, C. (1991) Influence of acid secretory status on absorption of omeprazole from enteric coated granules. *Br J Clin Pharmacol* **31**, 275-278

116. US FDA - Center for Drug Evaluation and Research. (2014) Prevacid (lansoprazole) Prescribing Information and Medication Guide. http://www.accessdata.fda.gov/drugsatfda_docs/label/2014/021428s028lbl020406s081lbl.pdf. Accessed: January 13, 2015.

117. US FDA - Center for Drug Evaluation and Research. (2014) Protonix (pantoprazole) Prescribing Information and Medication Guide. http://www.accessdata.fda.gov/drugsatfda_docs/label/2014/022020s011-020987s049lbl.pdf. Accessed: January 13, 2015.

118. US FDA - Center for Drug Evaluation and Research. (2014) Aciphex (rabeprazole) Prescribing Information and Medication Guide. http://www.accessdata.fda.gov/drugsatfda_docs/label/2014/020973s035204736s005lbl.pdf. Accessed: January 13, 2015.

119. US FDA - Center for Drug Evaluation and Research. (2014) Nexium (esomeprazole) Prescribing Information and Medication Guide. http://www.accessdata.fda.gov/drugsatfda_docs/label/2014/022101s014021957s017021153s050lbl.pdf. Accessed: January 13, 2015.

120. Ogilvie, B. W., and Parkinson, A. (2012) Mechanistic studies on the inactivation of CYP2C19 by esomeprazole, 5-*O*-desmethyl omeprazole, and omeprazole sulfone. *Drug Metab Rev* **44(S1)**, 40

121. Ohbuchi, M., Noguchi, K., Kawamura, A., and Usui, T. (2012) Different effects of proton pump inhibitors and famotidine on the clopidogrel metabolic activation by recombinant CYP2B6, CYP2C19 and CYP3A4. *Xenobiotica* **42**, 633-640

122. Clark, M. G., Beavers, C., and Osborne, J. (2015) Managing the acute coronary syndrome patient: Evidence based recommendations for anti-platelet therapy. *Heart Lung* **44**, 141-149

123. Pearce, R. E., McIntyre, C. J., Madan, A., Sanzgiri, U., Draper, A. J., Bullock, P. L., Cook, D. C., Burton, L. A., Latham, J., Nevins, C., and Parkinson, A. (1996) Effects of freezing, thawing, and storing human liver microsomes on cytochrome P450 activity. *Arch Biochem Biophys* **331**, 145-169

124. Paris, B. L., Yerino, P., Toren, P., Ogilvie, B. W., and Parkinson, A. (2008) An evaluation of ebastine hydroxylation and *N*-dealkylation as specific in vitro probes of human liver microsomal CYP2J2 and CYP3A4, respectively. *Drug Metab Rev* **40(S3)**, 396

125. Franklin, M. R. (1977) Inhibition of mixed-function oxidations by substrates forming reduced cytochrome P-450 metabolic-intermediate complexes. *Pharmacol Ther A* **2**, 227-245

126. Barbara, J. E. (2013) High-resolution MS: software, data processing and data management. in *Applications of High-Resolution Mass Spectrometry in Drug Discovery and Development* (Sleno, L. ed.), Future Science, Ltd., London, UK. pp 74-91

127. Barbara, J. E., Buckley, D. B., and Horrigan, M. J. (2013) Exploring the utility of high-resolution MS with post-acquisition data mining for simultaneous exogenous and endogenous metabolite profiling. *Bioanalysis* **5**, 1211-1228

128. Barbara, J. E., Kazmi, F., Muranjan, S., Toren, P. C., and Parkinson, A. (2012) High-resolution mass spectrometry elucidates metabonate (false metabolite) formation from alkylamine drugs during in vitro metabolite profiling. *Drug Metab Dispos* **40**, 1966-1975

129. Barbara, J. E., and Castro-Perez, J. M. (2011) High-resolution chromatography/time-of-flight MS^E with in silico data mining is an information-rich approach to reactive metabolite screening. *Rapid Commun Mass Spectrom* **25**, 3029-3040

130. Grimm, S. W., Einolf, H. J., Hall, S. D., He, K., Lim, H. K., Ling, K. H., Lu, C., Nomeir, A. A., Seibert, E., Skordos, K. W., Tonn, G. R., Van Horn, R., Wang, R. W., Wong, Y. N., Yang, T. J., and Obach, R. S. (2009) The conduct of in vitro studies to address time-dependent inhibition of drug-metabolizing enzymes: a perspective of the pharmaceutical research and manufacturers of America. *Drug Metab Dispos* **37**, 1355-1370

131. Rowland Yeo, K., Jamei, M., Yang, J., Tucker, G. T., and Rostami-Hodjegan, A. (2010) Physiologically based mechanistic modelling to predict complex drug-drug interactions involving simultaneous competitive and time-dependent enzyme inhibition by parent compound and its metabolite in both liver and gut - the effect of diltiazem on the time-course of exposure to triazolam. *Eur J Pharm Sci* **39**, 298-309

132. Renwick, A. B., Watts, P. S., Edwards, R. J., Barton, P. T., Guyonnet, I., Price, R. J., Tredger, J. M., Pelkonen, O., Boobis, A. R., and Lake, B. G. (2000) Differential Maintenance of Cytochrome P450 Enzymes in Cultured Precision-Cut Human Liver Slices. *Drug Metab Dispos* **28**, 1202-1209

133. Yang, J., Liao, M., Shou, M., Jamei, M., Yeo, K. R., Tucker, G. T., and Rostami-Hodjegan, A. (2008) Cytochrome P450 turnover: regulation of synthesis and degradation, methods for determining rates, and implications for the prediction of drug interactions. *Curr Drug Metab* **9**, 384-394

134. Obach, R. S., Walsky, R. L., and Venkatakrishnan, K. (2007) Mechanism-based inactivation of human cytochrome P450 enzymes and the prediction of drug-drug interactions. *Drug Metab Dispos* **35**, 246-255

135. Hassan-Alin, M., Andersson, T., Niazi, M., and Rohss, K. (2005) A pharmacokinetic study comparing single and repeated oral doses of 20 mg and 40 mg omeprazole and its two optical isomers, *S*-omeprazole (esomeprazole) and *R*-omeprazole, in healthy subjects. *Eur J Clin Pharmacol* **60**, 779-784

136. Wallace, J. L., and Sharkey, K. A. (2011) Pharmacotherapy of gastric acidity, peptic ulcers, and gastroesophageal reflux disease. in *Goodman and Gilman's The Pharmacological Basis of Therapeutics* (Brunton, L., Chabner, B., and Knollman, B. eds.), 12th Ed., McGraw-Hill, New York. pp 1001-1019

137. Furuta, T., Ohashi, K., Kobayashi, K., Iida, I., Yoshida, H., Shirai, N., Takashima, M., Kosuge, K., Hanai, H., Chiba, K., Ishizaki, T., and Kaneko, E. (1999) Effects of clarithromycin on the metabolism of omeprazole in relation to CYP2C19 genotype status in humans. *Clin Pharmacol Ther* **66**, 265-274

138. Li, X. Q., Andersson, T. B., Ahlstrom, M., and Weidolf, L. (2004) Comparison of inhibitory effects of the proton pump-inhibiting drugs omeprazole, esomeprazole, lansoprazole, pantoprazole, and rabeprazole on human cytochrome P450 activities. *Drug Metab Dispos* **32**, 821-827

139. US FDA - Center for Drug Evaluation and Research. (2014) Prilosec (omeprazole) Prescribing Information and Medication Guide. http://www.accessdata.fda.gov/scripts/cder/drugsatfda/index.cfm?fuseaction=Search.Label_ApprovalHistory#labelinfo. Accessed: January 14, 2015.

140. European Medicines Agency. (2010) Interaction between clopidogrel and proton-pump inhibitors. http://www.ema.europa.eu/docs/en_GB/document_library/Public_statement/2010/03/WC500076346.pdf. Accessed: January 14, 2015.

141. Sibbing, D., Koch, W., Gebhard, D., Schuster, T., Braun, S., Stegherr, J., Morath, T., Schomig, A., von Beckerath, N., and Kastrati, A. (2010) Cytochrome 2C19*17 allelic variant, platelet aggregation, bleeding events, and stent thrombosis in clopidogrel-treated patients with coronary stent placement. *Circulation* **121**, 512-518

142. Walsky, R. L., and Obach, R. S. (2004) Validated assays for human cytochrome P450 activities. *Drug Metab Dispos* **32**, 647-660

143. Nishiya, Y., Hagihara, K., Kurihara, A., Okudaira, N., Farid, N. A., Okazaki, O., and Ikeda, T. (2009) Comparison of mechanism-based inhibition of human cytochrome P450 2C19 by ticlopidine, clopidogrel, and prasugrel. *Xenobiotica* **39**, 836-843

144. Chen, B. L., Chen, Y., Tu, J. H., Li, Y. L., Zhang, W., Li, Q., Fan, L., Tan, Z. R., Hu, D. L., Wang, D., Wang, L. S., Ouyang, D. S., and Zhou, H. H. (2009) Clopidogrel inhibits CYP2C19-dependent hydroxylation of omeprazole related to CYP2C19 genetic polymorphisms. *J Clin Pharmacol* **49**, 574-581

145. Yueh, M. F., Kawahara, M., and Raucy, J. (2005) High volume bioassays to assess CYP3A4-mediated drug interactions: induction and inhibition in a single cell line. *Drug Metab Dispos* **33**, 38-48

146. Heyn, H., White, R. B., and Stevens, J. C. (1996) Catalytic role of cytochrome P4502B6 in the *N*-demethylation of *S*-mephenytoin. *Drug Metab Dispos* **24**, 948-954

147. Ko, J. W., Desta, Z., and Flockhart, D. A. (1998) Human *N*-demethylation of (*S*)-mephenytoin by cytochrome P450s 2C9 and 2B6. *Drug Metab Dispos* **26**, 775-778

148. Parkinson, A., Kazmi, F., Buckley, D. B., Yerino, P., Ogilvie, B. W., and Paris, B. L. (2010) System-dependent outcomes during the evaluation of drug candidates as inhibitors of cytochrome P450 (CYP) and uridine diphosphate glucuronosyltransferase

(UGT) enzymes: human hepatocytes versus liver microsomes versus recombinant enzymes. *Drug Metab Pharmacokinet* **25**, 16-27

149. Van, L. M., Heydari, A., Yang, J., Hargreaves, J., Rowland-Yeo, K., Lennard, M. S., Tucker, G. T., and Rostami-Hodjegan, A. (2006) The impact of experimental design on assessing mechanism-based inactivation of CYP2D6 by MDMA (ecstasy). *J Psychopharmacol* **20**, 834-841

150. Klotz, U. (2006) Clinical impact of CYP2C19 polymorphism on the action of proton pump inhibitors: a review of a special problem. *Int J Clin Pharmacol Ther* **44**, 297-302

151. Andersson, T., Cederberg, C., Edvardsson, G., Heggelund, A., and Lundborg, P. (1990) Effect of omeprazole treatment on diazepam plasma levels in slow versus normal rapid metabolizers of omeprazole. *Clin Pharmacol Ther* **47**, 79-85

152. Lefebvre, R. A., Flouvat, B., Karolac-Tamisier, S., Moerman, E., and Van Ganse, E. (1992) Influence of lansoprazole treatment on diazepam plasma concentrations. *Clin Pharmacol Ther* **52**, 458-463

153. Gugler, R., Hartmann, M., Rudi, J., Brod, I., Huber, R., Steinijans, V. W., Bliesath, H., Wurst, W., and Klotz, U. (1996) Lack of pharmacokinetic interaction of pantoprazole with diazepam in man. *Br J Clin Pharmacol* **42**, 249-252

154. Tran, M., Tafreshi, J., and Pai, R. G. (2010) Review article: combination of clopidogrel and proton pump inhibitors: implications for clinicians. *J Cardiovasc Pharmacol Ther* **15**, 326-337

155. Bates, E. R., Lau, W. C., and Angiolillo, D. J. (2011) Clopidogrel-drug interactions. *J Am Coll Cardiol* **57**, 1251-1263

156. Holmes, D. R., Jr., Dehmer, G. J., Kaul, S., Leifer, D., O'Gara, P. T., and Stein, C. M. (2010) ACCF/AHA Clopidogrel clinical alert: approaches to the FDA "boxed warning": a report of the American College of Cardiology Foundation Task Force on Clinical Expert Consensus Documents and the American Heart Association. *Circulation* **122**, 537-557

157. Zhang, H., Ragueneau-Majlessi, I., and Levy, R. H. (2009) Interaction between clopidogrel and proton pump inhibitors: hypothesis to explain multifactorial CYP2C19 inhibition. *Drug Metab Lett* **3**, 287-289

158. Abelö, A., Andersson, T. B., Antonsson, M., Naudot, A. K., Skånberg, I., and Weidolf, L. (2000) Stereoselective metabolism of omeprazole by human cytochrome P450 enzymes. *Drug Metab Dispos* **28**, 966-972

159. Baer, B. R., DeLisle, R. K., and Allen, A. (2009) Benzylic oxidation of gemfibrozil-1-*O*-β-glucuronide by P450 2C8 leads to heme alkylation and irreversible inhibition. *Chem Res Toxicol* **22**, 1298-1309

160. Li, X. Q., Weidolf, L., Simonsson, R., and Andersson, T. B. (2005) Enantiomer/enantiomer interactions between the *S*- and *R*-isomers of omeprazole in human cytochrome P450 enzymes: major role of CYP2C19 and CYP3A4. *J Pharmacol Exp Ther* **315**, 777-787

161. Andersson, T., Bredberg, E., Lagerstrom, P. O., Naesdal, J., and Wilson, I. (1998) Lack of drug-drug interaction between three different non-steroidal anti-inflammatory drugs and omeprazole. *Eur J Clin Pharmacol* **54**, 399-404

162. Wang-Smith, L., Fort, J., Zhang, Y., and Sostek, M. (2012) Pharmacokinetics and relative bioavailability of a fixed-dose combination of enteric-coated naproxen and non-enteric-coated esomeprazole magnesium. *J Clin Pharmacol* **52**, 670-680

163. Regårdh, C. G., Andersson, T., Lagerstrom, P. O., Lundborg, P., and Skånberg, I. (1990) The pharmacokinetics of omeprazole in humans - a study of single intravenous and oral doses. *Ther Drug Monit* **12**, 163-172

164. Wu, F., Gaohua, L., Zhao, P., Jamei, M., Huang, S., Bashaw, E. D., and Lee, S. (2014) Predicting nonlinear pharmacokinetics of omeprazole enantiomers and racemic drug using physiologically based pharmacokinetic modeling and simulation: application to predict drug/genetic interactions. *Pharm Res* **8**, 1919-1929

165. Tornio, A., Filppula, A. M., Kailari, O., Neuvonen, M., Nyronen, T. H., Tapaninen, T., Neuvonen, P. J., Niemi, M., and Backman, J. T. (2014) Glucuronidation converts clopidogrel to a strong time-dependent inhibitor of CYP2C8: A phase II metabolite as a perpetrator of drug-drug interactions. *Clin Pharmacol Ther* **96**, 498-507

166. Richter, T., Murdter, T. E., Heinkele, G., Pleiss, J., Tatzel, S., Schwab, M., Eichelbaum, M., and Zanger, U. M. (2004) Potent mechanism-based inhibition of human CYP2B6 by clopidogrel and ticlopidine. *J Pharmacol Exp Ther* **308**, 189-197

167. Zhang, H., Amunugama, H., Ney, S., Cooper, N., and Hollenberg, P. F. (2011) Mechanism-based inactivation of human cytochrome P450 2B6 by clopidogrel: involvement of both covalent modification of cysteinyl residue 475 and loss of heme. *Mol Pharmacol* **80**, 839-847

168. Foti, R. S., and Wahlstrom, J. L. (2008) CYP2C19 Inhibition: The impact of substrate probe selection on in vitro inhibition profiles. *Drug Metab Dispos* **36**, 523-528

169. Silverman, R. B. (1995) Mechanism-based enzyme inactivators. *Methods Enzymol* **249**, 240-283

170. Fontana, E., Dansette, P. M., and Poli, S. M. (2005) Cytochrome P450 enzymes mechanism-based inhibitors: common sub-structures and reactivity. *Curr Drug Metab* **6**, 413-454

171. Hollenberg, P. F., Kent, U. M., and Bumpus, N. N. (2008) Mechanism-based inactivation of human cytochromes P450s: experimental characterization, reactive intermediates, and clinical implications. *Chem Res Toxicol* **21**, 189-205

172. Kamel, A., and Harriman, S. (2013) Inhibition of cytochrome P450 enzymes and biochemical aspects of mechanism-based inactivation (MBI). *Drug Discov Today Technol* **10**, e177-189

173. Blobaum, A. L., Harris, D. L., and Hollenberg, P. F. (2005) P450 active site architecture and reversibility: inactivation of cytochromes P450 2B4 and 2B4 T302A by tert-butyl acetylenes. *Biochemistry* **44**, 3831-3844

174. Blobaum, A. L. (2006) Mechanism-based inactivation and reversibility: is there a new trend in the inactivation of cytochrome P450 enzymes? *Drug Metab Dispos* **34**, 1-7

175. Gawronska-Szklarz, B., Adamiak-Giera, U., Wyska, E., Kurzawski, M., Gornik, W., Kaldonska, M., and Drozdzik, M. (2012) CYP2C19 polymorphism affects single-dose pharmacokinetics of oral pantoprazole in healthy volunteers. *Eur J Clin Pharmacol* **68**, 1267-1274

176. Ernest, C. S., 2nd, Hall, S. D., and Jones, D. R. (2005) Mechanism-based inactivation of CYP3A by HIV protease inhibitors. *J Pharmacol Exp Ther* **312**, 583-591

177. Hanson, K. L., VandenBrink, B. M., Babu, K. N., Allen, K. E., Nelson, W. L., and Kunze, K. L. (2010) Sequential metabolism of secondary alkyl amines to metabolic-intermediate complexes: opposing roles for the secondary hydroxylamine and primary amine metabolites of desipramine, *S*-fluoxetine, and *N*-desmethyldiltiazem. *Drug Metab Dispos* **38**, 963-972

178. Stresser, D. M., Mason, A. K., Perloff, E. S., Ho, T., Crespi, C. L., Dandeneau, A. A., Morgan, L., and Dehal, S. S. (2009) Differential time- and NADPH-dependent inhibition of CYP2C19 by enantiomers of fluoxetine. *Drug Metab Dispos* **37**, 695-698

179. Andersson, T., Miners, J. O., Veronese, M. E., and Birkett, D. J. (1994) Identification of human liver cytochrome P450 isoforms mediating secondary omeprazole metabolism. *Br J Clin Pharmacol* **37**, 597-604

180. Jenkins, S. M., Zvyaga, T., Johnson, S. R., Hurley, J., Wagner, A., Burrell, R., Turley, W., Leet, J. E., Philip, T., and Rodrigues, A. D. (2011) Studies to further investigate the inhibition of human liver microsomal CYP2C8 by the acyl-β-glucuronide of gemfibrozil. *Drug Metab Dispos* **39**, 2421-2430

181. He, K., Bornheim, L. M., Falick, A. M., Maltby, D., Yin, H., and Correia, M. A. (1998) Identification of the heme-modified peptides from cumene hydroperoxide-inactivated cytochrome P450 3A4. *Biochemistry* **37**, 17448-17457

182. Correia, M., and Ortiz de Montellano, P. (2005) Inhibition of cytochrome P450 enzymes. in *Cytochrome P450: Structure, Mechanism, and Biochemistry* (Ortiz de Montellano, P. ed.), 3rd Ed., Kluwer Academic/ Plenum Publishers, New York. pp 247-322

183. Foti, R. S., Rock, D. A., Pearson, J. T., Wahlstrom, J. L., and Wienkers, L. C. (2011) Mechanism-based inactivation of cytochrome P450 3A4 by mibefradil through heme destruction. *Drug Metab Dispos* **39**, 1188-1195

184. He, K., Falick, A. M., Chen, B., Nilsson, F., and Correia, M. A. (1996) Identification of the heme adduct and an active site peptide modified during mechanism-based inactivation of rat liver cytochrome P450 2B1 by secobarbital. *Chem Res Toxicol* **9**, 614-622

185. Guengerich, F. P. (1978) Destruction of heme and hemoproteins mediated by liver microsomal reduced nicotinamide adenine dinucleotide phosphate-cytochrome P-450 reductase. *Biochemistry* **17**, 3633-3639

186. Ortiz de Montellano, P. R., and Reich, N. O. (1986) Inhibition of cytochrome P-450 enzymes. in *Cytochrome P-450: Structure, Mechanism and Biochemistry* (Ortiz de Montellano, P. R. ed.), 1st Ed., Plenum Press, New York. pp 273-314

187. Wong, S. G., and Marks, G. S. (1999) Formation of *N*-alkylprotoporphyrin IX after interaction of porphyrinogenic xenobiotics with rat liver microsomes. *J Pharmacol Toxicol Methods* **42**, 107-113

188. Strittmatter, P., and Velick, S. F. (1956) The isolation and properties of microsomal cytochrome. *J Biol Chem* **221**, 253-264

189. Brändström, A., Bergman, N.-A., Grundevik, I., Johansson, S., and Ohlson, L. (1989) Chemical reactions of omeprazole and omeprazole analogues. II. Kinetics of the reaction of omeprazole in the presence of 2-mercaptoethanol. *Acta Chemica Scand* **43**, 549-568

190. Brändström, A., Lindberg, P., Bergman, N.-A., Alminger, T., Ankner, K., Junggren, U., Nordberg, P., Erickson, M., Grundevik, I., Hagin, I., Hoffmann, K.-J., Johansson, S., Larsson, S., Löfberg, I., Ohlson, K., Persson, B., Skånberg, I., and Tekenbergs-Hjelte, L. (1989) Chemical reactions of omeprazole and omeprazole analogues. I. A survey of the chemical transformations of omeprazole and its analogues. *Acta Chemica Scand* **43**, 536-548

191. Ortiz de Montellano, P. R., and Mathews, J. M. (1981) Autocatalytic alkylation of the cytochrome P-450 prosthetic haem group by 1-aminobenzotriazole. Isolation of an NN-bridged benzyne-protoporphyrin IX adduct. *Biochem J* **195**, 761-764

192. Amunugama, H. T., Zhang, H., and Hollenberg, P. F. (2012) Mechanism-based inactivation of cytochrome P450 2B6 by methadone through destruction of prosthetic heme. *Drug Metab Dispos* **40**, 1765-1770

193. Mortishire-Smith, R. J., Castro-Perez, J. M., Yu, K., Shockcor, J. P., Goshawk, J., Hartshorn, M. J., and Hill, A. (2009) Generic dealkylation: a tool for increasing the hit-rate of metabolite rationalization, and automatic customization of mass defect filters. *Rapid Commun Mass Spectrom* **23**, 939-948

194. Boix, C., Ibanez, M., Sancho, J. V., Niessen, W. M., and Hernandez, F. (2013) Investigating the presence of omeprazole in waters by liquid chromatography coupled to low and high resolution mass spectrometry: degradation experiments. *J Mass Spectrom* **48**, 1091-1100

195. Baciocchi, R., Juza, M., Classen, J., Mazzotti, M., and Morbidelli, M. (2004) Determination of the dimerization equilibrium constants of omeprazole and pirkle's alcohol through optical-rotation measurements. *Helv Chim Acta* **87**, 1917-1926

196. Marom, H., Pogodin, S., and Agranat, I. (2014) Single enantiomer versus racemate: chiral distinction in the proton pump inhibitors omeprazole and esomeprazole. *Chirality* **26**, 214-227

197. Kajula, M., Tejesvi, M. V., Kolehmainen, S., Makinen, A., Hokkanen, J., Mattila, S., and Pirttila, A. M. (2010) The siderophore ferricrocin produced by specific foliar endophytic fungi in vitro. *Fungal Biol* **114**, 248-254

198. He, K., He, Y. A., Szklarz, G. D., Halpert, J. R., and Correia, M. A. (1996) Secobarbital-mediated inactivation of cytochrome P450 2B1 and its active site mutants. Partitioning between heme and protein alkylation and epoxidation. *J Biol Chem* **271**, 25864-25872

199. von Weymarn, L. B., Blobaum, A. L., and Hollenberg, P. F. (2004) The mechanism-based inactivation of P450 2B4 by tert-butyl 1-methyl-2-propynyl ether: structural determination of the adducts to the P450 heme. *Arch Biochem Biophys* **425**, 95-105

200. Correia, M. A., Sinclair, P. R., and De Matteis, F. (2011) Cytochrome P450 regulation: the interplay between its heme and apoprotein moieties in synthesis, assembly, repair, and disposal. *Drug Metab Rev* **43**, 1-26

201. Parkinson, A., Ogilvie, B. W., Paris, B. L., Hensley, T. N., and Loewen, G. J. (2010) Human biotransformation. in *Biotransformation and Metabolite Elucidation of Xenobiotics*, 1st Ed., John Wiley & Sons, Inc., Hoboken. pp 1-77

202. Berglund, M., and Wieser, M. E. (2011) Isotopic compositions of the elements 2009 (IUPAC Technical Report). *Pure Appl Chem* **83**, 397-410

203. Scientific Instrument Services. (2015) Exact Masses of the Elements and Isotopic Abundances. http://www.sisweb.com/referenc/source/exactmas.htm. Accessed: March 29, 2015.

204. Reynald, R. L., Sansen, S., Stout, C. D., and Johnson, E. F. (2012) Structural characterization of human cytochrome P450 2C19: active site differences between P450s 2C8, 2C9, and 2C19. *J Biol Chem* **287**, 44581-44591

APPENDIX 1: PERMISSION FROM PUBLISHER FOR CHAPTER 4

March 9, 2015

Brian W. Ogilvie
XenoTech, LLC
16825 W 116th St.
Lenexa, KS 66226

Email: bogilvie@xenotechllc.com

Dear Brian Ogilvie:

This is to grant you permission to include the following article in your dissertation entitled "An In Vitro Investigation Into the Mechanism of the Clinically Relevant Drug-Drug Interaction Between Omeprazole or Esomeprazole and Clopidogrel" for the University of Kansas Medical Center:

> Brian W. Ogilvie, Phyllis Yerino, Faraz Kazmi, David B. Buckley, Amin Rostami-Hodjegan, Brandy L. Paris, Paul Toren, and Andrew Parkinson, The Proton Pump Inhibitor, Omeprazole, but Not Lansoprazole or Pantoprazole, Is a Metabolism-Dependent Inhibitor of CYP2C19: Implications for Coadministration with Clopidogrel, *Drug Metab Dispos* November 2011 39:2020-2033

On the first page of each copy of this article, please add the following:

> Reprinted with permission of the American Society for Pharmacology and Experimental Therapeutics. All rights reserved.

In addition, the original copyright line published with the paper must be shown on the copies included with your thesis.

Sincerely yours,

Richard Dodenhoff
Journals Director

9650 Rockville Pike | Bethesda | MD | 20814-3995
P: (301) 634-7060 | F: (301) 634-7061 | E: info@aspet.org | www.aspet.org

APPENDIX 2: OTHER PUBLICATIONS INCLUDING THIS AUTHOR FROM 2008

1. **Ogilvie BW**, Torres R, Dressman MA, Baroldi P. Pharmacokinetics of tasimelteon, a novel dual melatonin receptor agonist, and CYP1A2 and CYP3A4-mediated drug-drug interactions. Accepted by: *J Clin Pharmacol*, March 26, 2015; DOI: 10.1002/jcph.507.

2. **Ogilvie BW**, Kazmi F, Parkinson A. Mechanistic studies on the inactivation of CYP2C19 by esomeprazole, 5-*O*-desmethyl omeprazole and omeprazole sulfone. To be submitted to *Drug Metab Dispos*.

3. **Ogilvie BW**, Barbara JE, Parkinson A. High-resolution mass spectrometry appears to reveal a false CYP2C19 heme adduct with esomeprazole: Implications for the use of mass-defect filtering. To be submitted to *Drug Metab Dispos*.

4. Rougée LRA, Buckley DB, **Ogilvie BW**, Hayman A, Helmstetter S, Otwell CJ, Woodworth ZW, Collier AC. The effects of age, obesity and sex on hepatic metabolism and modeled physiologically based pharmacokinetic (PBPK) clearance by Cytochromes P450. Submitted to: *Biochem Pharmacol*, September, 2014.

5. Oeser SG, Rougée LRA, Buckley DB, **Ogilvie BW**, Hayman A, Helmstetter S, Otwell CJ, Woodworth ZW, Coughtrie MWH, Milne AM, Collier AC. The effects of obesity and sex on hepatic metabolism and physiologically based pharmacokinetic (PBPK) clearance by UDP-Glucuronosyltransferases. To be submitted to: *Biochem Pharmacol*, May, 2015.

6. **Ogilvie BW** and Parkinson A (2014). Drugs as victims and perpetrators and the pharmacokinetic concept of maximum exposure. In *Handbook of Metabolic Pathways of Xenobiotics;* Vol. 2 (Prakash C, Gan L, Zhong D, Aizawa H, Lee P eds.). John Wiley & Sons, Hoboken, NJ. pp. 103 – 123. ISBN: 978-0-470-74910-4.

7. Parkinson A, **Ogilvie BW**, Buckley DB, Kazmi F, Czerwinski M, and Parkinson O. (2013) Biotransformation of xenobiotics, in: *Casarett and Doull's Toxicology: The Basic Science*

of Poisons (Klaassen CD, ed.), McGraw-Hill Medical Pub. Division, New York. pp. 185-367.

8. Eichenbaum G, Skibbe J, Parkinson A, Johnson MD, Baumgardner D, **Ogilvie B**, Usuki E, Tonelli F, Holsapple J, Schmitt-Hoffmann A. (2012) Use of enzyme inhibitors to evaluate the conversion pathways of ester and amide prodrugs: A case study example with the prodrug ceftobiprole medocaril. *J Pharm Sci* **101**(3): 1242-52.

9. Parkinson A, Kazmi F, Buckley DB, Yerino P, Paris BL, Holsapple J, Toren P, Otradovec SM and **Ogilvie BW**. (2011) An evaluation of the dilution method for identifying metabolism-dependent inhibitors of cytochrome P450 enzymes. *Drug Metab Dispos* **39**:1370-1387.

10. Watanabe T, Kusuhara H, Debori Y, Maeda K, Kondo T, Nakayama H, Horita S, **Ogilvie BW**, Parkinson A, Hu Z and Sugiyama Y. (2011) Prediction of the overall renal tubular secretion and hepatic clearance of anionic drugs and a renal drug-drug interaction involving organic anion transporter 3 in humans by in vitro uptake experiments. *Drug Metab Dispos* **39:**1031-1038.

11. Parkinson A, Kazmi F, Buckley DB, Yerino P, **Ogilvie BW**, Paris BL. (2010) System-dependent outcomes during the evaluation of drug candidates as Inhibitors of cytochrome P450 (CYP) and UDP-glucuronosyltransferase (UGT) enzymes: Human hepatocytes versus liver microsomes versus recombinant enzymes. *Drug Metab Pharmacokinet* **25**:16-27.

12. Parkinson A, **Ogilvie BW**, Paris BL, Hensley TN, Loewen GJ. (2010) Human Biotransformation, in: *Biotransformation and Metabolite Elucidation of Xenobiotics* (Nassar AF, ed.), John Wiley & Sons, Hoboken, NJ, 1-78.

13. Hirouchi M, Kusuhara H, Onuki R, **Ogilvie BW**, Parkinson A and Sugiyama Y. (2009) Construction of triple-transfected cells (OATP1B1/MRP2/MRP3 and OATP1B1/MRP2/MRP4) for analysis of the sinusoidal function of MRP3 and MRP4. *Drug Metab Dispos* **37**:2103-2111.

14. Paris BL, **Ogilvie BW**, Scheinkoenig JA, Ndikum-Moffor F, Gibson R and Parkinson A. (2009) In vitro inhibition and induction of human liver cytochrome P450 (CYP) enzymes by milnacipran. *Drug Metab Dispos* **37**:2045-2054.

15. Nassar AF, King I, Paris BL, Haupt L, Ndikum-Moffor F, Campbell R, Usuki E, Skibbe J, Brobst D, **Ogilvie BW** and Parkinson A. (2009) An in vitro evaluation of the victim and perpetrator potential of the anti-cancer agent laromustine (VNP40101M), based on reaction phenotyping and inhibition and induction of cytochrome P450 (CYP) enzymes. *Drug Metab Dispos* **37**:1922-1930.

16. **Ogilvie BW**, Usuki E, Yerino P and Parkinson A. (2008) In Vitro approaches for studying the inhibition of drug-metabolizing enzymes and identifying the drug-metabolizing enzymes responsible for the metabolism of drugs (reaction phenotyping) with emphasis on cytochrome P450, in: *Drug-Drug Interactions* (Rodrigues AD, ed.), Informa Healthcare, New York, 231-358.

17. Parkinson A and **Ogilvie BW**. (2008) Biotransformation of Xenobiotics, in: Casarett and Doull's *Toxicology: The Basic Science of Poisons* (Klaassen CD, ed.), McGraw-Hill Medical Pub. Division, New York, 161-304.